Site Response Characteristics of Marine Deposits of Eastern Coast of Cyprus

Maziar Bagheri

Submitted to the
Institute of Graduate Studies and Research
in partial fulfillment of the requirements for the degree of

Master of Science
in
Civil Engineering

Eastern Mediterranean University
October 2016
Gazimağusa, North Cyprus

Approval of the Institute of Graduate Studies and Research

Prof. Dr. Mustafa Tümer
Director

I certify that this thesis satisfies the requirements as a thesis for the degree of Master of Science in Civil Engineering.

Assoc. Prof. Dr. Serhan Şensoy
Chair, Department of Civil Engineering

We certify that we have read this thesis and that in our opinion, it is fully adequate in scope and quality as a thesis for the degree of Master of Science in Civil Engineering.

Assoc. Prof. Dr. Huriye Bilsel
Supervisor

Examining Committee

1. Prof. Dr. Zalihe Nalbantoğlu Sezai _____

2. Assoc. Prof. Dr. Huriye Bilsel _____

3. Assoc. Prof. Dr. Yeşim Gürtuğ _____

4. Asst. Prof. Dr. Giray Özay _____

5. Asst. Prof. Dr. Eriş Uygar _____

ABSTRACT

When an earthquake occurs, the site destruction is substantially affected by the soil response. For a long period, spectral acceleration and seismic resistant structures of the site has been employed for designing. The response of the site is computed as the spectra response of a specific site, in seismic response analysis. The parameters which are required for the seismic response analysis are the distance of the soil surface to bedrock, soil geotechnical properties, soil profile and its thickness, and shear wave velocity. The analysis of ground response is needed to estimate the movement of the ground surface for improvement of the design response spectrum and to assess the strain and dynamic stresses for appraisal of liquefaction potential. It is also required to distinguish forces from the earthquake which may lead to structures instability. A perfect evaluation of the ground response would also provide the mechanism of the rupture at an earthquake source, the growth of the stress waves which move through the earth up the bedrock beneath a given site, to distinguish how soil over the bedrock affects the movement of the ground surface. As a result, ground response analysis can be defined as how soil deposit responds to the movement of the rock beneath it. Therefore, soil properties are of utmost importance in this regard, as they determine the ground motions and movement especially in cases where soils are soft or loose. For this reason, the identification of the changes in period and acceleration parameters of the ground motion is very important.

In this study, shear wave velocity is obtained indirectly from CPT data of Tuzla area. For seismic response analysis all around the world, the ideal depth for soil profile and data is the upper 30 m of the ground which is considered for the area under

study. Seismic waves can be intensified or weakened by the condition of the subsurface soil. Therefore, for the investigation of seismic response, determination of the soil characteristics and shear wave variation associated with soil property variations is essential. In this study, the soil properties and liquefaction behavior were assessed using NovoCPT and LiqIT softwares respectively for Richter magnitudes of 6.0, 6.5, and 7.0, and the ground response was estimated using DeepSoil and SeismoSignal softwares. The analysis of the CPT data showed that there is no major risk for the liquefaction at the entire total depth as also justified by the empirical procedures apart from the 7 Richter magnitude earthquake. In fine-grained soils of Tuzla, however earthquakes ($M_w \geq 6.5$) might cause induced ground deformations, ground settlements and lateral spreads, which could not be evaluated with the available CPT based methods.

The response displacement, velocity and acceleration of the first layer and bedrock revealed that approximately during the first period when the amplitudes of ground motion are high based on high energy absorption in depth and soil characteristics, the acceleration, velocity and displacement are high. Whereas, when the amplitude decreases (during the second period) the absorbed energy is released and these parameters also dramatically decrease and reverse action will occur for the first layer, which was observed for all CPT locations. It was concluded that the amounts of response displacement, velocity and acceleration for all bedrock locations are nearly the same, whereas a varying trend can be observed for the response of first layers, which is directly related to soil characteristics in the region.

Keywords: Shear wave velocity, liquefaction potential, ground response analysis.

ÖZ

Bir deprem anında arazide oluşan yıkım önemli ölçüde arazi etkileşiminden kaynaklanır. Uzun süre depreme dayanıklı yapı tasarımında spektral ivme kullanılmıştır. Kısaca, bir arazinin depreme dayalı etkileşimi spektral etkileşim olarak çalışılmıştır. Sismik etkileşim analizi için gerekli değişkenler yer yüzeyinin ana kayaya olan mesafesi, geoteknik parametreler, zemin profili, derinliği ile kesme dalgası hızıdır. Tasarım etkileşim spektrumunu geliştirmek, ve sıvılaşma potansiyeli tesbiti için yer yüzeyinin hareketinin analiz edilmesi gerekmektedir. Mükemmel bir zemin etkileşim değerlendirmesi depremin kaynağındaki kırılma mekanizması, zemin içerisinde ana kayadan yukarı hareket eden gerilme dalgalarının büyümesi, ve anakaya üzerindeki zemin katmanın yüzey hareketlerini nasıl etkilediği hakkında bilgiler içermelidir. Kısaca, zemin etkileşimi üst katmanın anakayanın hareketine karşı nasıl bir etki yaptığını ifade eder. Dolayısıyla, zemin parametrelerini bilmek, özellikle yumuşak veya gevşek zeminlerde yer hareketlerini belirlemede çok önemlidir. Bu nedenle yer hareketlerinin peryoda bağlı değişimleri ve ivme parametreleri de önem arzeder.

Bu çalışmada, kesme dalgası dolaylı olarak Tuzla'da yapılan koni penetrasyon deney (CPT) sonuçlarından elde edilmiştir. Sismik etkileşim çalışmalarında çalışılması gereken derinlik 30 metredir ve bu araştırmada da böyle alınmıştır. Zeminin özelliklerine bağlı olarak sismik dalgaların gücü yükselebilir veya azalabilir. Dolayısıyla, sismik etkileşim çalışmasında zemin karakteristiği ve parametrelerinin değişiminin bilinmesi gerekir. Bu çalışmada, zemin parametreleri ve sıvılaşma davranışı NovoCPT and LiqIT yazılımları kullanılarak 6, 6.5, ve 7.0 Richter deprem

büyüklüklerinde tesbit edilirken, depreme dayalı zemin etkileşimi ise DeepSoil ve SeismoSignal yazılımları ile çalışılmıştır. CPT datası sonuçları 7.0 Richter büyüklüğünde deprem dışında önemli bir sıvılaşma riski olmadığını göstermiş, ayrıca empirik yöntemlerle de onaylanmıştır. Tuzla bölgesindeki ince taneli zeminlerden oluşan zemin katmanları ise en az 6.5 büyüklüğündeki depremlerle yer deformasyonları, oturmalar ve yanal yayılmalar gösterebilecektir, ancak bunlar CPT datası ile değerlendirlememektedir.

Zemin etkileşim çalışmasına bağlı olarak elde edilen grafiklerden, deprem esnasında, ilk periyodda yer hareketinin genliği, yüksek enerji emilimi ve zemin parametrelerine bağlı olarak yüksekse, ilk katman ve anakaya için zemin etkileşim ve deplasman, hız ve ivme davranışının da yüksek olacağı gözlemlenmiştir. Ancak ikinci periyodda genlik azaldıkça, emilen enerji serbest kalacak ve dolayısıyla bu parametrelerde de tüm CPT lokasyonlarında izlenen önemli bir azalma olacaktır. Sonuç olarak, etkileşim ve deplasman, hız ve ivme ilişkileri tüm anakaya lokasyonlarında yaklaşık olarak aynı iken, ilk katmandaki etkileşimde zemin parametrelerine bağlı olarak bir değişim izlenmektedir, bu da Tuzla Bölgesi'ndeki karma profilin zemin karakteristiğine bağlıdır.

Anahtar Kelimeler: Kesme dalga hızı, sıvılaşma potansiyeli, zemin etkileşim analizi.

To My Family

ACKNOWLEDGMENT

I would like to express my deep appreciation to my supervisor Assoc. Prof. Dr. Huriye Bilsel for her inspiration and guidance throughout this work. This thesis would not have been possible without her support.

I also would like to thank to my co-supervisor Assoc. Prof. Dr. Yeşim Gürtuğ for her constant support, availability and constructive suggestions, which were determinant for the accomplishment of the work presented in this thesis.

I would also like to thank the examining committee members Prof. Dr. Zalihe Nalbantoğlu Sezai, Asst. Prof. Dr. Giray Özay and Asst. Prof. Dr. Eriş Uygar for taking the time to review my thesis.

I would specially like to thank my amazing wife for the love, support, and constant encouragement I have gotten over the years. In particular, I would like to thank my parents. You are the salt of the earth, and I undoubtedly could not have done this without you.

I would also like to thank to other staff members of the Department of Civil Engineering of Eastern Mediterranean University, mainly to Ismail Safkan who has provided additional data and technical support in the preliminary stage of this work.

TABLE OF CONTENTS

LIST OF TABLES

LIST OF FIGURES

LIST OF ABBREVIATIONS

BH-1	Boreholes Number
CPT	Cone penetration test
E_S	Young modulus, Modulus of elasticity
S_u	Undrained shear strength
Vs	Shear wave velocity
G	Shear modulus
FS	Factor of safety
e	Void ratio
φ	Friction angle
γ	Soil unit weight
σ_v	Total vertical stress
σ'_v	Effective vertical stress
q_c	Cone tip resistance
f_s	Cone sleeve friction
u2	Pore water pressure
q_t	Corrected cone tip resistance
Q_t	Normalized cone resistance
Bq	Normalized pore pressure ratio
F_r	Normalized friction ratio
R_f	Friction ratio
I_c	Soil type index
S_v	Total overburden stress
S'_v	Effective overburden stress

C_c	Coefficient of compression for consolidation settlement
r_d	Stress reduction factor
CSR	Cyclic stress ratio
CRR	Cyclic resistance ratio
MSF	Magnitude scaling factor
SBT	Soil behavior type
SBT_N	Normalized soil behavior type
GMPE	Ground motion prediction equation
PGV	Peak ground velocity
PGA	Peak ground acceleration
PSA	Pseudo spectrum acceleration
ASI	Acceleration spectrum intensity
SI	Spectrum intensity
SA	Spectral acceleration
Vs_{30}	Shear velocity at the top 30 m of soil layer
W_D	Energy dissipation
W_S	Maximum strain energy
G_{sec}	secant shear modulus
G_{tan}	tangent shear modulus
A_{loop}	Area of the hysteresis loop
ξ	Damping ratio
γ_c	Shear strain
γ_{eff}	Effective shear strain
R_{Jb}	Closest distance to rupture plane

Chapter 1

INTRODUCTION

Soil liquefaction, SL is a fundamental geotechnical hazard which can be triggered by sudden tremor or movements of earth's tectonic crustal plate. SL usually happens due to rapid ground shaking during or after the earthquake and exhibits its characteristics as sudden reduction or strength and stiffness loss of soft sandy soils. Thus during strong ground shaking, saturated sediments act as sticky fluid. Hence the pore-water pressure exceeds the strength of soil particles causing the failure of masses. In its simplest explanation, the groundwater, sand, silt and soil mixtures combine during the tectonic crustal faulting line that generates seismic waves, which causes moderate to powerful earthquake that may result in liquefaction. The phenomenon called quicksand is the aftermath result of this hazardous geologic process. Immediately after the earthquake event, often the liquefaction takes place under the existing structures such as light buildings, foundations, roads, and other engineering structures. Then the structures sink and the buildings subjected to such phenomenon often collapse. Tilt or be subjected to severe damage. Then after the whole ground shaking process and liquefaction, the loose saturated soil deposits under the structures become firm again, and the water settles at a much deeper depth in underground. It has been observed in most cases, that region with sandy, sand-silt admixtures which are quite close to the groundwater are prone to the risk and damages related to liquefaction.

The 1998 Adana and 1999 Kocaeli earthquake events of magnitudes, M_w =5.9 and 7.4 respectively which happened in Turkey, are among the most recent case study of ground motion with devastated effect. As a result of these severe earthquakes, more than ten thousand buildings were subjected to destruction or severely damaged. About hundreds of civil engineering structures among which were poorly constructed structures bulged, dislocated, wrapped, tilted and deeply settled into the ground due to liquefaction and ground unstiffening (Sancio et al. 2002). By the same token, few years before Kocaeli earthquake, 1995, Kobe earthquake occurred in Japan which caused more than billions of dollars damage, in which liquefaction played a remarkable role. In fact, the liquefaction effect which occurs immediately after the earthquake often caused loss of lives (Hamada et al. 1995).

Over the last few decades, extensive studies have been carried out on liquefaction potential of sands and silty sands resulting from strong earthquakes and various methodologies, procedures, designs have been developed to determine safety factors against liquefaction during or after strong earthquakes (Youd et al., 2001). In this regard, Wang (1979) conducted a study on the liquefaction phenomenon by reviewing the initial field case studies of disasters experienced from liquefaction during Chinese earthquakes. Similarly, Seed et al. (1983) and many other researchers have developed the various laboratory-based criteria for the evaluation of liquefaction potential of any soil deposit (Robertson 1998). Also many other researchers have developed, proposed and suggested many empirical formulations generated from the in situ testing geotechnical methods such as cone penetration test (CPT), standard penetration test (SPT), penetrometer, etc. (Idriss and Boulanger 2006).

The cone penetration test in geotechnical practice is one of the most common techniques used for geotechnical site exploration and subsurface exploration. The cone penetration test is predictable in both the in situ and laboratory tests with the broad application as a tool for examining the liquefaction potential and its related parameters. In the literature review, comprehensive studies on some CPT-based liquefaction potential and resistance values have been investigated by a number of researchers such as Seed et al. (1983), Ishihara (1986), Robertson and Wride (1998), Juang et al. 2002, Idriss and Boulanger (2004) as presented by Moss et al. 2003. Therefore, the CPT Geotechnical application is used to interpret CPT data and generate several useful data to be used in engineering, design and application of numerous geotechnical studies such as shear wave velocity, pore water pressure and most importantly liquefaction potential.

In this thesis, the study was performed on the field at the Eastern Coast of Cyprus, situated in the north-west city of Famagusta. The study area is within the circumference area of one kilometre from the Famagusta Bay, Northern Cyprus. Tuzla area, known as Alasia nearly 4000 years ago is said to be a harbor town in 2000 B.C., was partly ruined when it was devastated by a strong earthquake event during 1300 B.C.

The recorded historical earthquakes in and around Cyprus indicates that the Eastern Coast of Cyprus has been an earthquake-prone area. Strong earthquakes of magnitudes 6.0 to 8.0 have been reported to occur along the coast of Famagusta. Despite this fact, the potential liquefaction and cyclic failure of the area under study needs to be investigated as there are not enough data and studies on this subject. In the most recent time, Durgunoğlu and Bilsel (2007) carried out the first liquefaction

assessment study in the Tuzla region in an attempt for a small scale microzonation. However, more detailed geotechnical investigations are necessary to generate more data and make available to find liquefaction susceptibility of local soils in Eastern Coast of Cyprus.

This study aimed to evaluate the soil liquefaction resistance of Eastern Coast of Cyprus by NovoCPT, LiqIT, DeepSoil and SeismoSignal software. The topics considered in this thesis include liquefaction potential index, the probability of liquefaction, liquefaction severity, evaluation of liquefaction potential based on CPT-criteria and site response analysis.

Finally, these studies correlated with each other for liquefaction assessment. In Chapter 2 the seismicity of Cyprus and the study area will be discussed while in Chapter 3, a literature review will be offered including information on the definition of soil liquefaction. The software programs and the CPT-based procedures used to analyze the liquefaction potential are presented in Chapter 4 while in chapter five the applications of methods and results will be discussed. Finally, in chapter 6, the summary and conclusions of the research will be presented.

Chapter 2

SEISMICITY OF CYPRUS

2.1 Introduction

The location of Cyprus is within the Alpine-Himalayan seismic region, which includes database records of approximately 15% of the total combination of world earthquake occurrence. The seismicity of Cyprus is dependent on the Cyprus Arc, which is a tectonic boundary between Africa and Eurasian continental plates, (Erdik et al., 1999). Cyprus Island has been subjected to many earthquake events in the record (15BC to 1900AD) based on both the historical evidence and archaeological findings. The more accurate data collection began in 1896, retrieved from the seismological stations operating in neighboring countries. The situation is improved since the mid1980s, with the creation of seismic stations in both the southern and northern parts of the Cyprus Island (Kalogeras. et al. 1999).

The creation of the Seismology Section Department, (SSD) of Cyprus in 1977 is for the monitoring of all seismic activities in Cyprus and the broader area of the Eastern Mediterranean region. The southeast maintains and operates the analogue section (1977-2013) and Digitalized Seismological Networks (2014-Till date). The network of accelerometer stations is on daily monitoring routine, recording, processing, and evaluation of the seismological data obtained at different locations. The immediate publication of the relevant information is available on SSD websites on a daily basis.

Although the operations of seismograph network began in Cyprus in 1997, Algermissen (2004) reported the long historical record of earthquake events on the island of Cyprus dated back to 92 BC. However, there are still limited data and information available for the active ground movements, plate tectonics, earthquake events, faulting lines in the offshore and onshore area of the Cyprus landmass.

In the last few years, scientists have been analysing the past and recent tectonic records of the island for the evaluation and prediction of the present day potential seismic hazards. During 2012-2013, the Geological Survey Department of Cyprus has achieved full implementation of the Seismological Network and Earthquake Hazard Assessment Center to work with the latest technological advances in seismology in the region. The funding of the earthquake site response facilities and equipment is by the United Nations Office for Project Services (UNOPS).

At every impulse of a ground movement, the seismological department section publishes the needful information attributed to the Cyprus seismicity and the broader sphere of the Eastern Mediterranean. The updates of such data (1977-till date) can be found on their website link (http://81.4.135.34:8080) with the relevant materials such as maps, catalogues, bulletins, articles, etc. for the general public assessments.

The locations of the seismological stations on the Cyprus Island are at Akamas (AKMS), Alaska (ALEF), Nata-Pafos (NATA), and Souni (SUNI). Also included are Asgata (ASGA), Athalassa (ATHA), Mavrovouni (MVOU), Paralimni (PARA), Troodos (TROD), CSNET (OBS1, OBS4), Nicosia (NIC), etc. The previously mentioned probabilistic seismic hazard materials obtained from the island and site survey analyses were often controlled following a revised seismic record data.

The regional earthquake event maps of Cyprus have been produced based on different parameters. Such parameters include the attenuation of strong ground motion for certain earthquake fault types, distribution of seismicity histories, maximum earthquake magnitudes, seismo-tectonic models, spatial rates of earthquake recurrence, etc. The variable required for the potential liquefaction calculations of Tuzla in North Cyprus, which is the study area of this thesis, is estimated from the analysis of the historical data.

2.2 Regional Geology and Tectonic

Cyprus has robust historical records of destructive earthquakes, (Kalogeras, 1999). The observation from the literature reviews has indicated that the seismotectonic operations on the Island of Cyprus lie either within or near the tectonic plate boundary between the African Plate and Eurasian Subplate, which is about 100 km west of the Arabian Plate. Figure 2.1 shows main tectonic settings in the Mediterranean Region (USGS, 1999).

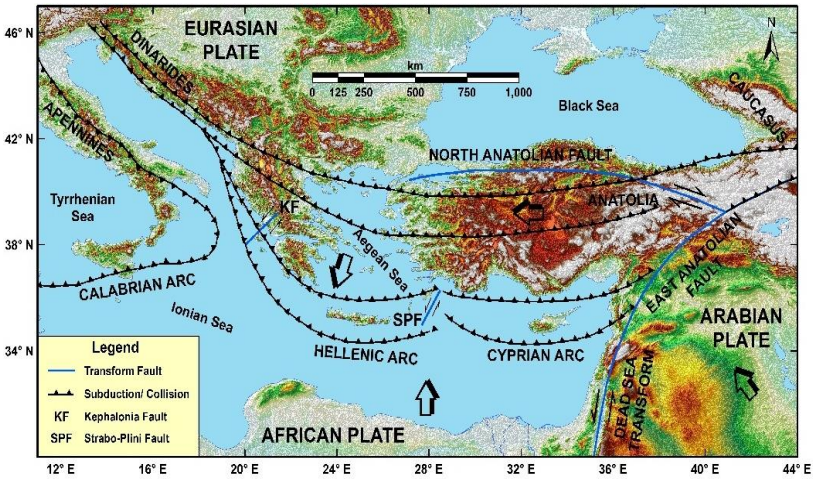

Figure 2.1: Tectonic map of the Eastern Mediterranean Region (Ziegler, Meulenkamp, 1988 and Dewey, 1989).

In the literature review, it is indicated that the African Plate is projecting toward northeast along with the Euro-Asian crustal plate whereas the Arabian Plate is

drifting toward north at a higher speed. Thus, the Eurasian minor plate is drifted toward west by the crustal crash of these two plates, and the Cyprus plate is moving together with it. Until now, the collective tectonic activities are well pronounced in the Cyprus and the region of the Eastern Mediterranean. From the past records and observations, it has been established that the destructive earthquakes took place along both the southern and eastern oceanic plates of Cyprus, more often at shallow depths. For this reason, it is necessary to study different factors that initiate the ground movements, including the behaviour of soil deposits and their corresponding cyclic mobility on the island.

Cyprus consists of four principal geological terrains: the Kyrenia Range to the north, the Mesaoria plain to the east, the Troodos range and the Circum-Troodos plain to the south as represented in Figure 2.2. The area where the information was obtained in this study is the east of Mesaoria plain, a plain land of Holocene-Miocene alluvial soil deposits.

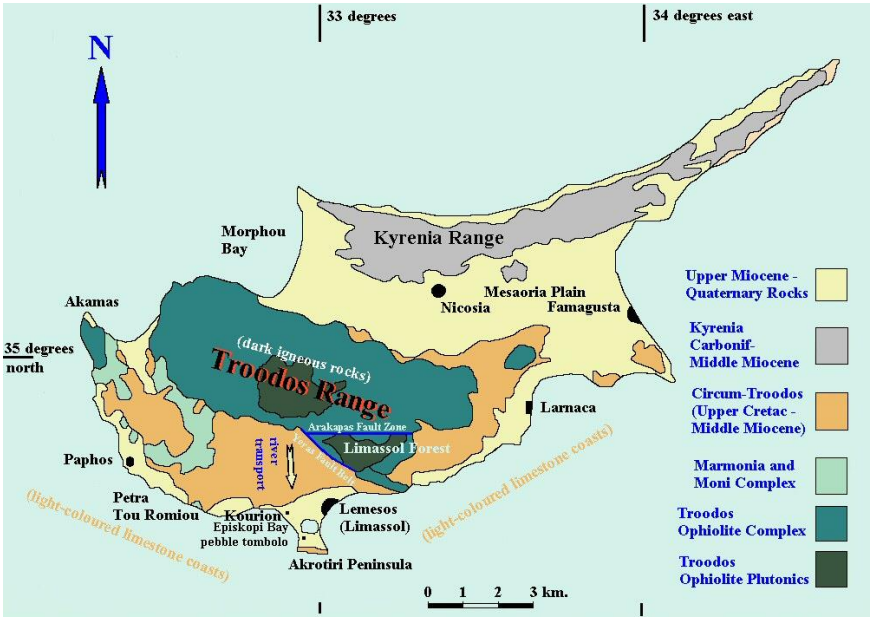

Figure 2.2: Geological Map of Cyprus, displaying the main Geological Terrains (Greensmith 1994; West and Bentley 2007).

In figure 2.3 (USGS, 2003), the continental faults of Cyprus is represented which its geological dating is not clear. Nevertheless, it is ascertained that a potentially active fault with temporal Holocene motion and peculiar Pliocene setting occupy the southern boundary of the Mesaoria plain basin, which is believed to initiate recurring mobility of soil deposits in the area under investigation. In the last three centuries, the records of powerful historical earthquakes are used as the main factor in evaluating the predictive ground motions that might happen in the next 50 years, which is the life cycle of new structures founded in soil deposits prone to the earthquakes. Therefore, to establish the geological records of these fault lines are critical. The US Geological Survey (USGS) considers the two faults Mia Milea and Main Ovgos near Nicosia of the modern age while considering the two other faults (South Mesaoria and Pergamos) as active.

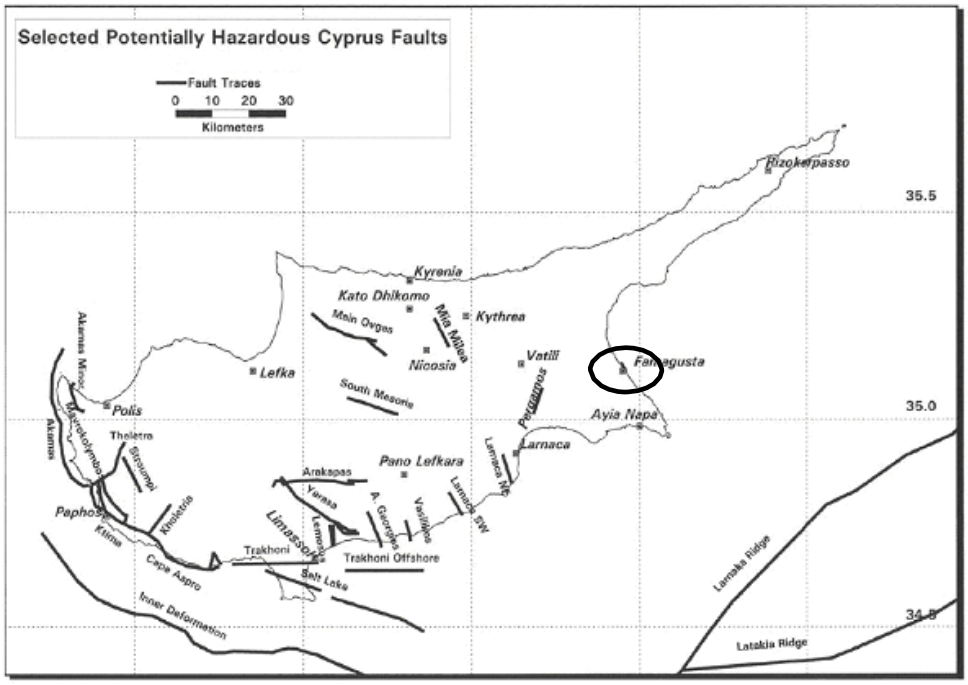

Figure 2.3: Mapped and Inferred Faults during Quaternary age in Cyprus **(**Algermissen and Rogers, 2004).

2.3 Regional Seismicity

A full description of historical earthquake records in Cyprus is offered in figure 2.4. Although the Island has not experienced many active earthquakes when compared to the neighbouring regions such as Israel, Greece, Syria, Turkey, and Lebanon, many destructive earthquakes have hit the area in the past. Despite the fact that seismicity have mostly occurred in the south of the Mesaoria plain, a number of disastrous earthquakes have been reported beneath Mesaoria. For this reason, Tuzla was chosen as the study area as it is located in the southeastern part of the Mesaoria plain following the literature review of the study and the report written by Algermissen and Rogers (2004).

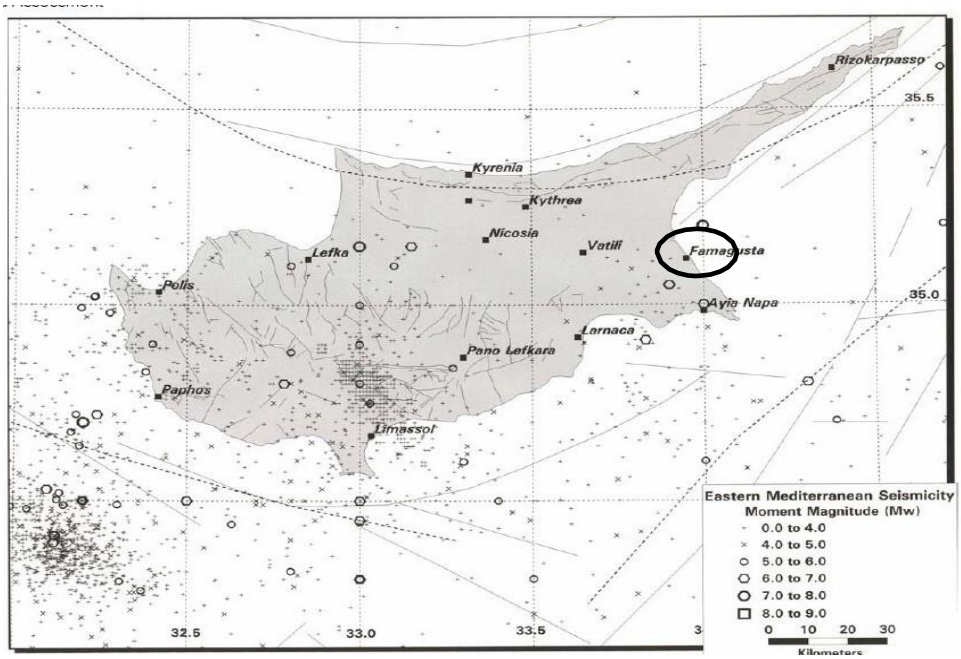

Figure 2.4: A Seismic Map of all Earthquakes in the Historical Record in the surrounding areas of Cyprus (Algermissen and Rogers, 2004).

2.4 Seismic Hazard Analysis

The peak ground acceleration, (PGA) values for Cyprus can be incorporated in analyzing ground motion if it is properly designed based on the standard codes. The

probabilistic hazard contour map was developed by two researchers, Cagnan & Tanircan (2010) on a hard rock location, to analyze and evaluate PGA values for Cyprus. From the contour map, the PGA range falls within 0.2g-0.4g. For Famagusta town considered in this micro-zonation study, it is taken approximately as 0.3g.

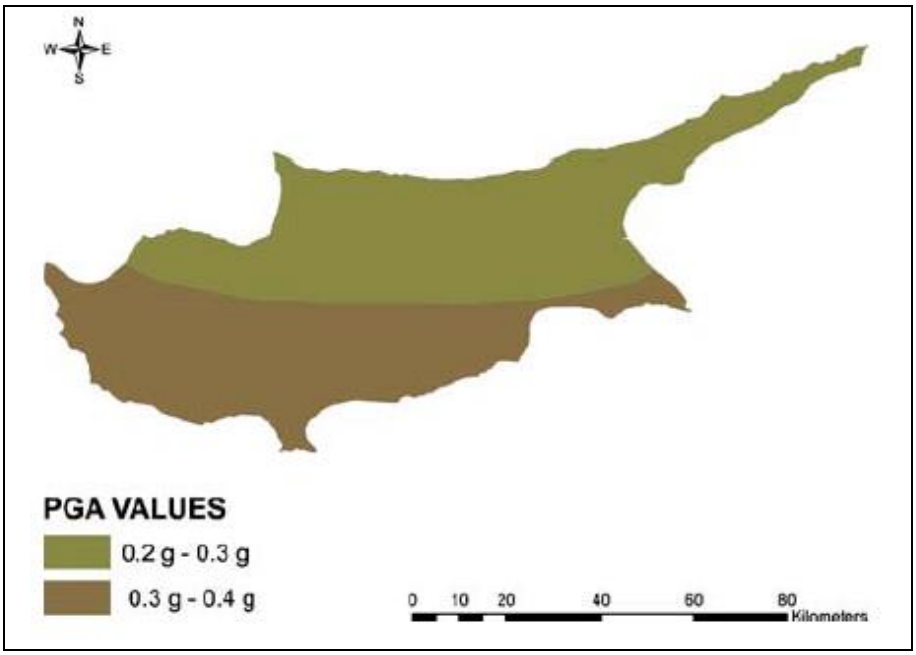

Figure 2.5: Distribution of PGA for Rock Situation in Cyprus during 50 Years with 10 Percent Probability of Exceedance (Cagnan & Tanircan, 2010).

Chapter 3

LITERATURE REVIEW

3.1 Soil Liquefaction Definition

Soil liquefaction is a occurrence attributed to moderate to large earthquake shaking or another sudden loading. Liquefaction causes loss of strength and stiffness of cohesionless, saturated soil deposits. The loss of strength is due to a rapid increase in pore water pressures and a sudden decrease in effective stress during a significant ground shaking. Liquefaction often causes great damages to bridges, buildings, dams, earth dams, highways, railways, natural habitats and other civil engineering structures.

A number of researchers have offered a definition of soil liquefaction. Marcuson (1978) defined it as “the alteration of particulate material from behaving as solid, then to flowing as liquid as a result of a sudden increase in pore-water pressure and a rapid reduction in effective stress”.

Liquefaction is seen as an earth-natural occurrence in which a deposit of soil body loses a large proportion of its shear resistance when cyclic, monotonic, or shock loading is exerted on it. It also has the capability to make the soil mass behave in the form likeable to a flowing fluid. The process continues until the shear stresses acting on the body reaches lesser than the shear resistance of the individual soil particles of the soil mass (Sladen et al. 1985).

Some researchers have tried to eliminate the ambiguous nature of the term "liquefaction" by providing the term "classic" (Seed et al., 2003). That is, "classic" cyclic liquefaction refers to a remarkable loss of stiffness and strength because of the cyclic pore pressure generation. Meanwhile, the "sensitivity" or loss of stiffness and strength is a result of monotonic shearing and remoulding due to more significant, monotonic (mono-directional) shear displacement.

Further, soil liquefaction is defined as a change from a solid to fluid state as an outcome of augmented pore pressures and decreased effective stresses.

For some time, soil liquefaction has been an issue of concern among various researchers. In this regard, two researchers, Terzaghi and Peck (1996) came up with the term "spontaneous liquefaction" to refer to the speedy strength loss of very loose sand deposits causing flow slides due to minimal disturbance. Moreover, Mogami and Kubo (1953) defined the term "liquefaction" as a phenomenon recognised during earthquakes. However, Niigata earthquake in 1964 in japan was the first earthquake in the world that attracted the researchers' attention soil liquefaction. Since then, researchers have commenced many research studies on liquefaction to define and understand it. The improvement of the study of this subject has been presented comprehensively in literature reviews, such as those by Holzer (2011), Seed (1981), Shihara (1993), and Robertson (1995). The huge earthquakes in 1964 and 1995 in Niigata and Kobe have shown the significance and generation of the enormity of destruction caused by soil liquefaction (Robertson and Wride, 1998).

However, "cyclic mobility" has been introduced as the main culprit in soil liquefaction phenomenon causing ground failures and ground deformations without

fluid-like flow. Castro and Poulos (1977) maintained that two phenomena cyclic mobility and liquefaction should be carefully differentiated as liquefaction refers to increasing pore pressures during undrained cyclic shear of saturated soils causing failures.

Further, Robertson and Wride (1998) offered a thorough classification of "soil liquefaction" by differentiating cyclic softening from flow liquefaction (strain-softening behavior). The further category of cyclic softening is the cyclic liquefaction and cyclic mobility.

Kramer (1996) summarized definitions of these concepts as follows:

1) Cyclic liquefaction: When extensive shear stress reversal occurs, the effective stresses approach zero, and, thus, triggers cyclic liquefaction. At the attainment of the condition of practically zero effective stress, significant deformations can occur. If cyclic loading persists, it increases distortions to a large extent.

2) Cyclic Mobility: If shear stress reversal does not occur, in general, it is impossible to attain the zero effective stress condition, and deformations will be smaller and as a result cyclic mobility will happen. Niigata in 1964 and Kobe in 1995 earthquakes are some examples of events where cyclic softening occurred in the form of sand boils. The occurrence caused huge damage such as lateral spreading, embankment slumpings, settlements, and cracks.

3) Cyclic softening: Cyclic softening can happen as a result of undrained cyclic loading such as rapid loading, for instance, earthquake loading. It should be mentioned here that soil density determines the magnitude and dimension of

deformations during cyclic loading, the intensity and duration of cyclic loading and the extent of shear stress reversal. That is, saturated sandy soils can cause cyclic softening if the cyclic loading is high enough in magnitude and duration.

4) Flow liquefaction: It occurs when the soil undergoes strain softening and is subject to collapse. Also, it also happens when the ultimate or the minimum soil mass strength reaches lesser than the gravitational shear stresses acting on it. The triggered mechanism can be either cyclic or monotonous. Flow liquefaction may occur in any moderate to high stable saturated soil, like a very weak fine cohesionless deposits, loess silt deposits, and very sensitive clays.

Cyclic softening is a commonly observed phenomenon in soil liquefaction experienced after earthquake loading. In the literature review, a number of studies investigating soil liquefaction concentrate on cyclic softening or cyclic liquefaction.

Based on the types of soils studied, researchers have offered a different definition of "liquefaction". A number of terms used in various studies will be reviewed here. In order to analyze and describe fine-grained soils Bray et al. (2004) used two terms "liquefaction" and "cyclic mobility". However, Durgunoglu and Bilsel (2007) used "cyclic failure" to describe liquefaction in the fine- grained soils.

Moreover, Boulanger and Idriss (2006) suggested that the "liquefaction" can be used to portray the emergence of increasing strains or strength loss in fine-grained soils manifesting sand-like behavior, since the term "cyclic softening failure" is employed to show much the same happening in fine-grained soils display clay-like behavior.

Furthermore, Moss et al. (2003) used the term “cyclic softening” to describe the failure mechanism for fine-grained soils. In this regard, some researchers have maintained that the soils susceptible to cyclic softening can have a more percentage of fines. These fine particles are susceptible to failure in a piece of plastic behavior. Further, such soils may show surface evidence exactly much the same to “classic” liquefaction examples, like building tilting, settlement, lateral spreading, and punching. However, the failure mechanism is entirely dissimilar to liquefaction phenomenon.

3.2 Failures Resulting from Soil Liquefaction

Liquefaction causes huge failures, loss of huge finances and human casualties and injuries. Liquefaction in soil also causes ground failures as well as engineering structure failures. Failures in a soil mass occur in the form of flow failures, ground oscillation, ground settlements, lateral spreads and sand boil. The failures in civil engineering structures are comprised of bearing capacity failures of foundations, the displacement of retaining walls, the floating of buried structures, and other construction failures.

3.2.1 Sand Boil

Extra pore water pressures triggered by soil liquefaction on the ground usually lead to an upward outflow. Then water and soil particles admixtures come forcefully to the surface of the ground either during and or after an earthquake shaking. In Figure 3.1, a case of sand boil from Nisqually earthquake in 2001 is shown. The observation of a sand boil is indicative of liquefaction when an earthquake happens in a place.

Figure 3.1: The Observation of Sand Boils after Nisqually Earthquake in Olympia, 2001.

3.2.2 Ground Oscillation

Due to the initiation of liquefaction at a particular depth with permits lateral displacement, the non-liquefiable soil blocks may eventually separate from one another and then vibrate in an upward and downward oscillation on the site of liquefaction. The subsequent ground shaking may be followed by the opening and closing such as fissures, cracks, voids, pores, and crevices. These pose a potential threat of damaging structures and underground utilities.

3.2.3 Ground Settlements

During earthquake loading, the underground water sprouts out to the ground surface making liquefied layers denser and consolidated in a short period of time. Further the resulting increased soil pore pressure and softening reduces the bearing capacity and ultimately such an increase from liquefaction can lead to potential ground settlements of loose granular soil layers. As a result, settlements may occur in both the levelling and sloping ground while the most deformation failures only occur on the levelling ground.

3.2.4 Lateral Spreads

Lateral spread is one of the most commonly observed phenomenon in ground failures triggered by liquefaction during earthquake shaking. In this case, the effective stresses tend to zero as the ground becomes liquefied and soil deposits begin to flow like a liquid. This causes the ground surface to be displaced horizontally towards the foot of a slope. Moreover, such movement of ground and foundation causes huge damage to bridges.

Figure 3.2: The Observation of Lateral Spread Failure after Nisqually Earthquake in Olympia, Capitol Interpretive Center (2001).

3.2.5 Flow Failures

The liquefiable soil on the ground slope can generate a flow failure. This failure occurs when the collapsed earth gravitates to a remote site. The flow can move a long distance at rather high speeds (Youd, 1978). In cases where in-situ static driving shear stresses in soil become larger than the reduced shear strength of the ground flow failures occur because when liquefaction occurs soil strength reduces significantly during soil strain softening (Zhang, 2001).

3.3 Soils Susceptible to Liquefaction

Some soils such as sandy soils are more likely to be liquefied during huge earthquakes. A large number of studies have investigated sandy soils but few studies have explored the liquefaction susceptibility of fine-grained soils.

A comprehensive study was conducted by Perlea (2000) on a number of strong earthquakes between the years of 1944 to 1989 through field observations of liquefaction. The researcher described the side effects of the magnitude of the earthquakes and epicentral distance of all soil types such as loose sands, cohesive (fine-grained) soils, sensitive clays and collapsible loess. In the literature review, the past results indicate that any soil, for instance, cohesive and sensitive in nature is susceptible to liquefaction considering the earthquake magnitude. For instance, if we ignore the collapsible loess (i.e. nonplastic silts) in fine-grained soils, they are more resistant to liquefaction than sands because fine-grained soils have been proved resistent to liquefaction to earthquakes with local Richter scale magnitude of less than 7.2, (Chang, 1987).

Soil liquefaction has been reported to have occurred during two strong earthquakes in 1999 in some cities in Turkey (Adapazari, Kocaeli) and Taiwan (Wu Feng, Yuan Lin and Nantou Chi-Chi). The soil liquefaction caused huge damages such as settlements and bearing failures of shallow-founded structures. It should be mentioned here that most of these damages occurred in cohesive soils. In this regard, Seed et al. (2003) found that cohesive soils (clays and plastic silts) are highly "sensitive" clay soil. Moreover, it should also be stated here that in cases where soils were remoulded or sheared, soils were reported to have lost significant strength.

Further, the recommendation is that the Modified Chinese Criteria is not a reliable means of study. It is because the overall contribution of the fines to plasticity is more important than "percent clay fines".

Bray et al. (2004) proposed a new empirical method to evaluate liquefaction susceptibility of fine-grained soils which is explained in great details in chapter 3. In the study which took place in Tuzla area in North Cyprus, the researchers carried out cyclic triaxial tests on the undisturbed samples of silty and clayey soils. The findings obtained from the cyclic tests indicated that the Chinese Criteria could not predict the liquefaction susceptibility of fine-grained soils. The observation of the liquefied Soils in Tuzla during past earthquakes basically was not compatible with the clay-size criterion of the Chinese Criteria. The results of the study indicated that the condition considered according to the amount of particles is not a suitable index of the soil's response and hence liquefaction susceptibility. Therefore, the index cannot be used in later studies and the best indicator is deemed to be the percentage of active clay minerals existing in the soils.

In another study which took place on a typical soft, sensitive clay in the north of Istanbul, Turkey, Durgunoglu et al. (2004) utilised cyclic triaxial tests on undisturbed samples. The study results revealed that even clays high plasticity (CH type) generated enormous strains in some cycles when a high cyclic stress ratio (CSR) was used which was not compatible with Chinese Criteria, CC. As a result, it was concluded that CC does not consider the magnitude of an earthquake which leads to anaomalies in its assessment and prediction.

Recently, Boulanger and Idriss (2006) used new liquefaction susceptibility evaluation criteria for saturated clays and silts according to the mechanics involved in their stress-strain behaviour. The study presented an upgraded approach for choosing engineering standard procedures to determine capacity strains and loss of strength during earthquake loading. The performance of the cyclic and monotonic undrained loading tests and their test results for clays and silts indicated a switch over a small number of plasticity indices (PI), from soils, which behaved more basically like sands (granular-like behaviour) to soils behaving more basically like clays (fine-like behaviour). In cases where fine-grained soils have PI $\geq$ 7, they are considered as clay.

The study results also suggested that fine-grained soils and the cyclic and monotonic undrained shear strengths are closely related showing apparently distinctive stress-strain normalised behaviours. Cyclic strengths then is estimated based on empirical correlations, in-situ testing programs and laboratory testing that are same to well-known methods of measuring the monotonic undrained shear strengths of such deposits. Further, Boulanger and Idriss (2006) also found out the unsuitability of Chinese criteria and suggested it to be eliminated.

Moreover, Seed et al. (2003) discussed the effect of fine particles on liquefaction potential as follows. Soils with abundant “fines” with particles smaller than 0.075 mm, or passing a #200 sieve to separate the coarser (> 0.075 mm) particulate matter, that is, the features of fines determine the potential of cyclically-induced liquefaction. When fines content are more than 15% to 35%, coarser particles can be easily separated which depends on soil gradation and the characteristics of fines. The well-graded soils have minor void ratios than uniformly-graded or gap-graded soils.

As a result, well-graded soils can be easily filled with little fines content which can also easily separate the large particles in a matrix of fines. It should be mentioned here that clay fines have higher void ratios than silt particles.

More recently, Boulanger and Idriss (2007) offered a new procedure to evaluate the potential for cyclic softening in saturated clays and silts during earthquakes. The suggested methods are suitable for clay-like fine-grained soils. The procedures offered by the researchers are similar to semi-empirical liquefaction methods.

Apparently, if the earthquake-induced strains are large enough, the consolidated or lightly consolidated sensitive clays and silts can experience a loss in both normal and cyclic strengths. However, generally clays and silts have higher cyclic strength and lower sensitivities with higher OCR, which cannot be influenced by even very massive shaking.

3.4 Evaluation of Liquefaction Potential by In-situ Soundings

In order to assess the liquefaction potential of saturated soils, cyclic laboratory tests need to be administered on high-quality undisturbed samples. However, sampling may pose dramatic challenges for the researchers as it is a costly process. Therefore, the easiest and most practical approach is to assess the cyclic resistance of soils through in-situ tests, such as standard penetration test (SPT) and cone penetration test (CPT).

3.4.1 Standard Penetration Test (SPT)

Standard Penetration Test (SPT) procedures were primarily developed to assess liquefaction in Niigata Earthquake (Kishida 1966) in Japan. The procedures used in

the study have been used in later studies especially in individual case studies (Boulanger and Idriss, 2004).

Further, Seed and Idriss (1970) proposed a procedure for estimating the liquefaction-inducing cyclic stress ratio (CSR) as a function of the N-value in the SPT by in situ performance record of sand deposits during the recent earthquake. The charts describe the liquefaction based on observations of liquefaction during past earthquakes. Seed et al. (1984, 1985) suggested the simplified method based on the relationship of SPT N-values, adjusted for effective overburden stress and energy.

Figure 3.3 is a graph for calculating cyclic stress ratio and corresponding data from sites that define the observation and non-observation of liquefaction effects of the past earthquakes with magnitudes of approximately 7.5. In Figure 3.3, the cyclic resistance ratio curves were intentionally positioned to divide regions with data showing liquefaction from areas with data showing non-liquefaction. The CRR curves in Figures 3.3 and 3.4 are valid only for earthquakes with magnitude of 7.5. The consideration of the earthquake magnitude scaling factor (MSF) of the earthquake is applicable when it is more than 7.5.

Shibata (1981) and Tokimatsu and Yoshimi (1983) have established similar correlations due to field performance based on the existing record of data gathered mostly from Japanese sites (Ishihara, 1996).

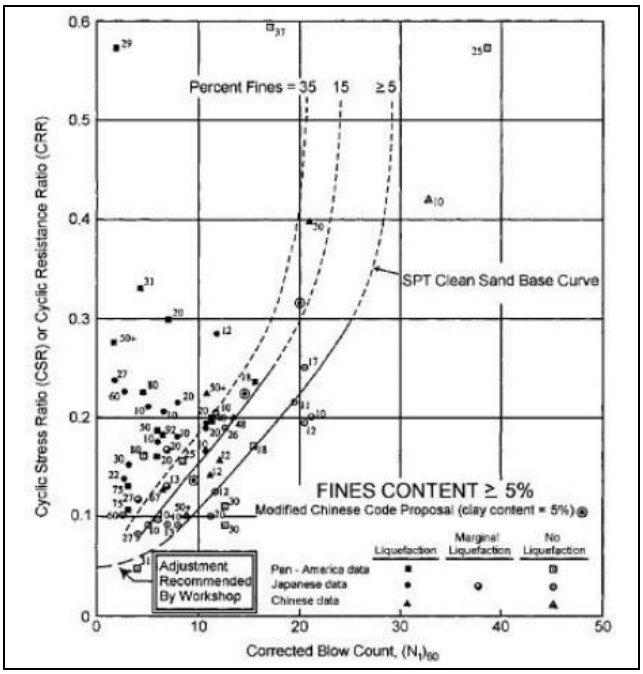

Figure 3.3: SPT Clean-Sand Curves for 7.5 Magnitude Earthquakes (Youd et al. 2001).

Cetin et al. (2000) re-analyzed and statistically expanded the SPT case history recorded data. Further, Seed et al. (1983) examined the database set of different 125 cases of active liquefaction and non-active liquefaction events in 19 earthquakes shaking. , In such situations, there were 65 cases for coarse sands with fine composition had FC ≤ 5%, 46 cases, and 14 cases had 6% ≤ FC ≤ 34% and FC ≥ 35% respectively of similar composition. Cetin et al. (2000) also examined around 67 cases of liquefaction/non-liquefaction in 12 earthquakes, of which 23 cases relevant to sands with FC ≤ 5%, 32 cases had fine content between 6% ≤ FC ≤ 34%, and 12 cases had more than 35% of fine content. He used their expanded database and site response analysis for determining CSR to establish revised deterministic and liquefaction probabilistic correlations.

Boulanger and Idriss (2004) presents an update on the semi- experimental in situ-based methods for examining the liquefaction potential of non-cohesive soils during

earthquake shaking. The provision of the re-examination of the SPT-based methodology included numerous modifications and parameter readjustments. The recommendation of CSR and (N1)60 values was re-analyzed using the revised CN, Kσ, MSF and $r_{d,}$ relationships and correlations.

3.4.2 Cone Penetration Test (CPT)

The cone penetration test (CPT) is predictable in situ index test with the broad application as a tool for examining the liquefaction potential and resistance of susceptible liquefiable soils. A number of researchers have investigated CPT-based liquefaction triggering potential and resistance (Idriss & Boulanger, 2004, Ishihara, 1985, Juang et al. 2003, Moss et al. 2006; Olsen 1984; Robertson & Wride, 1998, Seed et al. 1983, Stark & Olson, 1995, Suzuki 1995, Toprak et al. 1999).

Additionally, Gilstrap and Youd (1998) conducted a study by correlating liquefaction potential calculation and resistances against in situ efficacy at 19 sites. The study results showed that the CPT-criteria could properly assess the occurrence and non-occurrence of liquefaction with 85% reliability (Youd et al. 2001).

Because of the in situ challenges and deficient repeatability attributed to the SPT, numerous correlations have been postulated to determine the cyclic resistance ratio; CRR is using cone penetration resistance, CPT. Robertson and Wride (1998) have presented modern techniques to analyse liquefaction utilising the cone penetration test (CPT). The comprehensive procedure is explained in chapter 4. The suggested criteria for CPT can determine CRR using CPT penetration resistance. Robertson and Wride in 1998, prepared curve and figure 3.4 presented it for direct estimation of (CRR) for pure sands (FC ≤ 5 %) from CPT data. The chart presents the estimation of the cyclic resistance ratio (CRR) plotted as a function of corrected, dimensionless,

and normalized CPT tip resistance q_{c1N} from the field of either liquefaction or non-liquefaction. The CRR curve conservatively divides portions of the plot with recorded data showing liquefaction from regions indicating non-liquefaction.

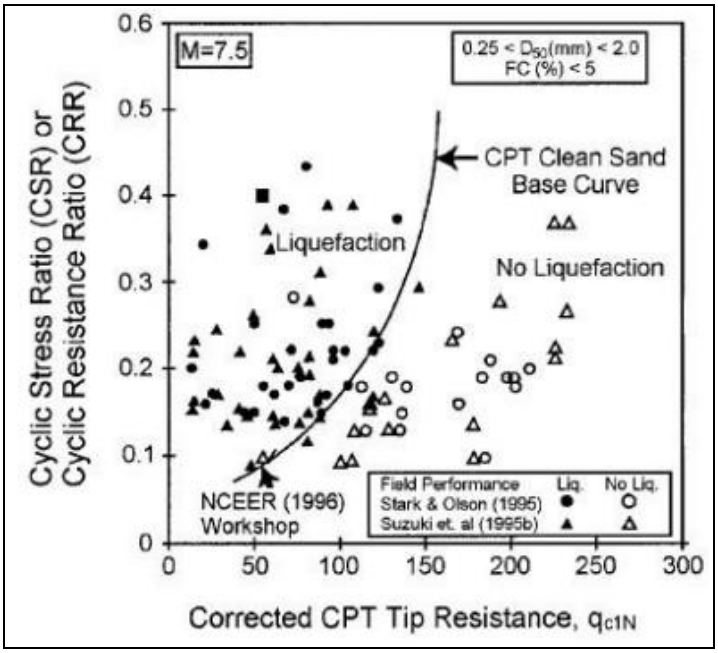

Figure 3.4: Calculation of CRR from CPT data along with Empirical Liquefaction data (Youd et al. 2001)

3.5 Site Response Analysis

To analyze seismic hazard, the future ground motions of earthquake need to be well estimated which is usually obtained through Ground Motion Prediction Equations. These equations offer a prediction of ground motion parameters such as the median and the standard deviation. In this regard, epsilon (ϵ) is used to refer to the differences between observed and predicted ground motions which are normalized by the standard deviation. For spectral accelerations, to guide ground motion selection, one needs to have access to the correlation structure of normalized residuals during oscillator timelines. The correlation structures have been

investigated in a large number of studies for large global datasets reflecting averaged effects in an entire dataset during the analyses.

Seismic hazard analyses and its related analyses of structural responses benefit a lot from the normalized residual values. To analyze nonlinear structures, one needs to have access to time history analyses. The input time histories are usually related to a certain spectral acceleration value in a fixed time, although, the ground motion needs to be well-matched with fixed target response spectra. Such matching is referred to as ground motion selection. Baker (2011) introduced Conditional Mean Spectra (CMS) method which offers the target response spectrum.

The ground motion data set was selected from the Next Generation Attenuation (NGA) database (PEER, 2005) which was collected from active shallow crustal earthquakes at rock stations. Care was taken to select unbiased dataset from NGA project. The resonance frequency of a soft soil site was estimated to be 1 Hz while it was predicted to be about 5 Hz for stiff soil site.

This literature review intends to review the most relevant and the up-to-date works on the topic of this thesis. In this thesis, effort was made to examine the effects of site response on the correlation structure of ground motion residuals. To have a better understanding of the relevant and related literature review, Attenuation relationships or ground motion prediction equations (GMPE) and the site response analysis will be discussed in length in this regard.

A large number of studies have been conducted on the effect of local site conditions on the nature of the ground motions and their consequent damage. The early studies in

this regard only considered the linear soil behavior and never took the soil non-linearity into account (Wu & Finn, 1997). However, for the first time, Seed and Idriss (1969) came to realize the effect of non-linearity by observing the earthquakes which occurred in Niigata and Alaska in 1964 and in Caracas in 1967, (Rodriguez-Marek, 2000).

The analyses of small amplitude recorded data and larger amplitude site response constitute the site amplification provisions in design codes. Previously, average spectral shapes for different soil conditions were used for code provisions which were based on Seed et al.'s (1976) statistical study of 21 earthquakes. Figure 3.5 displays the spectral shapes which are usually dependent on the site conditions obtained over a longer time periods. The idea of long period spectral shapes was used by the Applied Technology Council (1978) to come up with simplified response spectra shapes which later were modified by the Uniform Building Code of 1988 (Rodriguez-Marek, 2000).

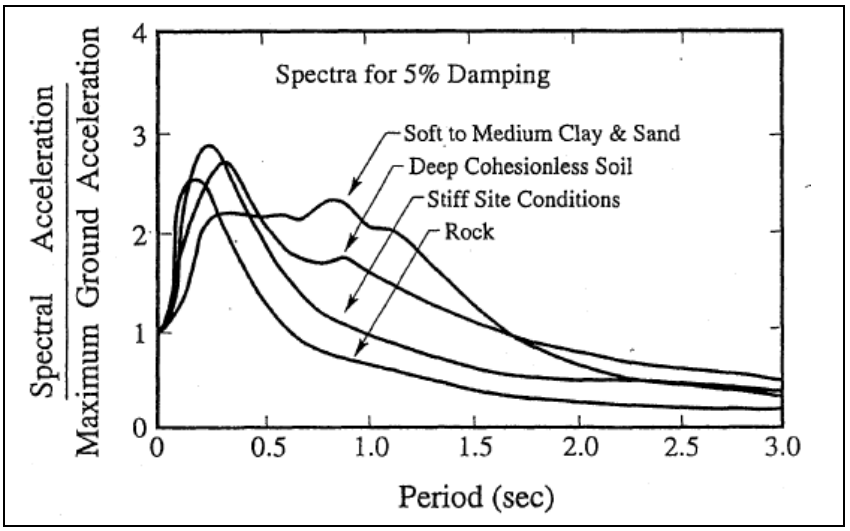

Figure 3.5: Average Spectral Shapes for Different Site Conditions, (Seed, 1976).

Ground response analysis is an indicator used to predict the effect of the earth conditions on the estimated response to the bedrock. It can also be used to estimate the design response spectra as well as the structural design. Kramer (1996) used the ground response analyses to predict dynamic stresses and strains for evaluation of liquefaction as well as the earthquake- induced forces causing damage to the earth and structures maintain the earth structures.

Various site response analysis methods have been proposed to investigate the effect of the site over the motion occurring at bedrock. These methods are classified according to the dimensionality of the problem, that is, in one-dimensional analysis, soil and rock surface are considered to be horizontal and the wave spread is seen vertically as horizontal shear waves go down through the rock. A popular method in this regard can be the linear approach which views soils as a linear elastic material.

The main elements in ground response analysis are the ground response transfer functions, referred to as amplification factor, which are used to calculate different response parameters such as ground surface acceleration from input motion parameters such as bedrock acceleration. In one-dimensional response analysis, the Fourier transform of the input time history is multiplied by the transfer function to obtain the Fourier transform of the ground surface motion. Finally, to the inverse Fourier transforms are used to the response parameter time history in the soil layers. Kramer, (1996) used transfer functions to investigate the bedrock frequency on amplification through soil deposit. The transfer function which is also referred to as Amplification Factor (AF) is the ratio of ground motion at the soil surface to the ground motion over the bedrock. These factors can be obtained for any ground

motion parameters; however, the most popular parameter to be used is the response spectral acceleration.

Bazzurro and Cornell (2004) conducted a study on the role of soil in the better identification of the AF parameters for a generic frequency in a saturated sandy site and a saturated soft clay site. The researchers studied Magnitude (*M*) and source-to-site distance (*R*) of input bedrock accelerogram together with a number of other parameters such as peak ground acceleration (PGA), the spectral acceleration values and the spectral acceleration at a generic frequency. The study findings revealed that the spectral acceleration could very well predict AF. Saturated soft clay and sandy sites are case studies that they considered.

Soil non-linearity methodologies have been around since 1960s. The idea of linearity behavior is no longer accepted in most of the engineering applications because of unrealistic approaches and assumptions in that regard. On the other hand, the nonlinear approach is not an ideal model for prediction of the real hysteretic stress-strain behavior of cyclically loaded soil. As a result, the only solution is the equivalent linear method modifying the linear approach (Kramer, 1996).

The equivalent linear model offers some parameters that are used to show the normal soil behavior that undergoes cyclic loading. The model has been designed based on a hysteresis loop (Figure 3.6) which has two main shape features; the preference of the loop contingent on the soil stiffness which can be measured through the secant stiffness (G_{sec}), and the breadth indicating the energy dissipation (W_D). Further, the Damping Ratio (ξ) is the energy dissipation measure which is shown below:

$$\xi = \frac{W_D}{4\pi W_S} = \frac{1}{2\pi} \times \frac{A_{loop}}{G_{sec}\gamma_c^2} \quad (1.1)$$

Where;

W_D = dissipated energy

W_S = maximum strain energy

γ_c = shear strain

A_{loop} = area of the hysteresis loop as is shown in Figure 3.6.

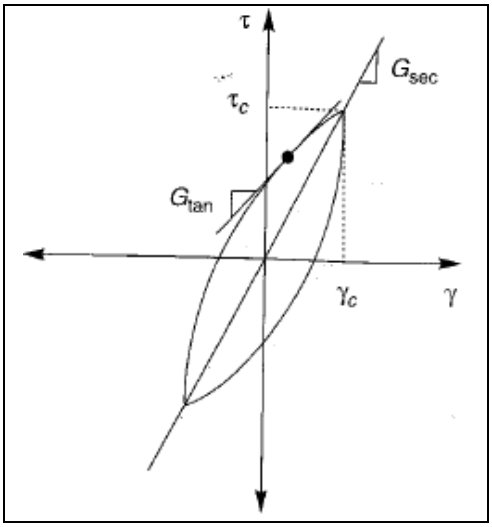

Figure 3.6: Relationship between G_{sec}, G_{tan}, ξ, and A_{loop}, (Kramer, 1996).

The two parameters, G_{sec} and ξ, are considered as linear material parameters varying from site to site or from soil layer to soil layer. Various laboratorial tests have shown that G_{sec}, hysteresis loop general inclination, represents cyclic shear strain amplitude. In the equivalent linear approach assumes G_{sec} and ξ constant for each soil layer for a certain strain level. First for each layer the shear strain is assessed and the new constant parameters should be computed for each layer in a way that the new parameters represent each layer's new shear strain appropriately, (Figure 3.7). In the equivalent linear method, the procedure is repeated to ensure the compatibility of the analysis parameters with the assessed strain level in all the layers (Kramer, 1996).

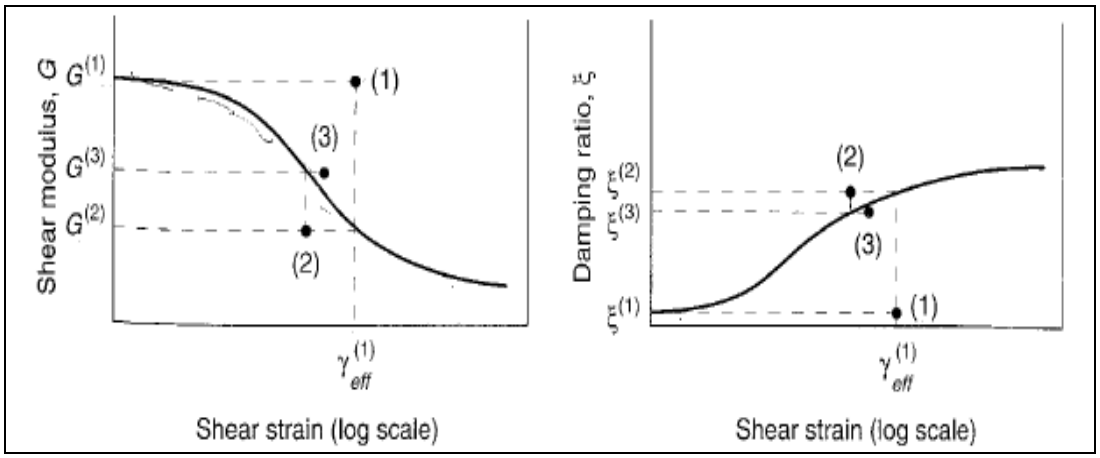

Figure 3.7: Equivalent linear approach process, (Kramer, 1996).

Bradley's (2011) study on the correlation between peak ground velocity (*PGV*) and spectrum intensity revealed that *PGV* had a strong correlation with spectrum intensity (SI) while had a moderate correlation with medium to long-period pseudo spectral acceleration (PSA), with short period spectral acceleration. During this study, Bradly considered 5 percent damping for spectral acceleration.

Chapter 4

METHODOLOGY

4.1 Introduction

The estimation of soil liquefaction potential is an important topic in geotechnical engineering practices (Youd et al. 2001). The cone penetration test (CPT) is widely accepted standard testing method for the determination of the field or in situ behavior and response to the liquefaction potential. Interestingly, the CPT technique has gained a sudden popularity due to the significant repeatability and reliability. Also, in the continuous nature of its stratigraphical profiling and sample availability when compared to other penetration tests.

In this study, the cone penetration in-situ test method was used to assess the liquefaction potential of soil deposits in the Tuzla region. Moreover, index and undrained shear strength (s_u) based approaches were also used. The potential liquefaction controls in this study draw mainly on Roberston and Wride (1998) procedure using CPT data. The procedures used also were updated during a workshop held by the National Center for Earthquake Engineering Research (NCEER), and Youd et al. (2001) published a summary report of them. The "simplified procedure" has been generated by field data based methods to assess the liquefaction resistance of soils over a -25-year period. Seed and Idriss (1971) published the procedures based on disastrous earthquakes occurred during 1964 in Alaska and Niigata in Japan (Youd et al. 2001).

4.2 Cone Penetration Test Method

The cone penetration test, CPT in geotechnical practice is one of the most accessible, standardised, fast and economical techniques used for geotechnical site exploration and subsurface exploration.

The application of CPT is suitable for the purpose of any subsurface research which includes the following:

- To evaluate the character and subsequence of the subsurface strata profiling.
- To quantify and determine the flow of groundwater conditions.
- To identify soil layers and assess their geotechnical parameters and design.
- To examine the mechanical and physical properties, of the subsurface layers.
- Finally the cone penetrometer, CP test is used to investigate the distribution and composition of contaminants in the geoenvironmental site investigation.

A CPT device comprises a cylindrical rod with a cone-shaped tip on the end. Also, have various sensors that record a continuous real-time estimation of soil properties such as the ground strength. The pushing of the CPT rods (sizes: 2 cm^2, 10 cm^2, 15 cm^2, 40 cm^2, etc. given in Figure 4.2) into the ground is continuous and at a constant speed of 2 cm/s. The CP rods are mounted on a heavy truck shown in Figure 4.3. There is resistance to penetration both at the cone and surface of the sleeve during the penetration. The data are measured and recorded at constant intervals (mostly 2 or 5cm) during the penetration. The CP is calibrated to record some different parameters such as the tip resistance, the sleeve friction and the pore pressure behind the tip. Tip resistance of cone probe is commonly used for the assessment of liquefaction potential and other related parameters.

The CPT finds application only in smooth soils, but with new large penetrating equipment and more strong cones, the CPT can be conducted on the soil profiling of stiff to very stiff soils (sand and clays). The main advantages of CPT are economical and productive, quick and continuous profiling, repeatable and trusty data (not operator or manager-related), immediate data availability and the strong theoretical basis for explanation and detailed subsurface exploration.

The corresponding disadvantages are: somewhat high capital procedures require skilled operators, no soil sample, during a CPT, penetration can be difficult in gravel/cemented layers. The cone resistance, q_c is defined as:

$$q_c = \frac{Q_c}{A_c} \tag{4.1}$$

Where:

Q_c = the total force acting on the cone,

$Ac =$ the projected area of the cone.

While the sleeve friction, f_s is defined as:

$$f_s = \frac{F_s}{As} \tag{4.2}$$

Where:

F_s = the frictional force acting on the friction sleeve.

$As =$ Surface area.

Pore pressure is measured as well in piezocones, generally behind the cone as shown in Figure 4.1.

Figure 4.1: Range of CPT Probes (from left: 2 cm^2, 10 cm^2, 15 cm^2, 40 cm^2)

Figure 4.2: The CPT Truck used in the General Study.

The Zemar Zemin Arastirma Company Ltd. Sti. from Ankara, conducted some cone penetration tests in the Tuzla region and obtained very good data on-site. The CPT has enhanced versions such as piezocone CPTu and seismic-SCPT. Since the inception of CPT application on the field, many extra recorders have been added to the cone. This includes the camera (visible light), dielectric, electrical resistivity/conductivity temperature, geophones (seismic wave velocity), laser and ultraviolet induced fluorescence, cover interface excavator pressuremeter, PH, oxygen exchange, radioisotope (gamma/neutron). These versions are used to determine other parameters which allowed the measurement of the of other needed

soil properties such as pore water pressures. The cone tip area and the friction sleeve area of the cone penetrometer are 10 cm^2, and 15 cm^2 are respectively. The most volume of the cone penetrometer during pushing and pulling processes are 20 tonnes and 30 tonnes respectively.

4.3 Assessments of Soil Liquefaction Potential using Software

In our study, the liquefaction potential was determined from three consecutive approaches using the geotechnical software. The following parameters were established: The factor of safety against liquefaction (FS), the liquefaction potential index (LPI) and the probability of liquefaction (PL).

The data obtained from 10 CPT excavation from the Eastern Coast of North Cyprus were evaluated and Several engineering properties have been obtained at different depths for each locations, (Erhan, 2009). These properties include the q_c, f_s, w, s_u etc. The three reliable geotechnical software used by other researchers (Bilsel et al., 2010) for similar studies were used to analyze data obtained from the field.

To estimate the soil liquefaction resistance of soils, the evaluation of two factor are needed. The cyclic stress ratio (CSR) is the follower of the peak amplitude acceleration, while the cyclic resistance ratio defines the capacity of soil to resist liquefaction. These parameters were determined by using the depth, q_c and f_s of the soil within the study site. The magnitude of the earthquake chosen is 6, 6.5 and 7 in order to study the expected liquefaction potential. Where the CSR surpasses the CRR, liquefaction is predictable to occur at locations. The properties were used to evaluate soil behaviour and their influence on liquefaction potential.

4.3.1 NovoCPT Software

The NovoCPT geotechnical software program is useful and practical for description of the data obtained from both the in situ or laboratory Cone Penetration Test, The data interface connected to the computer is easy to import to the CPT data files in the software program and perform the necessary engineering analysis. Such engineering analysis comprises of soil liquefaction, pile bearing capacity (LCPC method), pad footing bearing capacity and settlement analyses. The evaluation of the engineering data can be correlated to more than 35 soil parameters, (Afkhami, 2009). In this study, it was considered only about few soil variables and parameters. Robertson (2009) in Guide to Cone Penetration Testing suggested the evaluation method of liquefaction and the NovoCPT software is based on. All data are shown at each depth and plotted against depth on variety diagram. The columns of analysis of results are generated for more than 30 various parameters such as the following few examples as listed below:

S_v: Total overburden stress (σ_v)

S'_v: Effective overburden stress (σ'_v)

R_d: Stress reduction factor

D_r: Relative density of soil

γ_{max}: Maximum shear strain, calculated from D_r and liquefaction safety factor, at all depth,

ε_v: Volumetric strain (for settlement analysis), calculated from D_r and γ_{max}, at all depth

Kc: Fines content correction factor Q_{tn},

CSR: Cyclic stress ratio,

CRR: Cyclic resistance ratio,

Safety Factor against Liquefaction,

MSF: Magnitude scaling factor, etc.

The parameters used were depth, q_c, f_s at the earthquake magnitude of 6, 6.5 and 7 at different CPT locations. These soil parameters were then inputted into the software program to examine the CRR, CSR, Vs, unit weight, etc as shown in Figure 4.3.

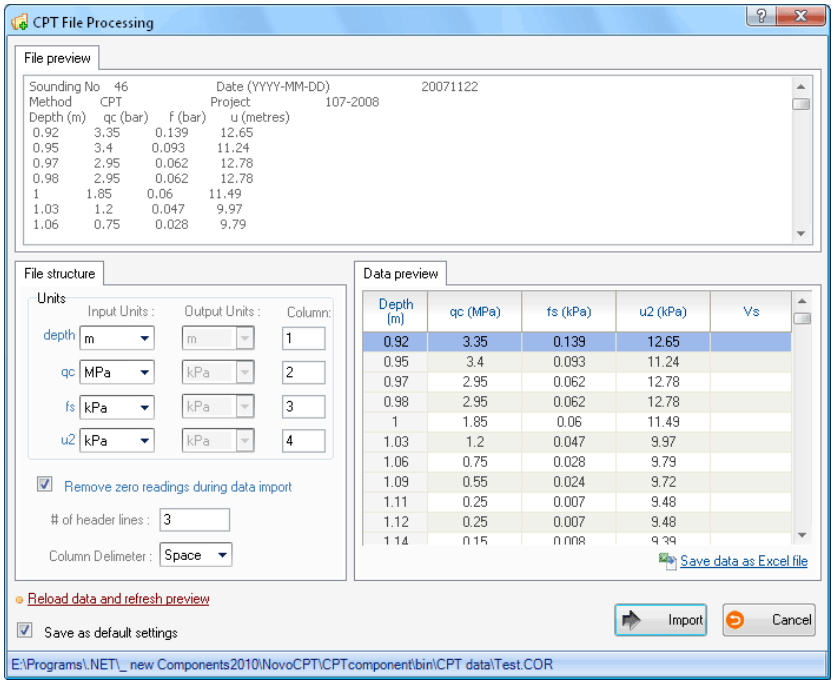

Figure 4.3: Input Data Page in NovoCPT Software

4.3.2 LiqIT Software

The LiqIT is a liquefaction analysis software program designed and developed to assess the liquefaction potential of loose saturated non-cohesive soils under the effect of ground motion. The parameters used were depth, q_c, f_s at the earthquake magnitude of 6.5 at different CPT locations. LiqIT is a software program for the evaluation of soil liquefaction based on commonly used field data. The input data parameters are listed as depth (m), q_c (MPa), f_s (MPa) and unit weight (kN/m^3) as shown in Figure 4.4. The calculation procedure includes, firstly, the evaluation of CRR (Cyclic Resistance Ratio), which is the soil strength, according to the available

field data (SPT, CPT or Vs). Secondly, the estimation of the induced seismic load expressed through cyclic stress ratio (CSR) and finally, the determination of the factor of safety against liquefaction.

Additionally, LiqIT can estimate:

1. The post-liquefaction induced settlements (both vertical and horizontal).

2. The overall liquefaction potential (Iwasaki liquefaction potential index LPI).

LiqIT implements the most recent and state-of-the-art calculation methods for both CSR and CRR. However, it should be considered that the results of these methods should be used according to the engineering judgment of the user and taking into consideration the uncertainties involved. In this study, the field data input from Cone Penetration Test (CPT) measurements was used to develop a deterministic-probabilistic liquefaction analysis method using the LiqIT software program. (GeoLogismiki, 2006).

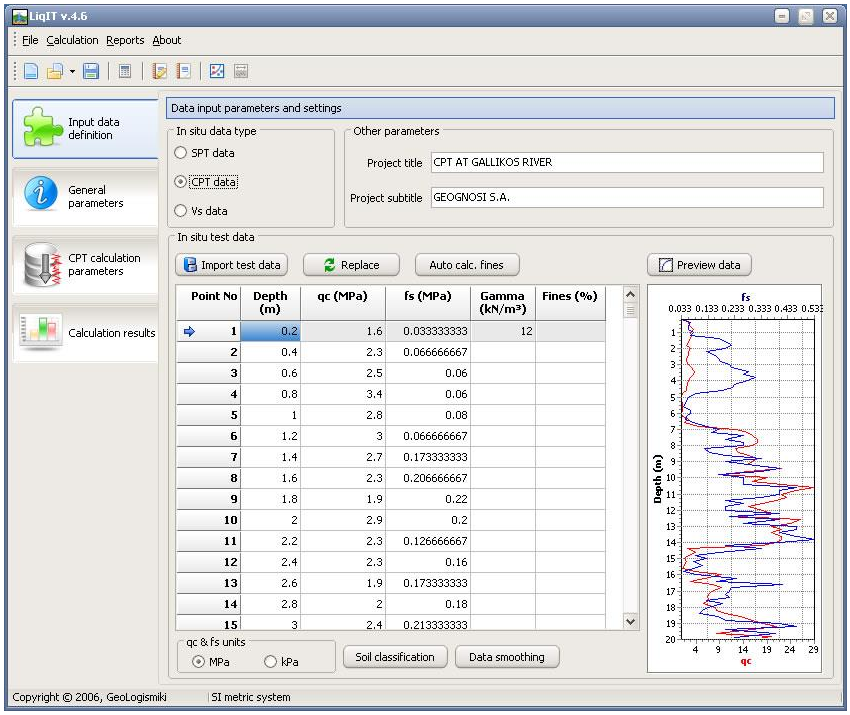

Figure 4.4: Input Data Page in LiqIT Software

4.3.3 DeepSoil Software

The DeepSoil software program is both applicable to unified equivalent linear and nonlinear site response assessment of engineering soil data analysis. The main features include the frequency-independent damping formulation, pore water pressure generation and dissipation models. Also, the graphical user interface, automated updating and parallel-processing capability are other components of the software program. In this study, this software program has been used to determine the layer thickness using the unit weight and shear wave parameters determined from the NovoCPT evaluation of the soil profiling long the depth and also different CPT locations, (Hashash, 2010). These parameters are used to start analysis with DeepSoil software as presented in Figure 4.5.

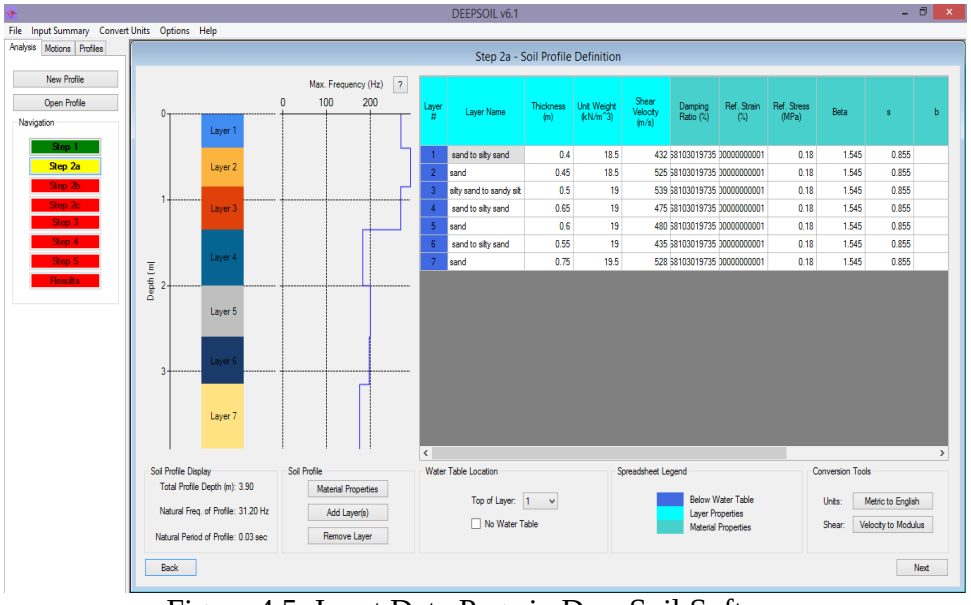

Figure 4.5: Input Data Page in DeepSoil Software

4.3.4 SeismoSignal Software

In this study, the Seismosignal software program was also used for the final evaluation of strong motion data. This software a user-friendly visual interface, easy

and efficient in its application. Displacement, velocity and acceleration are obtained by DeepSoil software, they are needed to start analysis by SeismoSignal software as presented in Figure 4.6. It can provide a significant number of outputs of strong-motion parameters often needed by earthquake engineers and engineer seismologists. In this study, the SeismoSignal software program was used to calculate the engineering parameters such as:

- Root-mean-square (RMS) of acceleration, velocity and displacement
- Sustained maximum acceleration (SMA) and velocity (SMV)

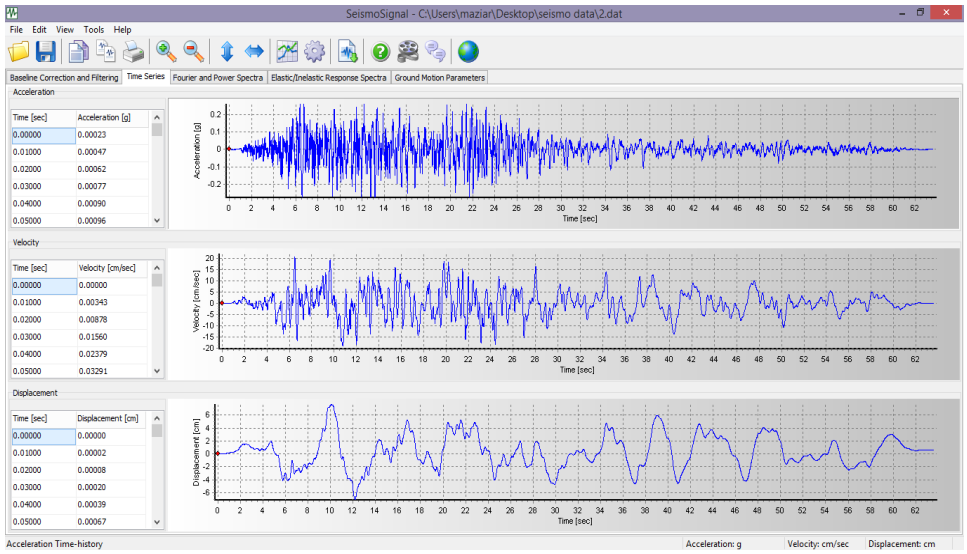

Figure 4.6: Input Data Page in SeismoSignal Software

4.4 Soil Liquefaction Assessment Procedures

The determination or valuation of the two most important variables is necessary for the calculation of liquefaction resistance of any susceptible soil deposits. The variables are the significant seismic values analyzed in soil strata. The liquefaction resistance is explained regarding the cyclic stress ratio, CSR and cyclic resistance ratio, CRR. The CSR represents the ability of the soil deposit to resist liquefaction or to generate or trigger liquefaction, while the CRR variable simply expresses the

liquefaction resistance ratio. Robertson and Wride (1998) first proposed the terminology of CRR during a workshop.

4.4.1 Evaluation of Factor of Safety for Liquefaction

The liquefaction potential can be determined by making a comparison between the earthquake loading (CSR) with the liquefaction resistance (CRR), this is typically expressed as;

$$FS = \frac{CRR}{CSR} \tag{4.3}$$

In previously used method, if FS ≤ 1, liquefaction is predicted to occur and supposed not to happen when FS > 1. The amounts of factor of safety were assessed for M = 6, 6.5, and 7 magnitudes of earthquake.

The safety factor against liquefaction is calculated based on some simple equations in the NovoCPT software.

$$FS = (\frac{CRR_{7.5}}{CSR}) \times MSF \times K_a \tag{4.4}$$

Where $CRR_{7.5}$the Cyclic Resistance Ratio for 7.5 earthquake magnitude, according the flowchart suggested by Robertson in 2004.

MSF is the magnitude scaling effect and,

K_α : Slope effect, approximately considered 1.0.

For LiqIT software tool the factor of safety against liquefaction is defined as ratio of CRR to CSR:

$$\text{Safety Factor} = (\frac{CRR}{CSR}) \times K_a \tag{4.6}$$

$$\text{CRR} = \text{CRR}_{7.5\ (ave)} \times MSF \tag{4.7}$$

4.4.2 Evaluation of Cyclic Stress Ratio

The cyclic stress ratio can be estimated for any given profile using the equation from the simplified procedure initially proposed by Seed and Idriss (1971) given as:

$$\text{CSR} = 0.65 \left(\frac{a_{max}}{g}\right) . \left(\frac{\sigma_{vo}}{\sigma' vo}\right) . (r_d) \quad (4.8)$$

where;

a_{max} = peak horizontal acceleration on the ground surface generated by the earthquake

g = acceleration of gravity

σ_{vo} = total vertical overburden stress (kN/m^2)

$\sigma' vo$ = effective vertical overburden stress (kN/m^2)

r_d = stress reduction coefficient

The equations provided in this section are all supported by both the NovoCPT and NovoLiq software tool programs. The initial simplified procedure for the estimation of the liquefaction potential proposed by Seed and Idriss (1971) was then later updated and modified by Youd et al. (2001). This new approach has become the latest methodology used worldwide for computation of liquefaction potential, and it is given as:

$$\text{CSR} = 0.65 \left(\frac{a_{max}}{g}\right) . \left(\frac{\sigma_{vo}}{\sigma' vo}\right) . S \quad (4.9)$$

Where S is defined as a 'soil parameter'.

Hence, as equation 4.8 and 4.9 are similar, therefore, $r_d = S$.

In the assessment of the stress reduction ratio, r_d according Youd et al. (2001), the relationship proposed by Liao and Whitman (1986) is a linear approximation equivalent of the average data from the simpfied procedure of Seed and Idris (1971).

The variable r_d can be calculated with the following equations provided by Liao and Whitman, 1986. Where, z is the depth beneath ground surface (NCEER, 1997 according to Seed and Idriss 1971).

$r_d = 1 - 0.00765z$ for $z \leq 9.15$ m (4.10)

$r_d = 1.174 - 0.0267z$ for $9.15 < z \leq 23$ m (4.11)

$r_d = 0744 - 0.008z$ for $23 < z \leq 30$ m (4.12)

$r_d = 0.05$ for $z > 30$ m (4.13)

Where;

z = depth underground surface in meters (m).

For the easier handling and understanding of the software, formulated equation changes to the following relation by Liao and Whitman (1986) and Youd et al. (2001).

$$r_d = \frac{1 - 0.4113.z^{0.5} + 0.04052.z + 0.001753.z^{1.5}}{1 - 0.4177.z^{0.5} + 0.05729.z^{1.5} + 0.00121.z^2} \quad (4.14)$$

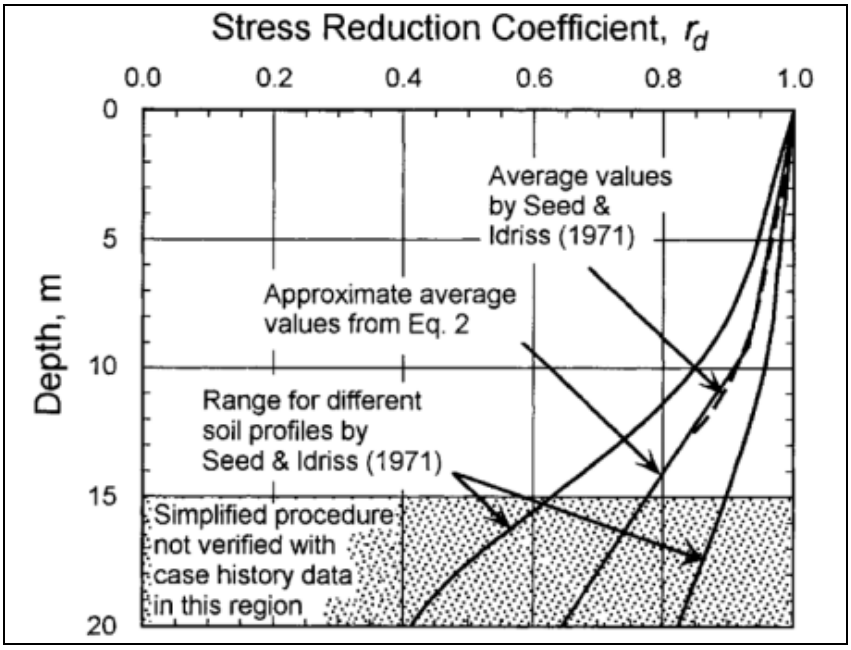

Figure 4.7: r_d Values - Depth Curves Established by Seed and Idriss (1971)

Therefore, the reduction factor to estimate the difference of cyclic shear stress with depth (z) underground level or gently sloping ground surface and represented by Figure 4.7 (Seed and Idriss 1971).

$$r_d = exp(\alpha(z) + \beta(z).M) \quad (4.15)$$

$$\alpha(z) = -1.012 - 1.126 \sin\left(\frac{z}{11.73} + 5.133\right) \quad (4.16)$$

$$\beta(z) = 0.0106 + 0.118 \sin\left(\frac{z}{11.28} + 5.142\right) \quad (4.17)$$

4.4.3 Evaluation of Liquefaction Resistance

The cyclic resistance of a layer is the cyclic stress needed to persuade liquefaction. The CRR be able to calculated through both laboratory and field tests. Field tests such as the standard penetration test (SPT) and the cone penetration test (CPT) and laboratory test are considered to be the unconsolidated-undrained tests (UU- test). Based on semi-empirical correlations from a database of field applications of in situ, which did not liquefy; using values of SPT $N_{1,\ 60cs}$ or CPT q_{c1Ncs} or V_{s1}. The charts are developed for the moment of magnitude 7.5, and all other magnitudes require a correction. Therefore, Seed and Idris (1971) proposed a factor of safety against liquefaction, FS given as:

$$FS = \frac{CRR_{7.5}}{CSR}$$

While, Youd et al. 2001 proposed a modified expression for Fs as:

$$FS = \frac{CRR.k_M.k_\sigma.k_\alpha}{CSR} \quad (4.18)$$

Where,

k_M = Magnitude correction

k_σ = Overburden correction

k_α = Sloping ground (driving static shear stress)

Bouglanger & Idriss (2006) applied the term sand-like to refer to soils with Plasticity Index of smaller than 7. Based on this, the procedures for SPT blow counts and CPT tip resistance were applied in sand-like soils as it will be described in the next section. Also, for soils with plasticity index of greater than 7, they are considered as clay-like material, and cyclic resistance ratio values were estimated by undrained shear strength (Bouglanger & Idriss, 2004).

4.4.4 Based Evaluation of Undrained Shear Strength (S_u)

In this study, we used the procedures recommended by Bouglanger and Idriss (2004) which can be used for fine-grained (clay-like) soils. To analyze the cyclic resistance ratio, the undrained shear strength, s_u was utilised by applying the following equation:

$$CRR_{7.5} = 0.8 \times \frac{S_u}{\sigma'_{\upsilon 0}} \times K_a \quad (4.19)$$

$\sigma'_{\upsilon 0}$ = effective overburden pressure (kN/m^2)

K_α (α, OCR) = the correction factor to exhibit the effects of primary static shear stress ratio $\alpha = \frac{\tau_s}{\sigma'_{\upsilon 0}}$ developed by Seed (1983)

OCR = the over consolidation ratio of the fine-grained soils.

4.4.5 Evaluation of Shear Wave Velocity

The CRR7.5 is a function of the shear wave velocity, V_s, which is evaluated based on the methods and procedures recommended by NCEER, 1997.

Robertson et al. (1992) suggested The stress-dependent liquefaction analytical procedure using the in-situ data obtained from the sites in the Imperial Valley, California.

These researchers normalised the shear wave velocity by:

$$V_{s1} = V_s \times (\frac{P_a}{\sigma'_{\upsilon 0}})^{0.25} \quad (4.20)$$

Where; P_a = 100 kPa, reference stress, approximately atmospheric pressure, and σ'_{vo} is effective overburden pressure in kPa. Liquefaction resistance curve is suggested by Robertson (1998) for 7.5 power magnitude earthquakes, as shown in Figure 4.8, with various sites where liquefaction occured or did not occure. Further liquefaction resistance boundaries presented by Kaye (1992) for 7 magnitude earthquake are also shown below.

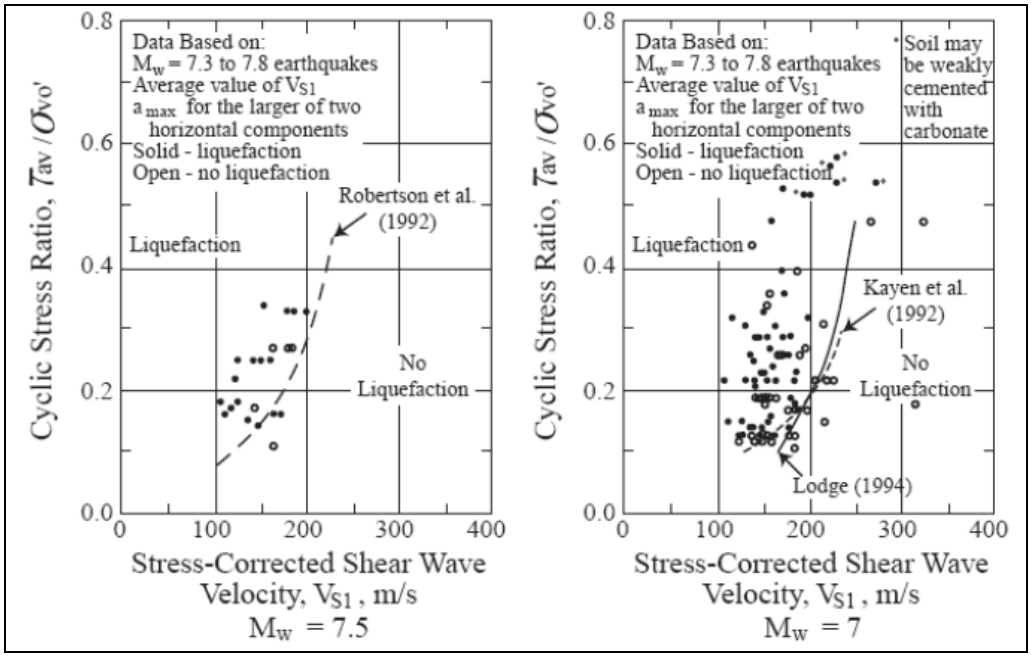

Figure 4.8: Cyclic Stress Ratio Based on Shear Wave Velocity.

Kayen et al. (2013) proposed a relationship which offers a conservative lesser boundary for liquefaction case histories with less than approximately 200 m/s for V_{s1} , while Ricardo proposed a relationship between CRR and constant average CSR to be V_{s1} ($V_{s1} \leq$ 125 m/s). The relationship by Robertson et al. (1998) is the minimum conservative of the three.

Andrus and Stokoe (2000), suggested higher values of $V_{s1,}$ the reason is that the CRR value should become asymptotic to some limiting values of V_{s1}. The limit makes the

dense granular soil to have tendency in exhibiting dilative behavior at high strains. Therefore, equation becomes modified into:

$$\frac{\tau_{av}}{\sigma'vo} = CRR = a \times (\frac{V_{s1}}{100})^2 + (\frac{b}{V_{s1c} - V_{s1}}) - \frac{b}{V_{s1c}} \quad (4.21)$$

Where;

V_{s1c} is the critical value of V_{s1} which separates contractive and dilative behavior, a and b are curve fitting factors.

4.4.6 CPT-Based Evaluation

Cone penetration test offers an approximately continuous profile by providing a comprehensive description of soil layers than the standard penetration test. Such stratigraphic capability makes the CPT exclusively beneficial for expanding liquefaction resistance profiles (Youd et al., 2001).

In this thesis, liquefaction potential was evaluated in two different ways using CPT data: factor of safety against liquefaction (FS), and liquefaction potential index (LPI) approaches.

4.5 Normalization of Cone Penetration Resistance

CPT procedure has to normalize tip resistance before liquefaction resistance is evaluated. For normalize tip resistance, Youd et al. (2001) applied the following equations:

$$q_{c1N} = C_Q(\frac{q_c}{P_a}) \quad (4.22)$$

$$C_Q = (\frac{P_a}{\sigma'_{vo}})^n \quad (4.23)$$

Where;

C_Q = normalizing factor of cone penetration resistance

P_a = 1 atm (100 kPa) of pressure in the similar units used for σ'_{vo}

n = power that varies with soil type

q_c = field cone penetration resistance measured at the tip (kN/m^2)

According to the earlier discussion, C_Q values >1.7 should not practical. The assessment of *n* differs from 0.5 to 1.0 depends on the grain physical characteristics of the soil profile (Olsen, 1997) as it will be explained further in the next section.

4.6 Non-Normalized SBT Charts

Robertson et al. (1986) suggested the most updated, dimensionless and commonly used CPT for soil behaviour types (SBT) chart as shown in Figure 4.9 and the similar interpretation of the ground response model is provided in below table. This chart is used the require CPT factors such as cone resistance, q_t and friction ratio, R_f. The specific chart is universal in nature and it can prepare suitable predictions of soil behaviour type for CPT excavations up to around 20m in depth. Overlap in several zones are expected and the zones corrected according to local experience.

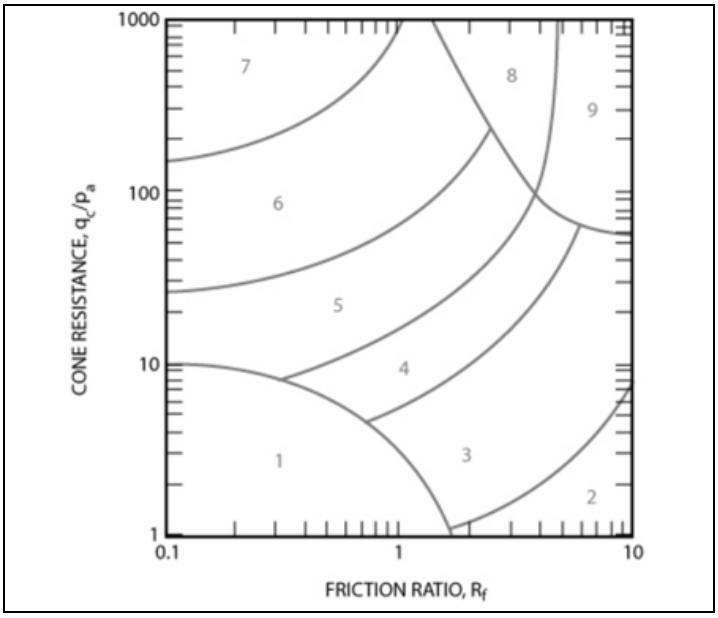

Figure 4.9: CPT Soil Behaviour Type Chart (Robertson 1986)

Zone	Soil Behaviour Type
1	Sensitive, fine-grained
2	Organic soils – clay
3	Clays – silty clay to clay
4	Silt admixtures – clayey silt to silty clay
5	Sand mixtures – silty sand to sandy silt
6	Sands – clean sand to silty sand
7	Gravelly sand to dense sand
8	Very hard sand to clayey sand*
9	Very stiff, fine-grained*

* Heavily over consolidated or cemented

4.7 Normalized SBTN Charts

The parameters such as the resistance to penetration and because of the increasing effective overburden stress in depth, sleeve friction is also increasing. The CPT data require normalisation for overburden stress for very shallow and very deep soundings. Robertson (1990) proposed the modern CPT soil behaviour chart based on normalised CPT data as shown in Figure 4.10. The soil behaviour chart was improved using 1 for *n*, which is the suitable value for clayey soil types, on the other hand for clean sands, 0.5 for *n* value is ideal, and value within a range between 0.5 and 1.0 can be ideal for silts and sandy-silts (Youd et al. 2001).

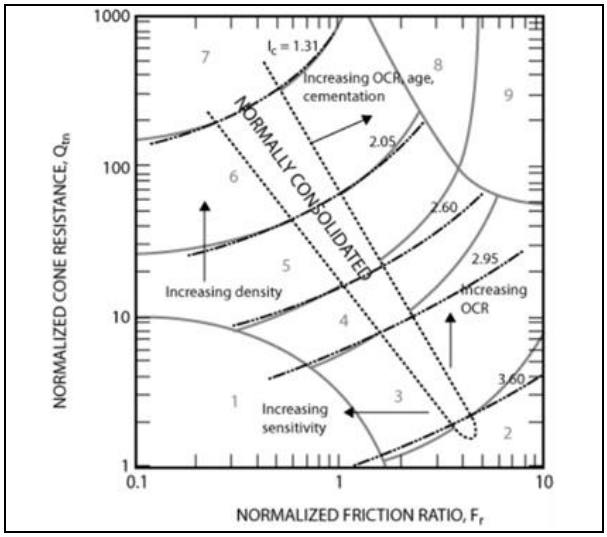

Figure 4.10: Normalized CPT Soil Behavior Type Chart, (Robertson, 1990)

Zone	Soil Behaviour Type	I_C
1	Sensitive, fine-grained	N/A
2	Organic soils – clay	> 3.6
3	Clays – silty clay to clay	2.95 – 3.6
4	Silt mixtures – clayey silt to silty clay	2.60 – 2.95
5	Sand mixtures – silty sand to sandy silt	2.05 – 2.6
6	Sands – clean sand to silty sand	1.31 – 2.05
7	Gravelly sand to dense sand	< 1.31
8	Very hard sand to clayey sand*	N/A
9	Very stiff, fine-grained*	N/A

* Heavily over consolidated or cemented

The basic method that was applied for determining the soil behaviour type index I_c was described by Roberston and Wride (1998). The first level is the variation of non-liquefiable layers (clays) from the liquefiable layers (sands and silts). This distinction was made by considering 1 for exponent *n* (clays characteristic) and the dimensionless CPT tip resistance C_Q was obtained from the Equation 4.16.

If I_c is more than 2.6 for $n = 1$, the soil was categorized like clayey and was reflected too clay-rich to liquefy, and the analysis was performed for clayey parts.

Robertson (1990) proposed the full normalised SBT_N charts and also an additional chart based on the normalised parameter such as pore pressure, Bq, as shown in Figure 4.10, where;

$$Bq = \frac{\Delta u}{q_n} \quad (4.24)$$

and excess pore pressure, $\Delta u = u_2 - u_0$ (4.25)

Net cone resistance, $q_n = q_t - \sigma'_{vo}$ (4.26)

The Q_t – Bq chart can help to recognize the soft, saturated fine-grained soils where the excess pore pressures can be remarkable in CPT penetration. totally, this chart is

not universally used for onshore CPT because of the absence of repeatability for the results of pore pressure (poor or loss of saturation of the filter element).

According to Youd et al. (2001), due to the increasing fines content and soil plasticity, the CPT friction ratio (sleeve resistance f_s divided by cone tip resistance q_c) increases. CPT data were also used to obtain a rough estimation of soil type and fines content. Robertson and Wride (1998) prepared the chart reproduced in Figure 4.8 for estimation of soil type. The radius of the circles, defining the soil behaviour type indexI_C, is calculated from the following equation given by Youd et al. (2001):

$$I_C = \sqrt{(3.47 - \log Q)^2 + (1.22 + \log F)^2} \quad (4.27)$$

Where,

Q = normalized cone penetration resistance (dimensionless):

$$Q = \frac{(q_c - \sigma_{vo})}{P_a} \cdot \left(\frac{P_a}{\sigma' vo}\right)^n \quad (4.28)$$

F = normalized friction ratio, in %:

$$F = \left[\frac{f_s}{q_c - \sigma' vo}\right] \times 100\% \quad (4.29)$$

At the time, q_{c1N} was calculated with 0.5 for exponent *n*, and it was used to determine resistance of liquefaction. However, in cases where recalculated I_c was more than 2.6, the soil reflected likely to be very silty and probably plastic. In such cases, the earlier procedure was repeated, and I_c was recalculated with 7 for intermediate exponent *n*. Then, q_{c1N} was recalculated with the intermediate exponent.

4.8 Magnitude Scaling Factor

As mentioned earlier, The CRR equations can be only applied in 7.5 Richter magnitude earthquakes. For an earthquake magnitude of M_w other than 7.5, a magnitude scaling factor is used.

Amounts of MSF for undrained shear strength (s_u) based estimation was calculated conferring to Bouglanger & Idriss (2004) from the correlation in below:

$$\text{MSF} = 6.9.exp[(-M)/4] - 0.058 \leq 1.8 \quad (4.30)$$

Consequently, factor of safety against liquefaction was calculated as follows:

$$FS = (\text{CRR}_{7.5}/\text{CSR}).\text{MSF} \quad (4.31)$$

According to the LiqIT software tool, the CSR and $\text{CRR}_{7.5}$ are modified in such a way that the MSF should be multiplied at $\text{CRR}_{7.5}$ to modify its value for the target earthquake magnitudes (Tokimatsu and Seed 1987, Idriss NCEER 1997).

4.9 Liquefaction Potential Index

The liquefaction potential index, LPI was originally developed by Iwasaki et al. (1978, 1984) to evaluate and predict the possibility of liquefaction to trigger foundation damage at a site. Also, Yegian and Whitman (1978) defined the Liquefaction Potential Index as the ratio of the shear stress triggered by the earthquake to the resistance of cohesionless sand during shaking.

The in-situ testing techniques, ITT is a common practice in most countries for the evaluation of liquefaction factors and susceptibility. However, the independent use of ITT is not adequate for calculation of liquefaction potential. Sonmez (2003) proposed the liquefaction potential index (LPI) to evaluate the intensity of liquefaction.

More simplified methods for a specific location and depth within the soil can be used to estimate the liquefaction potential (Seed and Idriss, 1971). Therefore, simpler additional approaches were proposed to quantify the liquefaction potential for the whole boring during the in situ methods (Iwasaki et al. 1982). The development of

liquefaction potential index (LPI) has become a tool to determine the liquefaction potential over boring depth and to obtain an evaluation of liquefaction-related surface damage for a boring position (Lenz, 2007).

At the beginning Iwasaki et al in 1978 defined LPI to illustrate the factors of safety against liquefaction and thickness of potentially liquefiable soil profiles according to the depth. It supposes that the liquefaction severity is proportionally related to:

- The thickness of liquefied layers.
- Vicinity of liquefied layers to the surface.
- The value of factor safety (FS) is less than 1.0,

FS is the ratio of soil capacity to resist liquefaction to seismic burden by the earthquake.

The LPI based on the method by Iwasaki et al. (1982), is defined as:

Where;

$$LPI = \int_0^{20} F(z)\, W(z)\, dz \tag{4.32}$$

$$F(z) = 1 - FS \quad \text{for} \quad FS \leq 1 \tag{4.33}$$

$$F(z) = 0 \quad \text{for} \quad FS > 1 \tag{4.34}$$

$$W(z) = 10 - 0.5\, z \tag{4.35}$$

Where,

z = depth (meters)

$W(z)$= weighting factor ranges 0 to 20m

dz = the differential increment of depth

Iwasaki et al. (1978) suggested *w(z)*, from one at the surface at zero to 20 m. F=0 top of the water table. The assumed severity of liquefaction should be proportional to the:

1- Thickness of the liquefied layer

2- The vicinity of the liquefied layer to the surface

The value of the factor of safety against liquefaction (FS) is less than 1 where it is the ratio of resistance on liquefaction when the earthquake is occurred.

In this thesis, the liquefaction potential formula provided by Sonmez (2003) was applied which defined F_L as:

$$F_L = 0 \quad \text{for} \quad FS \geq 1.2 \tag{4.36}$$

$$F_L = 1 - FS \quad \text{for} \quad FS < 0.95 \tag{4.37}$$

$$F_L = 2 \times 10^{6}\, e^{-18.427 \cdot FS} \quad \text{for} \quad 1.2 > FS > 0.95 \tag{4.38}$$

Liquefaction had been reported by using the equation which is suggested by Iwasaki in 1982 for six historical earthquakes in Japan, as summarized in Table 4.1.

Table 4.1: Liquefaction potential classifications (Iwasaki et al. 1982)

Liquefaction Potential Index	**Liquefaction Potential Classification**
0	Very low
$0 < LPI \leq 5$	Low
$5 < LPI \leq 15$	High
$15 > LPI$	Very high

The next liquefaction potential classifications were used in this study proposed by Sonmez (2003) as mentioned in Table 4.2.

Table 4.2: Liquefaction potential classifications (Sonmez, 2003)

Liquefaction Potential Index	Liquefaction severity Classification
0	Non-liquefiable
$0 < LPI \leq 2$	Low
$2 < LPI \leq 5$	Moderate
$5 < LPI \leq 5$	High
$15 > LPI$	Very high

In this study, the amounts of LPI were established with estimated factor of safety values from CPT soundings.

4.10 Probability of Liquefaction

There is a need to use the deterministic method to calibrate the severity of liquefaction, so that the meaning of the calculated factor of safety, FS becomes meaningful in terms of probability of liquefaction (Chen and Juang, 2000). It has been observed that Chen's approach, Juang and Jiang (2000) is a modified calibration of the Robertson and Wride (1998) method and thus provided the appropriate mapping function to analyze the probability of liquefaction;

Table 4.3: Liquefaction probability classification (Chen and Juang, 2000)

Probability (PL) ranges	Description
$0.85 \leq PL < 1.00$	Almost certain that it will liquefy
$0.65 \leq PL < 0.85$	Very likely
$0.35 \leq PL < 0.65$	Liquefaction/non-liquefaction is equally likely
$0.15 \leq PL < 0.35$	Unlikely
$0.00 \leq PL < 0.15$	Almost certain that it will not liquefy

$$P_L = \frac{1}{\left(1+\frac{FS}{A}\right)B} \quad (4.39)$$

The coefficients of A = 0.96 and B = 4.5.

Table 4.4: Liquefaction severity classification (Sonmez and Gokceoglu, 2005)

Liquefaction Severity (L_S)	**Description**
$85 \leq L_S < 100$	Very High
$65 \leq L_S < 85$	High
$35 \leq L_S < 65$	Moderate
$15 \leq L_S < 35$	Low
$0 < L_S < 15$	Very Low
$L_S = 0$	Non-liquefied

The use of Factor of safety to predict the liquefaction potential of any given layer does not directly offer a categorization on the level of severity. Iwasaki et al. (1982) suggested single approach procedure to eliminate a few limitations of factor of safety, the classification of severity and potential index as illustrated in the previous part. After Iwasaki et al. (1982) and Lee et al. (2004) assessed a new empirical approach with the consideration of defined probability function as proposed by Juang et al. (2003). A new approach, of the Factor of Safety term F(z) term of the LPI was then offered by Iwasaki et al. (1982) which was substituted by P_L and LPI was renamed as a risk of liquefaction index (I_R).

$$I_R = \int_0^{20} P_L\ (z).W\ (z)\ .dz \quad (4.40)$$

Where,

P_L = Probability of liquefaction

FS = Safety factor against liquefaction

Sonmez and Gokceoglu (2005) suggested different empirical procedure by using Lee et al. (2003) concept. The only difference of this new empirical methodology is the investigators used the replaced the term liquefaction risk index, I_R with liquefaction severity index, L_S.

$$I_R = Ls = \int_0^{20} P_L\ (z).w\ (z)\ .dz$$

$$w\ (z) = 10 - 0.5z \tag{4.41}$$

$$I_R = Ls = \int_0^{20} P_L\ (z).(10 - 0.5z)\ .dz$$

$$I_R = 100\ P_L(z) \tag{4.42}$$

or

$$I_R = Ls = \int_0^{20} P_L\ (z).w(z).dz$$

$P_L = \frac{1}{(1+ F_S/0.96)^{4.5}}$ For FS ≤ 1.411

$P_L = 0$ For FS > 1.411

Where,

L_S = Liquefaction severity index

P_L = Probability of liquefaction

FS = Factor of safety against liquefaction

z = depth (m)

dz = the variance increment of depth

4.11 Evaluation of Site Response Analysis

Site response analysis could be the first step to study seismic soil-structure. Geotechnical earthquake engineering is trying to find the perfect solution for analyzing the ground responses when the earthquake loadings happen, then this study

has tried to analyze the ground response for eastern coast of Cyprus during 6.5 magnitude earthquakes loading.

This study is tried to site response analysis on the Tuzla area with ground motion residuals. Deep Soil software is useful to do it. This software needs some parameters such as unit weight, shear wave velocity and soil distribution for each layer in depth to analyze the site response. These parameters are estimated according to NovoCPT software, and for each location according to soil behavior type 7 to 10 layers are defined depends on depth and distribution of soil. In order to compare the results of this application, specific reference or database is required. Ground motion recorded in the past on bedrock, these ground motion data (NGA) could be find through Peer Berkeley website by choosing the criteria magnitude earthquake (M_w), shear wave velocity and closest distance to rupture plane (R_{Jb}) for study area.

Although, DeepSoil software originally has 13 ground motion as a default of this program but for the better comparing and understanding of the site response results in this study, 10 extra ground motions are selected through Peer Berkeley website which are recorded in the past, and also they are near and has an approximately same conditions with Cyprus. 6.5 magnitude earthquake is chosen to site response analysis during this thesis and because of bedrock condition in eastern coast of Cyprus, very dense soil and soft rock, shear wave velocity is obtained 700 m/s, (Wair et al, 2012). These NGA are selected as following parameters in below:

$6.0 < M_w < 8.0$

$500 \text{ m/s} < Vs_{30} < 1000 \text{ m/s}$

$20 \text{ km} < R_{Jb} < 150 \text{ km}$

$\xi = 5\%$

Site response could be analyzed for all defined layers in all CPT location by DeepSoil software, so first layer with 2 or 3 meter depth is chosen for response analysis for locations and compares them according to input motions. Displacement, velocity and acceleration during earthquake period for all layers will be obtained by using DeepSoil software. Pseudo spectral velocity and acceleration curves are two important parameters for site response analysis; these curves are shown as results of DeepSoil application. The period of building is possible to calculate according to pseudo spectral acceleration graph while comparing with input motion curve. The amount of earthquake magnitude can be extremely influential on the spectral shapes, while, the distance between the source of earthquake and the site cannot be much effective on them.

SeismoSignal software could be another program in this thesis to site response analysis by using displacement, velocity and acceleration for each CPT location according to DeepSoil software results.

Response displacement, velocity, and acceleration curves versus period for first layer and bedrock for whole CPT locations are as results of analyzing by SeismoSignal software. These curves show the different behavior of response displacement, velocity, and acceleration during the first amplitude of earthquake and second amplitude when the first layer and bedrock curves cut off each other.

All comments relating to the results of NovoCPT, DeepSoil, and SeismoSignal software have been reported in chapter five and extra information about them are presented during the Appendix A to C.

The summary of methodology is shown as following figure 4.11:

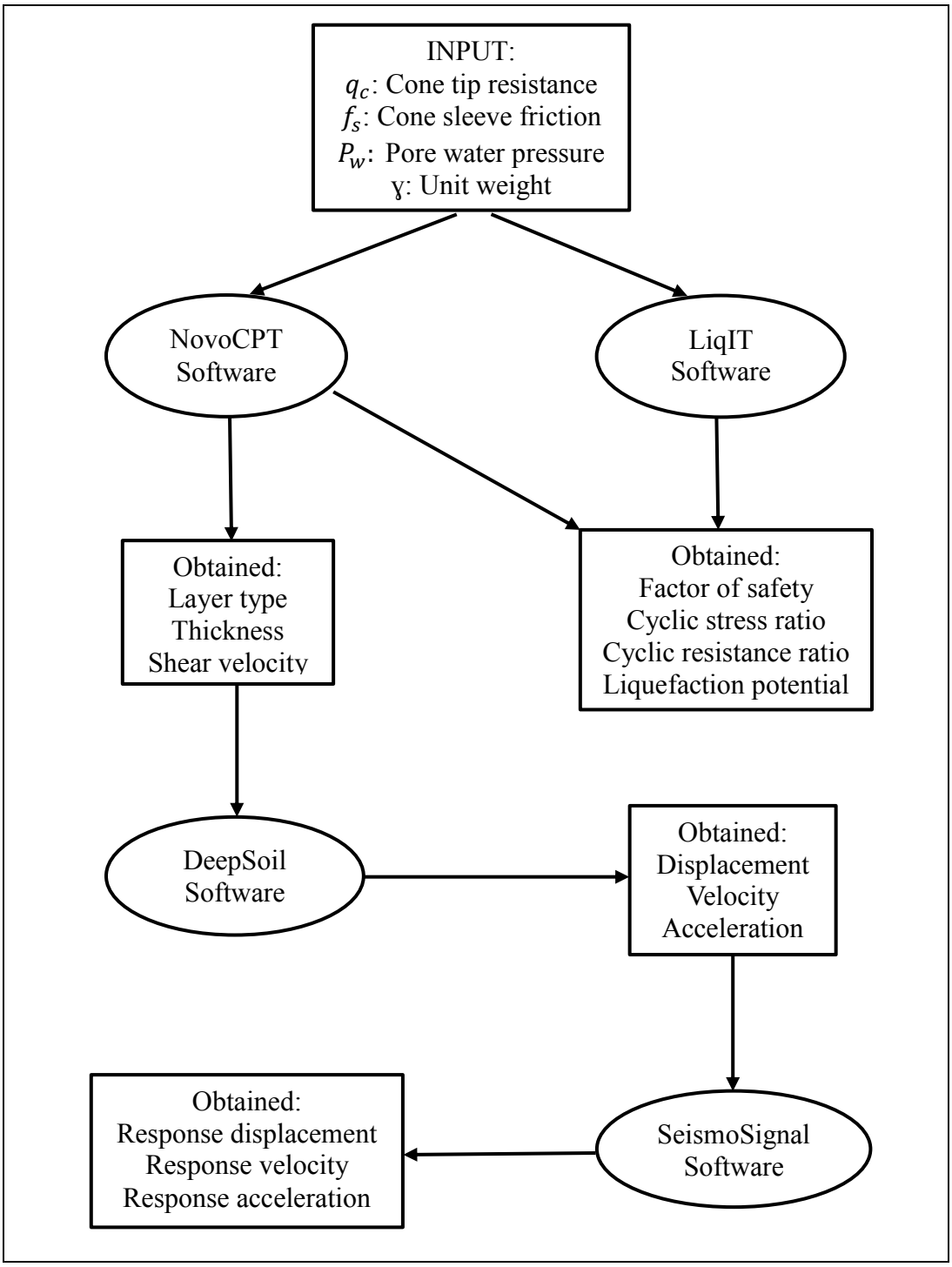

Figure 4.11: Summary of Methodology

Chapter 5

RESULTS AND DISCUSSIONS

5.1 CPT Locations

In this study, the standardized in situ technique of cone penetration test (CPT) method was used to investigate the liquefaction potential. During the investigation, a total of ten CPT sounding probes was installed and drilled in the eastern coast of Cyprus (Tuzla region) to study the subsurface strati graphical layers (Erhan,2009), conditions and properties. The CPT locations, their corresponding boreholes with underground depths between 3.9 to 20m and coordinates are shown in Figure 5.1 and Table 5.1.

Figure 5.1: CPT Locations in the Study Area (Google Earth Image of Tuzla, 35° 09′15" N 33°52′ 58.91"), (Erhan, 2009).

Table 5.1: Coordinates of CPT and BH locations (Erhan, 2009)

Study locations	CPT no	Coordinate	
		N	E
TUZLA	CPT 1 & BH 1	3893360.648	582572.078
	CPT 2	3893974.781	582340.869
	CPT 3	3892722.659	581636.071
	CPT 4	3892662.347	581287.023
	CPT 5 & BH 2	3892662.347	580986.784
	CPT 6	3892044.763	580602.898
	CPT 7 & BH 3	3891639.905	580608.541
	CPT 8 & BH 4	3891033.562	581574.409
	CPT 9	3891594.14	581002.622
	CPT 10 & BH 5	3890709.144	581658.505

5.2 Liquefaction Assessment

In weak soils with saturated conditions Liquefaction will be happen, that is, underground soil layers within the first depth of 20 m from the ground surface and with the factor of safety, FS values less than 1.0 are categorized as liquefiable. The test results are obtained from the analysis of the CPT data in the ten borehole probes. There is an observation of liquefiable potential within the few meters in the dimension of the soil layer at some of the CPT locations. Therefore, in this study, different conditions and classifications class have been applied to define the liquefaction probability, severity, potential of the soil layers at various CPT locations.

5.3 CPT-Based Assessment of Liquefaction Parameters

The safety factor (FS), cyclic stress ratio (CSR), cyclic resistance ratio (CRR), liquefaction potential index (LPI) values, etc., were calculated to classify the liquefaction potential of the subsurface soil by using the in situ CPT probes at the Tuzla area. Also, the estimation of the factor of safety, probability ranges (P_L), liquefaction severity (Ls) categories as they represent the liquefaction potential of each profile per borehole position.

5.3.1 Assessment of Liquefaction Factor of Safety

From the analysis of CPT data by the NovoCPT and LiqIT software programs, useful liquefaction parameters were generated for the assessment of liquefaction. One of these parameters is the factor of safety against liquefaction. The condition factor of safety, FS when it greater than one, that is, FS > 1 indicates that the soil layer is categorized as non-liquefiable, but when FS < 1 it means that the soil layer is classified liquefiable. Therefore, it was observed from the analysis of the CPT data by the NovoCPT and LiqIT software programs for 6, 6.5 and 7 earthquake magnitude that the soil layer within the liquefiable zone (of remarkable few meters) are of low to moderate or high liquefiable class, while the entire soil layer (about the total thickness) are acceptably non-liquefiable given in Table 5.12.

Although, LiqIT software is usefull for assessment of liquefaction potential but during this thesis is tried to use another software, on the other hand, the summary of liquefaction potential for each CPT location according to LiqIT results are presented in Appendix B. Total information about liquefaction parameters such as factor of safety , CRR, CSR, and also soil behavior type in total depth for each CPT location are obtained by NovoCPT software, and they presented in Table 5.2 to 5.11 and

Figure 5.2 to 5.11. Appendix A consist of factor of safeties graphs for M_w = 6, 6.5, and 7.0 and soil distribution chart and soil behavior type for each location that they proposed by Robertson et al, 1990 and Jefferies & Been, 2006.

Table 5.2 shows CPT 1 parameters which are obtained from NovoCPT Software such as soil behavior type, cone tip resistance, shear velocity and factor of safety for three senarios magnitude earthquake. Shear wave velocity and factor of safety against liquefaction for 6, 6.5 and 7 magnitude earthquake are obtained for different depths and it is considered after 4 meter soil behavior is susceptible to liqufaction due to the FS is going to equal 1 and liquefaction will be happen when 7 magnitude earthquake occured. Overal, CPT 1 with 17.80 m depth consist of sand, silty sand and silty clay to clay, according to Robertson et al, 1986, as shown in Figure 5.2.

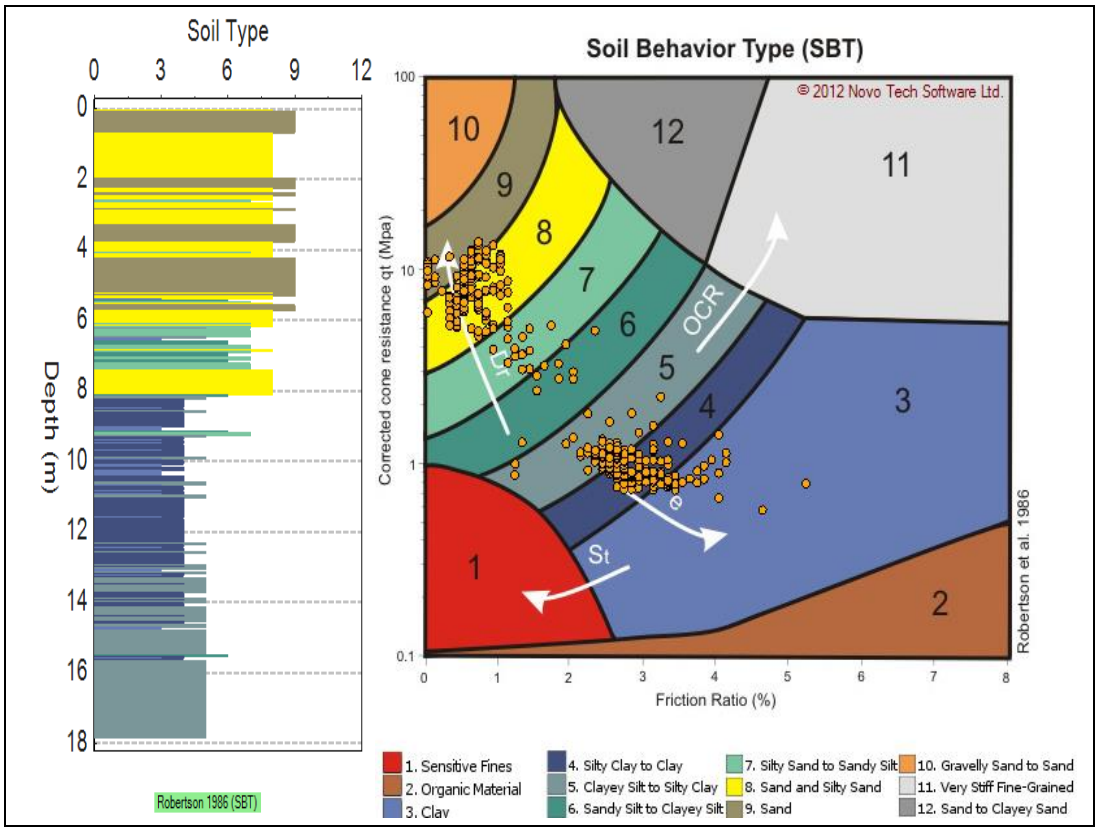

Figure 5.2: Soil Classification by NovoCPT Software for CPT 1

Table 5.2: Liquefaction Results by NovoCPT Software for CPT 1

Depth	**SBT**	**q_c (MPa)**	**Vs (m/s)**	**FS $_6$**	**FS $_{6.5}$**	**FS $_7$**
0 - 1	sand	8.74	516	4.21	3.42	2.83
1.05 - 2.4	sand to silty sand	7.69	475.1	4.24	3.45	2.86
2.45 - 4	sand to silty sand	9.3	534.7	3.41	2.77	2.3
4.05 - 7.4	silty sand to sandy silt	7.58	457.3	2.32	1.89	1.54
7.45 - 8.5	sandy silt to clayey silt	4.98	344.8	1.77	1.45	1.19
8.55 - 9.68	silty sand to sandy silt	1.27	148.2	2.27	1.84	1.53
9.7 - 11.15	silty clay to clay	0.85	124.7	1.96	1.6	1.32
11.2 - 14.35	clay	0.88	129.8	1.76	1.44	1.19
14.4 - 17.8	clayey silt to silty clay	1.05	144.5	1.84	1.5	1.24

Table 5.3 and Figure 5.3 show the NovoCPT results for CPT 2, this location with 3.9 meter depth involve sand and sand to silty sand in different depth. 7 layers are defined for this location and shear wave velocity and factor of safety are calculated for each layer and it seems that FS tend to decrease after 3 meter, so CPT 2 maybe trend to liquefaction after sixth layer with high shaking and earthquake magnitude. This potential has investigated in the next part of this chapter.

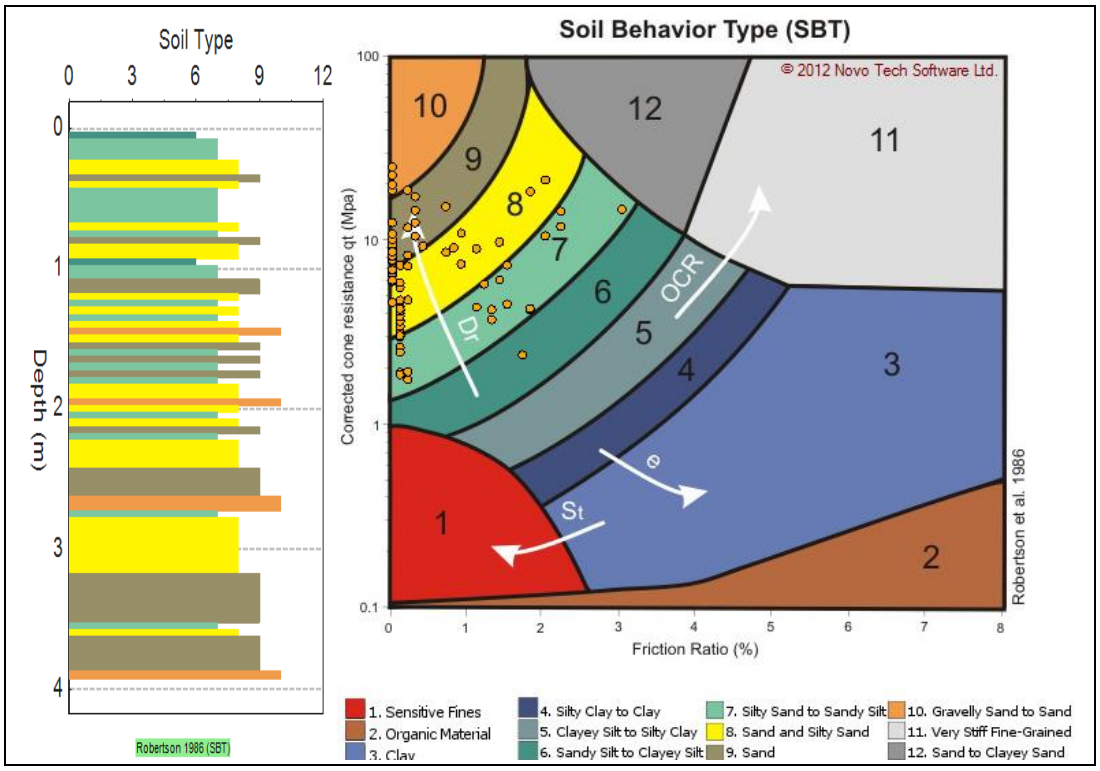

Figure 5.3: Soil Classification by NovoCPT Software for CPT 2

Table 5.3: Liquefaction Results by NovoCPT Software for CPT 2

Depth	SBT	q_c (MPa)	Vs (m/s)	FS $_6$	FS $_{6.5}$	FS $_7$
0 - 0.4	sand to silty sand	6.79	431.6	4.19	3.41	2.83
0.45 - 0.85	sand	9.41	525	4.2	3.43	2.84
0.9 - 1.35	silty sand to sandy silt	9.82	535.8	4.06	3.31	2.73
1.4 - 2	sand to silty sand	8.54	474.6	3.25	2.65	2.13
2.05 - 2.6	sand	8.33	480.8	3.02	2.46	2.03
2.65 - 3.15	sand to silty sand	7.46	434.8	1.68	1.37	1.13
3.2 - 3.9	sand	9.22	527.4	2.73	2.22	1.79

Silty sand to sandy silt, silty clay to clay and clay are founded as a soil behavior type through analyzing by NovoCPT software for CPT 3 location with 18.6 meter depth, as displayed in Figure 5.4. liquefaction is predictable in this location after 10 meter depth because of th FS is intended for less than 1, reported in Table 5.4.

Table 5.4: Liquefaction Results by NovoCPT Software for CPT 3

Depth	**SBT**	**q_c (MPa)**	**Vs (m/s)**	**FS $_{6}$**	**FS $_{6.5}$**	**FS $_{7}$**
0 – 0.5	silty sand to sandy silt	3.82	307	4.19	3.42	2.83
0.55 - 3	clay	1.42	155.6	5.62	4.58	3.79
3.05 – 5.95	clay	0.48	81.2	2.56	2.08	1.72
6 - 7.6	silty clay to clay	1.02	126	2.47	2.02	1.67
7.65 – 9.7	silty sand to sandy silt	2.6	230.6	3.42	2.79	2.31
9.75 – 10.95	clay	0.74	108.3	1.64	1.33	1.1
11 - 13.15	silty clay to clay	0.43	75.8	0.56	0.45	0.38
13.2 – 15.6	clay	0.54	92.3	0.79	0.64	0.53
15.65 - 17.4	silty clay to clay	0.83	120.2	1.35	1.1	0.91
17.45 – 18.6	clay	0.76	116.6	1.14	0.93	0.77

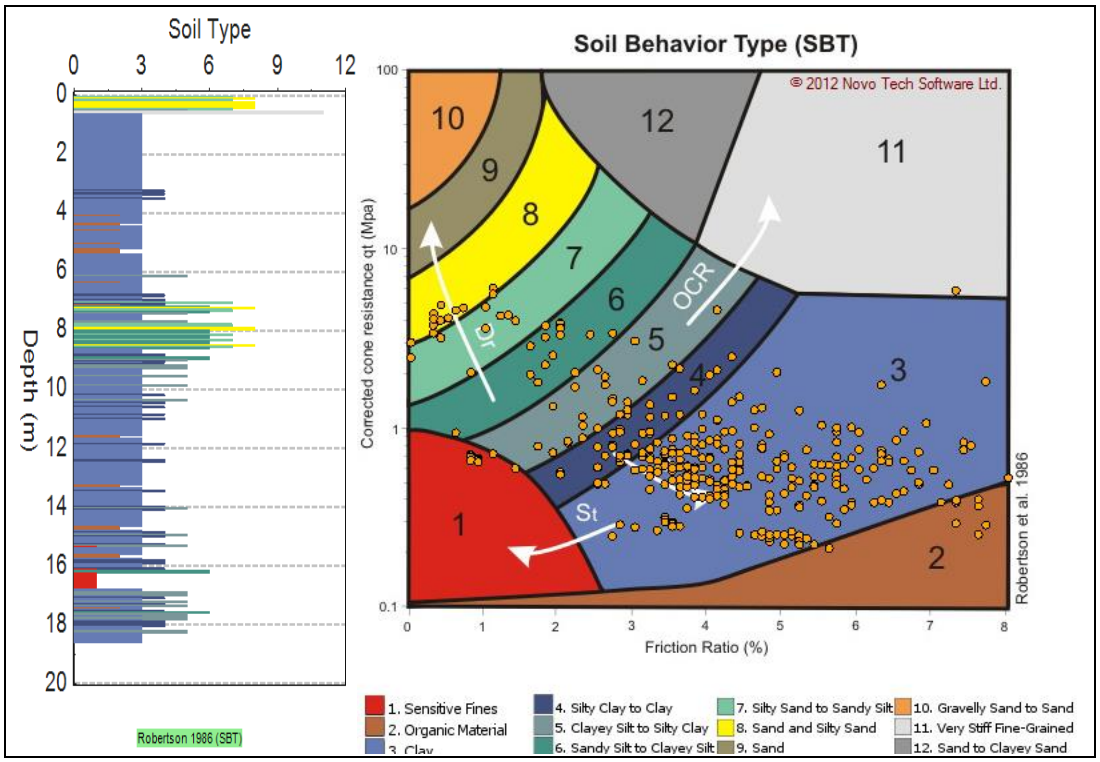

Figure 5.4: Soil Classification by NovoCPT Software for CPT 3

NovoCPT results for CPT 4 to CPT 7 locations are presented in the next pages. Table 5.5 and Figure 5.5 are reported about the results of CPT 4 by NovoCPT software, this excavation with 17.95 meter consist of clay and clayey silt to silty clay as a soil classification and according to amounts of FS in this location for three scenarios assumption, liquefaction accrues by 6.5 and 7 magnitude earthquake in 8 meter depth and more.

CPT 5 included silty sand to sandy silt, clay silt to silty clay and clay in 15.55 meter depth, as shown in Figure 5.6. Factor of safeties are estimated less than 1 for layers after 5 meter depth, Table 5.6, this location has high potential to liquefaction when the earthquake happened with more than 6 magnitudes. In continue, Table 5.5 to 5.6 and Figure 5.5 to 5.6 are reported the liquefaction parameters and soil behavior types for CPT 4 and CPT 5 locations.

Table 5.5: Liquefaction Results by NovoCPT Software for CPT 4

Depth	SBT	q_c (MPa)	Vs (m/s)	FS $_6$	FS $_{6.5}$	FS $_7$
0 – 1.9	clay	1.73	168.9	5.43	4.42	3.66
1.95 – 4.65	clayey silt to silty clay	0.9	113.7	3.24	2.64	2.18
4.7 – 7.35	clayey silt to silty clay	1.2	141.7	3.02	2.46	2.04
7.4 – 8.65	clay	0.64	99.2	1.83	1.5	1.24
8.7 – 10	clay	0.58	94.1	1.34	1.09	0.9
10.05 – 12	silty clay to clay	0.58	96.5	1.17	0.95	0.79
12.05 - 13.3	clay	0.56	98.7	1.04	0.85	0.7
13.35 – 14.7	clay	0.56	102.4	1.01	0.82	0.68
14.75 – 16.15	clay	0.65	110.9	1.11	0.91	0.75
16.2 – 17.95	silty clay to clay	0.68	115.1	1.1	0.89	0.74

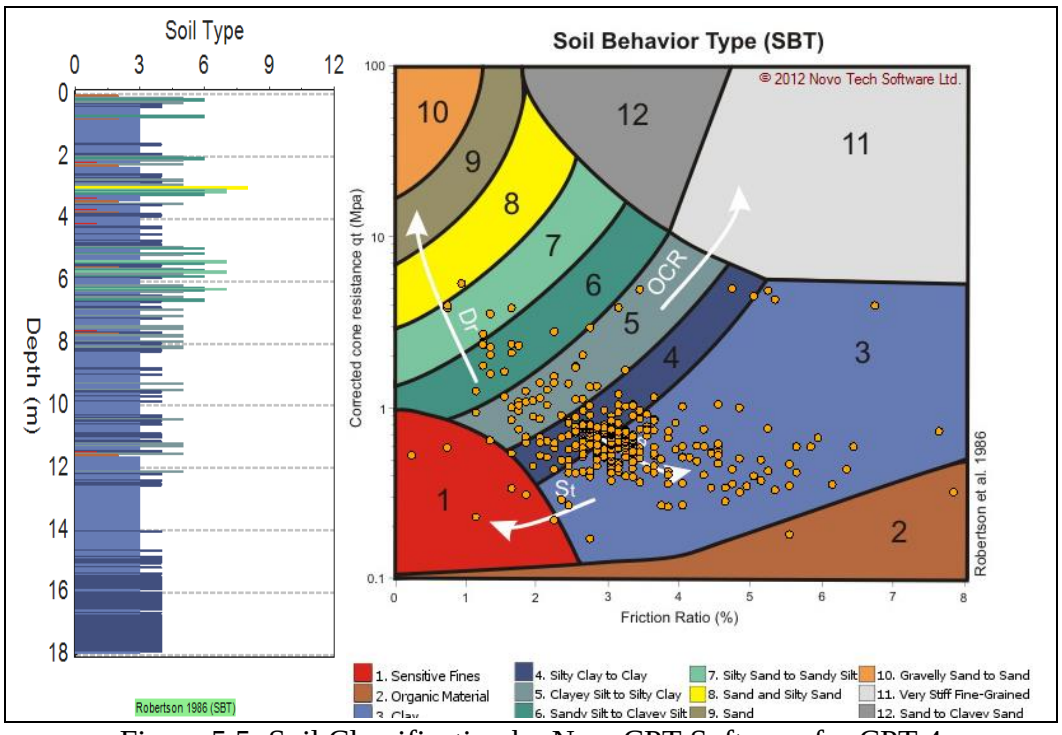

Figure 5.5: Soil Classification by NovoCPT Software for CPT 4

Table 5.6: Liquefaction Results by NovoCPT Software for CPT 5

Depth	SBT	q_c (MPa)	Vs (m/s)	FS $_6$	FS $_{6.5}$	FS $_7$
0 – 0.65	silty sand to sandy silt	6.7	418.7	4.05	3.3	2.72
0.7 – 2.65	clay	1.57	170.8	4.9	3.99	3.3
2.7 – 5.35	clayey silt to silty clay	2.16	193.9	3.87	3.16	2.58
5.4 – 8.3	clay	0.39	73.9	1.39	1.13	0.94
8.35 – 10.1	clay	0.38	78.3	1.02	0.83	0.69
10.15 – 11.85	clay	0.38	81.1	0.87	0.71	0.59
11.9 - 13.55	clay	0.45	90.3	0.93	0.76	0.63
13.6 – 15.15	clay	0.5	96.6	0.95	0.77	0.64
15.2 – 16.4	clayey silt to silty clay	1.48	168.4	2.91	2.37	1.96
16.45 – 17.55	clay	1.11	138	1.36	1.11	0.86

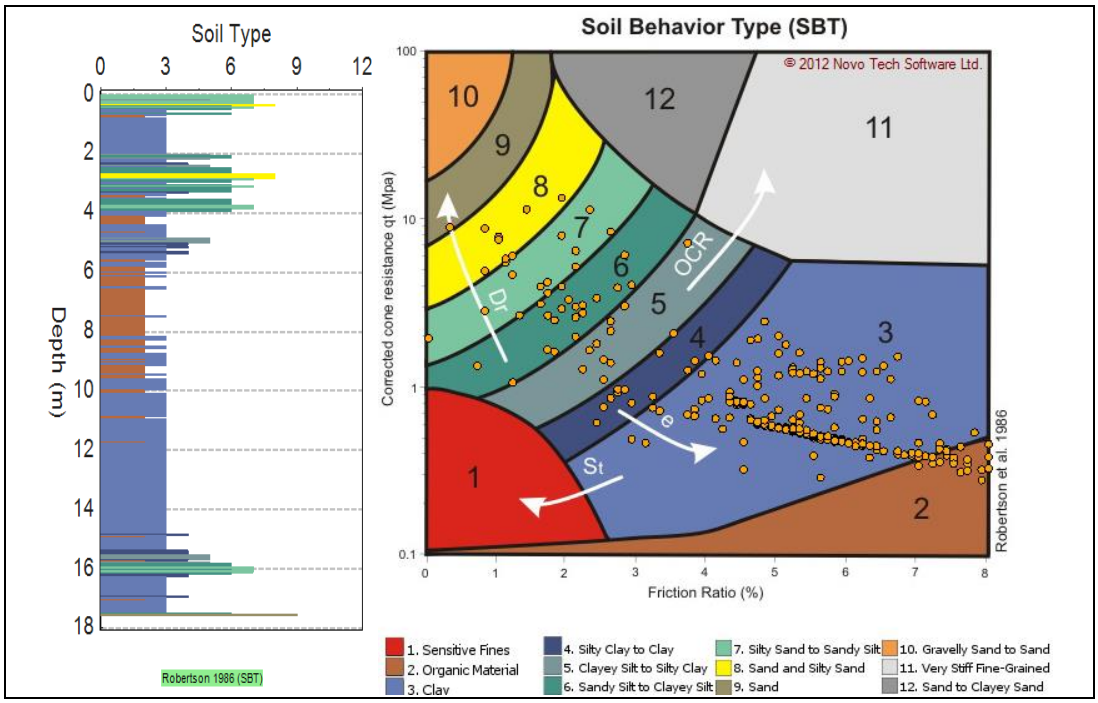

Figure 5.6: Soil Classification by NovoCPT Software for CPT 5

According to Figure 5.7, clay and silty clay to clay are formed the soil behavior type of CPT 6 location with 20.1 meter depth. The results of factor of safety for each layer are shown that this location trend to liquefaction, this phenomenon is predictable after 6, 6.5 and 7 magnitude earthquake because FS is less than 1 after third layer in 7 meter depth, shown in Table 5.7.

The results of CPT 7 are presented in Table 5.8 and Figure 5.8. Clay, sand to silty sand and silty clay to clay are the classification of soil in this location with 15.3 meter depth. The results show FS in two last layers is less than one and it is possible to liquefaction, it needs to more evaluation with other methods such as Iwasaki or Sonmez's methods, these methods are applied in the next parts.

Table 5.7: Liquefaction Results by NovoCPT Software for CPT 6

Depth	**SBT**	**q_c (MPa)**	**Vs (m/s)**	**FS $_6$**	**FS $_{6.5}$**	**FS $_7$**
0 – 2	clay	1.52	164.5	5.21	4.24	3.56
2.05 – 5	clay	0.5	86.7	3.93	3.2	2.65
5.05 – 7	silty clay to clay	0.71	102.5	2.8	2.28	1.89
7.05 – 9.5	clay	0.51	88	1.5	1.22	1.01
9.55 – 12.1	clay	0.39	81.7	0.84	0.68	0.56
12.15 – 14.1	clay	0.5	94.4	0.93	0.76	0.63
14.15 - 15.3	clay	0.51	97	0.87	0.71	0.59
15.35 – 17.65	clayey silt to silty clay	1.31	160.9	2.55	2.08	1.72
17.7 – 18.9	clay	0.77	120.8	1.21	0.98	0.82
18.95 – 20.1	clay	0.84	127.8	1.36	1.1	0.92

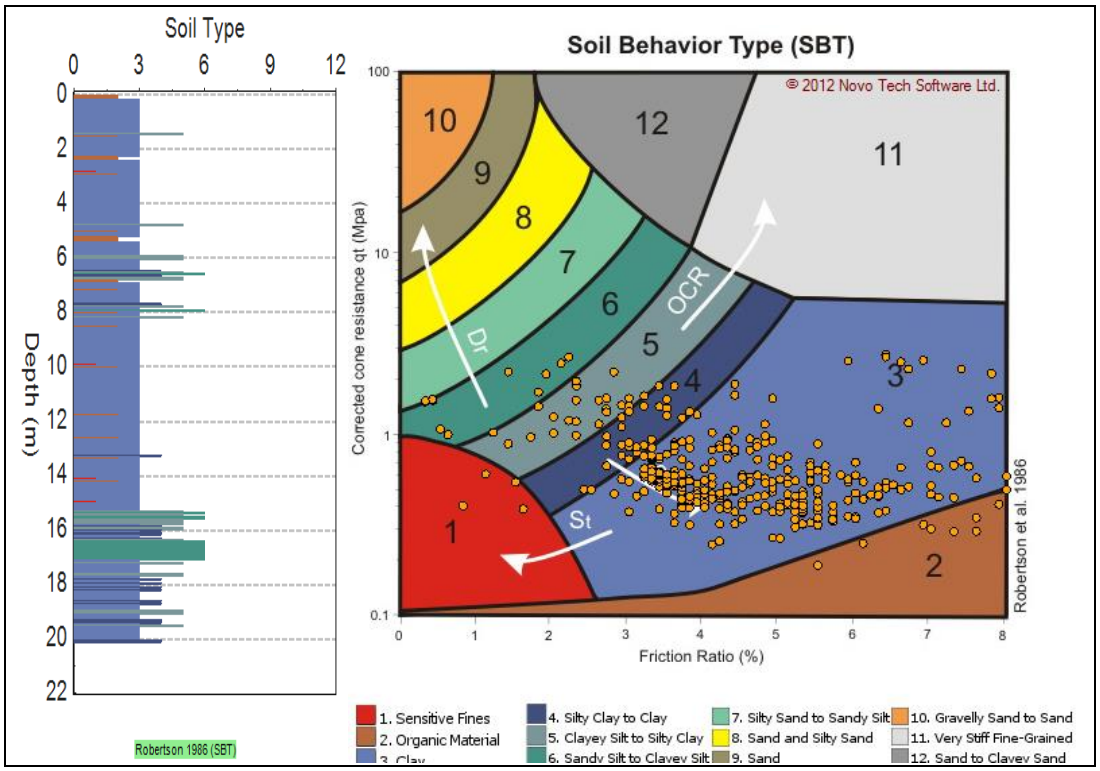

Figure 5.7: Soil Classification by NovoCPT Software for CPT 6

Table 5.8: Liquefaction Results by NovoCPT Software for CPT 7

Depth	SBT	q_c (MPa)	Vs (m/s)	FS $_{6}$	FS $_{6.5}$	FS $_{7}$
0 – 1.6	clay	3.19	240.9	4.86	3.96	3.27
1.65 – 3.2	clay	0.82	116.5	6.98	5.68	4.7
3.25 – 4.8	clay	0.64	100.5	4.15	3.38	2.79
4.85 – 6.4	clay	0.35	69.2	1.44	1.17	0.97
6.45 – 7.6	clay	1.02	123.9	2.78	2.27	1.87
7.65 – 9	sand to silty sand	4.35	325	3.87	3.15	2.61
9.05 – 11.4	clayey silt to silty clay	0.87	117.4	1.82	1.48	1.23
11.45 – 13.2	silty clay to clay	0.57	93	0.98	0.79	0.66
13.25 – 15.3	clay	0.61	98.6	0.91	0.74	0.61

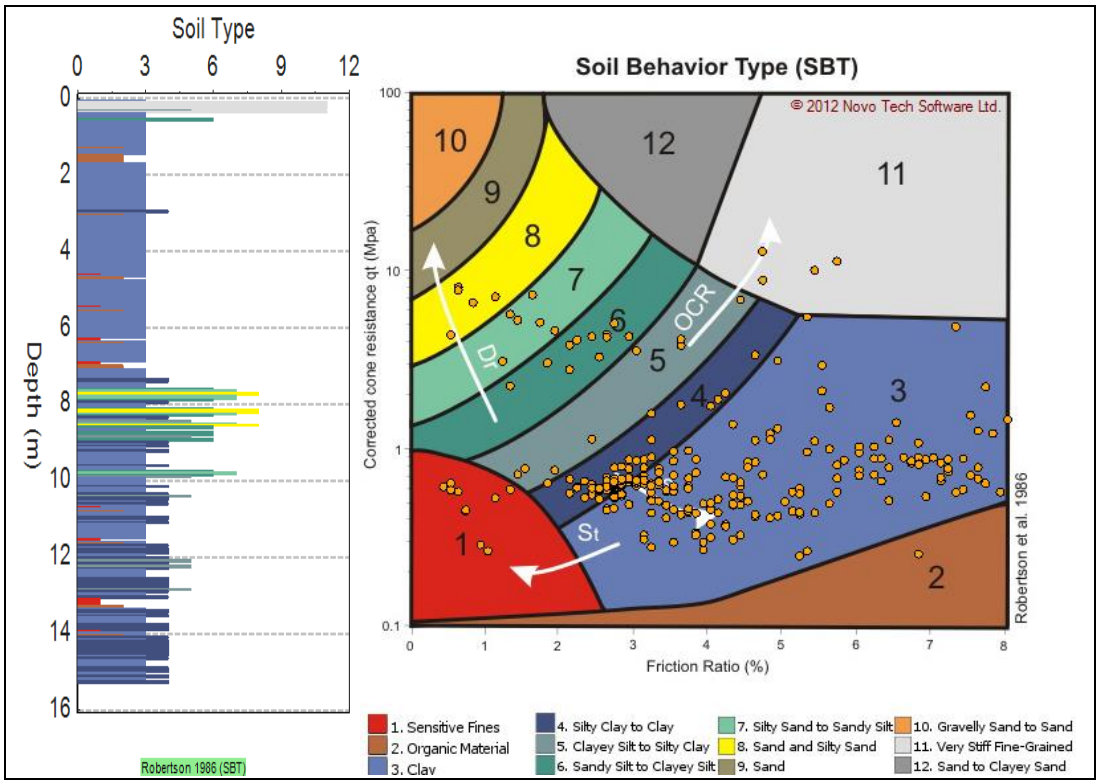

Figure 5.8: Soil Classification by NovoCPT Software for CPT 7

Most of the soil behavior type in CPT 8 with 7.85 meter depth is clay and some small thickness after 7 meter depth is included of sand and silty sand as shown in Figure 5.9, because of that for this location seven layers defined for analyze as a clay. Table 5.9 shows the FS parameters in each layer and most of them is more than 1, so liquefaction is not predictable with low magnitude earthquake and it probably accrued during or after 7 or more Richter earthquake.

Table 5.9: Liquefaction Results by NovoCPT Software for CPT 8

Depth	**SBT**	**q_c (MPa)**	**Vs (m/s)**	**FS $_6$**	**FS $_{6.5}$**	**FS $_7$**
0 – 1.8	clay	3.7	278.9	4.88	3.98	3.29
1.85 – 3.2	clay	0.78	109.1	4.67	3.8	3.15
3.25 – 4.9	clay	0.29	62	1.64	1.33	1.1
4.95 – 6.55	clay	0.32	66	1.3	1.06	0.87
6.6 – 7.85	clay	3.23	255.1	3.19	2.6	2.15

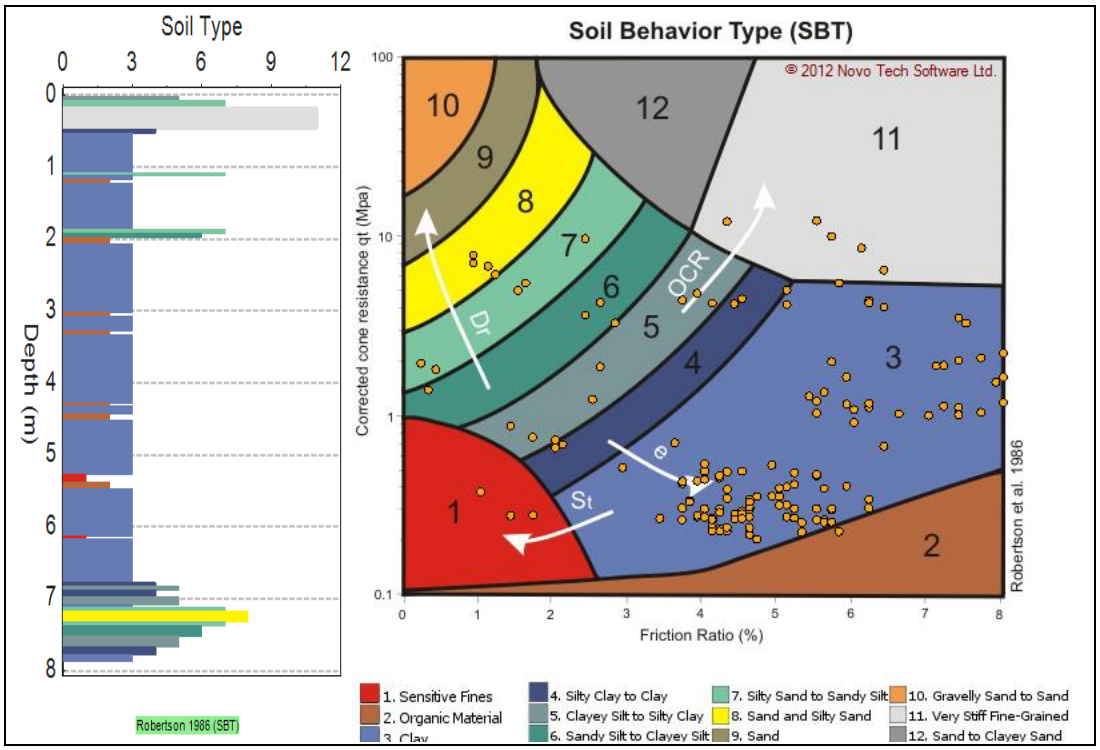

Figure 5.9: Soil Classification by NovoCPT Software for CPT 8

CPT 9 with 13.85 m excavation consist of clayey silt to silty clay, clay and silty clay as it shown in Figure 5.10 according to Robertson' chart in 1986. Table 5.10 is presented that FS values is decreasing to 1 or less than one after 4 meter depth, it shows liquefaction maybe happened when magnitude earthquake is more than 6.5. More information about probability of liquefaction is reported in following parts.

According to the FS results by NovoCPT software, presented in Table 5.11, CPT 10 has critical condition to liquefaction; this location with 18.75 meter excavation involved of clay and silty clay to clay for soil classification and also sensitive fine is observed after 6 meter depth, as shown in Figure 5.11. Most of the factor of safety values after second layer are less than one for three scenario assumed in this study, so the percentage of liquefaction probability in CPT 10 is higher than most of the another locations.

Table 5.10: Liquefaction Results by NovoCPT Software for CPT 9

Depth	SBT	q_c (MPa)	Vs (m/s)	FS $_6$	FS $_{6.5}$	FS $_7$
0 – 2	clayey silt to silty clay	3.8	283	4.87	3.97	3.28
2.05 – 4	clay	0.79	114.5	5.98	4.87	4.03
4.05 – 6.5	clay	0.56	91.8	2.63	2.14	1.77
6.55 – 8.75	silty clay to clay	0.95	123	2.66	2.17	1.79
8.8 – 11.05	clayey silt to silty clay	2.4	204	2.83	2.31	1.91
11.1 – 12.55	clay	0.7	105	1.32	1.08	0.89
12.6 - 13.85	clay	0.83	116.4	1.51	1.23	1.02

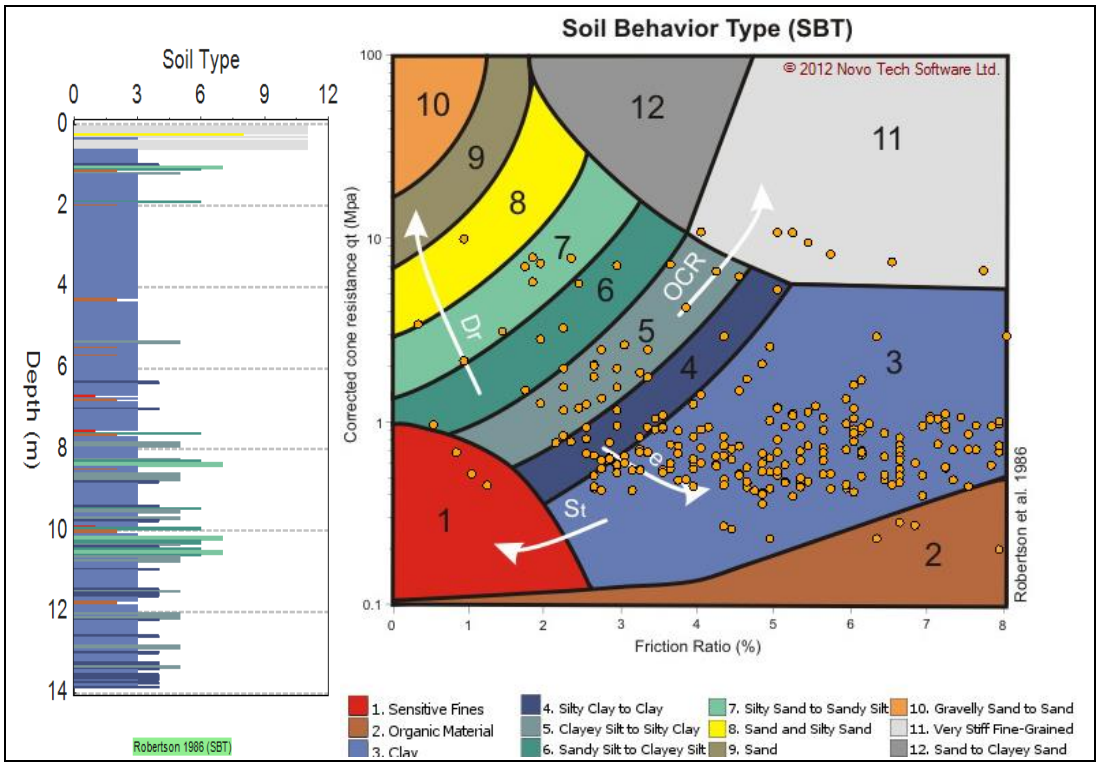

Figure 5.10: Soil Classification by NovoCPT Software for CPT 9

Table 5.11: Liquefaction Results by NovoCPT Software for CPT 10

Depth	SBT	q_c (MPa)	Vs (m/s)	FS $_6$	FS $_{6.5}$	FS $_7$
0 – 3	clay	1.28	146.3	5.64	4.59	3.89
3.05 – 6.6	clay	0.75	110	4.25	3.46	2.86
6.65 – 9.95	silty clay to clay	0.34	68.2	0.83	0.68	0.56
10 – 11.65	clay	0.41	79	0.76	0.62	0.51
11.7 – 13.65	silty clay to clay	0.42	82.5	0.82	0.66	0.55
13.7 – 15.75	clay	0.53	98.1	0.88	0.72	0.59
15.8 – 17.25	silty clay to clay	0.58	103.8	0.89	0.72	0.6
17.3 – 18.75	silty clay to clay	0.67	113.6	1.02	0.83	0.69

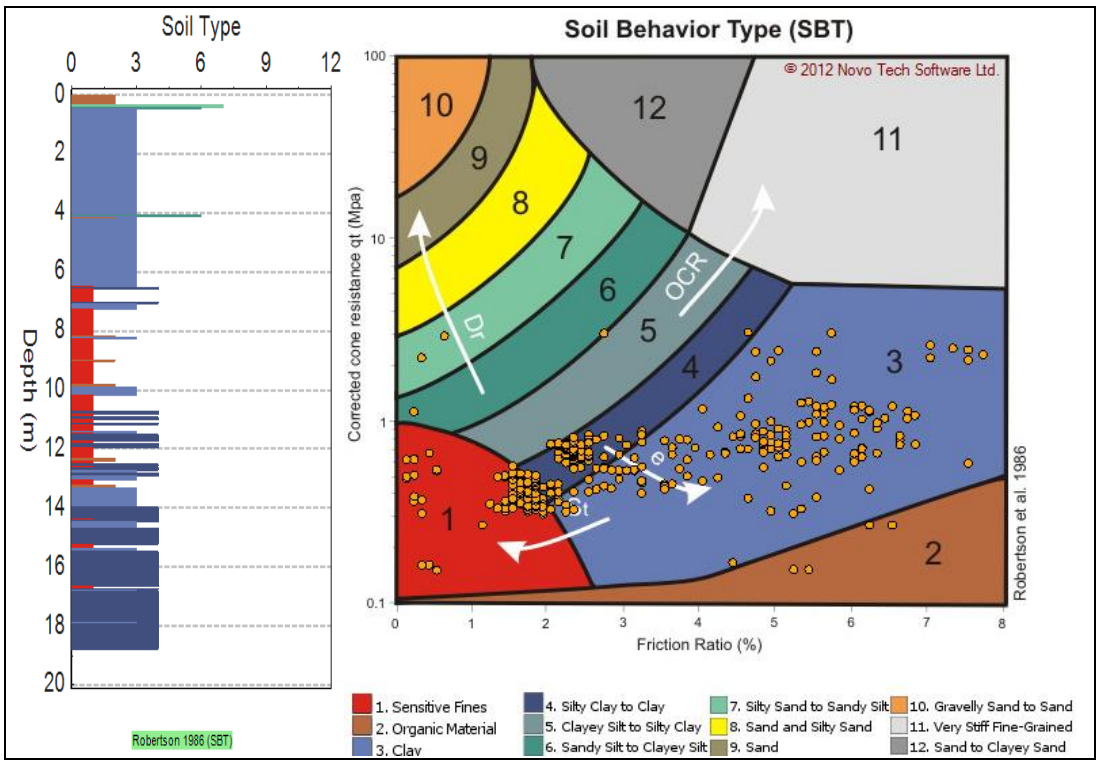

Figure 5.11: Soil Classification by NovoCPT Software for CPT 10

Summary of NovoCPT results for all CPT locations are presented in Table 5.12. This table included total depth for each location, liquefiable depth, it means that which depth of each location is predictable to liquefaction according to FS values, shear average of shear wave velocity, CSR and CRR in total depth, and also FS is estimated in two parts, average of total FS in total depth and average of FS in liquefiable depth for all CPT locations for all scenarios magnitude earthquake assumed in this study. Most of the factor of safety against liquefaction value as it shown in Table 5.12 are near to 1 or less than one, especially for 7 magnitude earthquake and it seems that liquefaction will happen for most of the 10 locations during or after 6.5 or more than 6.5 magnitude earthquake and of course it depends on soil behavior type in each location.

5.3.2 Assessment of Liquefactıon Potential Index, Probability and Severity

For the purpose of this study, empirical formulas, in-situ CPT data and these software programs applications are combined to produce a better realistic liquefaction assessment. The various standardized empirical methods as proposed by Chen and Juang (2000), Iwasaki et al. (1982), Sonmez and Gokceoglu (2005), to quantify *LPI*, P_L and *Ls* were utilised in this study to interpret the results obtained.

These parameters were generated for the earthquake magnitude that is more peculiar to the Tuzla region, which is M_w = 6.0, M_w = 6.5, M_w = 7 at a_{max} = 0.3g but another software information for M_w = 6.5 is included in Appendix A and B. The results are given in Table 5.12, and the P_L parameters were categorized according to Chen and Juang, (2000) and Yalcin et al. (2008). For the three power earthquake magnitude, the liquefiable zone, and the total depth were considered for each of the CPT locations.

Table 5.12: Potential liquefaction parameters for different earthquake magnitudes in study area

CPT #	Depth(m)	Liquefiable Depth	Vs (m/s)	CSR	CRR	M_w = 6		M_w = 6.5		M_w = 7	
						FS total	FS liq	FS total	FS liq	FS total	FS liq
CPT 1	17.8	6.3 - 8	294.5	0.173	0.236	2.41	1.53	1.96	1.3	1.62	1.07
CPT 2	3.9	2.75 - 3	489.3	0.192	0.348	3.21	1	2.61	0.84	2.15	0.74
CPT 3	18.6	7 - 18.5	126.8	0.172	0.243	3.36	1.53	1.93	1.25	1.59	1.03
CPT 4	17.95	8.4 - 17.9	117.3	0.173	0.231	2.25	1.14	1.83	0.92	1.51	0.76
CPT 5	17.55	5.9 - 17.45	132	0.174	0.224	2.2	0.91	1.79	0.77	1.47	0.6
CPT 6	20.1	7 - 15	110.2	0.168	0.227	2.28	1.05	1.85	0.86	1.54	0.71
CPT 7	15.3	11.5 - 15	137.5	0.178	0.306	2.92	0.94	2.38	0.76	1.97	0.64
CPT 8	7.85	4.5 - 6.7	153	0.189	0.334	3.11	1.2	2.53	0.98	2.09	0.81
CPT 9	13.85	11.7 - 12.75	150	0.181	0.338	3.23	1.22	2.63	0.98	2.18	0.88
CPT 10	18.75	7.15 - 18.6	101	0.171	0.236	2.28	0.84	1.85	0.69	1.54	0.59

In all the CPT locations, the minimum to maximum liquefiable zone by thickness ranges from 0.5 m to 12 m out the total depth of 20 m. The liquefiable zone dimension by percentage to total depth is thus 1.5% to 60% by dimensional size.

The CSR_{avg}, CRR_{avg} and FS_{avg} values provided have indicated that within the liquefiable zone, the soil types shown are prone to liquefaction. The factor of safety against liquefaction for all the CPT locations suggested that the liquefiable zone within the total depth locations have the potential for liquefaction.

For the earthquake magnitude of $M_w = 6$ at $a_{max} = 0.3g$, The CPT 5, 7 and 10 locations comprise the sand, silt and gravel mixtures which are susceptible to low or moderate liquefaction. For the earthquake magnitude of $M_w = 6.5$ at $a_{max} = 0.3g$, all The CPT locations except CPT 1 and CPT 3 are majorly of organic soil, sand and silt mixture, which are also trend to liquefaction potential. Similar parameters were obtained for CPT 1 and CPT 3 locations for the earthquake magnitude of $M_w = 7.0$ at $a_{max} = 0.3g$.

From all indications, it is observed during earthquake magnitude of $M_w = 6$ at $a_{max} = 0.3g$ according to Iwasaki et al. (1982) as indicated in Table 5.13 that the liquefiable zone shows very low to very high classification for liquefaction potential index (*LPI*), and also, similar parameters show indications of very low to very high categories liquefaction during earthquake magnitude of $M_w = 6.5$ and 7 at $a_{max} = 0.3g$ according to Iwasaki et al. (1982) as indicated in Table 5.14 to Table 5.15. Meanwhile, in more general terms, and for more classification, Sonmez (2003) modified classification, *FS* term was applied to the liquefaction severity (L_S) by

considering the threshold value of 1.2 between the non-liquefiable and slightly liquefied classification as provided in Table 5.16 to Table 5.18.

Therefore, as a result of Sonmez (2003) classification, the soil layers in the liquefiable zone and all CPT locations fall into the classification categories from Non-liquefied to very high for liquefaction severity. Meanwhile, the classification for the whole layers for all CPT locations is broadly non-liquefiable. This is an indication that it is only a few meters of the soil layers within the whole thickness of soil deposit at each CPT probe location that are liquefiable. On a general note, the study area, the Tuzla zone is not potentially susceptible or trend to liquefaction and it does not mean that the probability of liquefaction in this area is zero percent because according to the results In some parts of the drilling there is possibility of severe liquefaction and it depends on the soil type in that area and also size and duration of cyclic loading. The results showed that potential and probability of liquefaction during the earthquake with 7 magnitude is more than earthquakes with 6.5 or 6 magnitudes.

Table 5.13: Liquefaction potential categories for M_w=6, a_{max}=0.3g (Iwasaki, 1982)

CPT #	***LPI***	**Liquefaction Potential Classification**
1	0	Very low
2	1.98	Low
3	0	Very low
4	0.15	Low
5	9	High
6	0.79	Low
7	6	High
8	0	Very low
9	0	Very low
10	16	Very High

Table 5.14: Liquefaction potential categories for M_w=6.5, a_{max}=0.3g (Iwasaki, 1982)

CPT #	*LPI*	Liquefaction Potential Classification
1	0	Very low
2	16	Very High
3	0	Very low
4	8	High
5	23	Very High
6	14	High
7	24	Very High
8	2.87	Low
9	2.87	Low
10	31	Very High

Table 5.15: Liquefaction potential categories for M_w=7, a_{max}=0.3g (Iwasaki, 1982)

CPT #	*LPI*	Liquefaction Potential Classification
1	0.54	Low
2	26	Very High
3	1.14	Low
4	24	Very High
5	40	Very High
6	29	Very High
7	36	Very High
8	19	Very High
9	12	High
10	41	Very High

Table 5.16: Liquefaction severity categories for M_w=6, a_{max}=0.3g (Sonmez, 2005)

CPT #	L_S	Liquefaction Severity Classification
1	0	Non-liquefied
2	45	Moderate
3	0	Non-liquefied
4	31	Low
5	56	Moderate
6	40	Moderate
7	52	Moderate
8	26	Low
9	25	Low
10	64	Moderate

Table 5.17: Liquefaction severity categories for M_w=6.5, a_{max}=0.3g (Sonmez, 2005)

CPT #	L_S	Liquefaction Severity Classification
1	27	Low
2	64	Moderate
3	23	Low
4	54	Moderate
5	73	High
6	62	Moderate
7	74	High
8	47	Moderate
9	47	Moderate
10	81	High

Table 5.18: Liquefaction severity categories for M_w=7, a_{max}=0.3g (Sonmez, 2005)

CPT #	L_S	Liquefaction Severity Classification
1	38	Moderate
2	76	High
3	42	Low
4	74	High
5	89	Very High
6	79	High
7	86	Very High
8	68	High
9	59	Moderate
10	90	Very High

Therefore, to explain the liquefaction potential of the soil within the liquefiable zone and total depth, Cheng and Juang (2000) classification was employed. According to the liquefaction probability values obtained for the soil layer total depth, it was observed that about 50% of the total CPT locations analyzed are unlikely or almost certain that it will not liquefy during earthquake magnitude of M_w = 6 at a_{max} = 0.3g which are the CPT 1, 3, 4, 8 and 9 locations. Also, another 50% at CPT locations of CPT 2, 5, 6, 7 and 10 are of the class in which liquefaction or non-liquefaction is equally likely to occur. During earthquake magnitude of M_w = 6.5, CPT 1 and 3 are unlikely, CPT 2, 4, 6, 8, 9 are Liquefaction/non-liquefaction is equally likely, and CPT 5 and 7 are very likely. For the 7 magnitude earthquake CPT 1, 3 and 7 are Liquefaction/non-liquefaction is equally likely and another CPT locations are very likely and almost certain that it will liquefy. This is well represented in Table 5.19 to 5.21, and it is remarkably supported by the analysis illustrated in Table 5.16 to 5.18.

Table 5.19: Liquefaction probability classification for M_w=6, a_{max}=0.3g (Chen and Juang, 2000)

CPT #	(P_L)	Description
1	0	Almost certain that it will not liquefy
2	0.45	Liquefaction/non-liquefaction is equally likely
3	0	Almost certain that it will not liquefy
4	0.31	Unlikely
5	0.56	Liquefaction/non-liquefaction is equally likely
6	0.4	Liquefaction/non-liquefaction is equally likely
7	0.52	Liquefaction/non-liquefaction is equally likely
8	0.26	Unlikely
9	0.25	Unlikely
10	0.64	Liquefaction/non-liquefaction is equally likely

Table 5.20: Liquefaction probability classification for M_w=6.5, a_{max}=0.3g (Chen and Juang, 2000)

CPT #	(P_L)	Description
1	0.27	Unlikely
2	0.64	Liquefaction/non-liquefaction is equally likely
3	0.23	Unlikely
4	0.54	Liquefaction/non-liquefaction is equally likely
5	0.73	Very likely
6	0.62	Liquefaction/non-liquefaction is equally likely
7	0.74	Very likely
8	0.47	Liquefaction/non-liquefaction is equally likely
9	0.47	Liquefaction/non-liquefaction is equally likely
10	0.81	Very likely

Table 5.21: Liquefaction probability classification for M_w=7, a_{max}=0.3g (Chen and Juang, 2000)

CPT #	(P_L)	Description
1	0.38	Liquefaction/non-liquefaction is equally likely
2	0.76	Very likely
3	0.42	Liquefaction/non-liquefaction is equally likely
4	0.74	Very likely
5	0.89	Almost certain that it will liquefy
6	0.79	Very likely
7	0.86	Almost certain that it will liquefy
8	0.68	Very likely
9	0.59	Liquefaction/non-liquefaction is equally likely
10	0.9	Almost certain that it will liquefy

5.3.3 Assessment of Site Response Analysis

Site response analysis could be the first step to study seismic soil-structure. Geotechnical earthquake engineering is trying to find the perfect solution for analyzing the ground responses when the earthquake loadings happen, then this study has tried to analyze the ground response for eastern coast of Cyprus during 6.5 magnitude earthquakes loading.

The DeepSoil code which has the capability of performing the linear and nonlinear analysis is adopted to evaluate the site response analysis. DeepSoil software originally has 13 motions such as Chichi, Kobe, Coyote, etc. these motions are as a default of software which can be useful for comparison with another profile (Hashash et al. 2010). On the other hand in this study, 10 ground motions has founded (http://peer.berkeley.edu) which occurred and recorded in the past and are too close to study area are added to DeepSoil software to achieve the realistic

analysis data. The Tuzla region located in Famagusta North Cyprus is selected as the study site, consisting of marine or alluvial deposits, and for earthquake resistant design in this area, shear wave velocity (Vs) was considered as 700 m/s for bedrock and 5% damping in total, (Wair & Shantz, 2012).

Site response analysis is so important to design structures. Site response curves included spectral acceleration versus period. This curve is founded by peak ground acceleration and shear wave velocity for each area depends on soil classification. There are some standard codes to define the special period, for instance, current periods to estimation of spectral acceleration in Cyprus are 0.2 sec, 1.0 sec and 1.2 sec, Bommer & Pinho, (2004). These periods in deeded to evaluation of period of building and they will applied during building design in civil engineering. So in this study by using DeepSoil software, response analysis for each CPT locations is done and response acceleration for first layer compared with input motion and the values of ground acceleration for 0.2, 1.0, and 1.2 sec and the average of total amount of PSA for first layer and input motion are estimated, as given in Table 5.22.

According to the DeepSoil chart for each CPT location, which shows that most of the first layers at the CPT probe location are below the critical input motion value except CPT 1, 2, 4, and 9. In consideration of the average of the first layer within all the CPT locations, there is only one CPT location, precisely CPT 2 which has a higher value than the corresponding critical input motion value. This is due to the response spectrum of CPT 2 is 0.805 at period 0.2 sec and 0.524 at period 1.2 sec.

Although, some of the response spectra periods for the first layer are higher than the critical input motion, their average total value in this layer is less than the critical

input motion. Then these values cannot be significant for the response spectrum or to consider these parameters for further analysis. Generally, because of 5% damping, 0.3g for peak ground acceleration, soil behavior type and liquefaction tendency in this area, ground oscillation, and natural frequency can be critical during vibration or ground surface shaking induced by large earthquake magnitude scales such as 7 Richter and higher values.

Table 5.22: Response spectrum for all CPT locations by DeepSoil software

CPT #	Response Spectrum Acceleration			Average of PSA	
	0.2 (sec)	1 (sec)	1.2 (sec)	First Layer	Input Motion
CPT 1	0.209	0.305	0.457	0.199	0.361
CPT 2	0.805	0.198	0.524	0.43	0.361
CPT 3	0.101	0.094	0.137	0.118	0.361
CPT 4	0.29	0.174	0.673	0.177	0.361
CPT 5	0.063	0.117	0.185	0.097	0.361
CPT 6	0.154	0.133	0.195	0.153	0.361
CPT 7	0.095	0.17	0.235	0.129	0.361
CPT 8	0.134	0.209	0.232	0.133	0.361
CPT 9	0.19	0.378	0.362	0.187	0.361
CPT 10	0.093	0.1	0.164	0.086	0.361
AVERAGE	**0.204**	**0.188**	**0.316**	**0.171**	**0.361**

Although, the average of spectral acceleration for first layers in all CPT locations except CPT 2 because of the shallow drilling in there, but critical time of acceleration during earthquake loading is required to any structure design. Figure 5.12 consist of pseudo spectral acceleration curve for 10 CPT locations is offered to find the critical period of acceleration. CPT locations are numbered (a) to (j) respectively.

Critical value of period is a particular time when spectral acceleration curve for first layer (blue line) cut off the input motion (black line) as a high level, it means that after this time the value of PSA for first layer should be more than the value of input motion. This parameter for each location is reported in below, this parameter was not applicable for CPT 2 due to the shallow drilling in this location.

CPT #	1	2	3	4	5	6	7	8	9	10
Period (sec)	0.73	0.0	2.09	1.35	1.53	1.44	1.27	0.93	0.68	1.85

Extra information such as PGA (g), maximum shear strain (%), stress ratio curve versus depth and also pseudo spectral velocity diagram for each location are analyzed, as given in Appendix C.

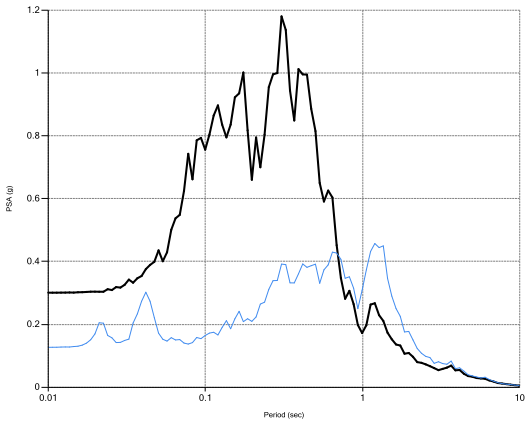

(a)

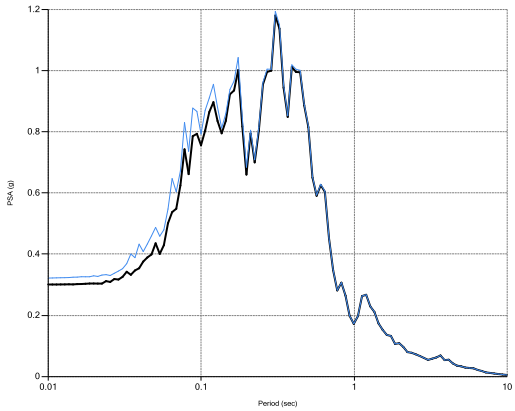

(b)

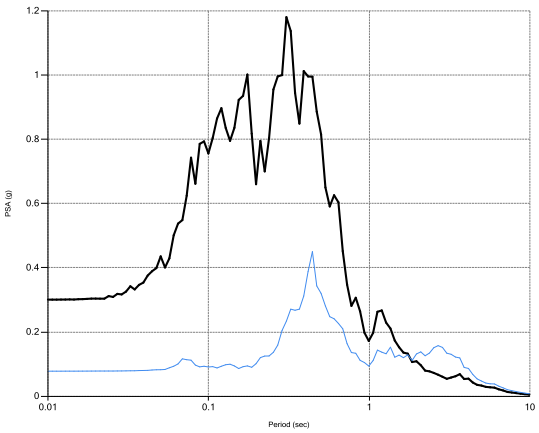

(c)

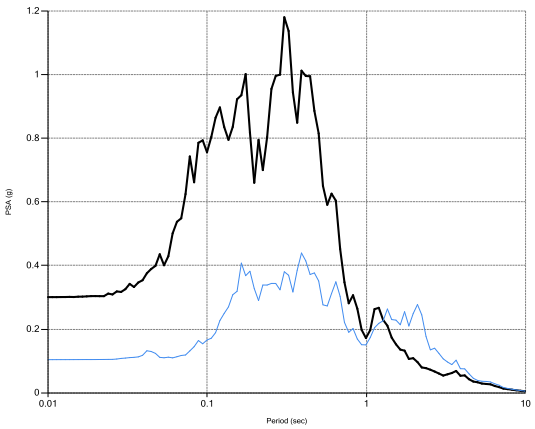

(d)

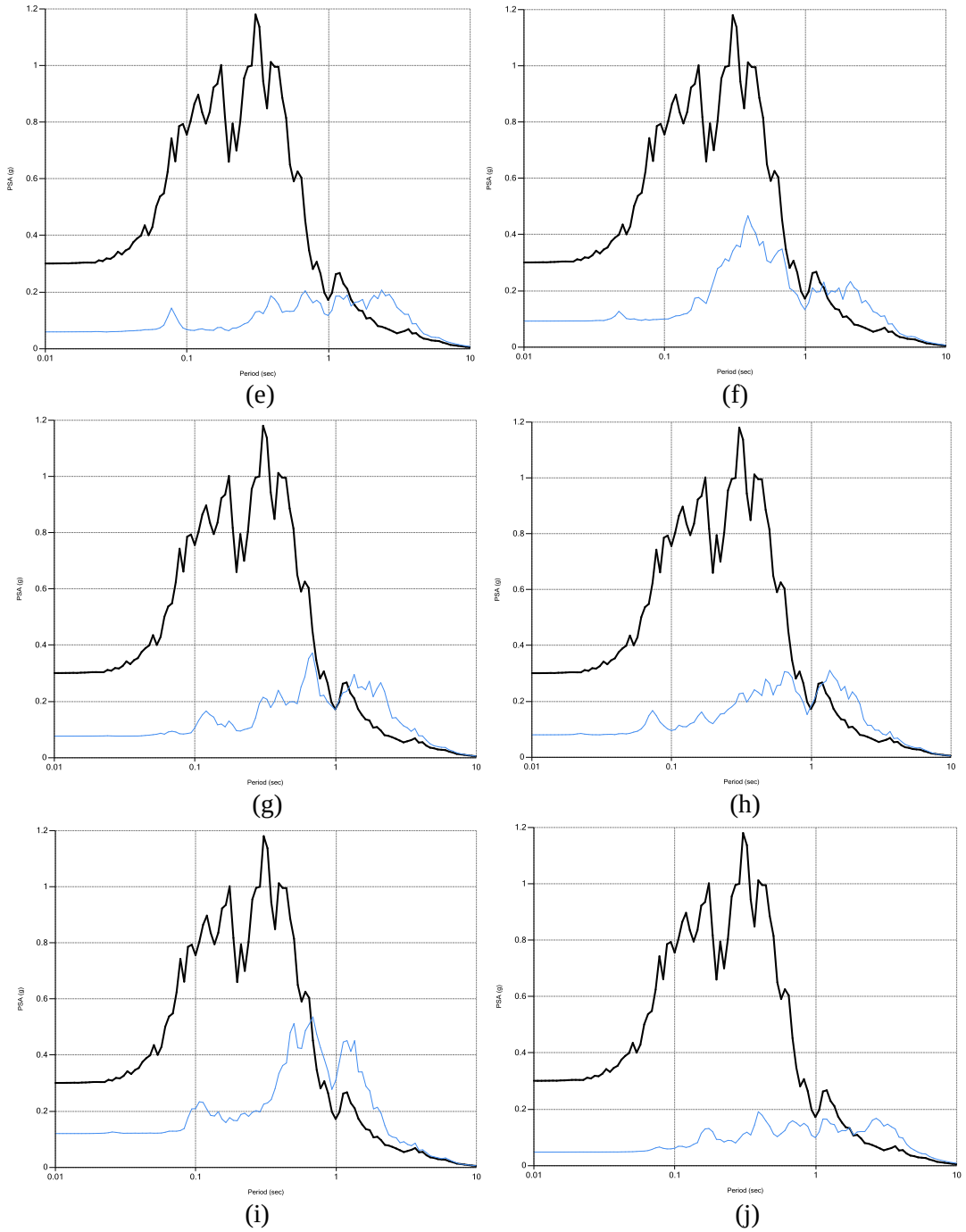

(e) (f)

(g) (h)

(i) (j)

Figure 5:12: Comparison of Response Spectral Acceleration for all CPT locations by DeepSoil Software. (Blue line shows first layer and input motion is Black)

Figure 5.13 is divided into two parts, first part shows all first layer's PSA curve, included CPT 1 to 10 and input motion and second part is presented the average of total PSA curves compared with input motion. Critical period for first layers average curve is calculated 1.27 sec.

Therefore engineers must be aware of this issue that the period of building should not be considered less than 1.27 sec, so they should be sure about appropriate consolidation and compaction of soil before designing and constructing structure in this area. This is in good correlation with the results obtained from the analysis of the CPT data using the NovoCPT and LiqIT software programs.

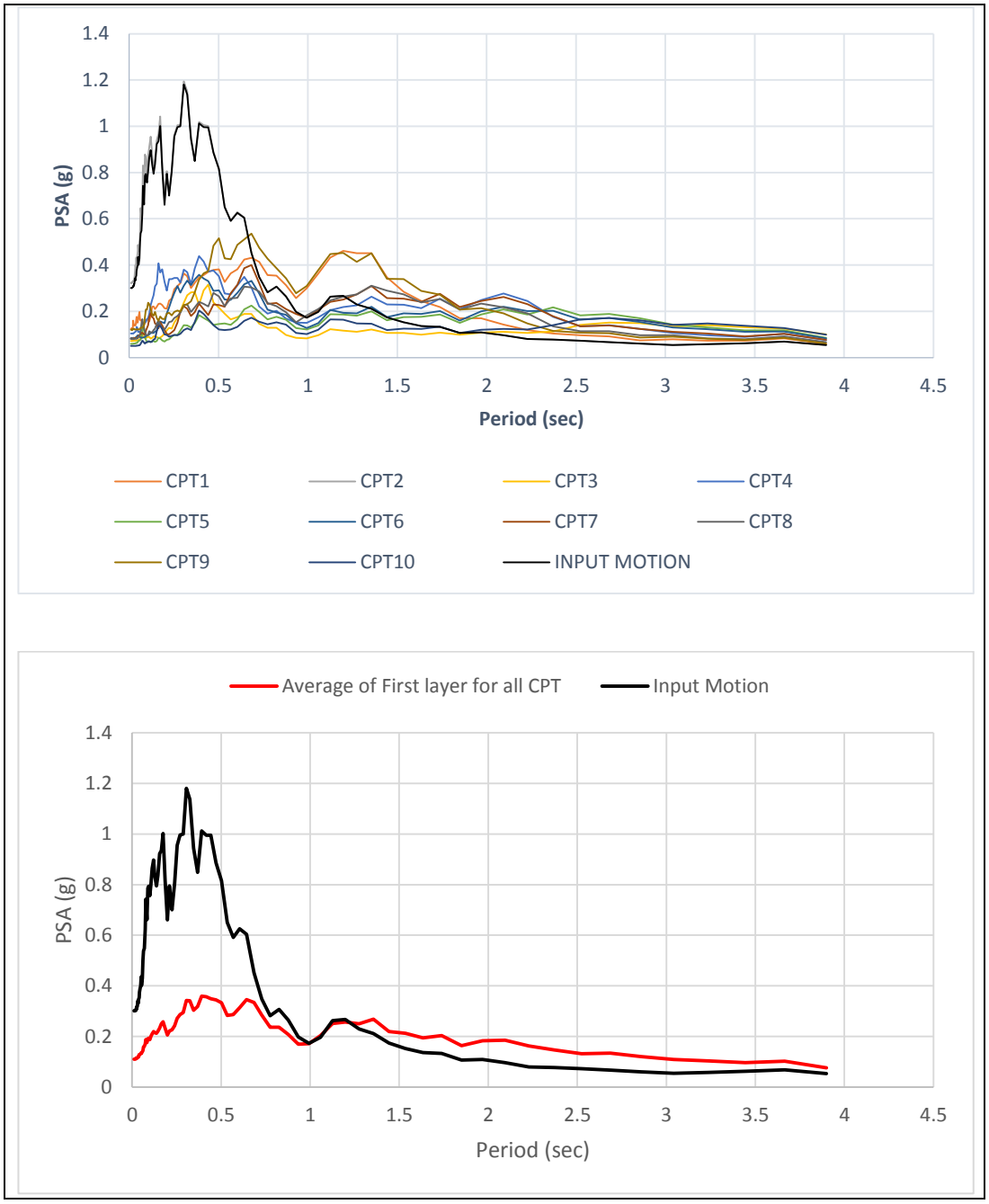

Figure 5:13: Average of Response Spectral Acceleration for all CPT Locations between Input Motion and First Layers

5.3.4 Assessment of Response Displacement, Velocity and Acceleration

In this section of the thesis, the response displacement, velocity and acceleration of the first layer and bedrock were investigated by using DeepSoil software and then they were scaled by using SeismoSignal software with 5.0% damping. As indicated in Table 5.23.

Response acceleration, velocity and displacement versus period (sec) scaled base on study assumption and they are shown in Figure 5.14 to 5.23. Soil depth, H, is one of the effective parameters so the first layer and bedrock for each CPT locations were modeled and compared.

In this study, it was considered that the first layer is surface of the earth and bedrock has different depths according to defenition of DeepSoil software by using the NovoCPT results in each CPT logs. Therefore always higher acceleration occurs in bedrock layer because of Strength of earthquake, density, and nature of frequency compared to the first layer, displacement and velocity are higher in first layer when compared to bedrock. According to these three types of graphs for each CPT locations, given in Figure 5.14 to 5.23, and the results in Table 5.23, it can be observed that the depth has considerable effect on acceleration because all response acceleration values in bedrock are more than response acceleration values in the first layer and less impressive on velocity and displacement values for bedrock due to the higher value of response displacement and velocity in the first layer than bedrock. Values of response acceleration for all CPT location are near to each other, but other values are different because of the soil behavior type, the impaction, density of aggregates and nature frequency that they can be effective on these values.

According to these figures, approximately during the first period when the amplitudes of ground motion are high based on high energy absorption in depth and soil characteristics, the acceleration, velocity and displacement are high. On the other hand, when the amplitude decreases (during the second period) the absorbed energy is released and these parameters also dramatically decrease and reverse action will be happen for the first layer. This phenomenon has happened for all CPT locations.

The amounts of response displacement, velocity and acceleration for all bedrock locations are near to each other and variety values can be observed for the response of first layers and it exactly depends on soil behavior type and soil distribution in Tuzla area.

Table 5.23: Response analyzes by SeismiSignal software

CPT #	Period (sec)	Response Displacement		Response Velocity		Response Acceleration	
		First Layer	Bed Rock	First Layer	Bed Rock	First Layer	Bed Rock
CPT 1	4	14.08	10.19	46.63	39.11	0.199	0.217
CPT 2		10.51	10.49	41.4	41.08	0.23	0.228
CPT 3		16.53	10.13	38.56	39.51	0.13	0.22
CPT 4		17.32	10.16	48.63	39.46	0.19	0.218
CPT 5		18.84	10.22	47.7	39.6	0.15	0.21
CPT 6		18.32	10.15	48.82	39.3	0.17	0.21
CPT 7		17.74	10.21	49.64	39.87	0.18	0.22
CPT 8		15.54	10.38	45.3	40.58	0.17	0.225
CPT 9		15.69	10.24	51.96	39.46	0.21	0.218
CPT 10		17.77	10.15	41.75	39.53	0.13	0.219
AVERAGE		**16.23**	**10.23**	**46.04**	**39.75**	**0.179**	**0.221**

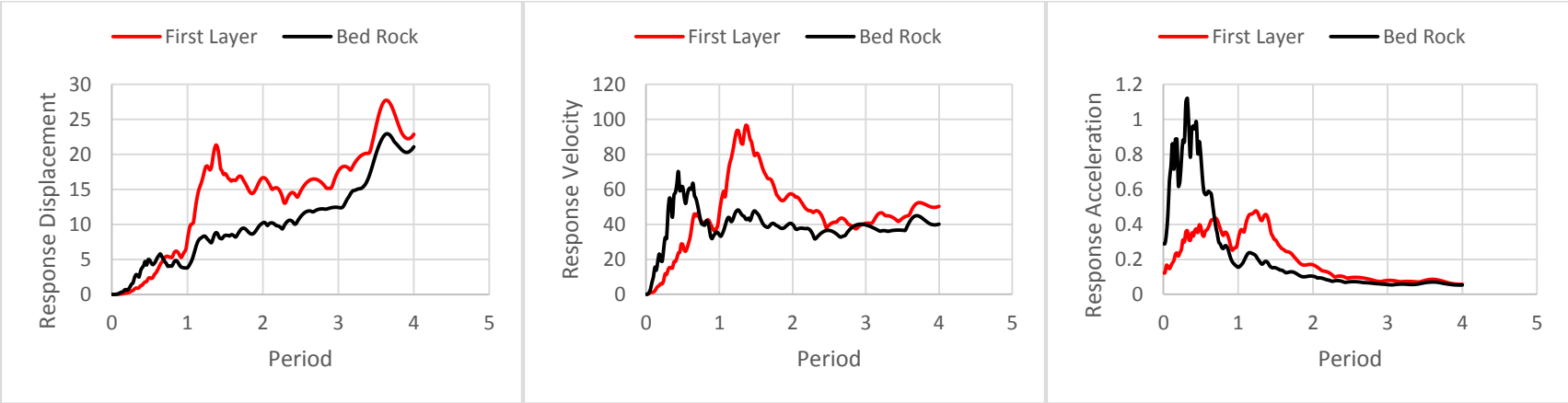

Figure 5.14: Response Analysis by SeismoSignal for CPT 1

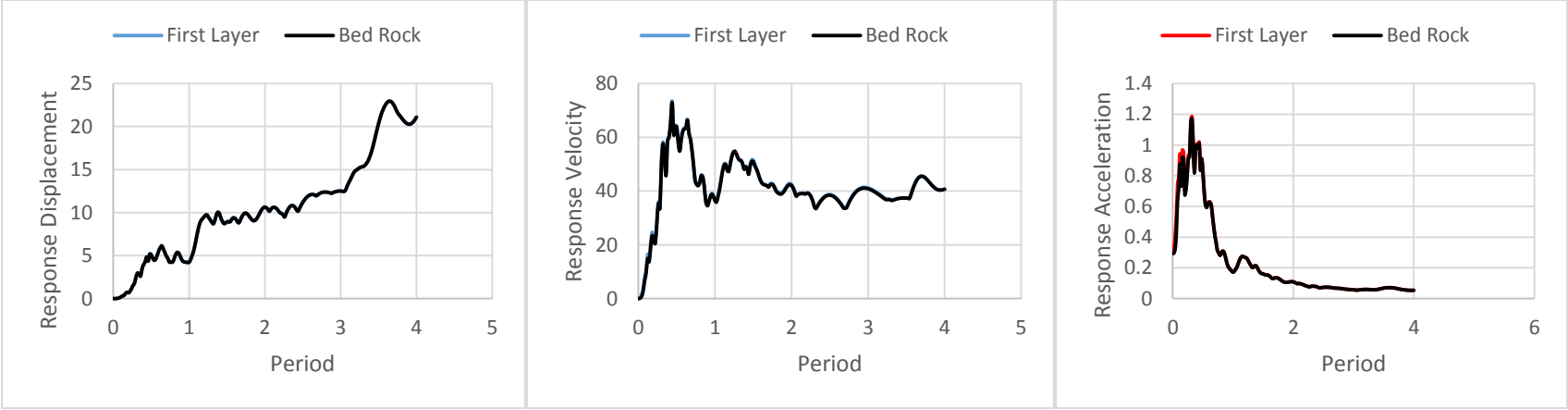

Figure 5.15: Response Analysis by SeismoSignal for CPT 2

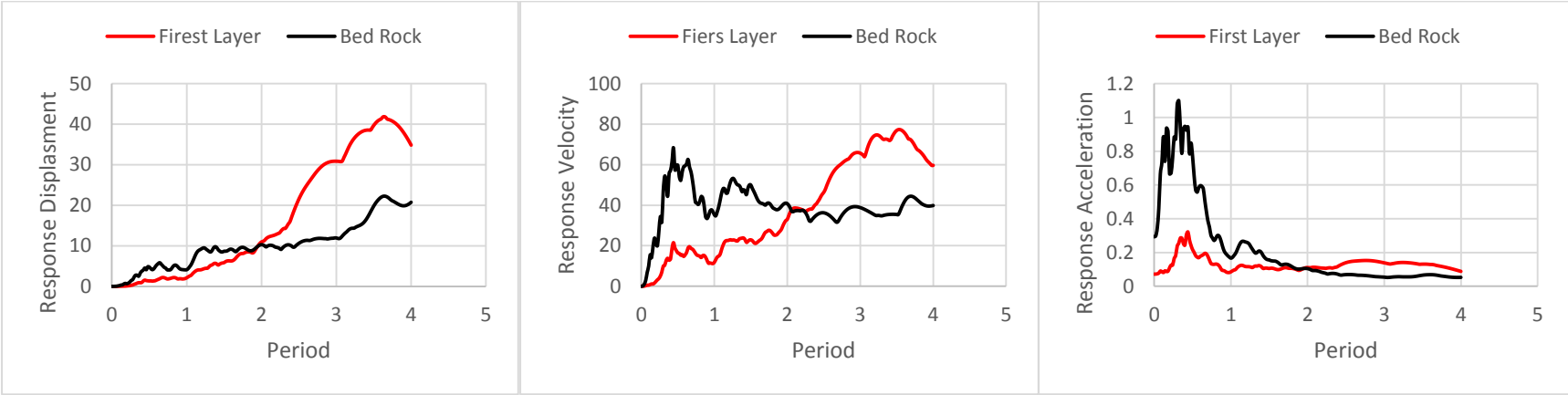

Figure 5.16: Response Analysis by SeismoSignal for CPT 3

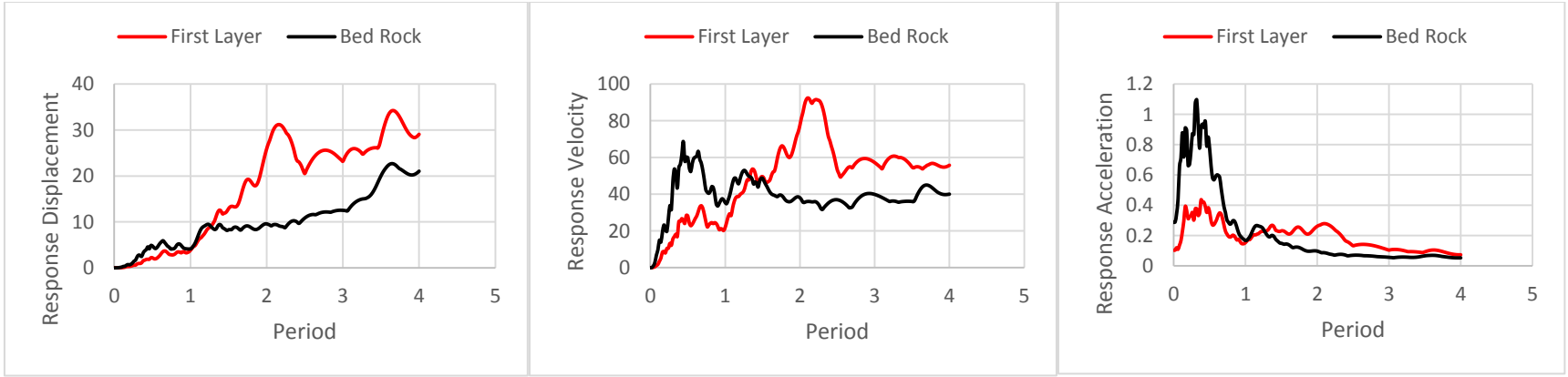

Figure 5.17: Response Analysis by SeismoSignal for CPT 4

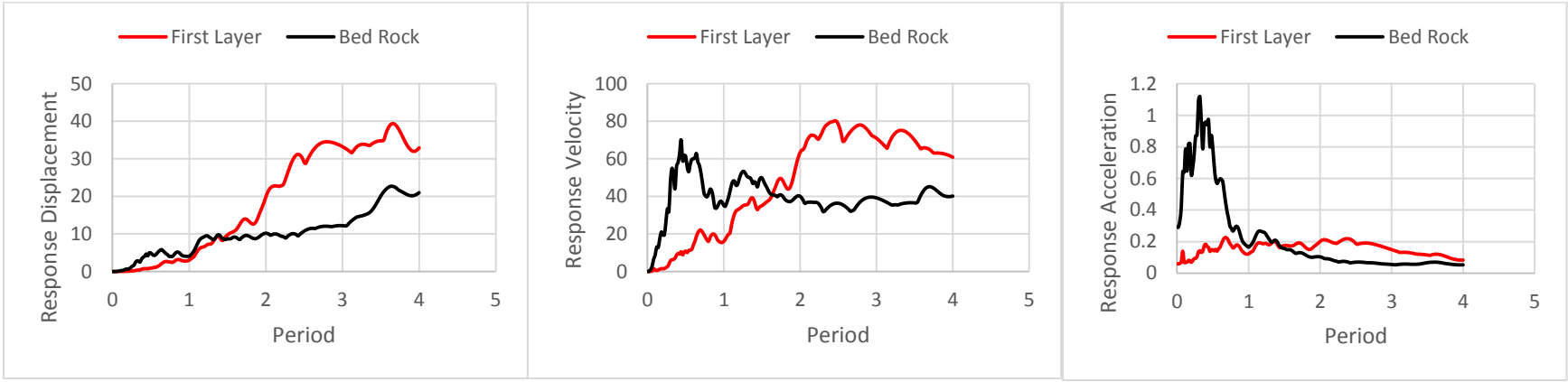

Figure 5.18: Response Analysis by SeismoSignal for CPT 5

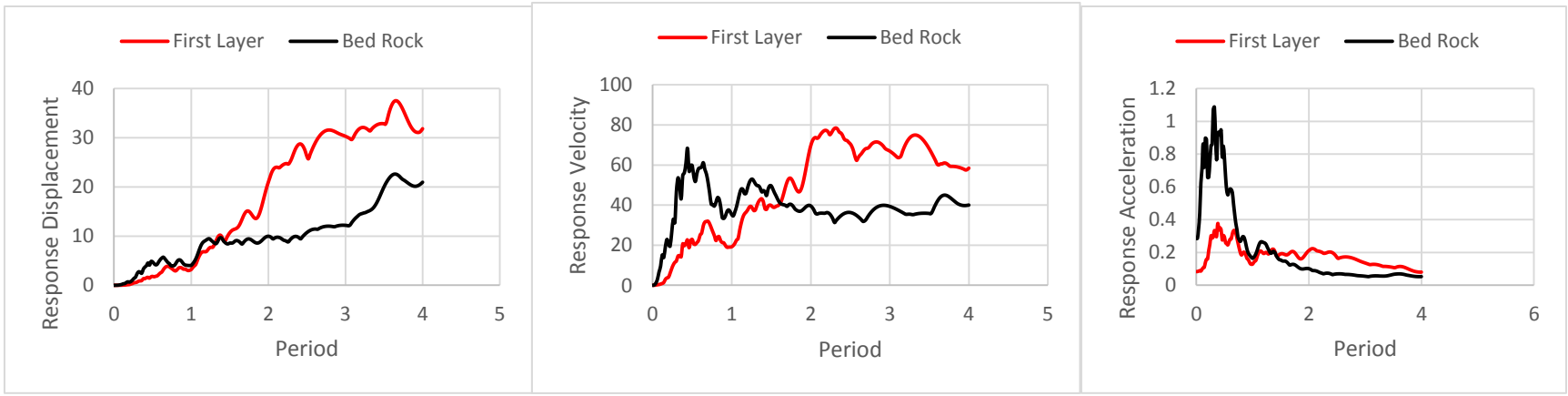

Figure 5.19: Response Analysis by SeismoSignal for CPT 6

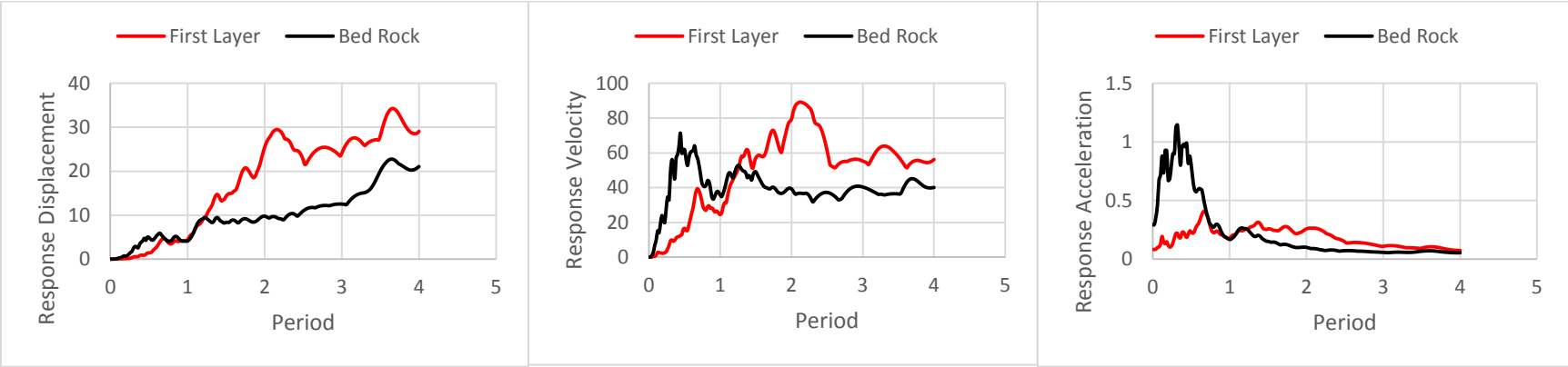

Figure 5.20: Response Analysis by SeismoSignal for CPT 7

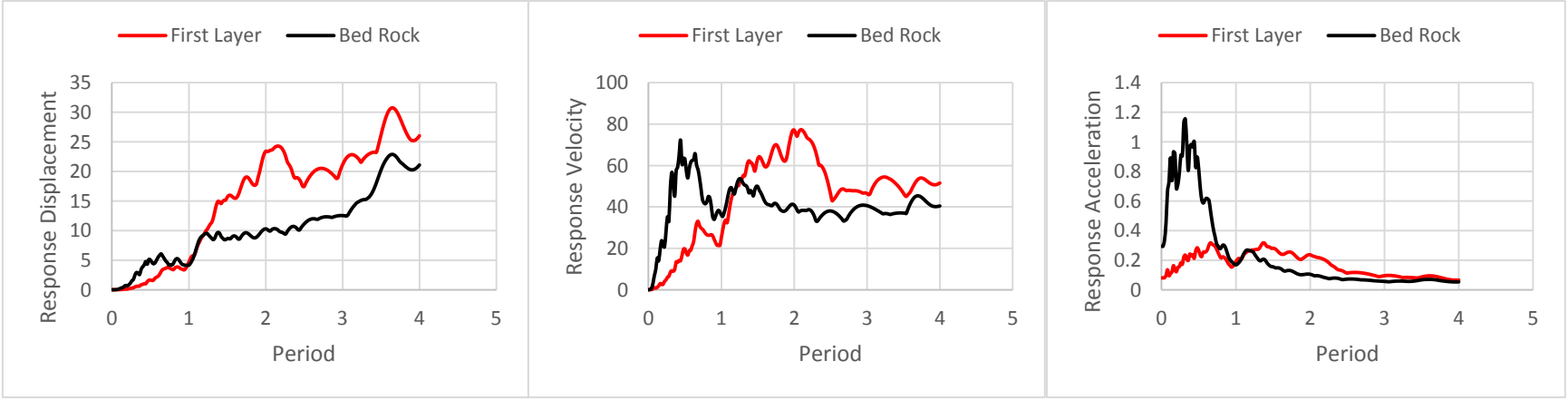

Figure 5.21: Response Analysis by SeismoSignal for CPT 8

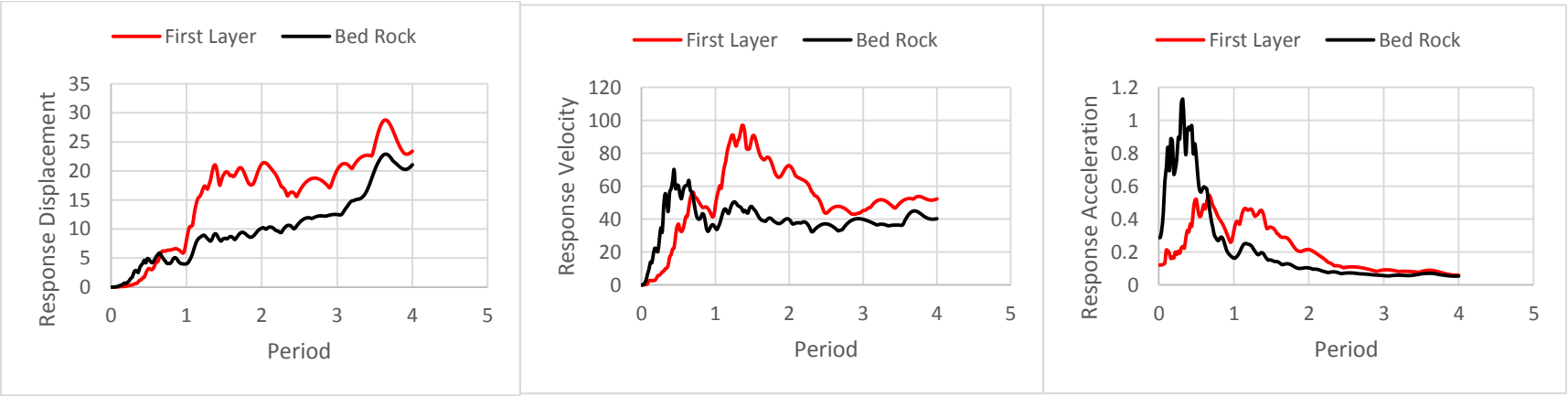

Figure 5.22: Response Analysis by SeismoSignal for CPT 9

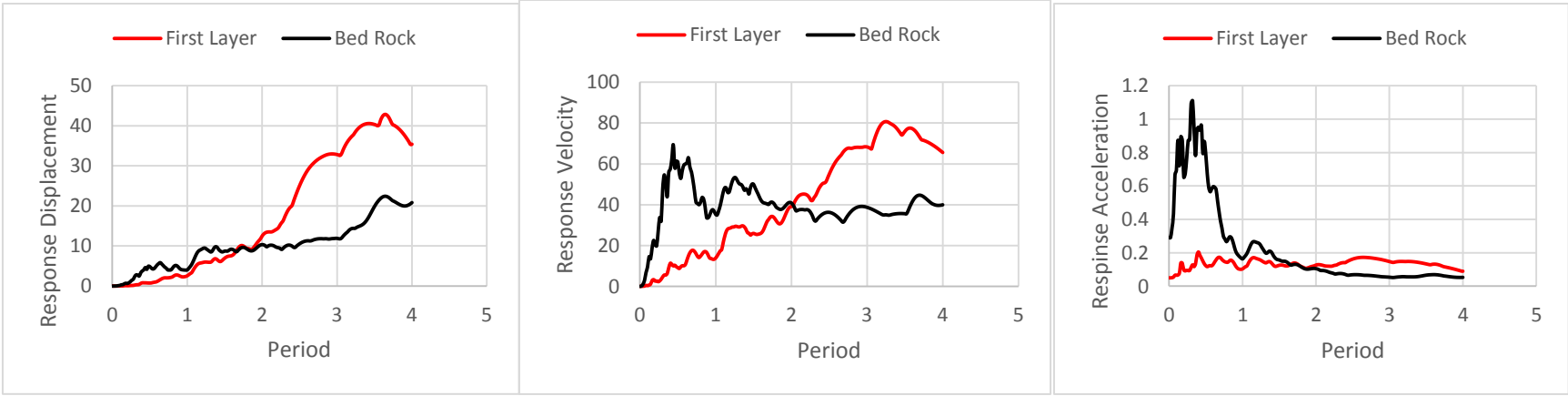

Figure 5.23: Response Analysis by SeismoSignal for CPT 10

Although, different values of first amplitude are observed in Figure 5.14 to 5.23 for response displacement, velocity, and acceleration diagrams, but Figure 5.24 is shown the total average of these parameters in study location. Duration of first amplitude for response displacement and acceleration are estimated 1.0 sec and 1.3 sec for velocity.

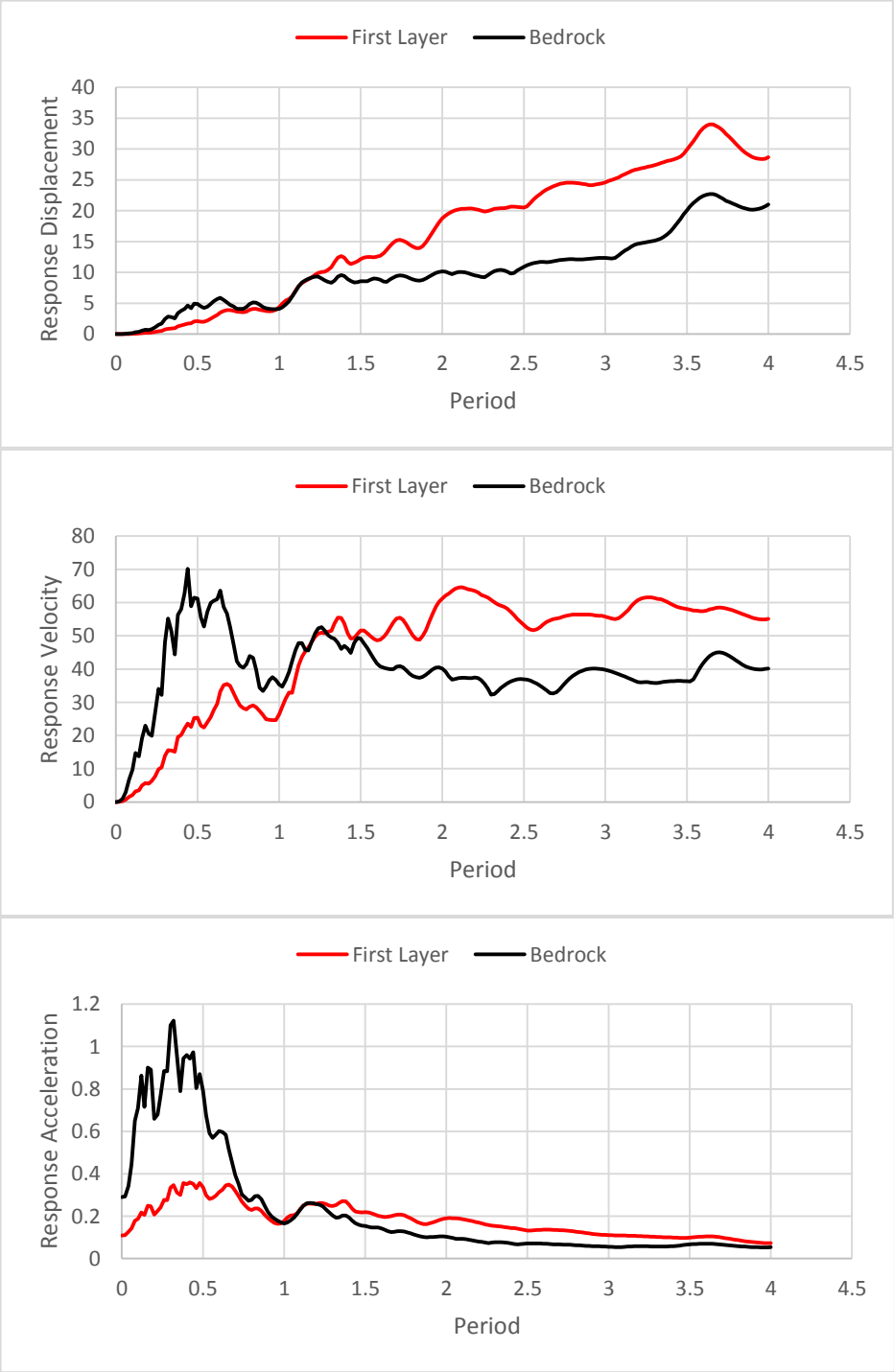

Figure 5.24: Average Response Analysis for First Layers and Bedrock

Chapter 6

CONCLUSION

This thesis studies the assessment of liquefaction properties such as CRR, CSR, liquefaction potential, probability, severity, factor of safety, shear wave velocity, magnitude scaling factor of the soil deposits in the eastern coast of Cyprus. The evaluation of the liquefaction parameters is quite a demanding task in the geotechnical investigation and exploration due to the complexity in the heterogeneous nature of the soils and the involvement of factors that determine the occurrence of liquefaction after the earthquake events at different regions of the world.

In this study, in-situ CPT method was deployed to acquire the required data for the various liquefaction analysis of the underground subsoil strata. According to the analyzed data, the soil stratigraphy comprises sand, silt, sand mixtures with gravels, organic soils and sensitive soils. The following conclusions were derived from the CPT analysis data obtained from the field:

1. The CPT data were obtained from the in situ field methods where the ten CPT locations were probed and the data acquired were subjected to the selected software program tools. These software program tools generated parameters useful for all kinds of analysis related to liquefaction. The CPT in-situ method was applied in this

study to evaluate liquefaction or cyclic failure susceptibility of soil deposit in Eastern coast of Cyprus.

2. The output data obtained from the CPT methods are analyzed by using the NovoCPT, LiqIT, DeepSoil and SeismoSignal software. The NovoCPT and LiqIT analyzed the input data to generate parameters used for the evaluation of liquefaction potentials and other related parameters. The DeepSoil was used for the site response analysis and the SeismoSignal was employed to monitor the response analysis for displacement, velocity and acceleration versus period.

3. The factor of safety (FS) a very important parameter being used against liquefaction to quantify other parameters was utilized from CPT data. The factor of safety values were determined for all layers at all CPT locations with earthquake magnitudes Mw = 6, 6.5, and 7.0. Since the whole testing was conducted in-situ, different empirical procedures were used to analyze the output data from the software. The analysis of the test results showed that FS from NovoCPT and LiqIT for the ranges of depth indicated was moderate to high at the liquefiable zone, while, it indicates no major risk for the liquefaction at the entire total depth. This is clearly analyzed according to the empirical procedures of Iwasaki et al. (1982), Chen and Juang (2000), Sonmez and Gokceoglu, (2005), and Yalcin et al. (2008). According to safety factors against liquefaction, liquefaction is expected to occur during 7 Richter magnitude earthquakes for the eastern coast of Cyprus.

4. Liquefaction potential was estimated through CPT soundings. The CPT also always offers a record of data for the penetration resistance and is less likely to be affected by operator error compared to other in situ testing methods. Meanwhile, the

soil strata of the Tuzla area are mainly composed of soft, saturated sands, silts, organic and sensitive clays. Most commonly CPT-based liquefaction potential evaluation criteria were deemed suitable to study sandy soils in the area under study. Moreover, the procedure used in this study is based on a study conducted by Roberston and Wride (1998) that indicated liquefaction potential of Tuzla soil deposit depends on cyclic loading or high magnitude earthquake. It should however be mentioned here that high sensitivity of soft soils causes a significant loss in shear strength hence causing low bearing capacity and lateral spreading when earthquake occurs.

5. Following CPT sounding, the calculated factor of safeties (FS) was used to develop liquefaction potential index (LPI) and liquefaction severity index (LS) values. “Very likely” or “Liquefaction/non-liquefaction is equally likely” liquefaction potential was obtained through the probability approach proposed by Juang (2002). While ‘moderate to very high liquefaction potential’ is usually obtained from liquefaction potential index based approach in most of CPT locations Iwasaki (1982), liquefaction severity index based approach categorizes most of CPT locations as high severity class during the third earthquake scenario.

6. As a result, liquefaction severity index based approach (Sonmez & Gokceoglu, 2005) is concluded to be an unsuitable method for the area under study. This is due to the fact that soft to very soft cohesive soils possess a different failure property which is usually due to recurrent cyclic loading of soils, therefore, attributing this behavior to soil liquefaction is not considered a sound approach.

7. Due to the fine-grained soils of Tuzla area earthquake shaking may not cause liquefaction. However, huge earthquakes ($M_w \geq 6.5$) may cause induced ground deformation, ground settlements and lateral spreads in Tuzla. The available techniques and methods nowadays can only evaluate liquefaction potential rather than estimate liquefaction-induced ground deformations. That is, none of the available CPT based methods can estimate ground settlements and lateral displacements properly.

8. Site response analysis has been studied using DeepSoil Software and the average of response spectrum for the first layer is compared with the average of ten input motions of past earthquakes from areas considered to be similar to the study area, and repeated for each CPT location. Then displacement, velocity and acceleration parameters are scaled by using SeismoSignal software for the first layer and bedrock for all CPT logs to find the response displacement, velocity and acceleration versus period. These parameters are used to describe the influence of earthquake or nature of frequency on soil and structures. In fact by averaging spectra for the past earthquakes, a summary of frequency of displacement, velocity, acceleration and also structural dynamics was obtained, useful for engineers in the design of structures to resist earthquakes by considering lateral force requirements in building codes. The amount of earthquake magnitude can be extremely influential on the spectral shapes, while, the distance between the source of earthquake and the site cannot be much effective on them.

6.1 Summary of Future Study

Future studies are recommended using advanced software to find more realistic displacement and velocity or acceleration for microzonation study area, and

proposing appropriate ways to reduce soil subsidence or soil liquefaction caused by earthquakes or cyclic loading to improve design and construction of structures.

REFERENCES

Afkhami, A. (2009). NovoCPT User Manual. North Vancouver: Novo Tech Software.

Andrus, R. D., & Stokoe II, K. H. (2000). Liquefaction resistance of soils from shear-wave velocity. *Journal of geotechnical and geoenvironmental engineering*, *126*(11), 1015-1025.

Algermissen, T., & Rogers, A. (2004). A Cyprus earthquake hazard assessment: maps of probabilistic peak ground acceleration and uniform-hazard pseudo-absolute acceleration spectral response. *UNOPS Seismic Hazard and Risk Assessment of the Greater Nicosia Area Report*.

Bazzurro, P., & Cornell, C. A. (2004). Nonlinear soil-site effects in probabilistic seismic-hazard analysis. *Bulletin of the Seismological Society of America*, *94*(6), 2110-2123.

Bilsel, H., Erhan, G., & Durgunoglu, T. (2010). Assessment of Liquefaction/Cyclic Failure Potential of Alluvial Deposits on the Eastern Coast Of Cyprus.

Boulanger, R. W., & Idriss, I. M. (2007). Evaluation of cyclic softening in silts and clays. *Journal of geotechnical and geoenvironmental engineering*, *133*(6), 641-652.

Boulanger, R. W., & Idriss, I. M. (2004). *Evaluating the potential for liquefaction or cyclic failure of silts and clays* (p. 131). Center for Geotechnical Modeling.

Boulanger, R. W., & Idriss, I. M. (2006). Liquefaction susceptibility criteria for silts and clays. *Journal of geotechnical and geoenvironmental engineering*, *132*(11), 1413-1426.

Bradley, B. A. (2012). Empirical correlations between cumulative absolute velocity and amplitude-based ground motion intensity measures. *Earthquake Spectra*, *28*(1), 37-54.

Bray, J. D., Sancio, R. B., Riemer, M. F., & Durgunoglu, T. (2004, January). Liquefaction susceptibility of fine-grained soils. In *Proc., 11th Int. Conf. on Soil Dynamics and Earthquake Engineering and 3rd Int. Conf. on Earthquake Geotechnical Engineering* (Vol. 1, pp. 655-662). Stallion Press, Singapore.

Cagnan, Z., & Tanircan, G. B. (2010). Seismic hazard assessment for Cyprus. *Journal of Seismology*, *14*(2), 225-246.

Castro, G., & Poulos, S. J. (1977). Factors affecting liquefaction and cyclic mobility. *Journal of Geotechnical and Geoenvironmental Engineering*, *103*(6).

Cetin, K. O., Seed, R. B., Moss, R. E., Der Kiureghian, A., Tokimatsu, K., Harder Jr, L. F., & Kayen, R. E. (2000). Field case histories for SPT-based in situ liquefaction potential evaluation.

Chang, N. Y. (1987). *Liquefaction susceptibility of fine-grained soils preliminary study report*. Colorado Univ at Denver Dept of Civil and Urban Engineering.

Chen, C. J., & Juang, C. H. (2000). Calibration of SPT-and CPT-based liquefaction evaluation methods. *Geotechnical Special Publication*, 49-64.

Durgunoglu, H. T., & Bilsel, H. (2007). A Microzonation Study Based On Liquefaction and Cyclic Failure Potential of Fine Grained Soils.

Erdik, M., Biro, Y. A., Onur, T., Sesetyan, K., & Birgoren, G. (1999). Assessment of earthquake hazard in Turkey and neighboring. *Annals of Geophysics*, *42*(6).

Erhan, G. (2009). Assessment of liquefaction / cyclic failure potential of Tuzla soils, M.S. Thesis, EMU.

Gilstrap, S. D., & Youd, T. L. (1998). *'CPT based liquefaction resistance analyses using case histories* (Vol. 1). Tech. Rep. CEG-90.

Hamada, M., Isoyama, R., & Wakamatsu, K. (1997). The Hyogoken-Nanbu (Kobe) Earthquake: Liquefaction, Ground Displacement and Soil Condition in Hanshin Area. Association for Development of Earthquake Prediction.

Hashash, Y., Phillips, C., & Groholski, D. R. (2010). Recent advances in non-linear site response analysis.

Holzer, T. L., Noce, T. E., & Bennett, M. J. (2011). Liquefaction probability curves for surficial geologic deposits. *Environmental & Engineering Geoscience*, *17*(1), 1-21.

Idriss, I. M., & Boulanger, R. W. (2006). Semi-empirical procedures for evaluating liquefaction potential during earthquakes. *Soil Dynamics and Earthquake Engineering*, *26*(2), 115-130.

Ishihara, K. (1996). *Soil behaviour in earthquake geotechnics*. Clarendon Press; Oxford University Press.

Iwasaki, T., Arakawa, T., & Tokida, K. I. (1984). Simplified procedures for assessing soil liquefaction during earthquakes. *International Journal of Soil Dynamics and Earthquake Engineering*, *3*(1), 49-58.

Iwasaki, T., Tokida, K., Tatsuoka, F., Watanabe, S., Yasuda, S., & Sato, H. (1982, June). Microzonation for soil liquefaction potential using simplified methods. In *Proceedings of the 3rd International Conference on Microzonation, Seattle* (Vol. 3, pp. 1310-1330).

Iwasaki, T., Tatsuoka, F., Tokida, K. I., & Yasuda, S. (1978, November). A practical method for assessing soil liquefaction potential based on case studies at various sites in Japan. In *Proc., 2nd Int. Conf. on Microzonation* (pp. 885-896). Washington, DC: National Science Foundation.

Jayaram, N., Lin, T., & Baker, J. W. (2011). A computationally efficient ground-motion selection algorithm for matching a target response spectrum mean and variance. *Earthquake Spectra*, *27*(3), 797-815.

Juang, C. H., & Jiang, T. (2000). Assessing probabilistic methods for liquefaction potential evaluation. In *Soil dynamics and liquefaction 2000* (pp. 148-162). ASCE.

Juang, C. H., Jiang, T., & Andrus, R. D. (2002). Assessing probability-based methods for liquefaction potential evaluation. *Journal of Geotechnical and Geoenvironmental Engineering*, *128*(7), 580-589.

Kalogeras, I., Stavrakakis, G., & Solomi, K. (1999). The October 9, 1996, earthquake in Cyprus: seismological, macroseismic and strong motion data.

Kayen, R. E., Mitchell, J. K., Seed, R. B., Lodge, A., Nishio, S. Y., & Coutinho, R. (1992). Evaluation of SPT-, CPT-, and shear wave-based methods for liquefaction potential assessment using Loma Prieta data. In*Technical Report NCEER* (Vol. 1, No. 92-0019, pp. 177-204). US National Center for Earthquake Engineering Research (NCEER).

Kayen, R., Moss, R. E. S., Thompson, E. M., Seed, R. B., Cetin, K. O., Kiureghian, A. D., & Tokimatsu, K. (2013). Shear-wave velocity–based probabilistic and deterministic assessment of seismic soil liquefaction potential. *Journal of Geotechnical and Geoenvironmental Engineering*, *139*(3), 407-419.

Kishida, H. (1966). Damage to reinforced concrete buildings in Niigata city with special reference to foundation engineering. *Soils and Foundations*, *6*(1), 71-88.

Kramer, S. (1996). Geotechnical Earthquake Engineering. Delhi (India): Pearson Education Ptd. Ltd.

Lee, D. H., Ku, C. S., & Yuan, H. (2004). A study of the liquefaction risk potential at Yuanlin, Taiwan. *Engineering Geology*, *71*(1), 97-117.

Liao, S. S., & Whitman, R. V. (1986). *A catalog of liquefaction and non-liquefaction occurrences during earthquakes*. Department of Civil Engineering, MIT.

López, M., Bommer, J. J., & Pinho, R. (2004). Seismic hazard assessments, seismic design codes, and earthquake engineering in El Salvador. *Geological Society of America Special Papers*, *375*, 301-320.

Marcuson, W. F. (1978). Definition of terms related to liquefaction. *Journal of the Geotechnical Engineering Division*, *104*(9), 1197-1200.

Mogami, T., & Kubo, K. (1953). The behavior of soil during vibration. In *Proc. 3rd Inter. Conf. on Soil Mech. And Found. Energy* (Vol. 1, pp. 152-155).

Moss, R. E. (2003). CPT-Based Probabilistic Assessment of Seismic Soil Liquefaction Initiation. *Dissertation*.

Olsen, R. S., & Idriss, I. M. (1997). Cyclic liquefaction based on the cone penetrometer test. In *Technical Report NCEER* (Vol. 97, pp. 225-76). US National Center for Earthquake Engineering Research (NCEER).

Perlea, V. G., Pak, R. Y. S., & Yamamura, J. (2000). Liquefaction of cohesive soils. In *Soil dynamics and liquefaction 2000. Proceedings of sessions of Geo-Denver 2000, Denver, Colorado, USA, 5-8 August 2000.* (pp. 58-76). American Society of Civil Engineers.

Robertson, P. K. (1990). Soil classification using the cone penetration test.*Canadian Geotechnical Journal*, *27*(1), 151-158.

Robertson, P. K. (2004). Evaluating soil liquefaction and post-earthquake deformations using the CPT. in *Proc. 2nd Int. Conf. on Site Characterization ISC* (Vol. 2, pp. 233-249).

Robertson, P. K., & Wride, C. E. (1998). Evaluating cyclic liquefaction potential using the cone penetration test. *Canadian Geotechnical Journal*, *35*(3), 442-459.

Rodriguez-Marek, A., Bray, J. D., & Abrahamson, N. A. (2000). A geotechnical seismic site response evaluation procedure. In *Proceeding of* (Vol. 12).

Rogers, A. M., & Algermissen, S. T. (2004). An Earthquake Hazard Assessment of Cyprus. *Report prepared for the United Nations Office for Project Services, Nicosia, Cyprus*.

Sancio, R. B., Bray, J. D., Stewart, J. P., Youd, T. L., Durgunoğlu, H. T., Önalp, A., & Karadayılar, T. (2002). Correlation between ground failure and soil conditions in Adapazari, Turkey. *Soil Dynamics and Earthquake Engineering*, *22*(9), 1093-1102.

Seed, R. B., Cetin, K. O., Moss, R. E., Kammerer, A. M., Wu, J., Pestana, J. M., ... & Faris, A. (2003). Recent advances in soil liquefaction engineering: a unified and consistent framework. In *Proceedings of the 26th Annual ASCE Los Angeles Geotechnical Spring Seminar: Long Beach, CA*.

Seed, H. B., Idriss, I. M., & Kiefer, F. W. (1969). Characteristics of rock motions during earthquakes. *Journal of Soil Mechanics & Foundations Div*.

Seed, H. B., & Idriss, I. M. (1970). Soil moduli and damping factors for dynamic response analyses.

Seed, H., & Idriss, I. (1981). Evaluation of liquefaction potential of sands deposits based on observations of performance in previous earthquakes. Session on in situ testing to evaluate liquefaction susceptibility, ASCE National Convention, St. Louis, MO, 81, 544.

Seed, H. B., Idriss, I. M., & Arango, I. (1983). Evaluation of liquefaction potential using field performance data. *Journal of Geotechnical Engineering*, *109*(3), 458-482.

Sladen, J. A., D'hollander, R. D., & Krahn, J. (1985). The liquefaction of sands, a collapse surface approach. *Canadian Geotechnical Journal*, *22*(4), 564-578.

Sonmez, H. (2003). Modification of the liquefaction potential index and liquefaction susceptibility mapping for a liquefaction-prone area (Inegol, Turkey). *Environmental Geology*, *44*(7), 862-871.

Sonmez, H., & Gokceoglu, C. (2005). A liquefaction severity index suggested for engineering practice. *Environmental Geology*, *48*(1), 81-91.

Terzaghi, K., Peck, R. B., & Mesri, G. (1996). *Soil mechanics in engineering practice*. John Wiley & Sons.

Tokimatsu, K., & Seed, H. B. (1987). Evaluation of settlements in sands due to earthquake shaking. *Journal of Geotechnical Engineering*, *113*(8), 861-878.

Wair, B. R., DeJong, J. T., & Shantz, T. (2012). Pacific Earthquake Engineering Research Center.

Wang, W. (1979). *Some findings in soil liquefaction*. Earthquake Engineering Department, Water Conservancy and Hydroelectric Power Scientific Research Institute.

Wu, G., & Finn, W. L. (1997). Dynamic nonlinear analysis of pile foundations using finite element method in the time domain. *Canadian Geotechnical Journal*, *34*(1), 44-52.

Yalcin, A., Gokceoglu, C., & Sönmez, H. (2008). Liquefaction severity map for Aksaray city center (Central Anatolia, Turkey). *Natural Hazards and Earth System Sciences*, *8*(4), 641-649.

Yegian, M. K., & Whitman, R. V. (1978). Risk analysis for ground failure by liquefaction. *Journal of Geotechnical and Geoenvironmental Engineering*, *104*(ASCE 13900 Proceeding).

Youd, T. L. (1978). Major Cause of An Earthquake Damage Is Ground Failure. *Civil Engineering*, *48*(4).

Youd, T. L., & Idriss, I. M. (1997). Magnitude scaling factors. In *Technical Report NCEER* (Vol. 97, pp. 149-65). US National Center for Earthquake Engineering Research (NCEER).

Youd, T. L., Idriss, I. M., Andrus, R. D., Arango, I., Castro, G., Christian, J. T., & Ishihara, K. (2001). Liquefaction resistance of soils: summary report from the 1996 NCEER and 1998 NCEER/NSF workshops on evaluation of liquefaction resistance of soils. *Journal of geotechnical and geoenvironmental engineering*, *127*(10), 817-833.

Zhang, G. (2001). Estimation of liquefaction-induced ground deformations by CPT & SPT-based approaches.

APPENDICES

Appendix A: NovoCPT Software Results

A.1 Soil Classification and Factor of Safeties for CPT 1

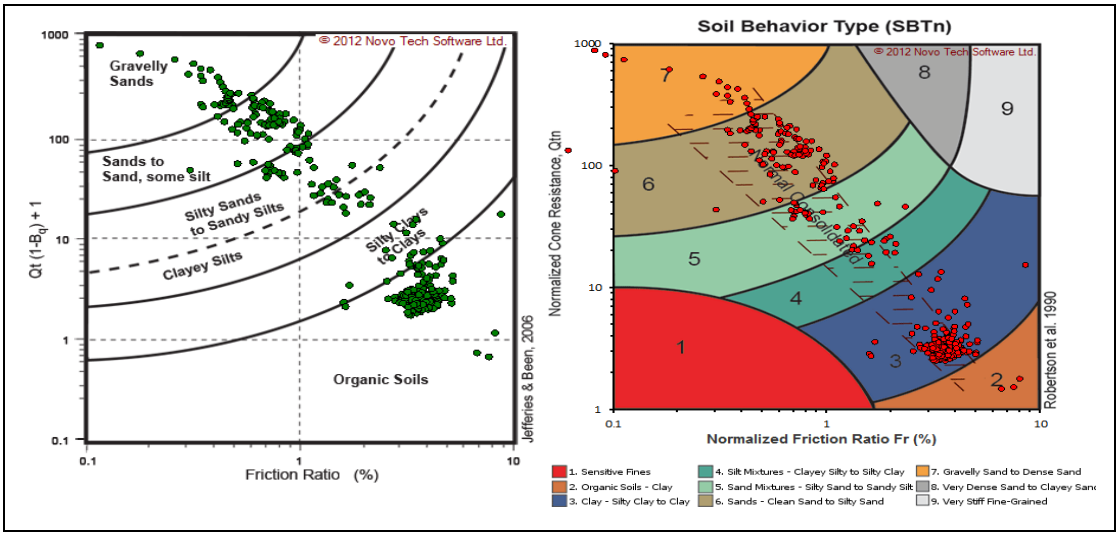

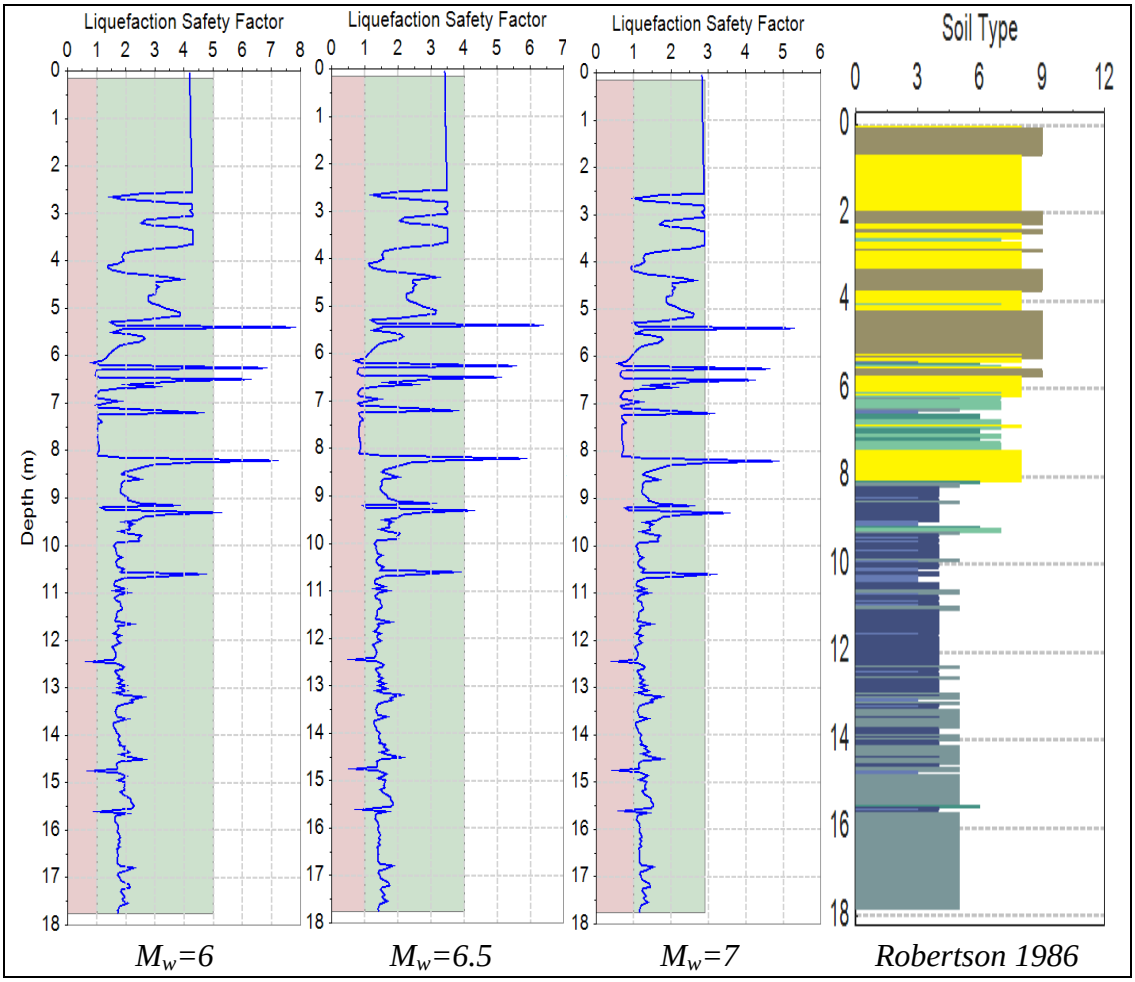

A.2 Soil Classification and Factor of Safeties for CPT 2

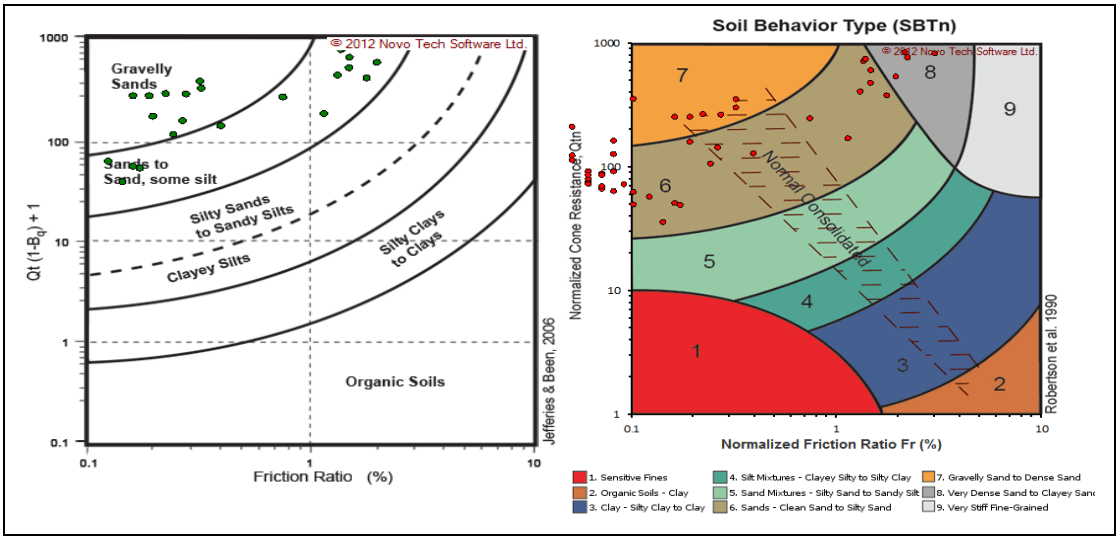

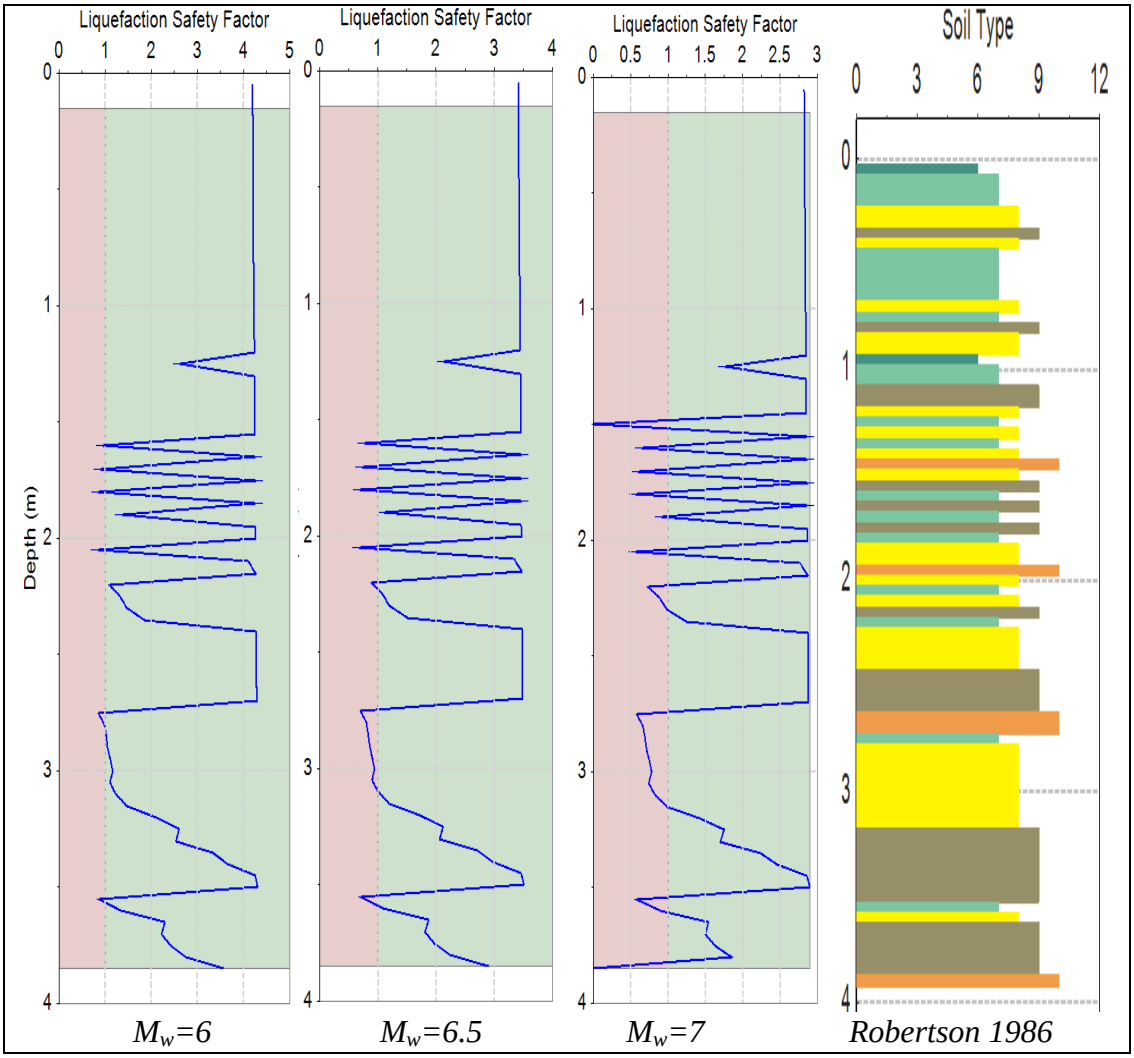

A.3 Soil Classification and Factor of Safeties for CPT 3

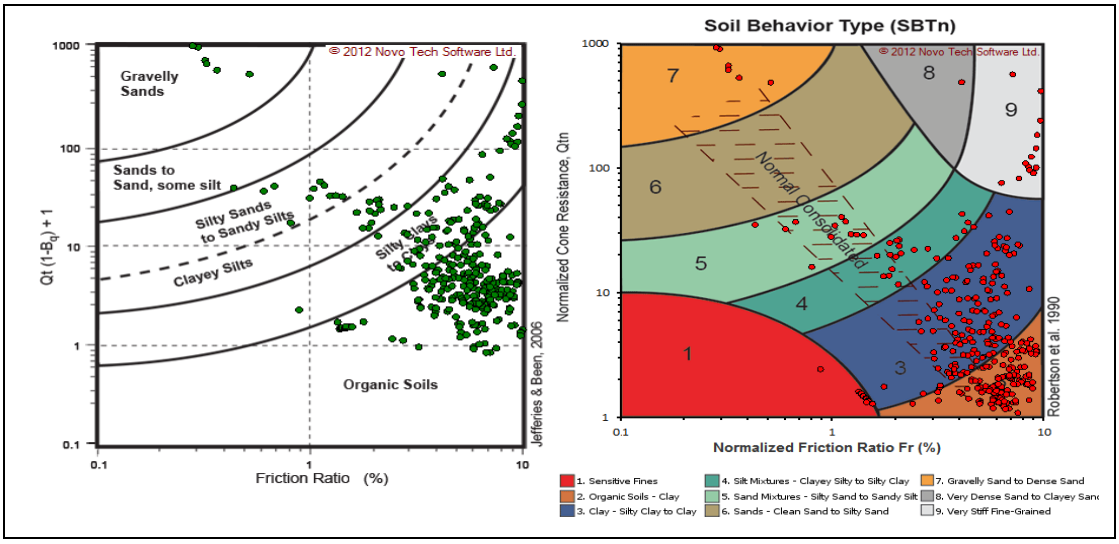

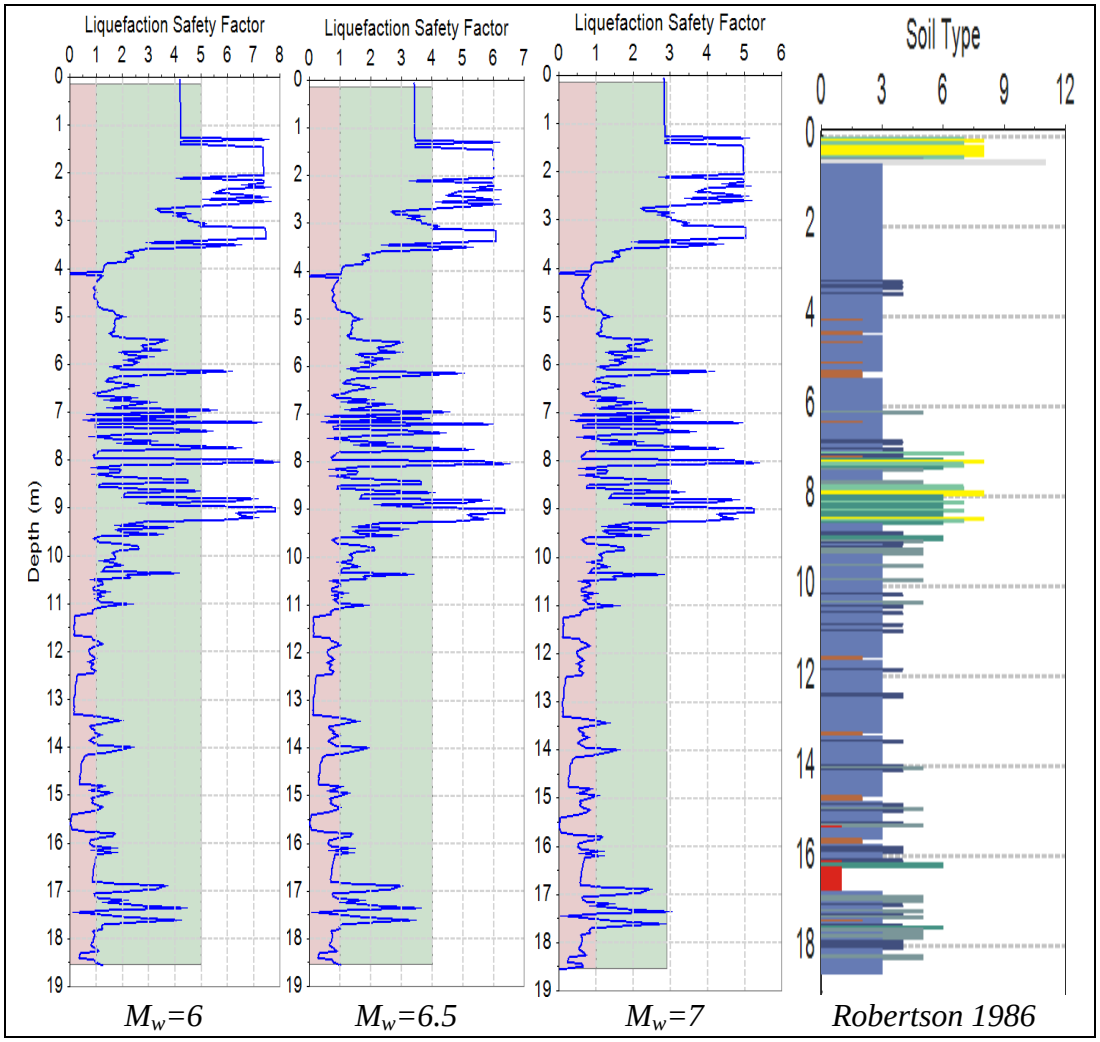

A.4 Soil Classification and Factor of Safeties for CPT 4

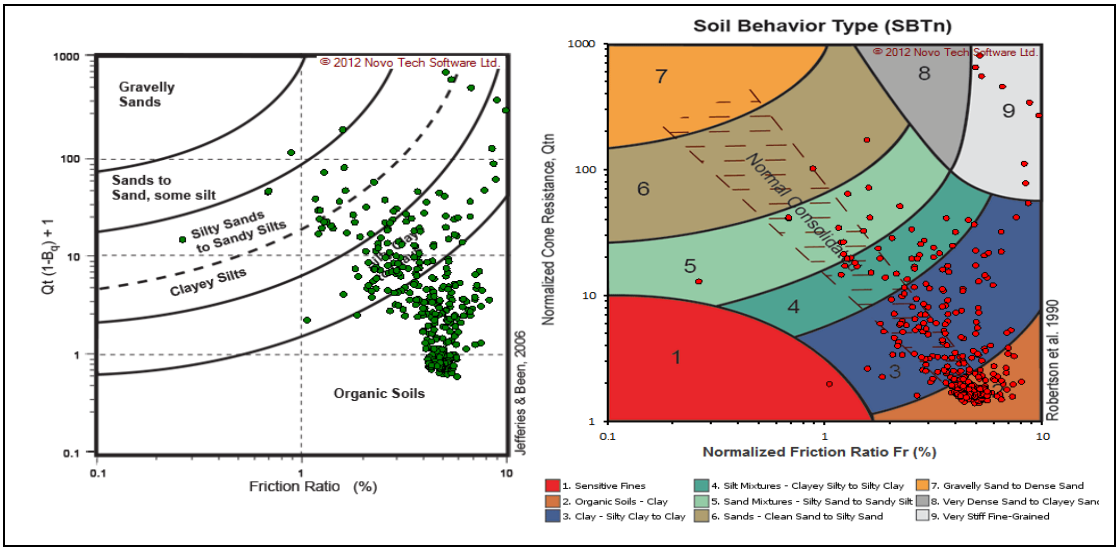

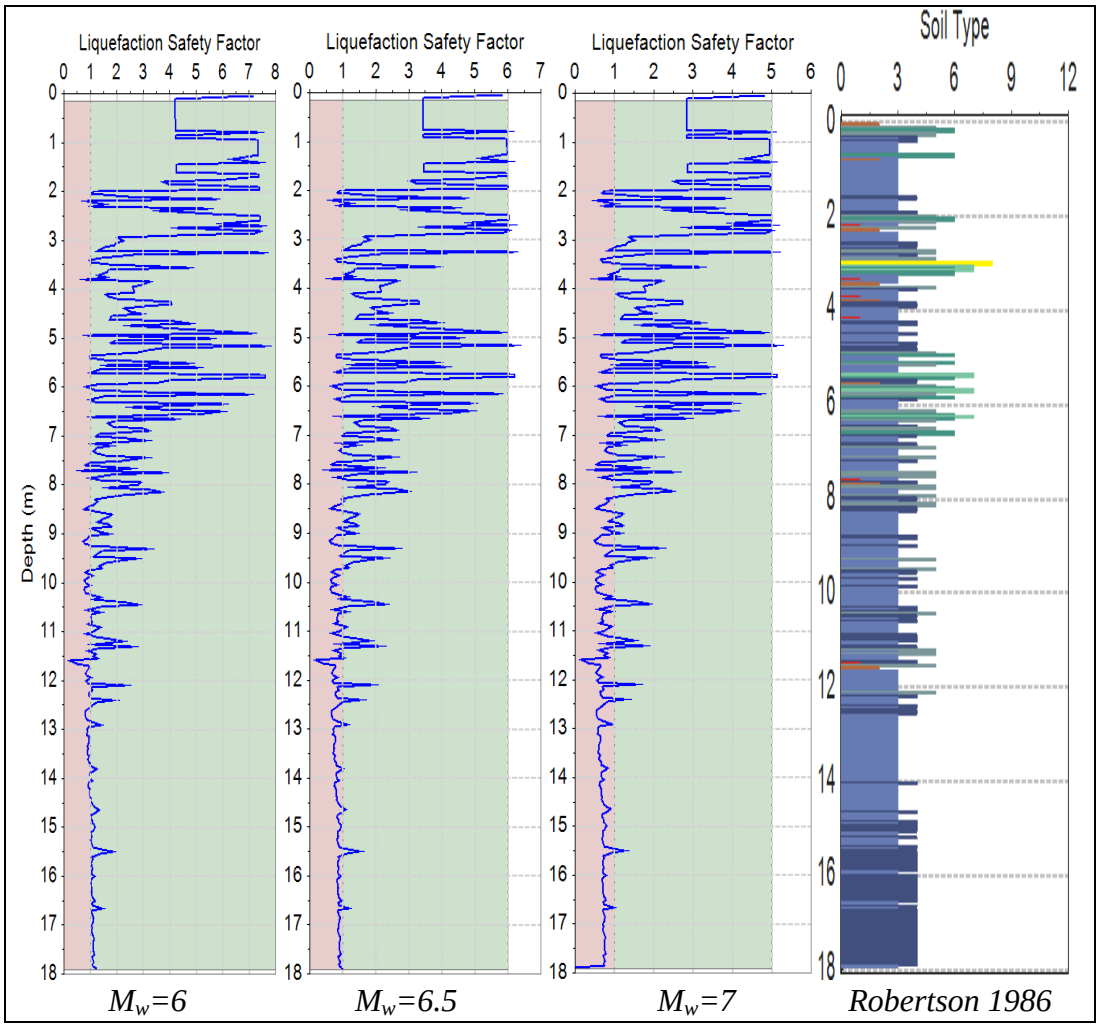

A.5 Soil Classification and Factor of Safeties for CPT 5

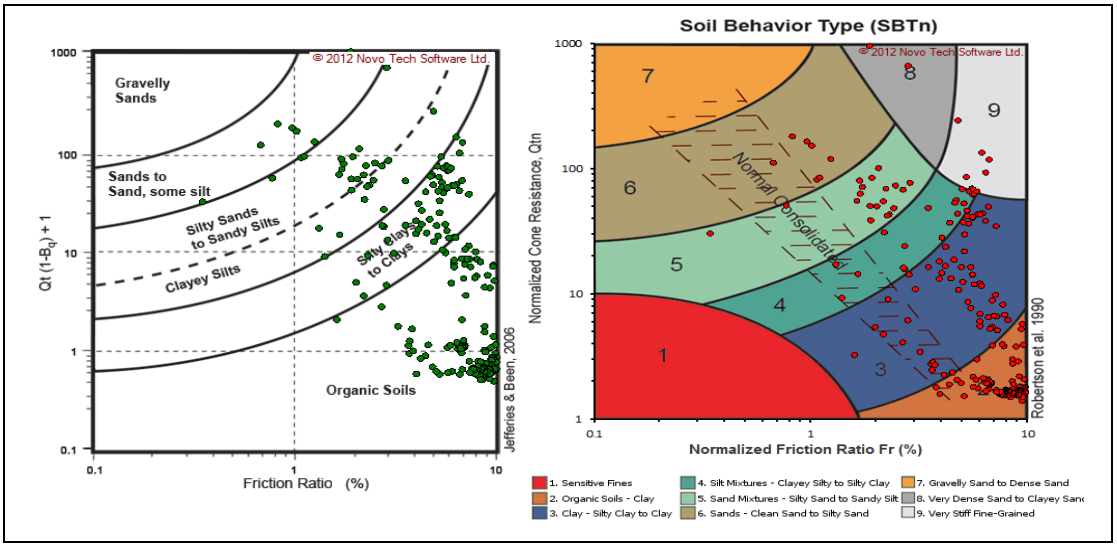

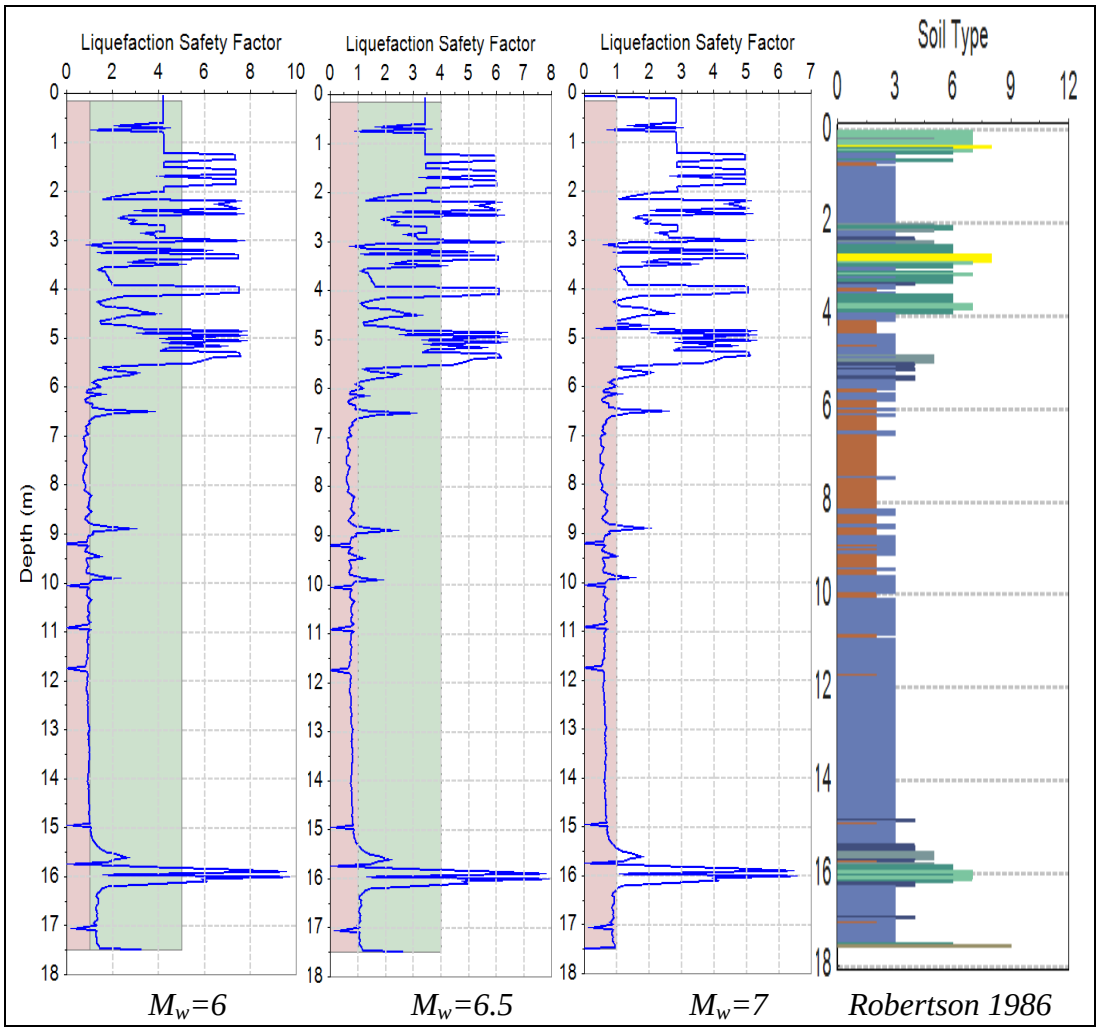

A.6 Soil Classification and Factor of Safeties for CPT 6

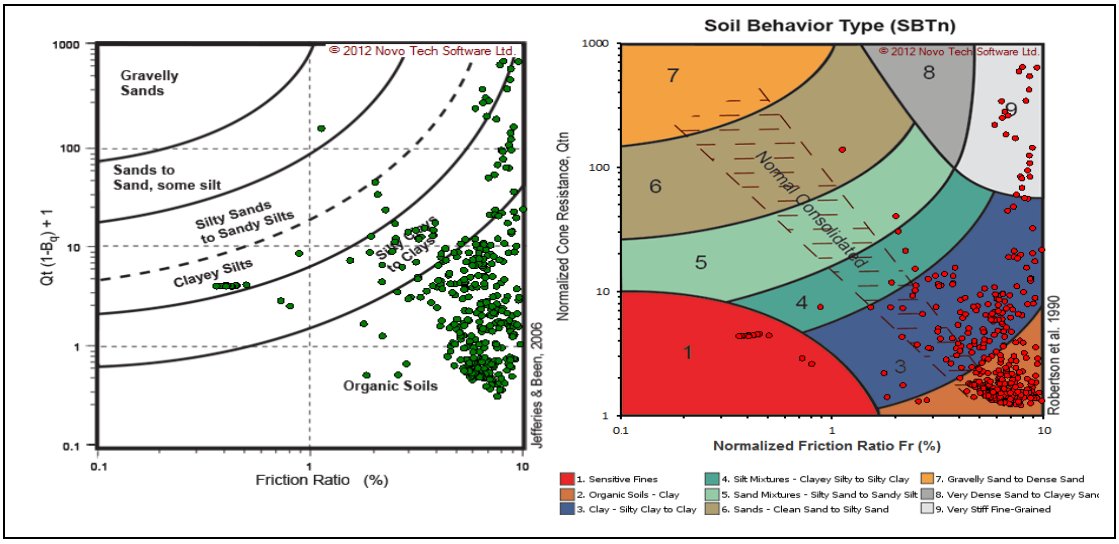

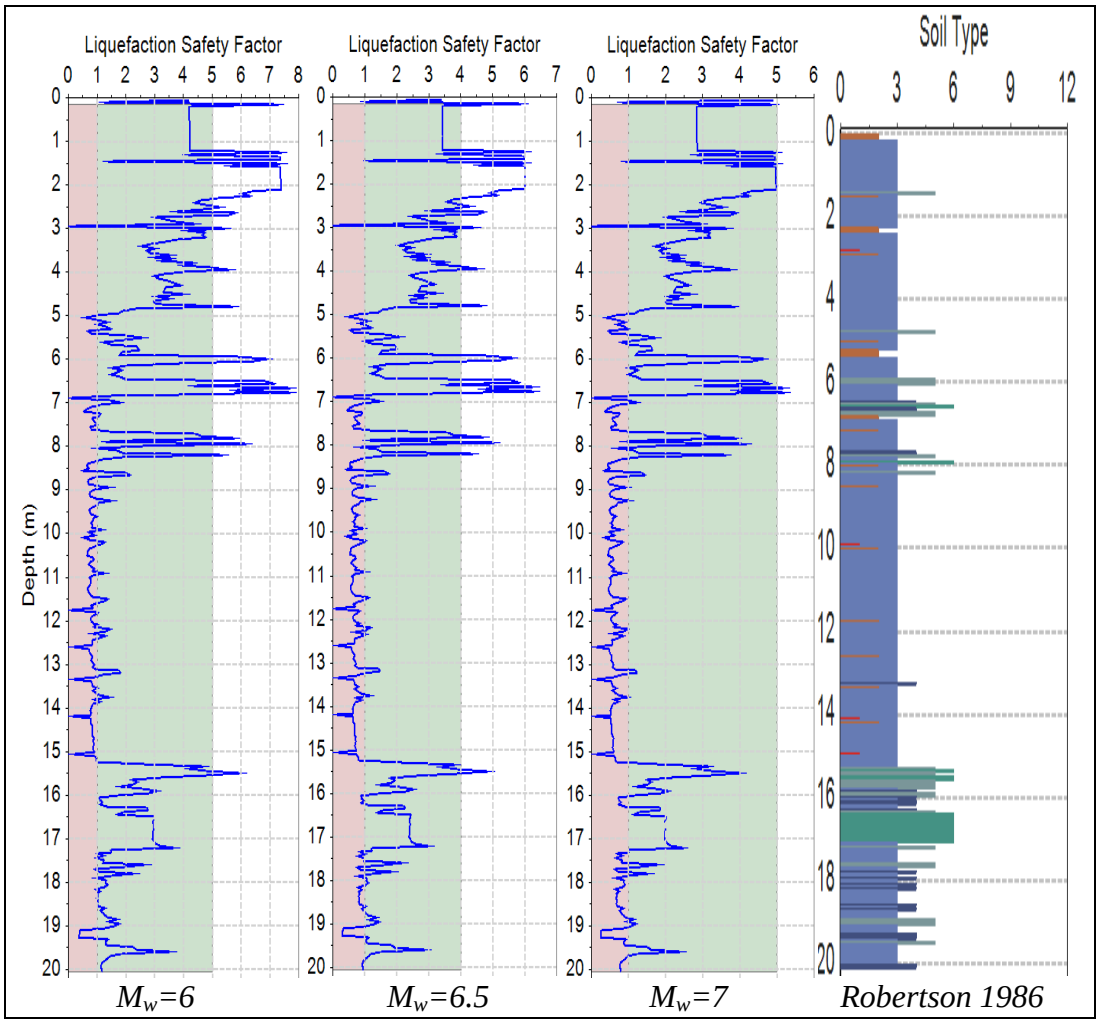

A.7 Soil Classification and Factor of Safeties for CPT 7

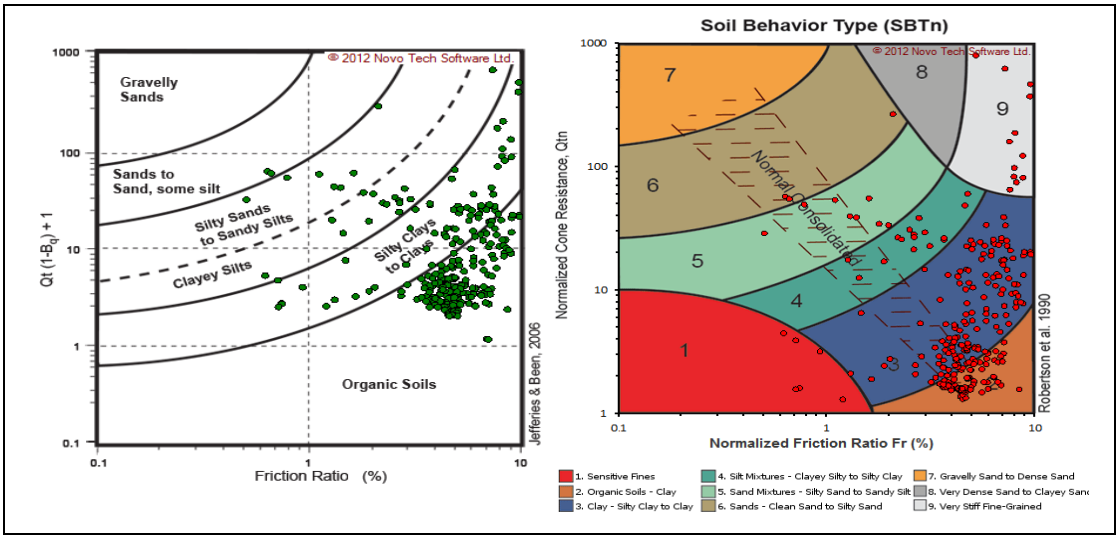

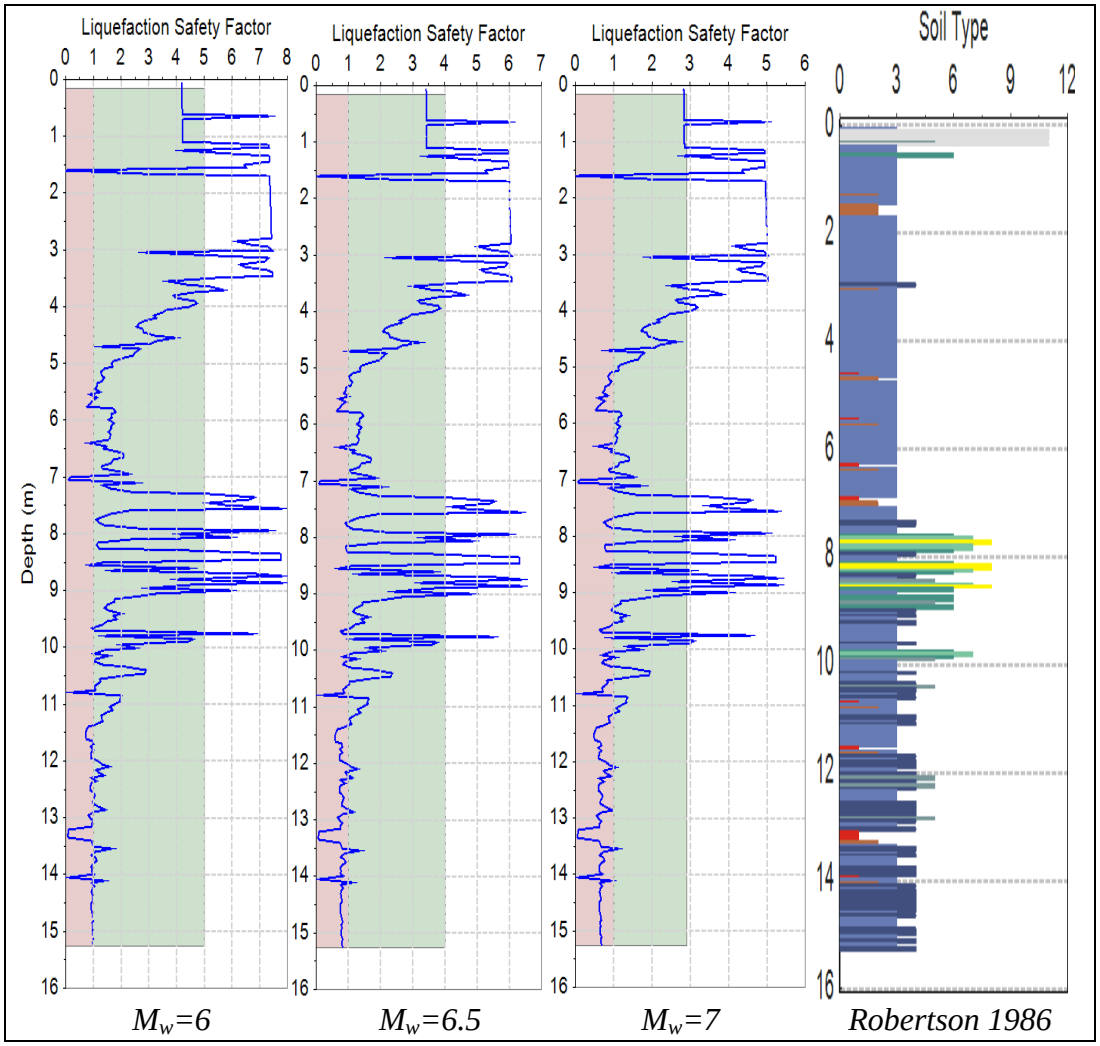

A.8 Soil Classification and Factor of Safeties for CPT 8

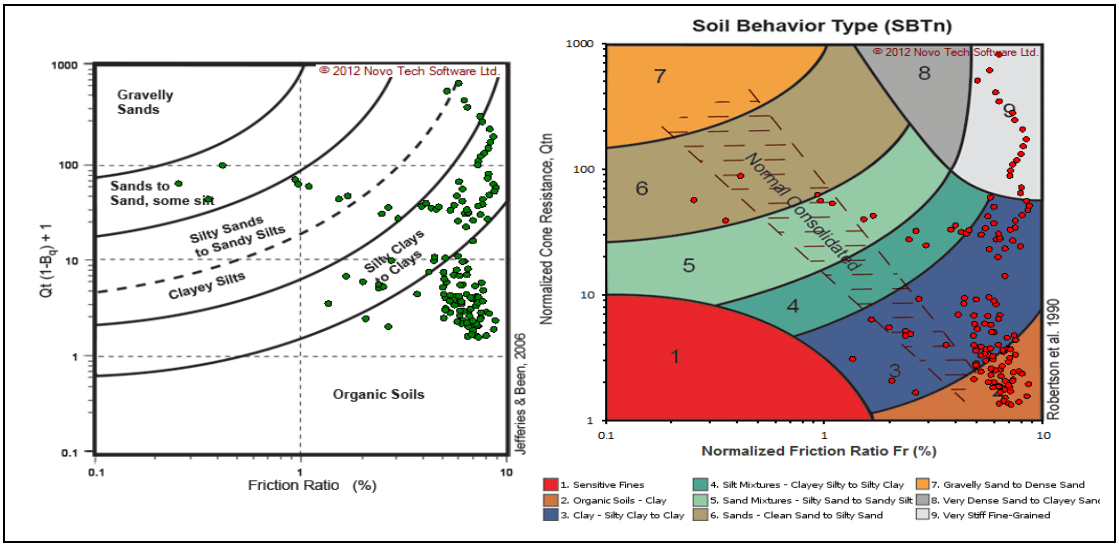

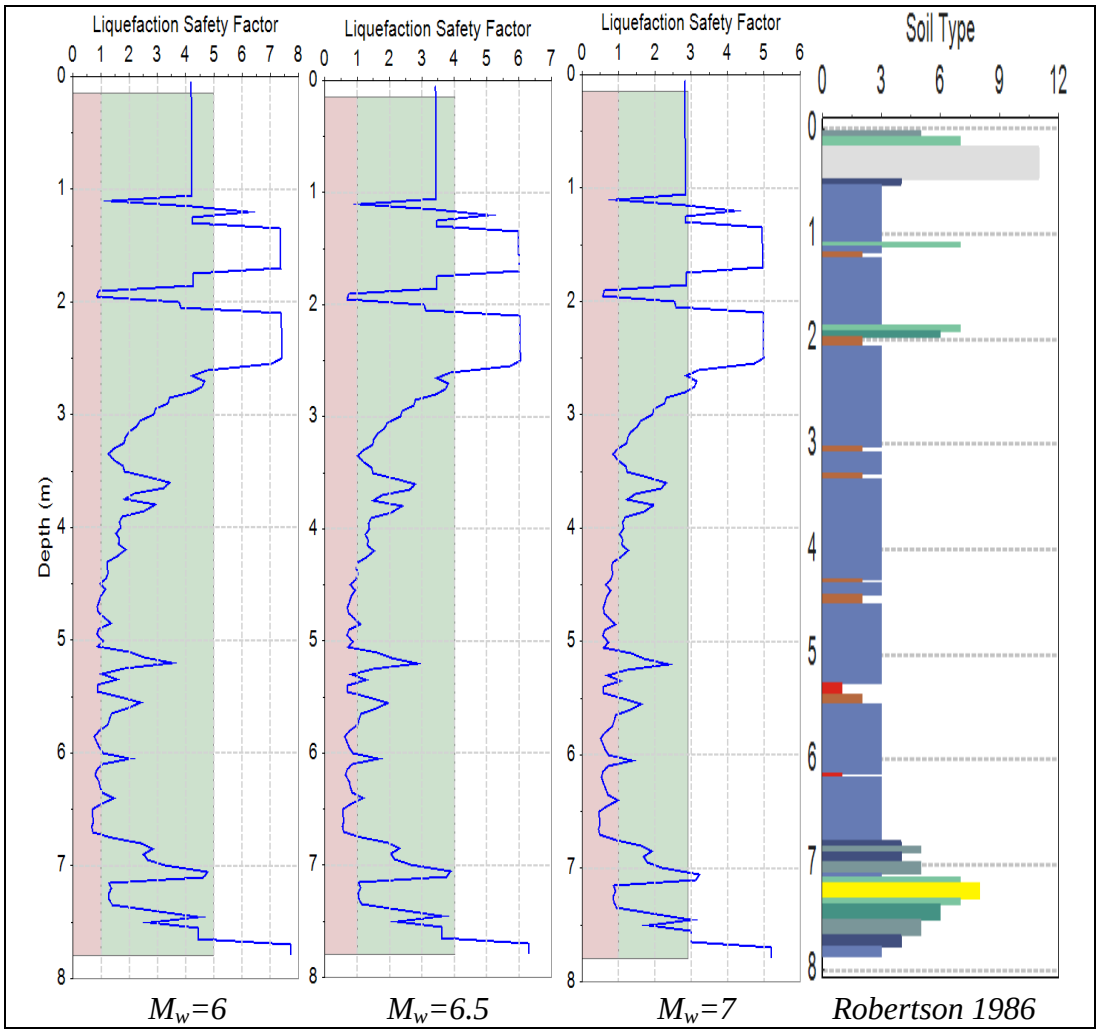

A.9 Soil Classification and Factor of Safeties for CPT 9

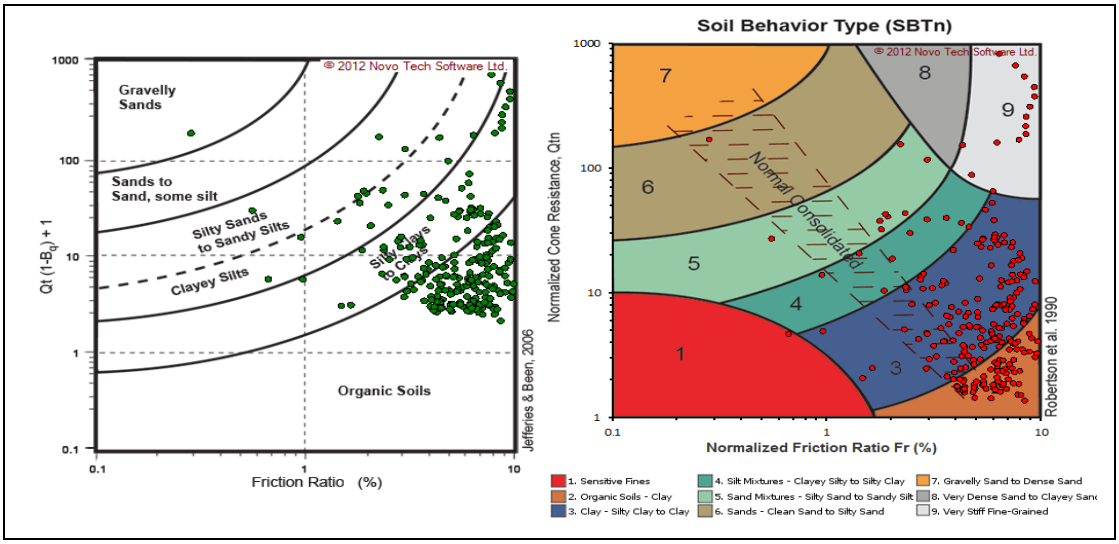

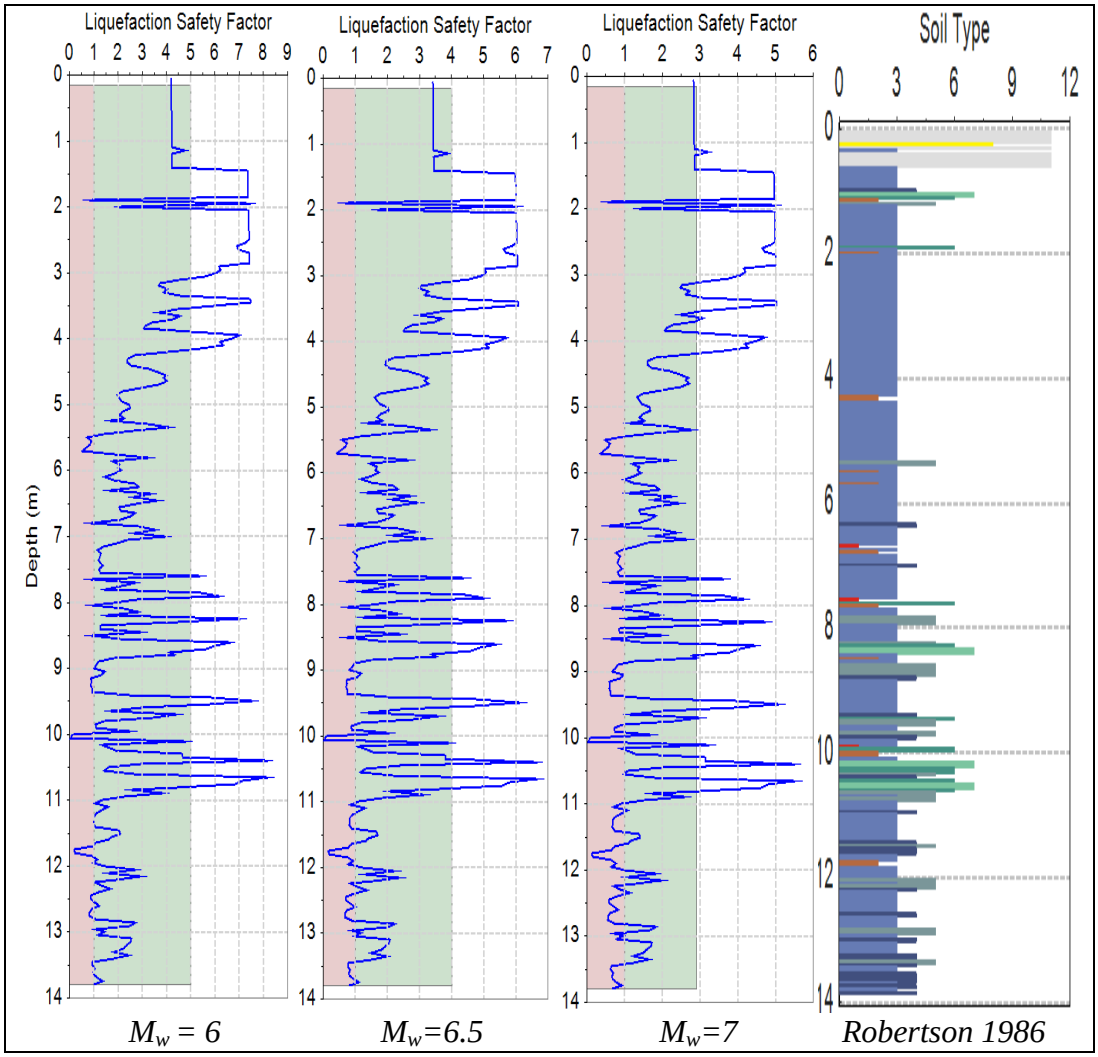

A.10 Soil Classification and Factor of Safeties for CPT 10

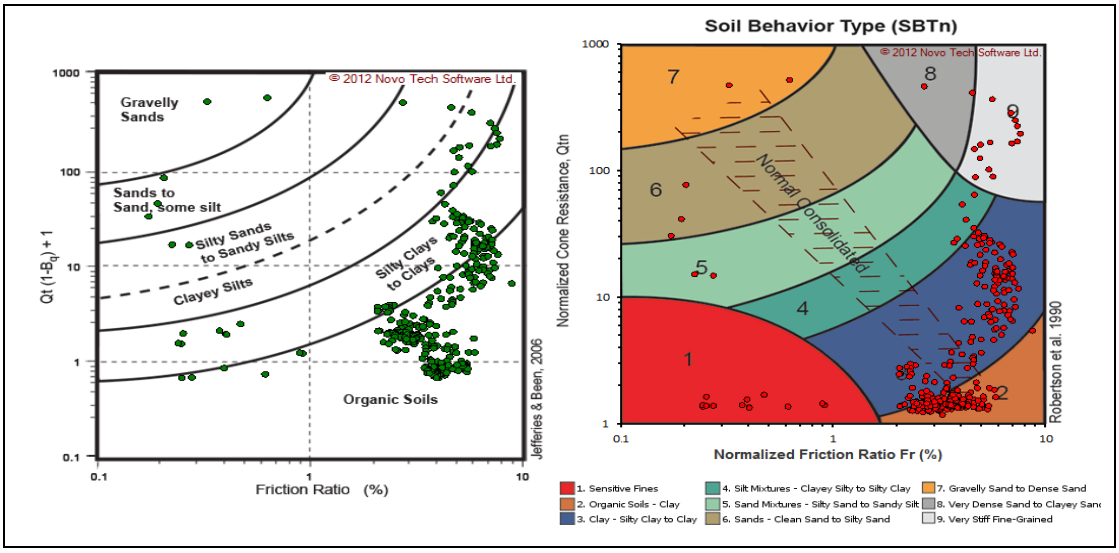

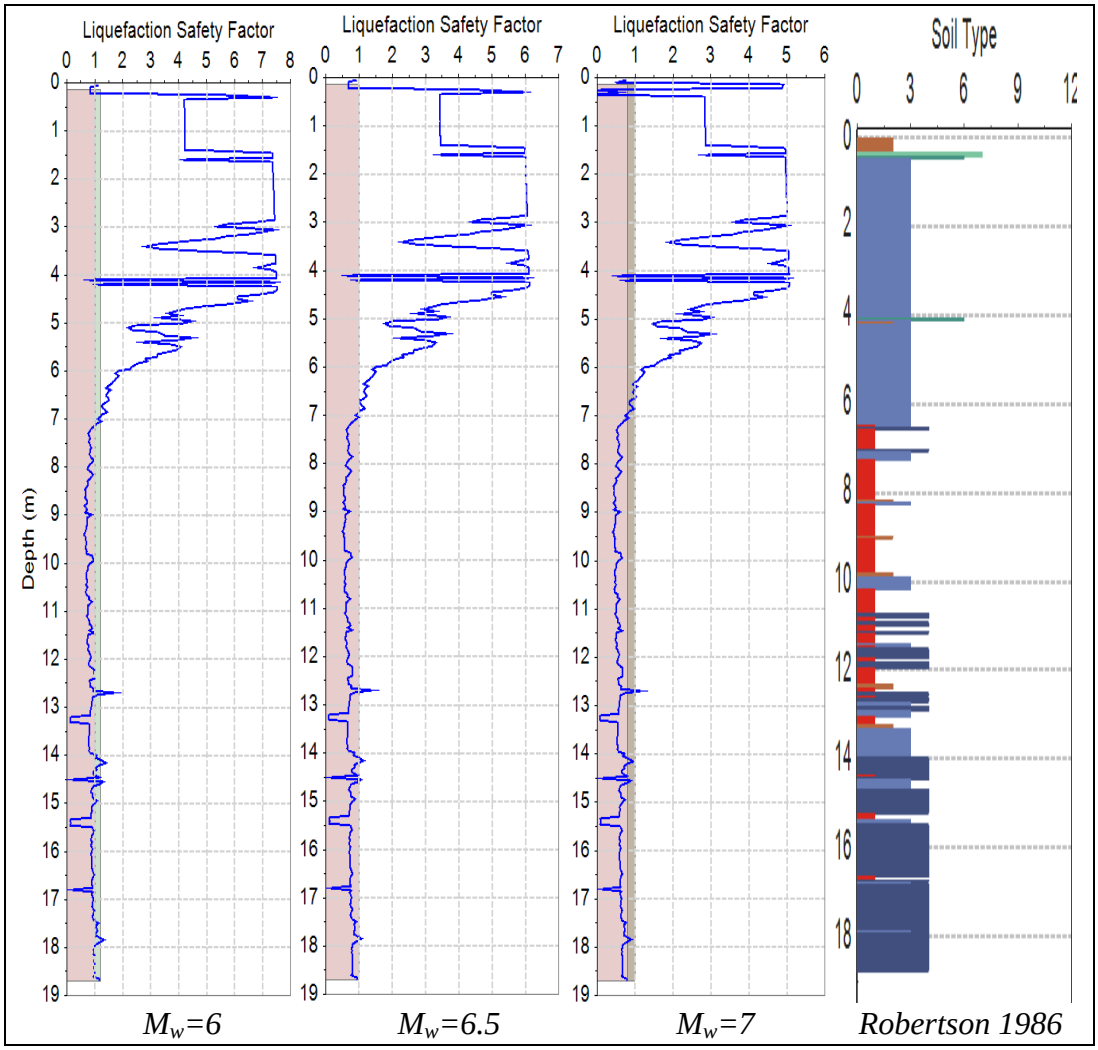

Appendix B: LiqIT Software Results

B.1 Liquefaction Information for CPT 1

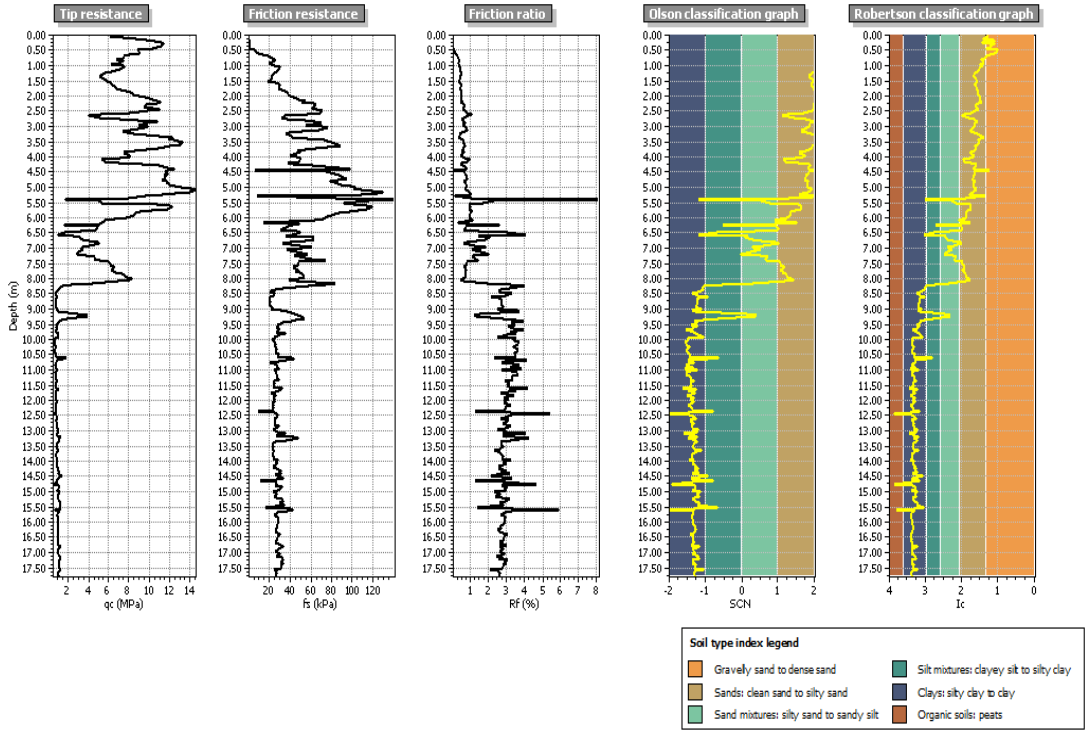

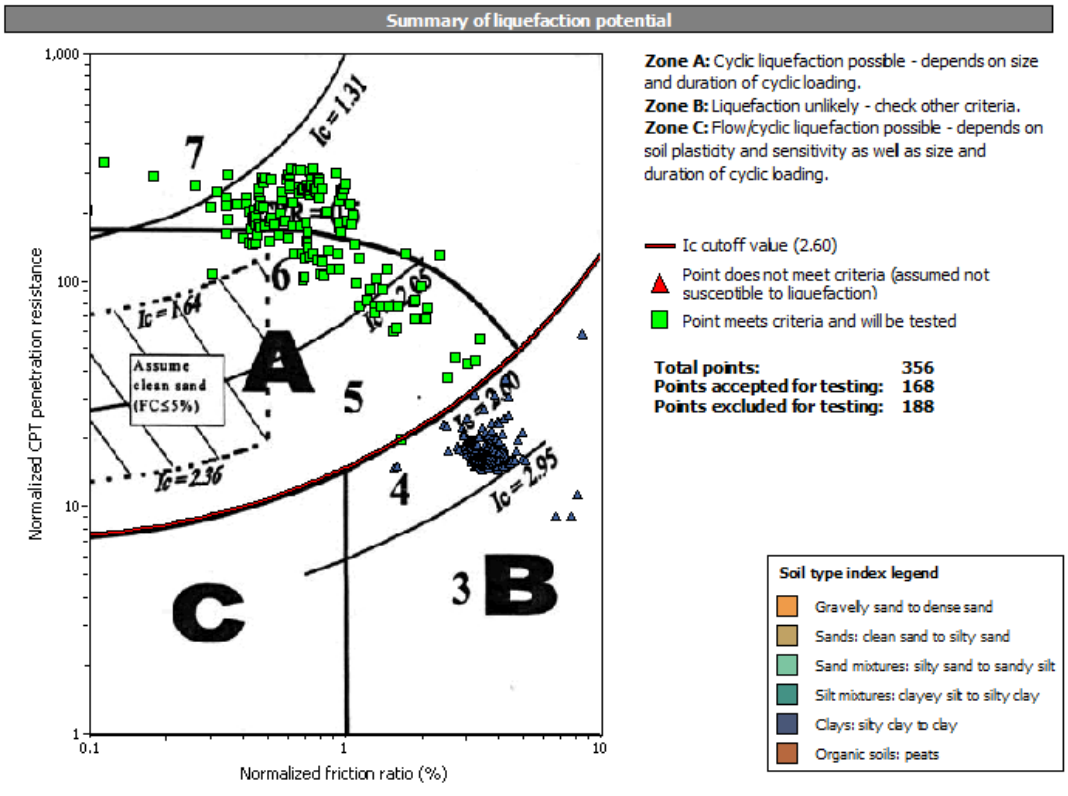

LIQUEFACTION ANALYSIS REPORT

Project title :

Project subtitle :

Input parameters and analysis data

In-situ data type:	Cone Penetration Test	Depth to water table:	1.00 m
Analysis type:	Deterministic	Earthquake magnitude M_w:	6.50
Analysis method:	Robertson (1998)	Peak ground accelaration:	0.30 g
Fines correction method:	Robertson (1998)	User defined F.S.:	1.00

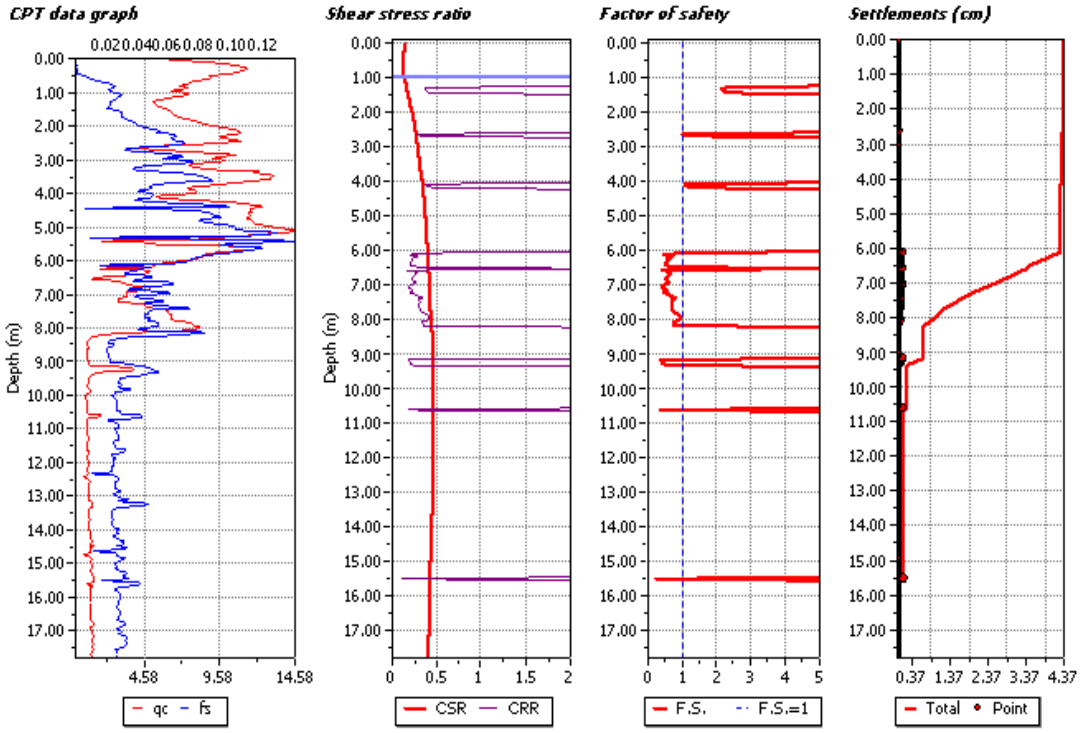

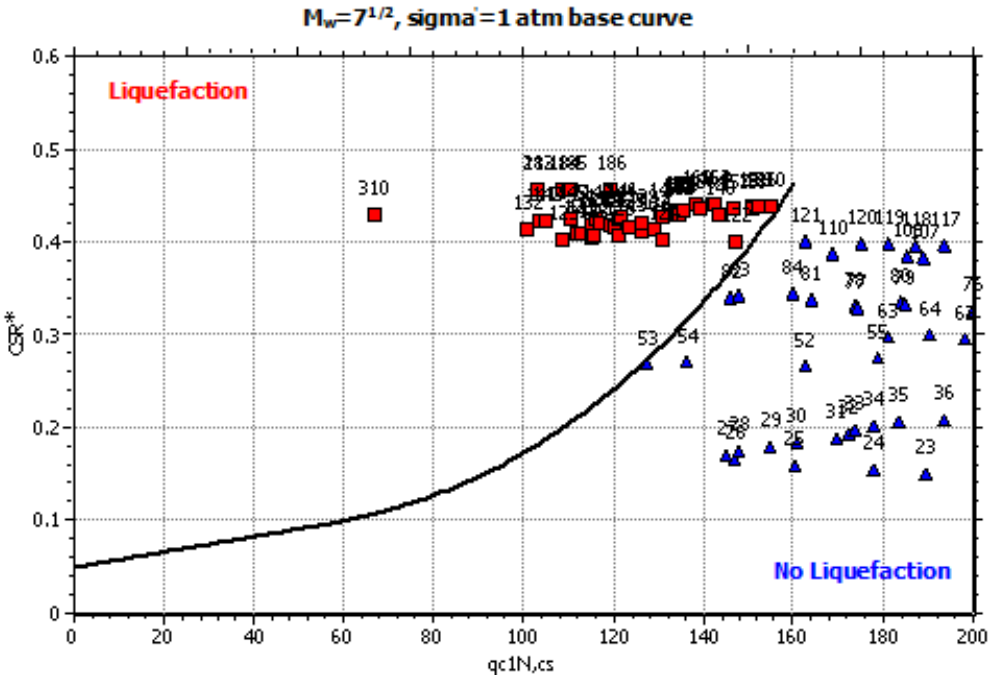

B.2 Liquefaction Information for CPT 2

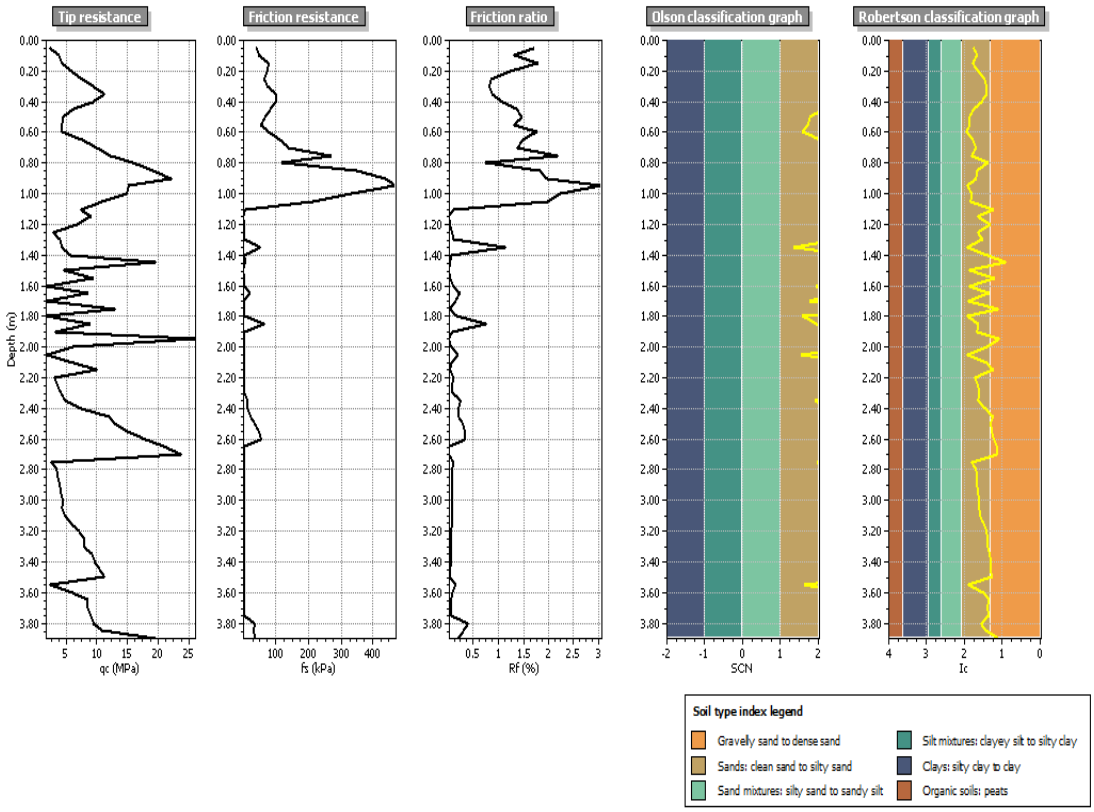

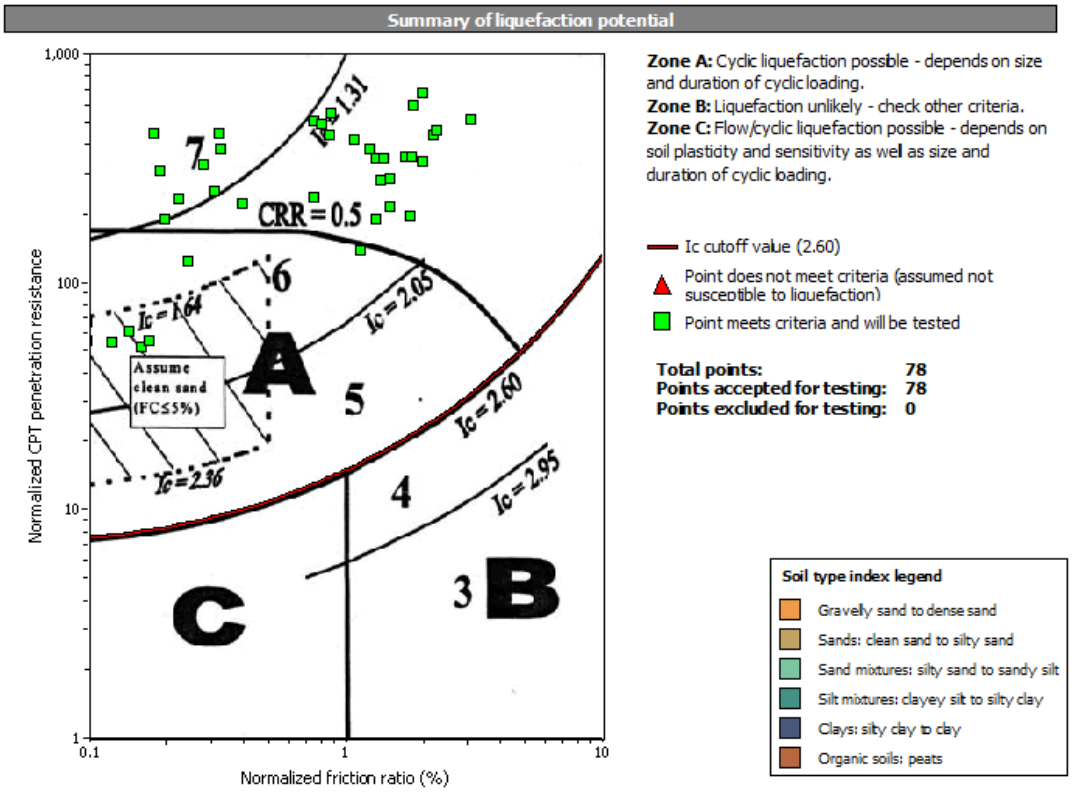

LIQUEFACTION ANALYSIS REPORT

Project title :

Project subtitle :

Input parameters and analysis data

In-situ data type:	Cone Penetration Test	Depth to water table:	1.00 m
Analysis type:	Deterministic	Earthquake magnitude M_w:	6.50
Analysis method:	Robertson (1998)	Peak ground accelaration:	0.30 g
Fines correction method:	Robertson (1998)	User defined F.S.:	1.00

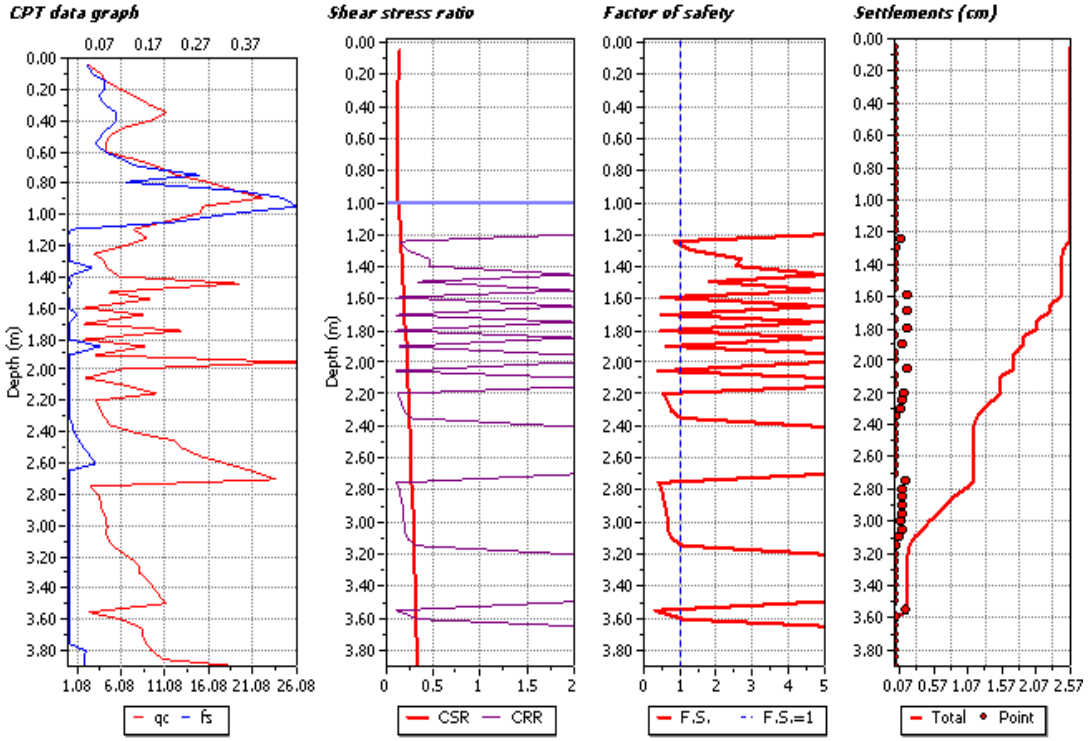

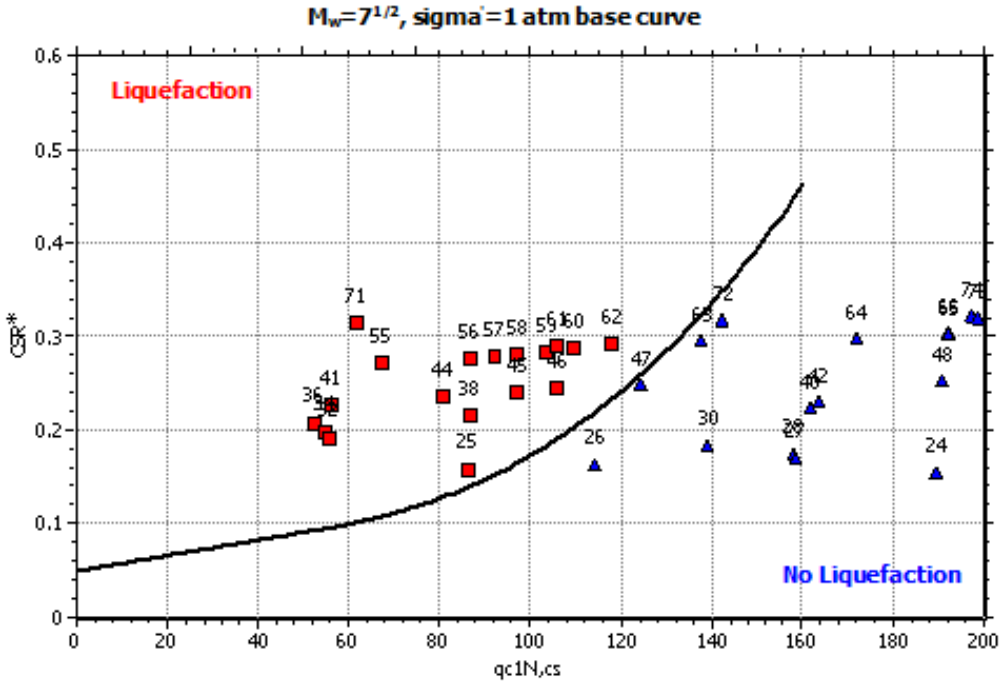

B.3 Liquefaction Information for CPT 3

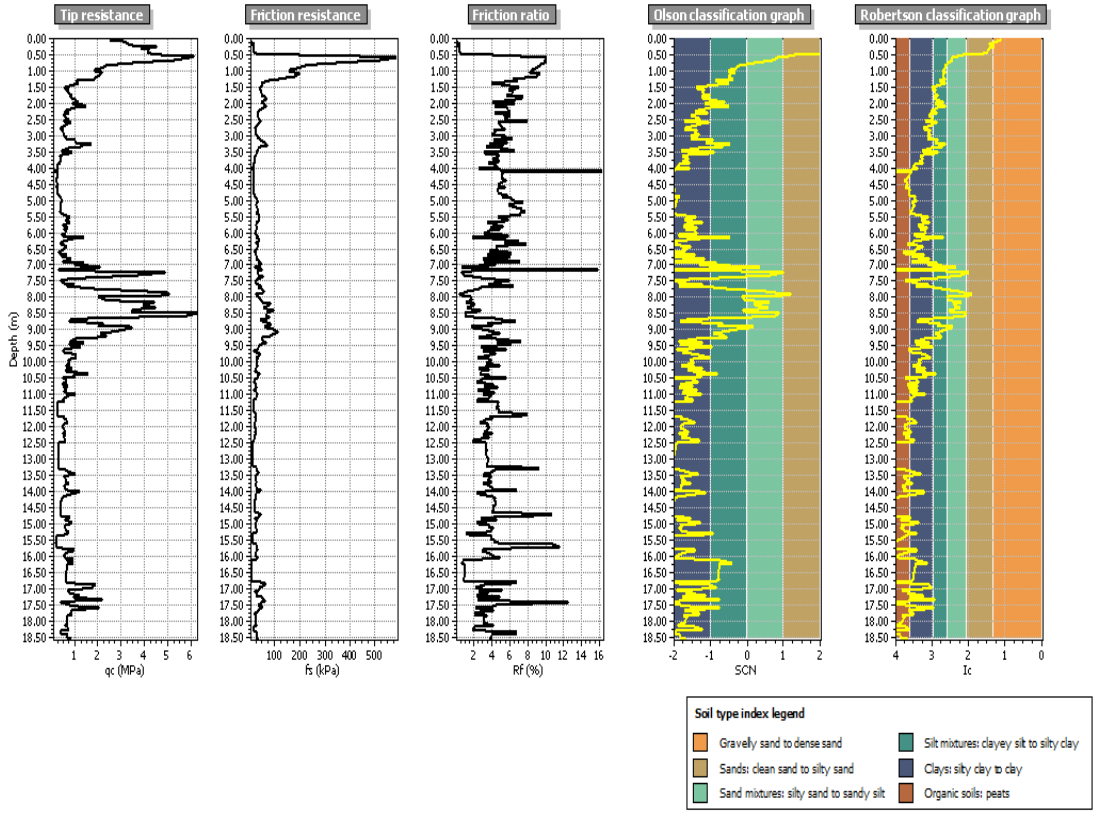

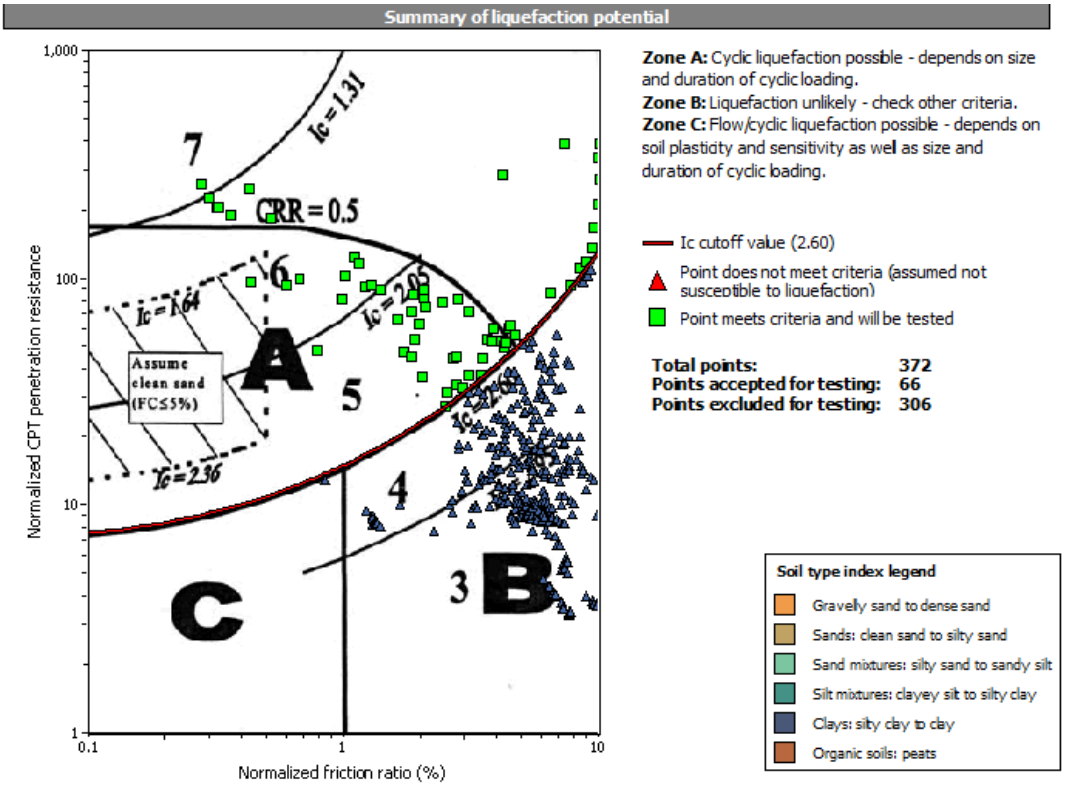

LIQUEFACTION ANALYSIS REPORT

Project title :

Project subtitle :

Input parameters and analysis data

In-situ data type:	Cone Penetration Test	Depth to water table:	1.00 m
Analysis type:	Deterministic	Earthquake magnitude M_w:	6.50
Analysis method:	Robertson (1998)	Peak ground accelaration:	0.30 g
Fines correction method:	Robertson (1998)	User defined F.S.:	1.00

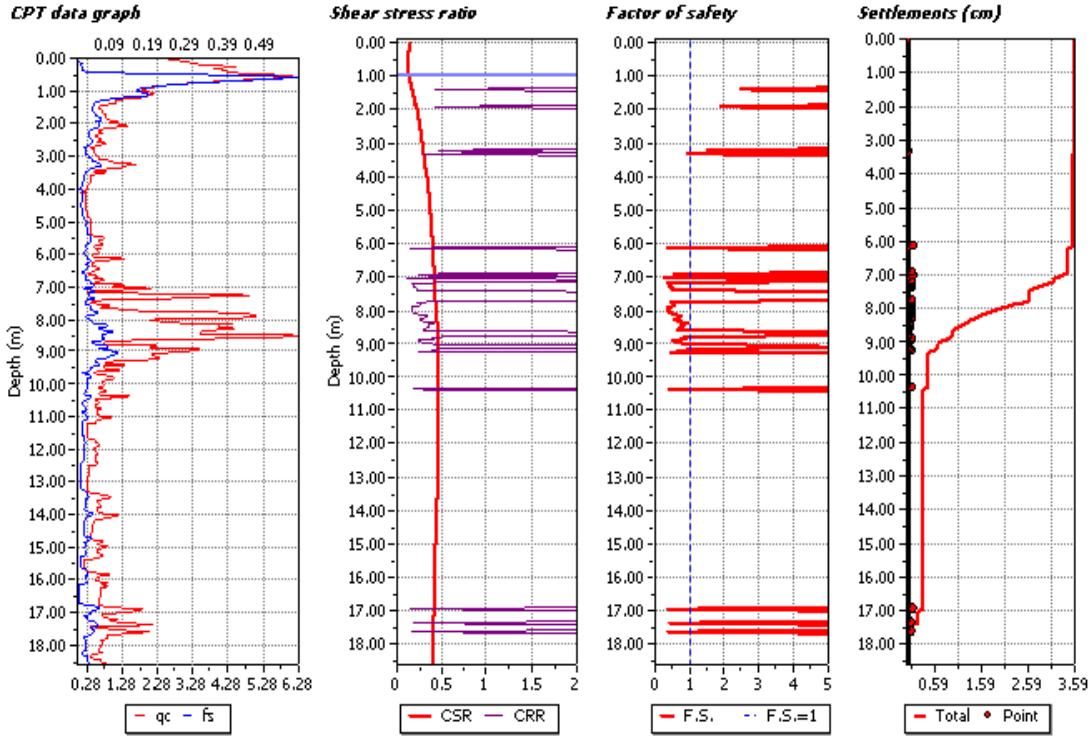

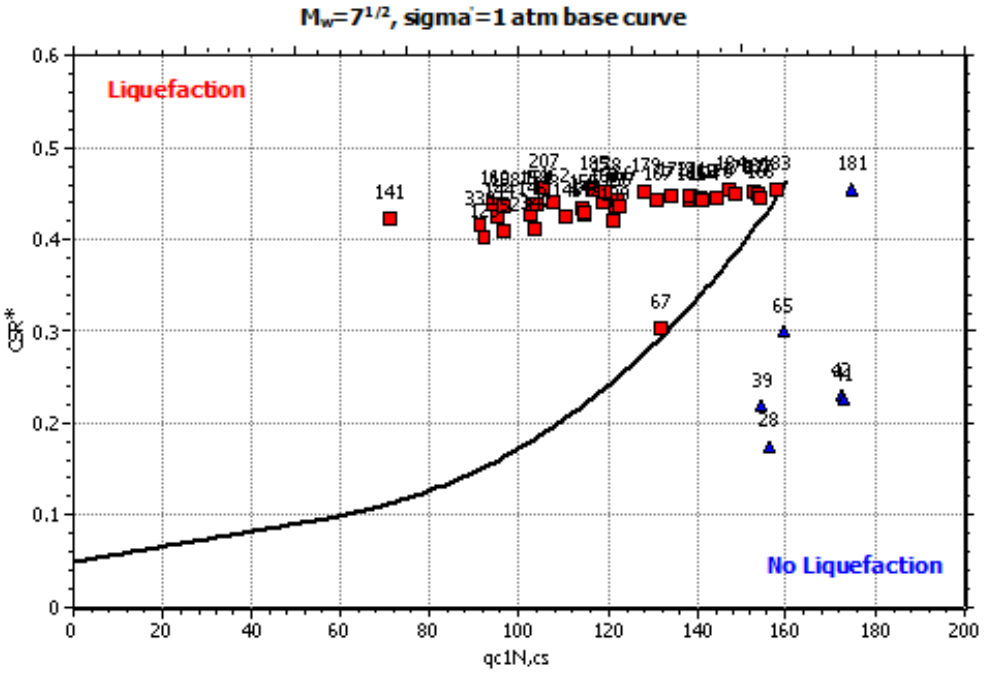

B.4 Liquefaction Information for CPT 4

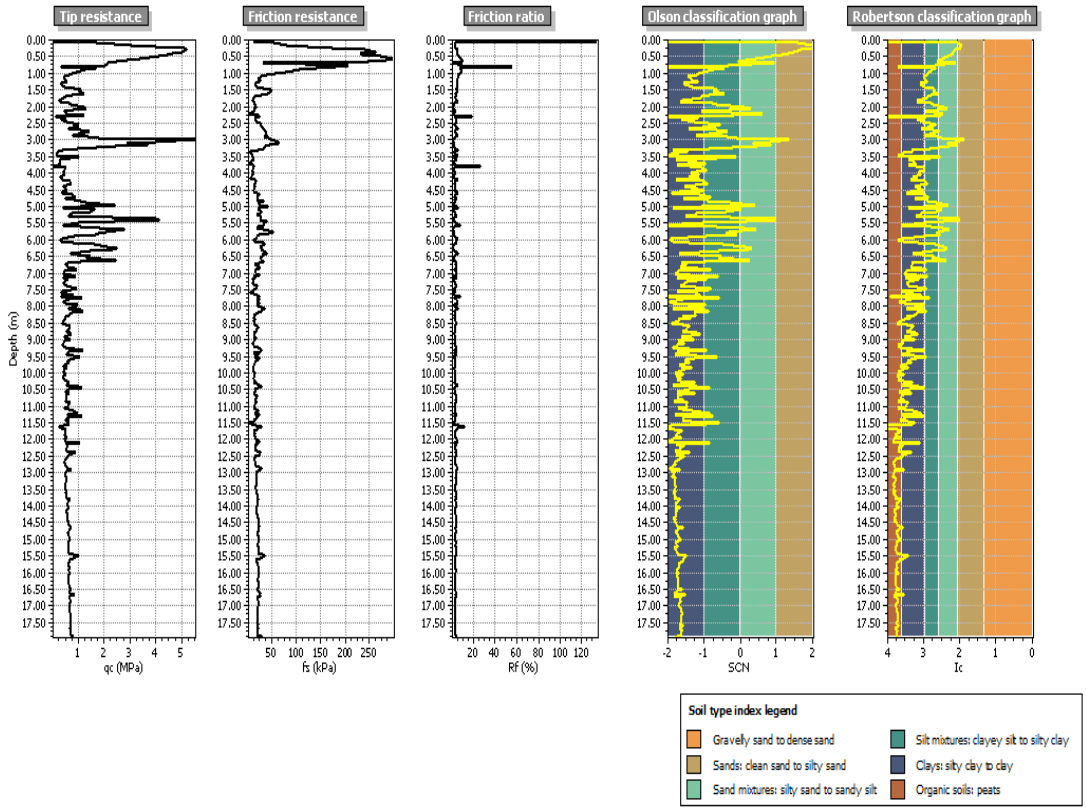

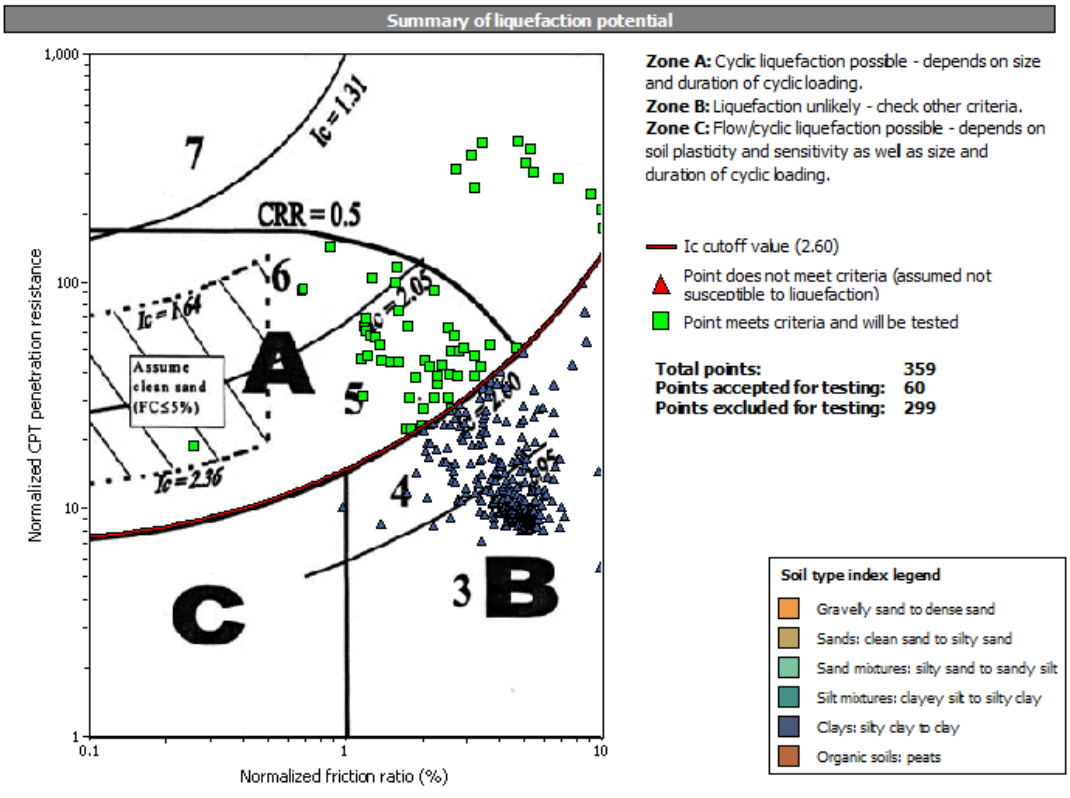

LIQUEFACTION ANALYSIS REPORT

Project title :

Project subtitle :

Input parameters and analysis data

In-situ data type:	Cone Penetration Test	Depth to water table:	1.00 m
Analysis type:	Deterministic	Earthquake magnitude M_w:	6.50
Analysis method:	Robertson (1998)	Peak ground accelaration:	0.30 g
Fines correction method:	Robertson (1998)	User defined F.S.:	1.00

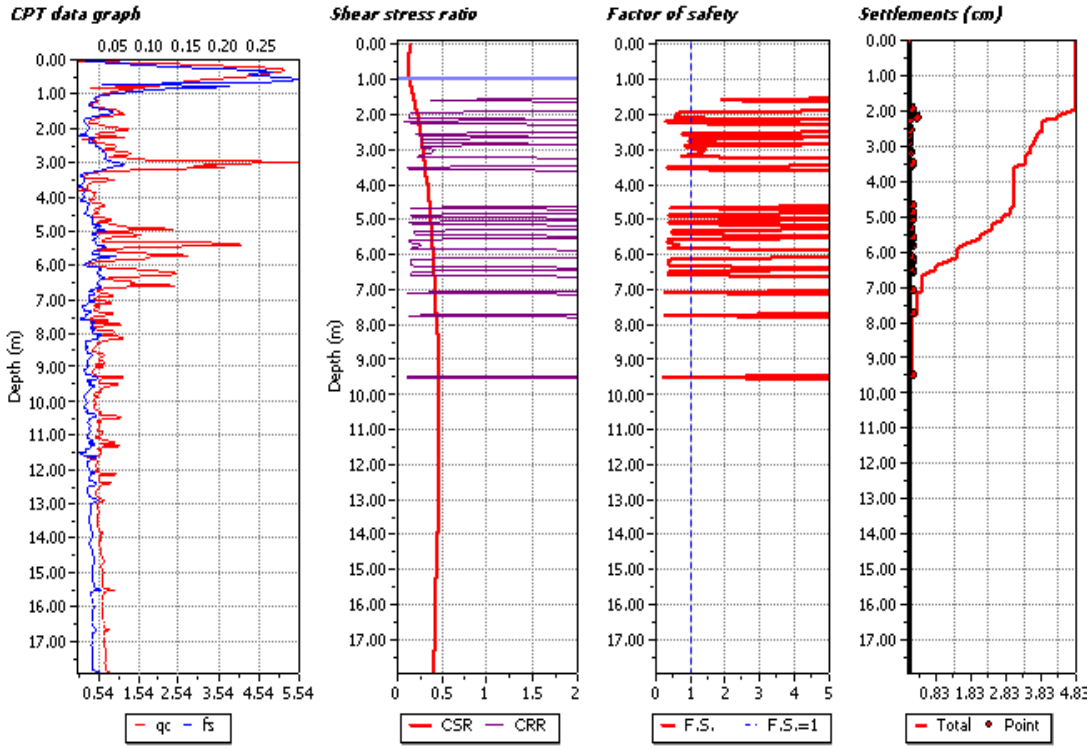

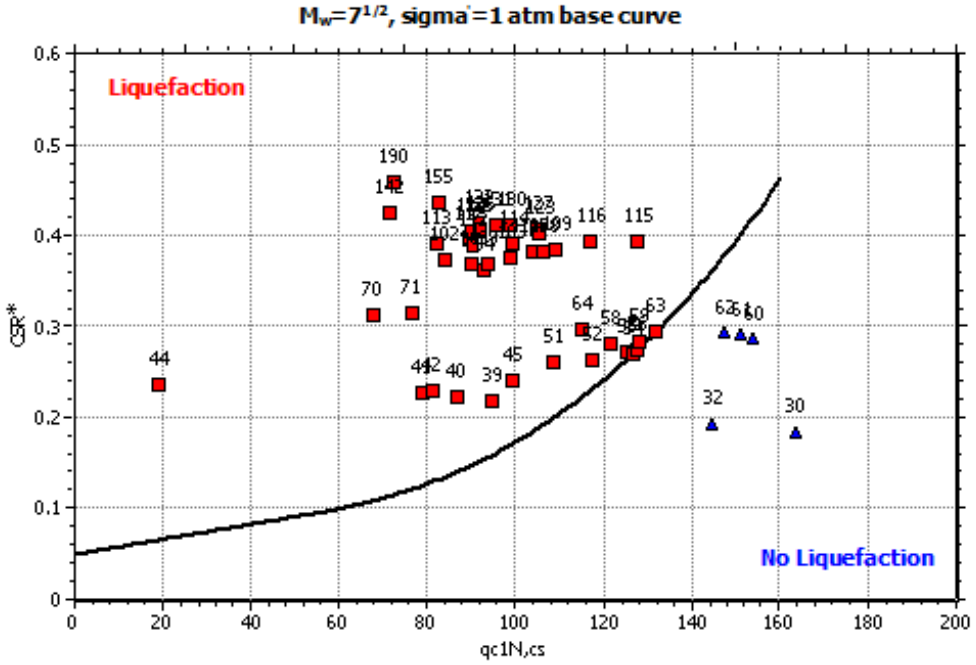

B.5 Liquefaction Information for CPT 5

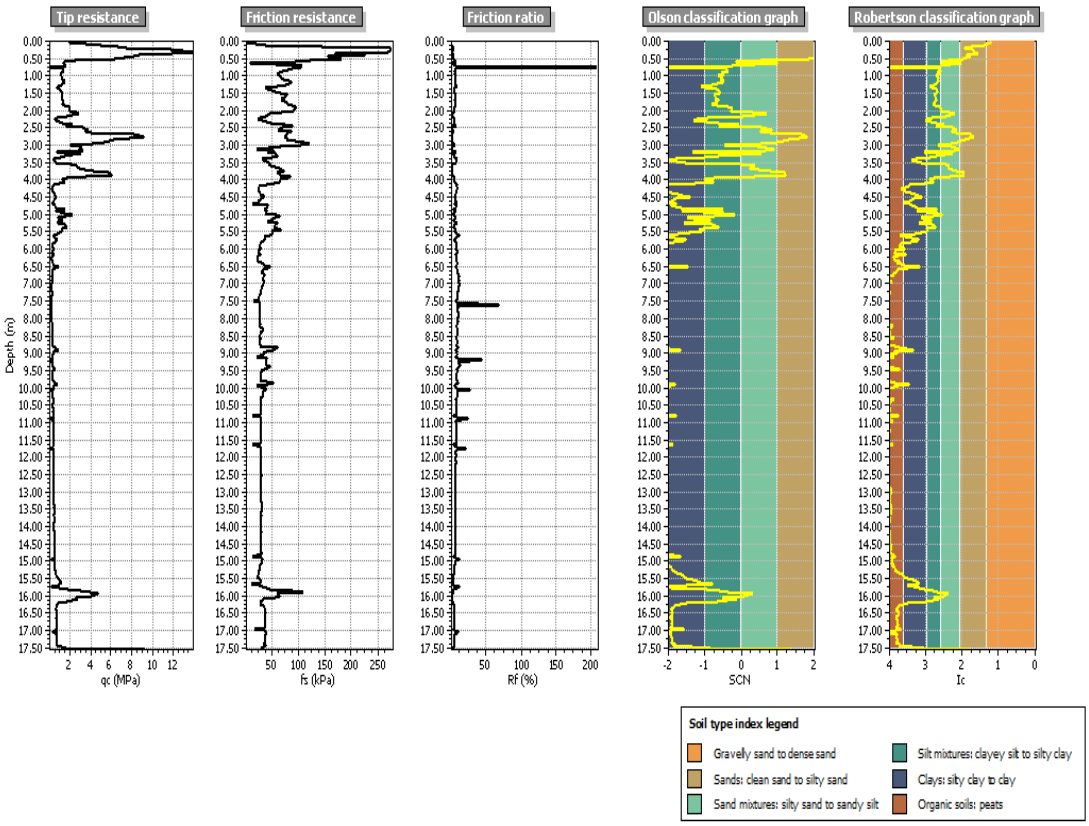

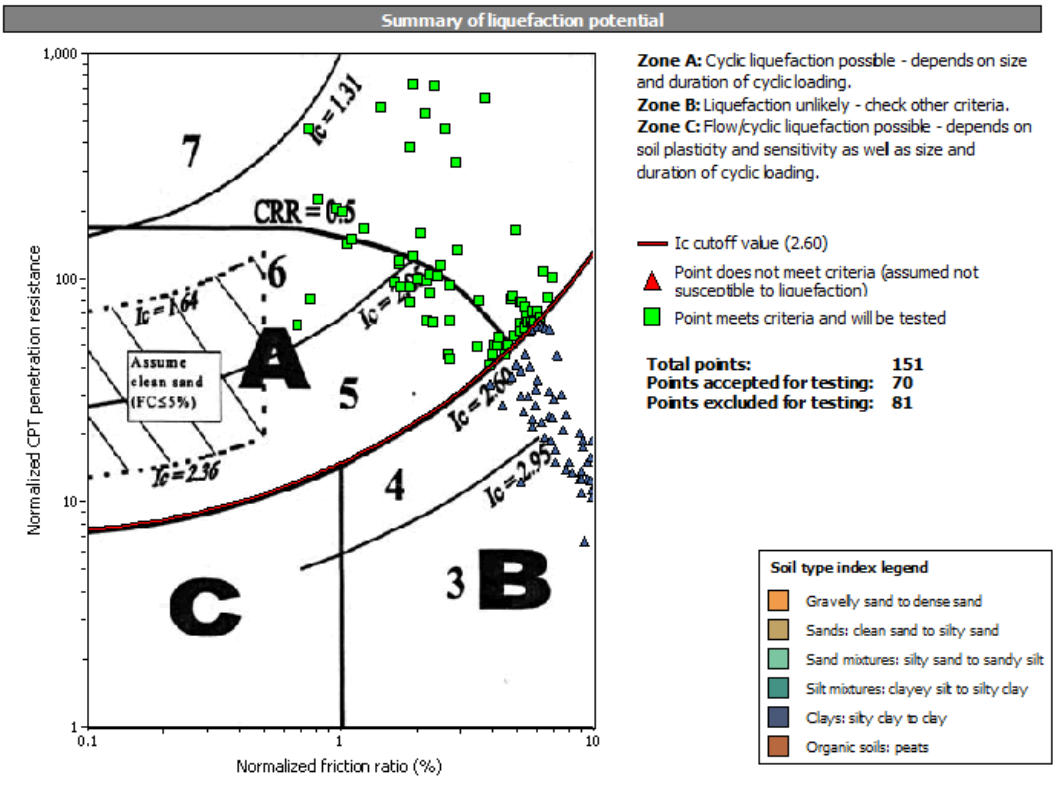

LIQUEFACTION ANALYSIS REPORT

Project title :

Project subtitle :

Input parameters and analysis data

In-situ data type:	Cone Penetration Test	Depth to water table:	1.00 m
Analysis type:	Deterministic	Earthquake magnitude M_w:	6.50
Analysis method:	Robertson (1998)	Peak ground accelaration:	0.30 g
Fines correction method:	Robertson (1998)	User defined F.S.:	1.00

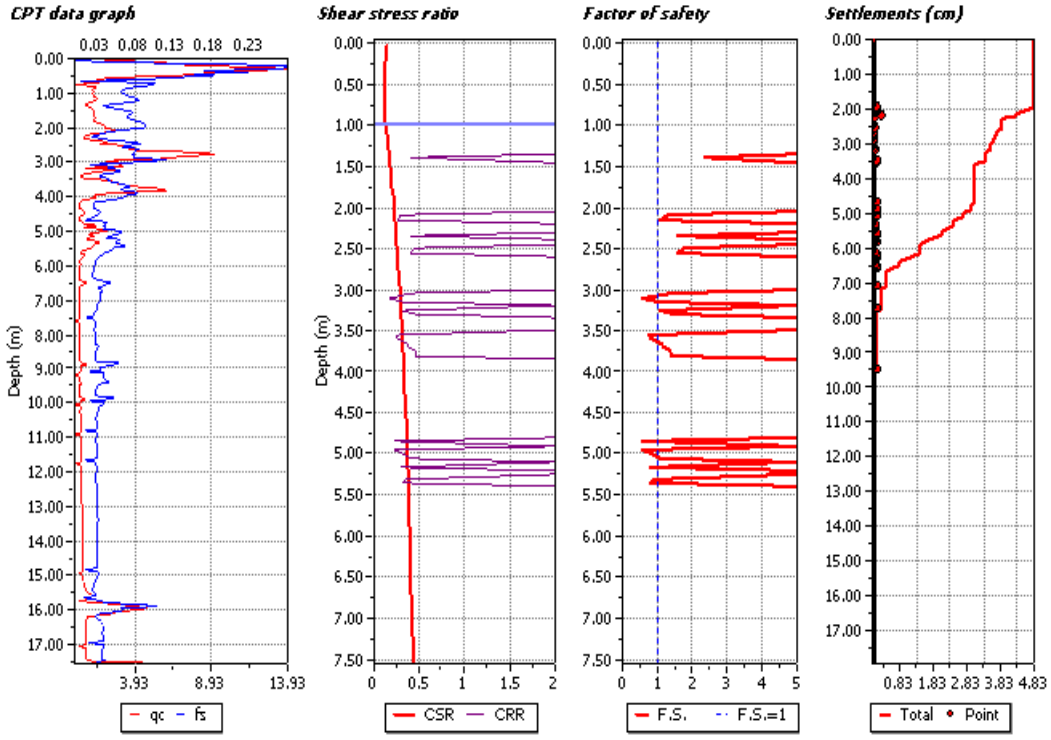

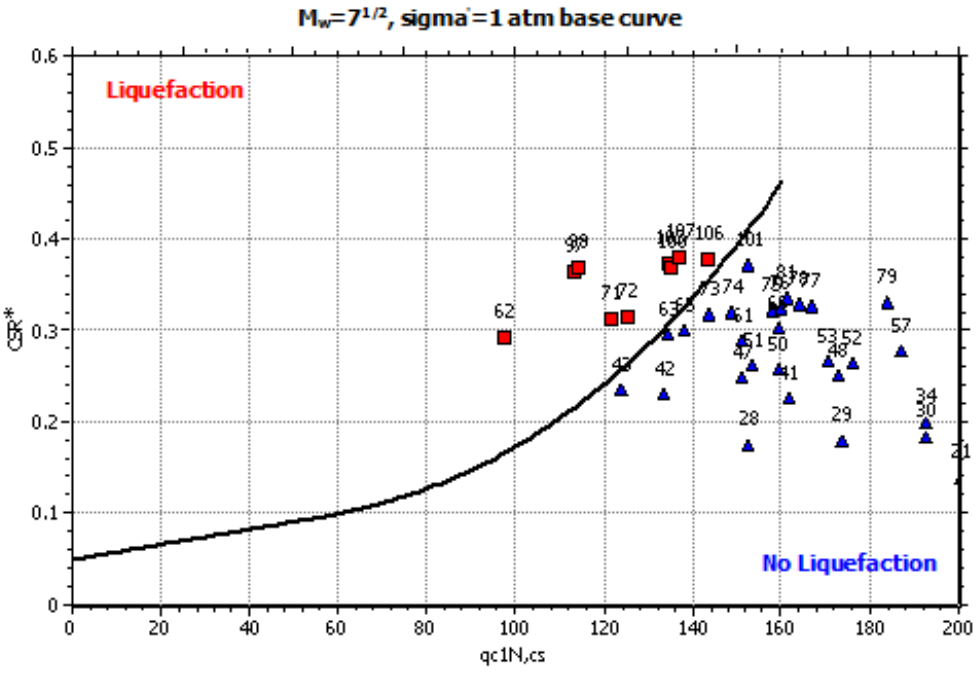

B.6 Liquefaction Information for CPT 6

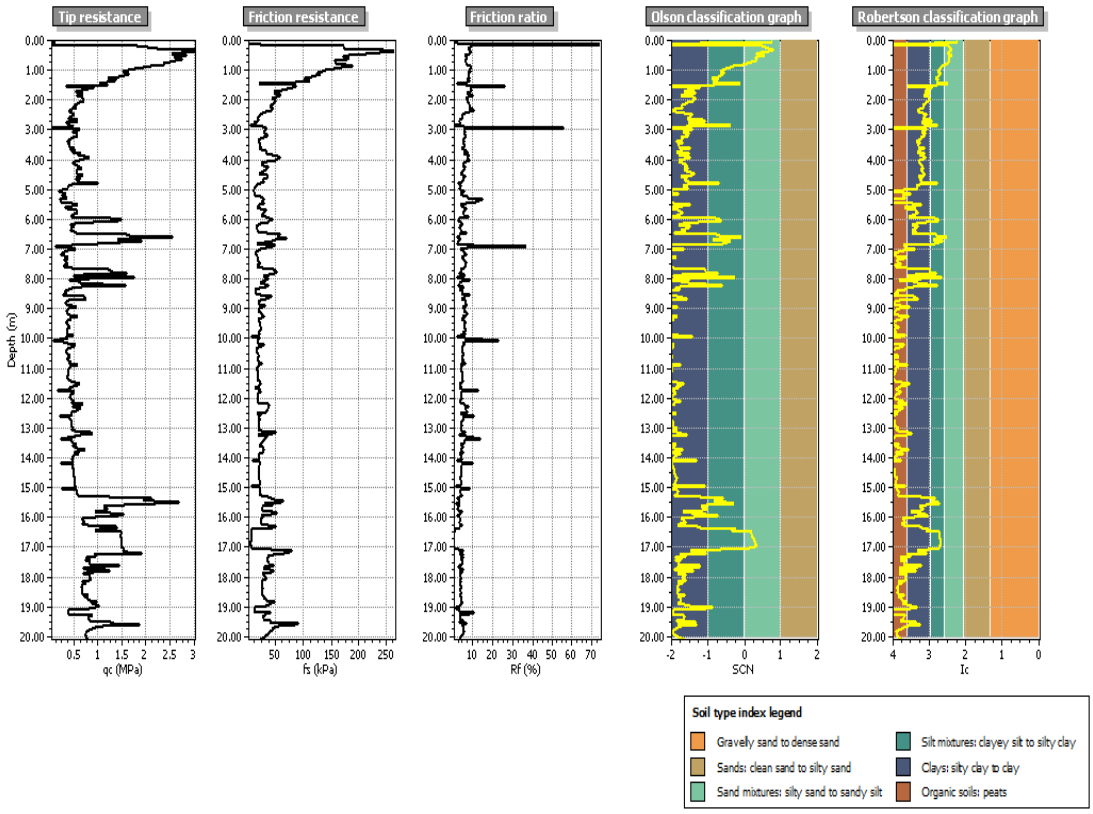

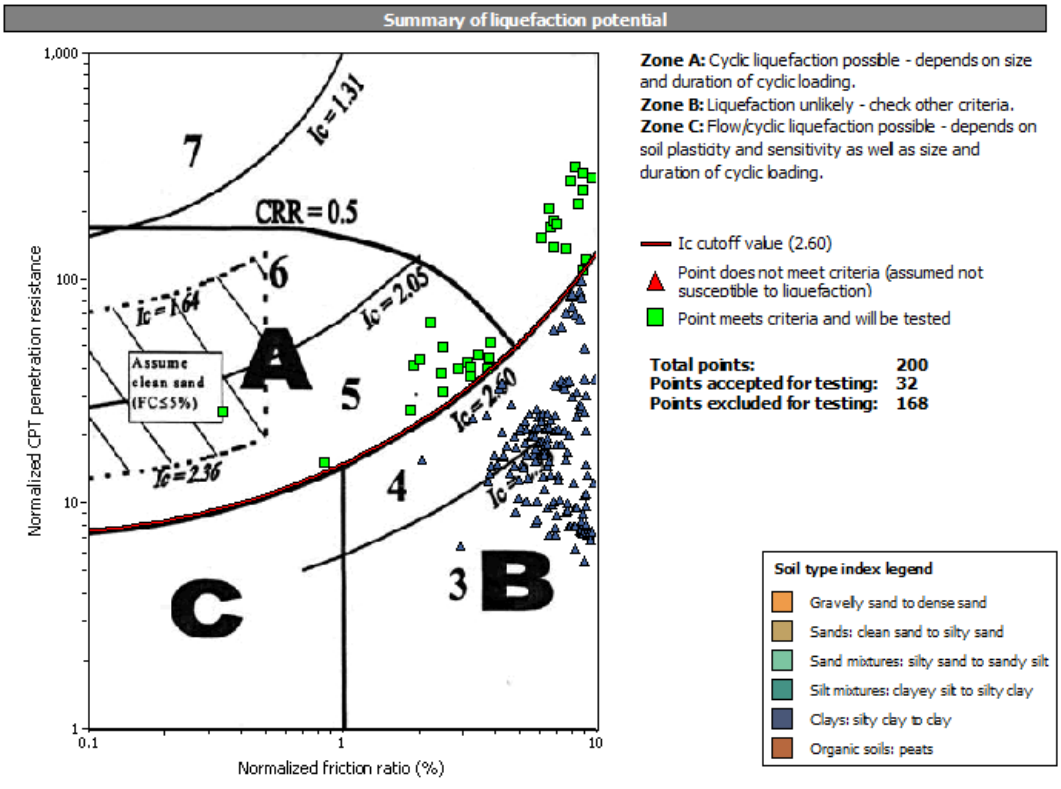

LIQUEFACTION ANALYSIS REPORT

Project title :

Project subtitle :

Input parameters and analysis data

In-situ data type:	Cone Penetration Test	Depth to water table:	1.00 m
Analysis type:	Deterministic	Earthquake magnitude M_w:	6.50
Analysis method:	Robertson (1998)	Peak ground accelaration:	0.30 g
Fines correction method:	Robertson (1998)	User defined F.S.:	1.00

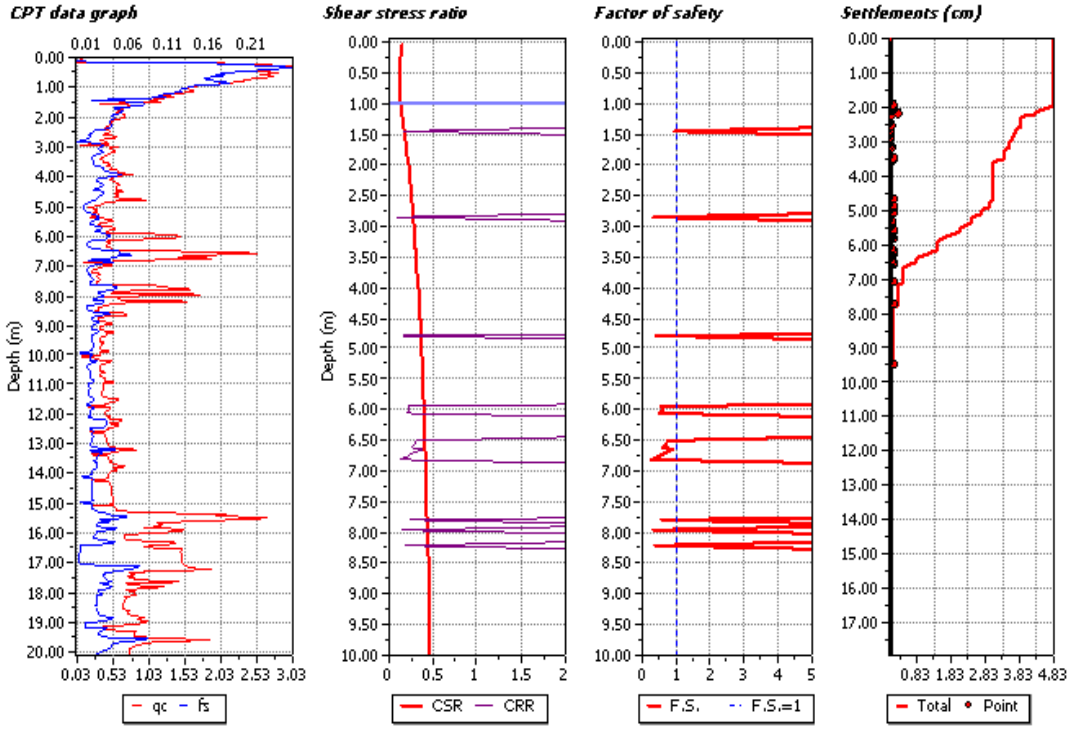

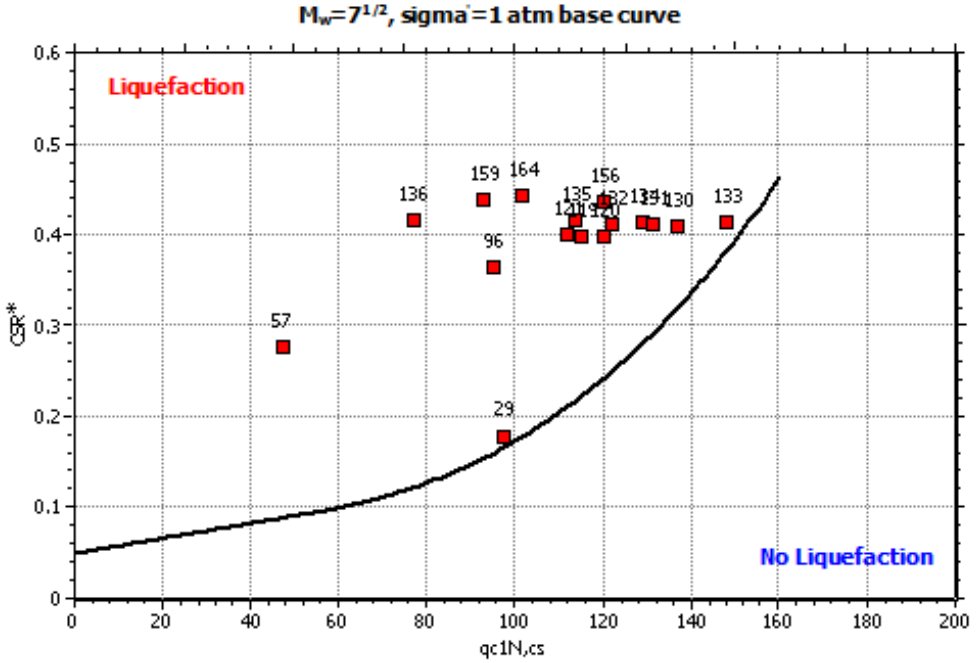

B.7 Liquefaction Information for CPT 7

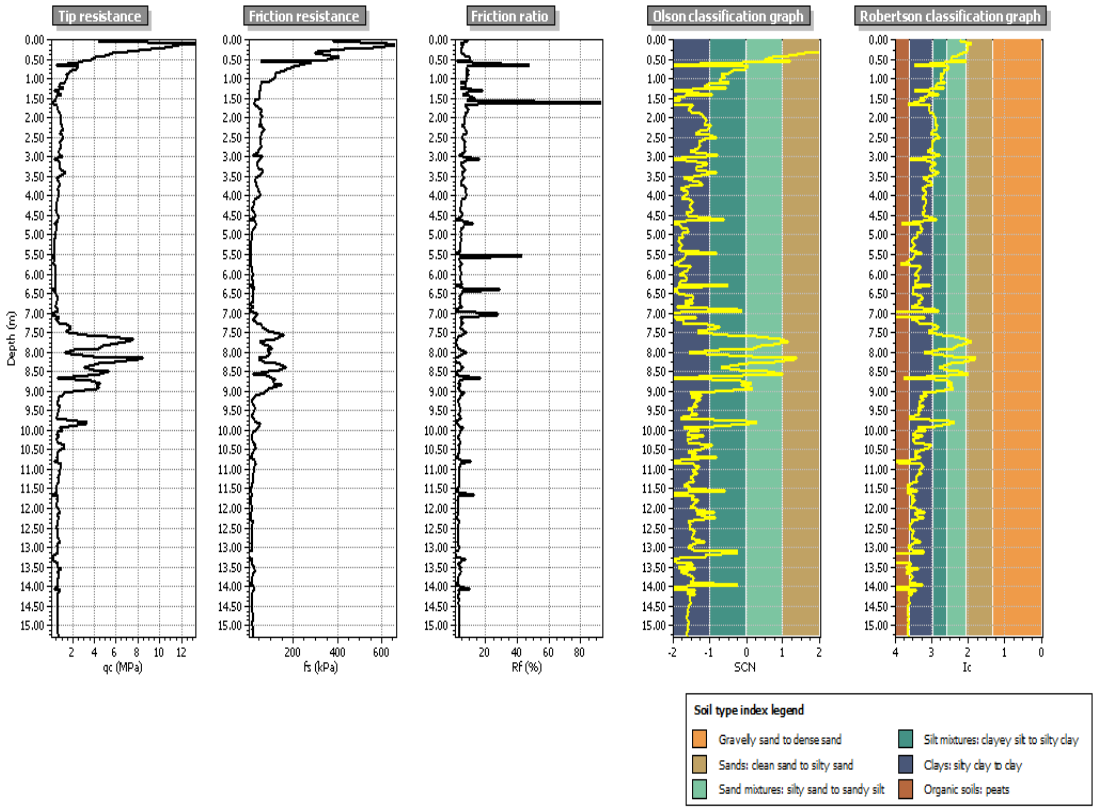

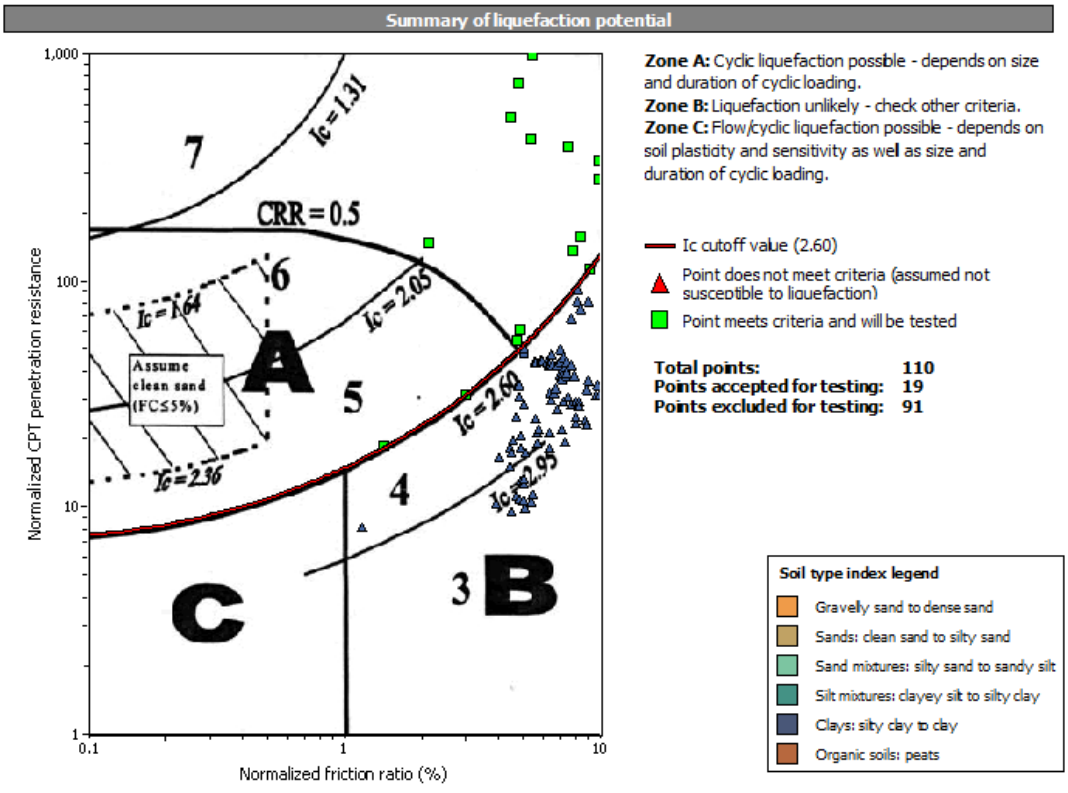

LIQUEFACTION ANALYSIS REPORT

Project title :

Project subtitle :

Input parameters and analysis data

In-situ data type:	Cone Penetration Test	Depth to water table:	1.00 m
Analysis type:	Deterministic	Earthquake magnitude M_w:	6.50
Analysis method:	Robertson (1998)	Peak ground accelaration:	0.30 g
Fines correction method:	Robertson (1998)	User defined F.S.:	1.00

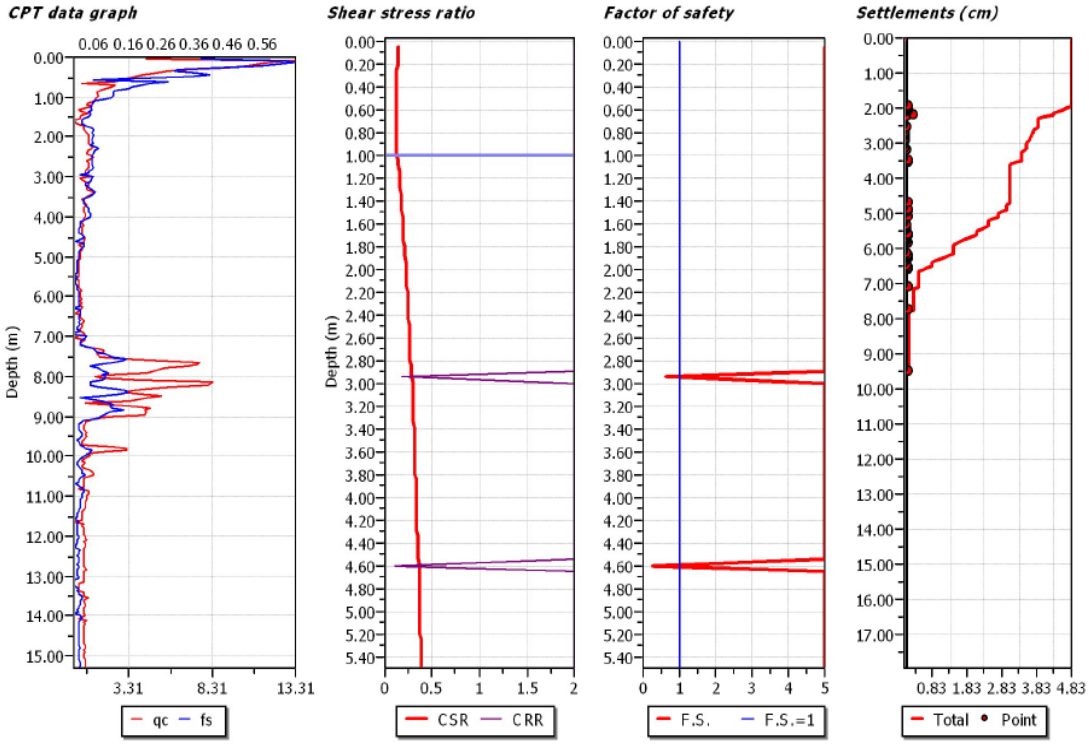

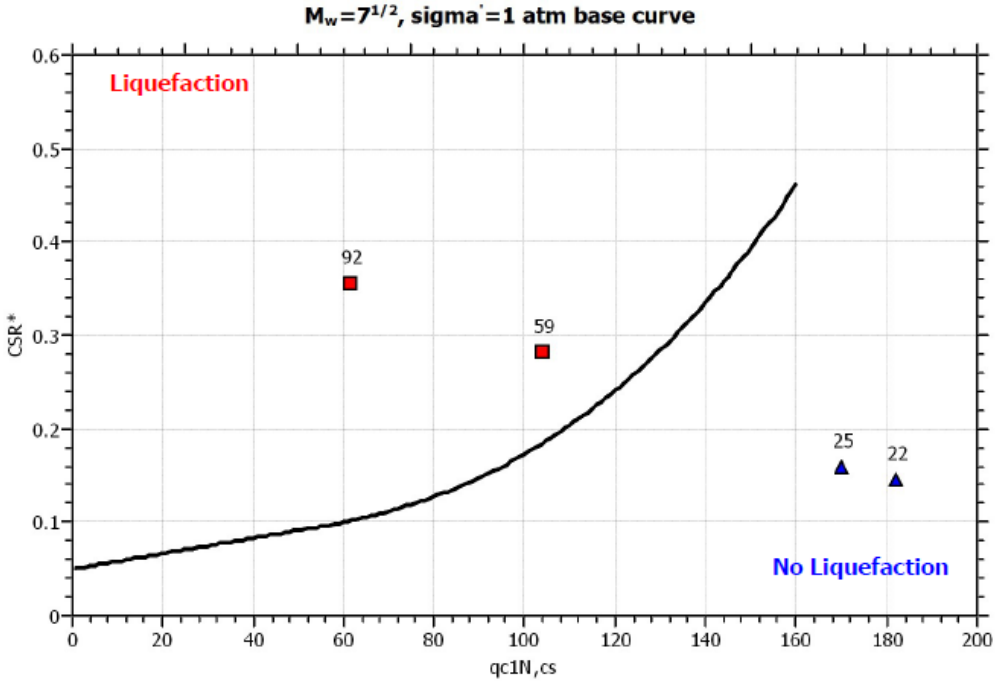

B.8 Liquefaction Information for CPT 8

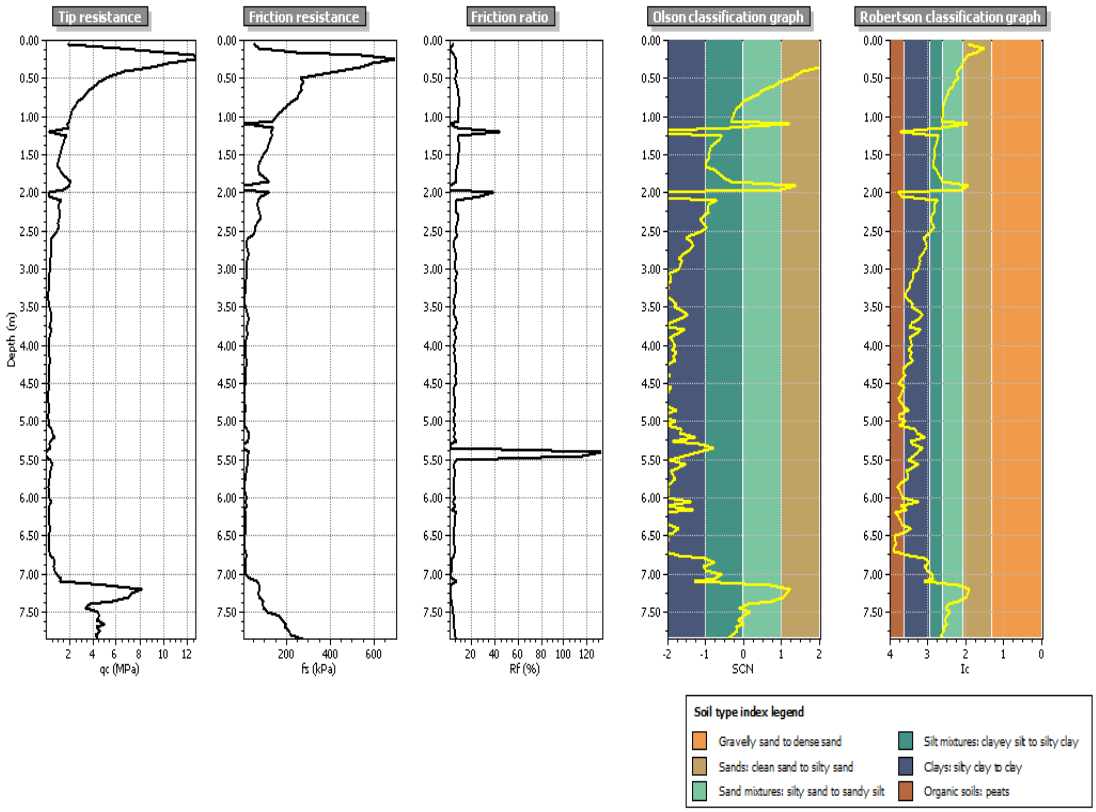

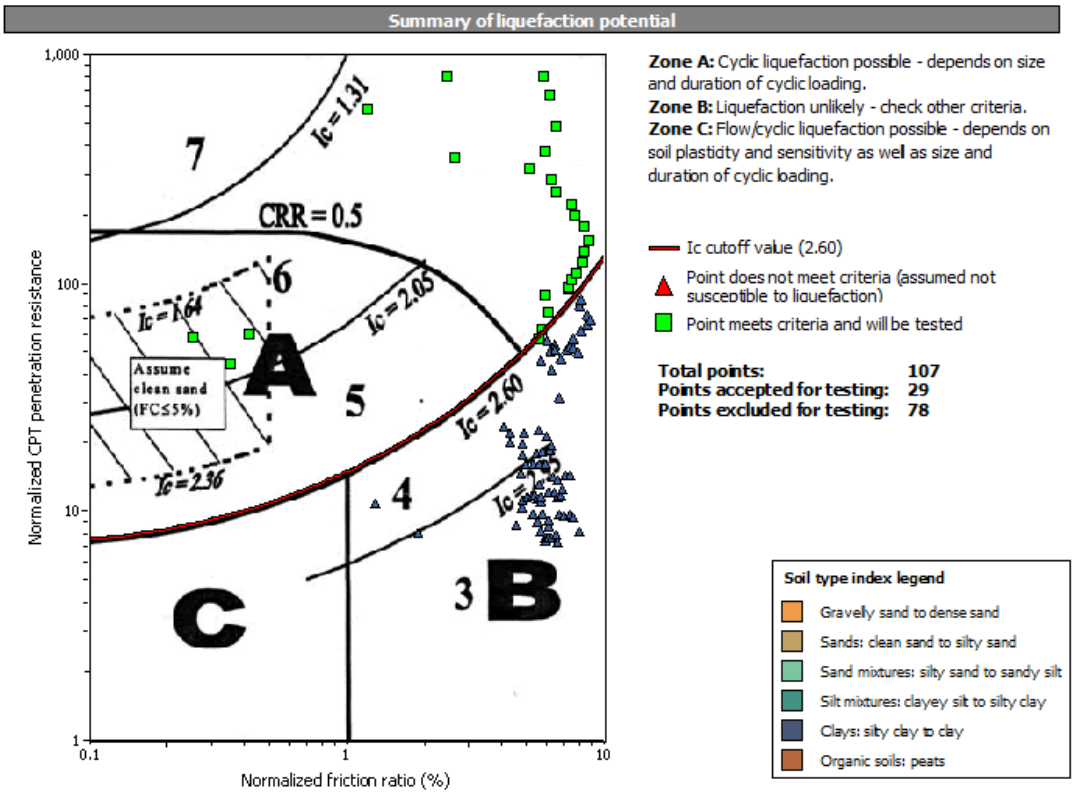

LIQUEFACTION ANALYSIS REPORT

Project title :

Project subtitle :

Input parameters and analysis data

In-situ data type:	Cone Penetration Test	Depth to water table:	1.00 m
Analysis type:	Deterministic	Earthquake magnitude M_w:	6.50
Analysis method:	Robertson (1998)	Peak ground accelaration:	0.30 g
Fines correction method:	Robertson (1998)	User defined F.S.:	1.00

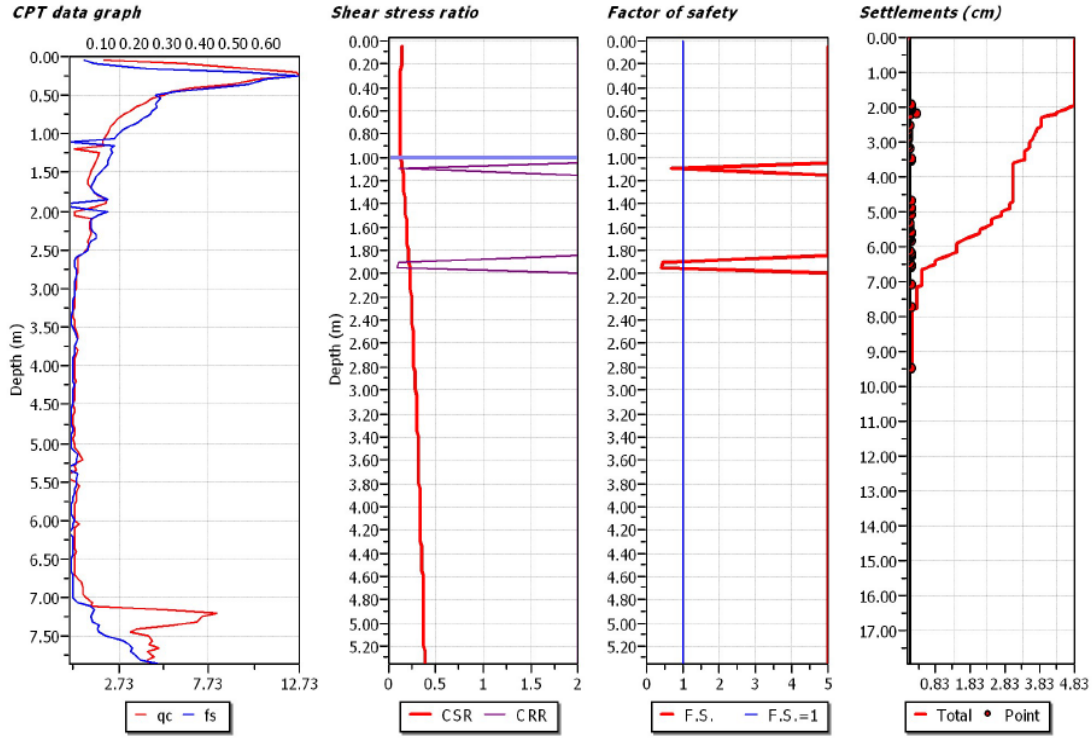

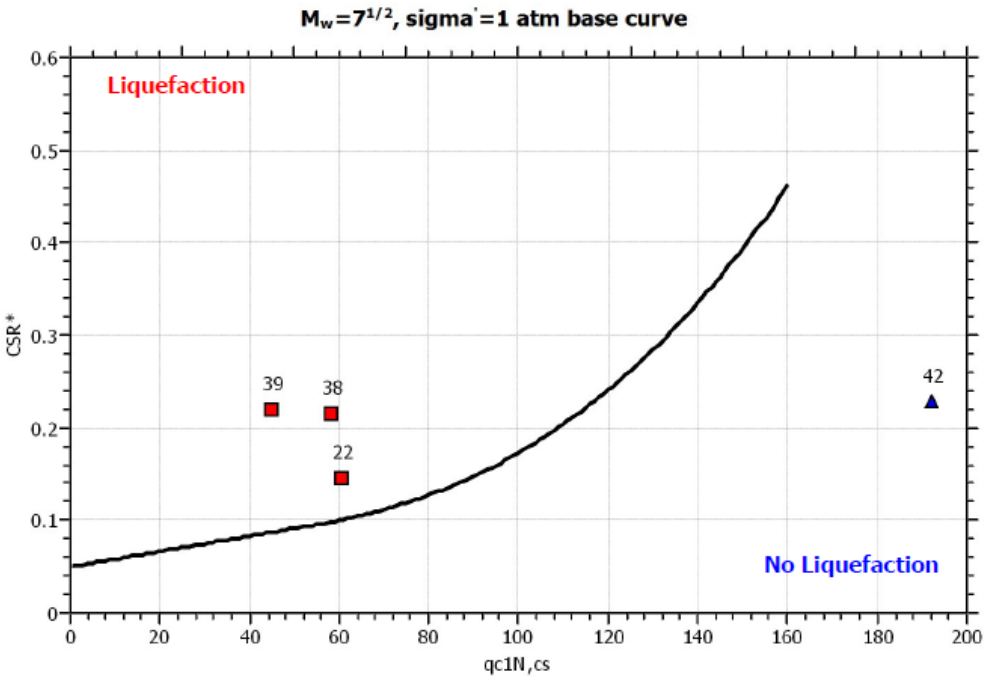

B.9 Liquefaction Information for CPT 9

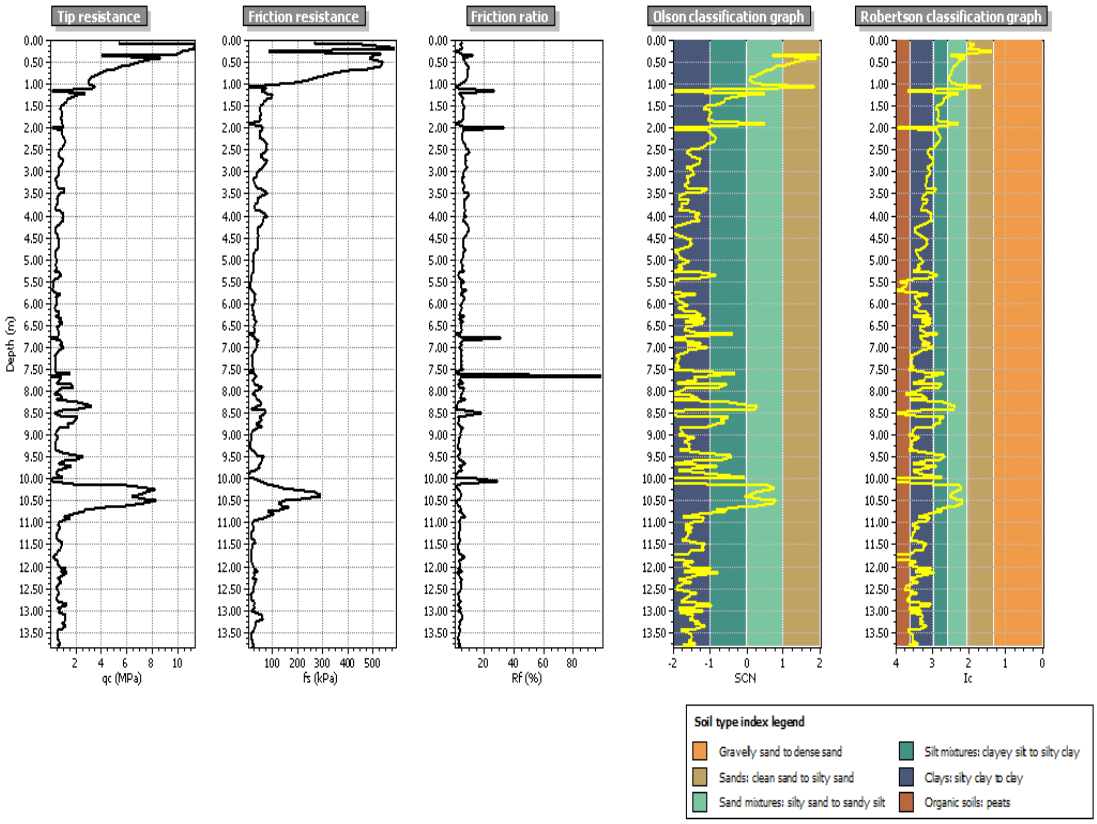

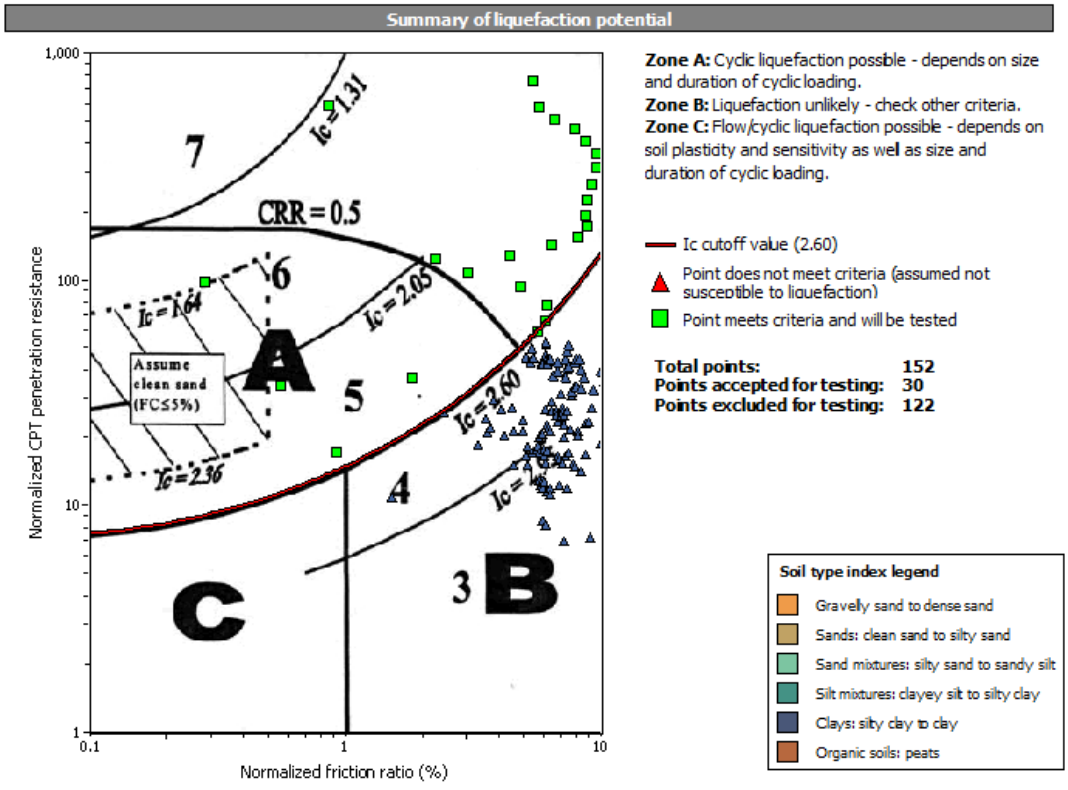

LIQUEFACTION ANALYSIS REPORT

Project title :

Project subtitle :

Input parameters and analysis data

In-situ data type:	Cone Penetration Test	Depth to water table:	1.00 m
Analysis type:	Deterministic	Earthquake magnitude M_w:	6.50
Analysis method:	Robertson (1998)	Peak ground accelaration:	0.30 g
Fines correction method:	Robertson (1998)	User defined F.S.:	1.00

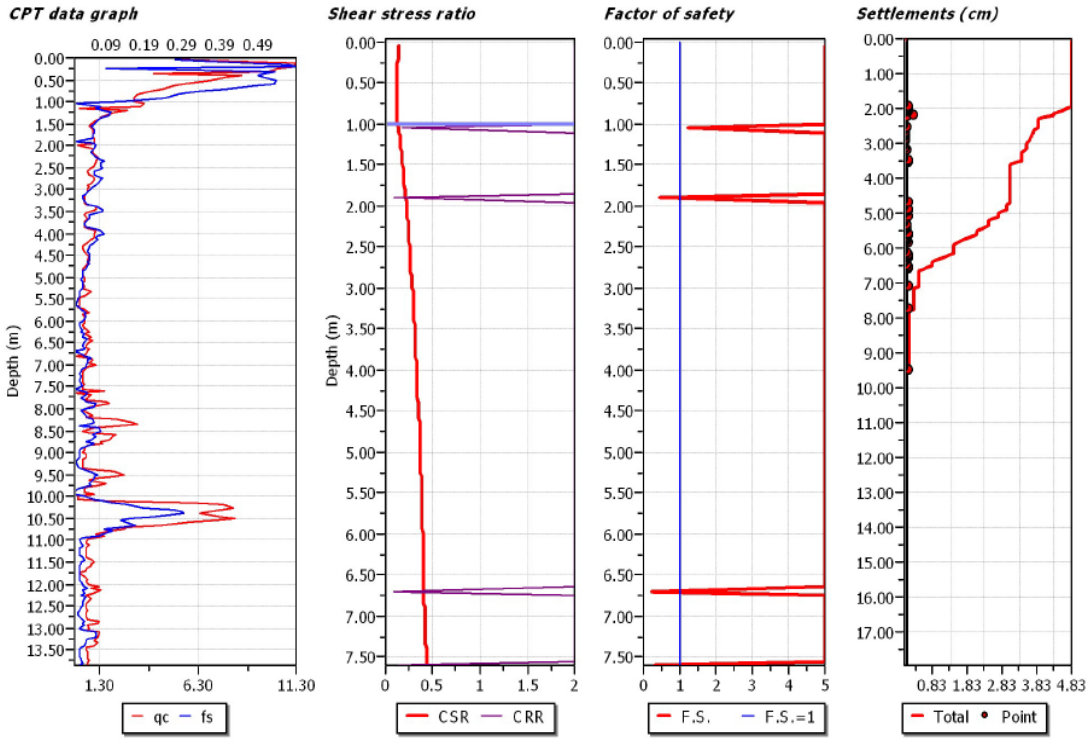

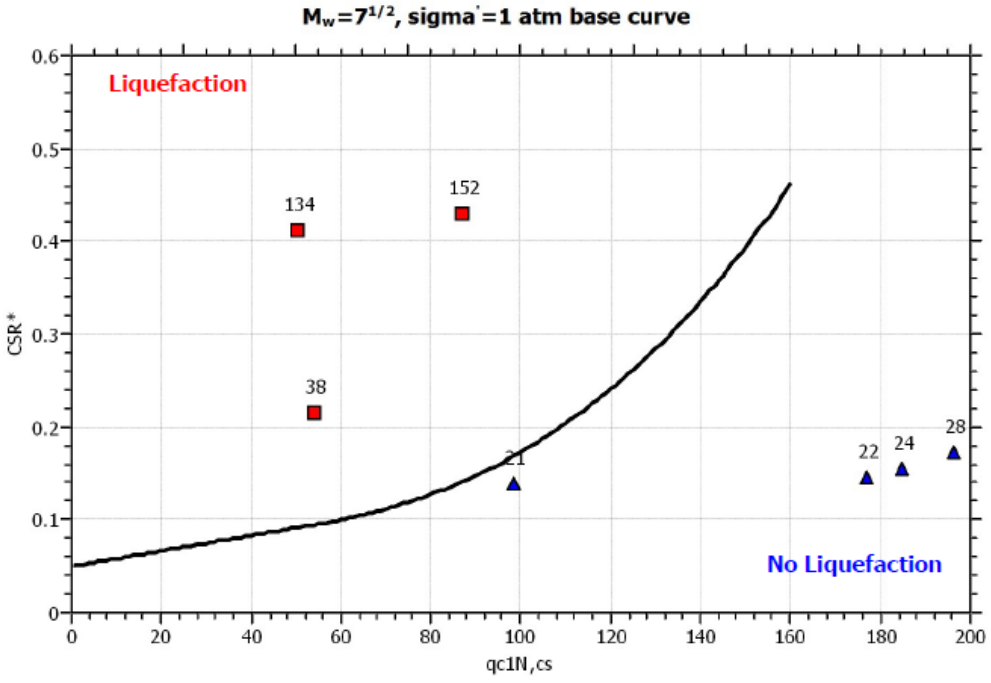

B.10 Liquefaction Information for CPT 10

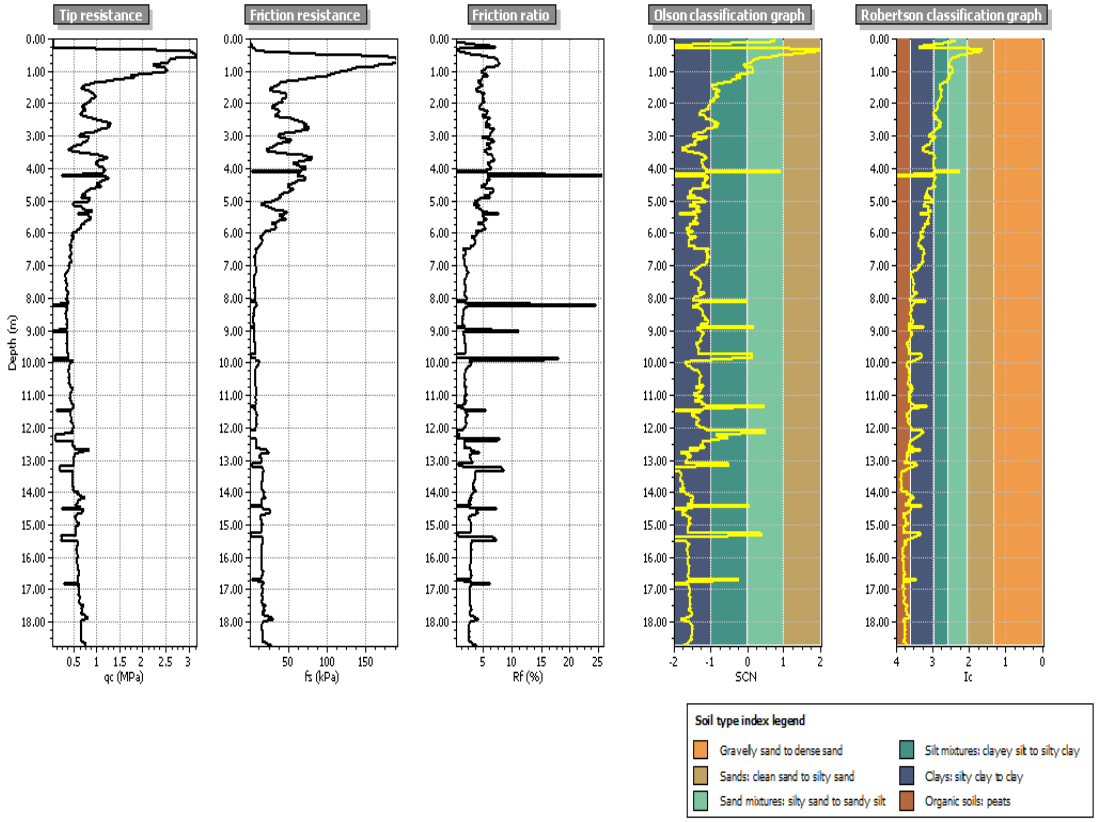

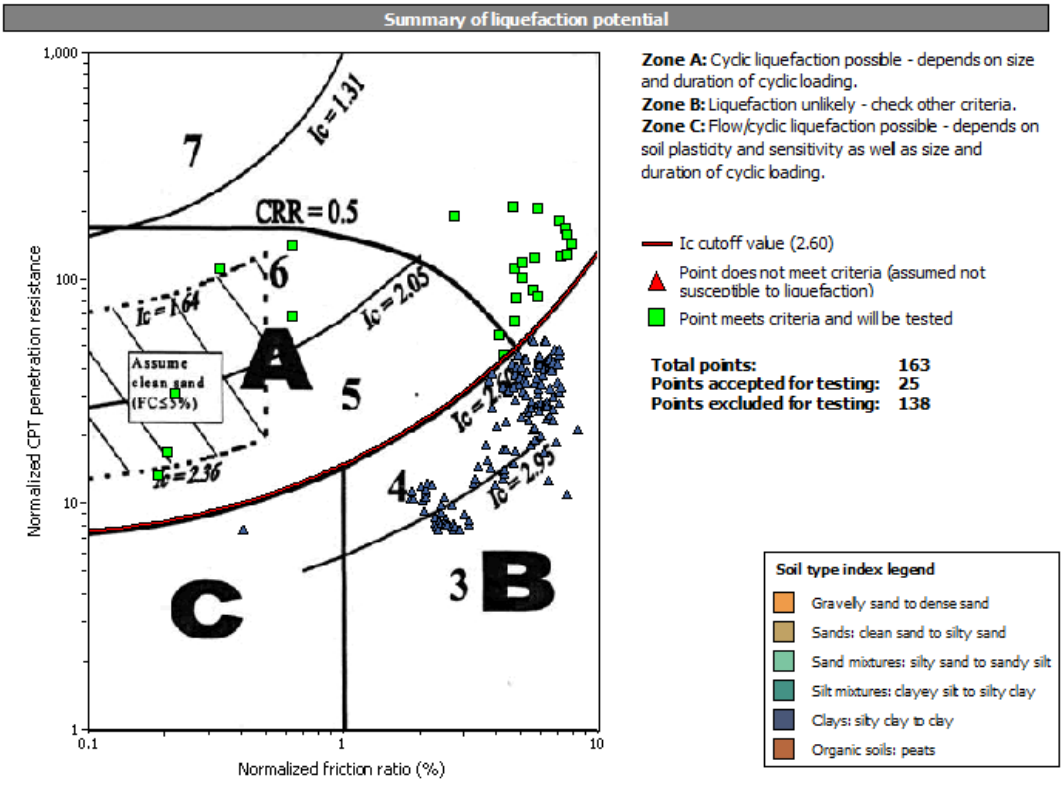

LIQUEFACTION ANALYSIS REPORT

Project title :

Project subtitle :

Input parameters and analysis data

In-situ data type:	Cone Penetration Test	Depth to water table:	1.00 m
Analysis type:	Deterministic	Earthquake magnitude M_w:	6.50
Analysis method:	Robertson (1998)	Peak ground accelaration:	0.30 g
Fines correction method:	Robertson (1998)	User defined F.S.:	1.00

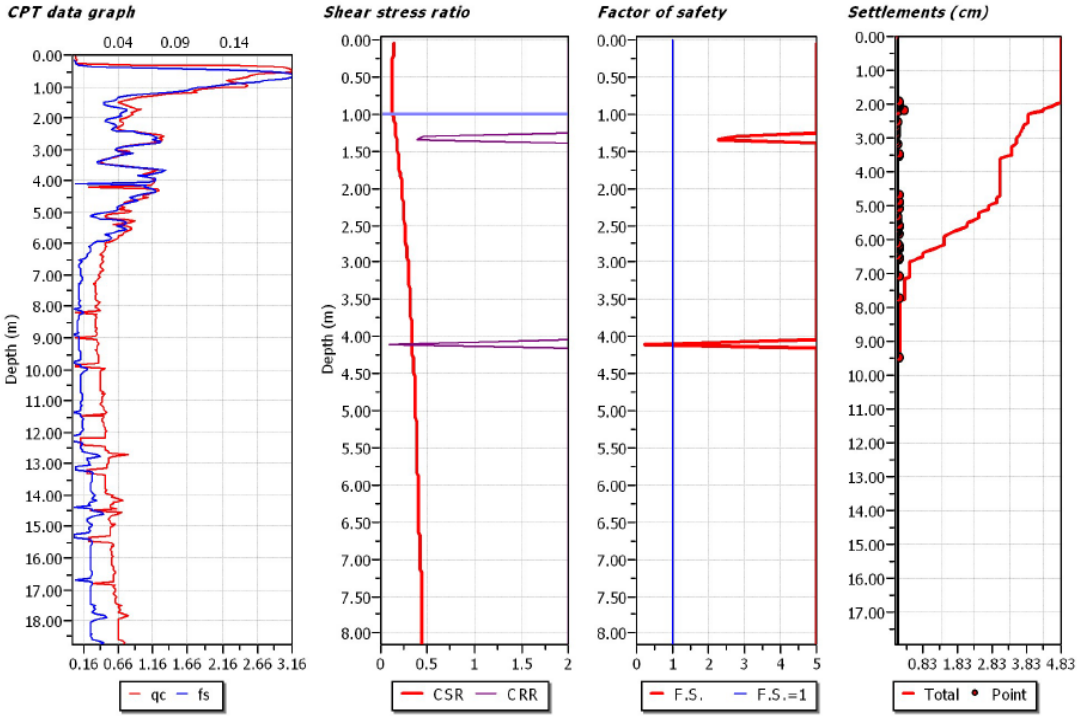

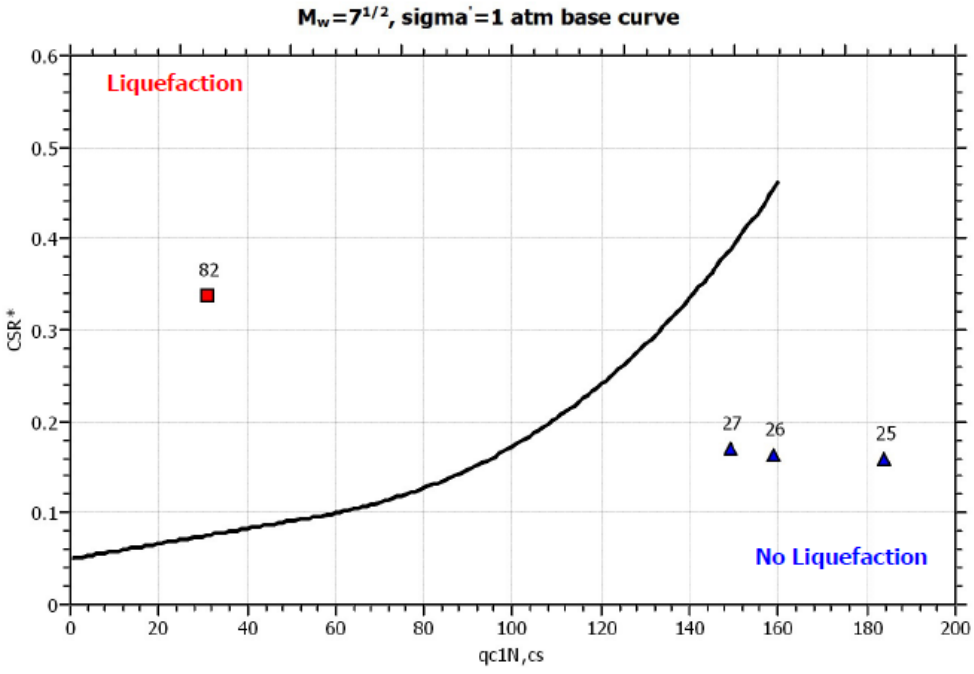

Appendix C: DeepSoil Software Results

C.1 Results of CPT 1

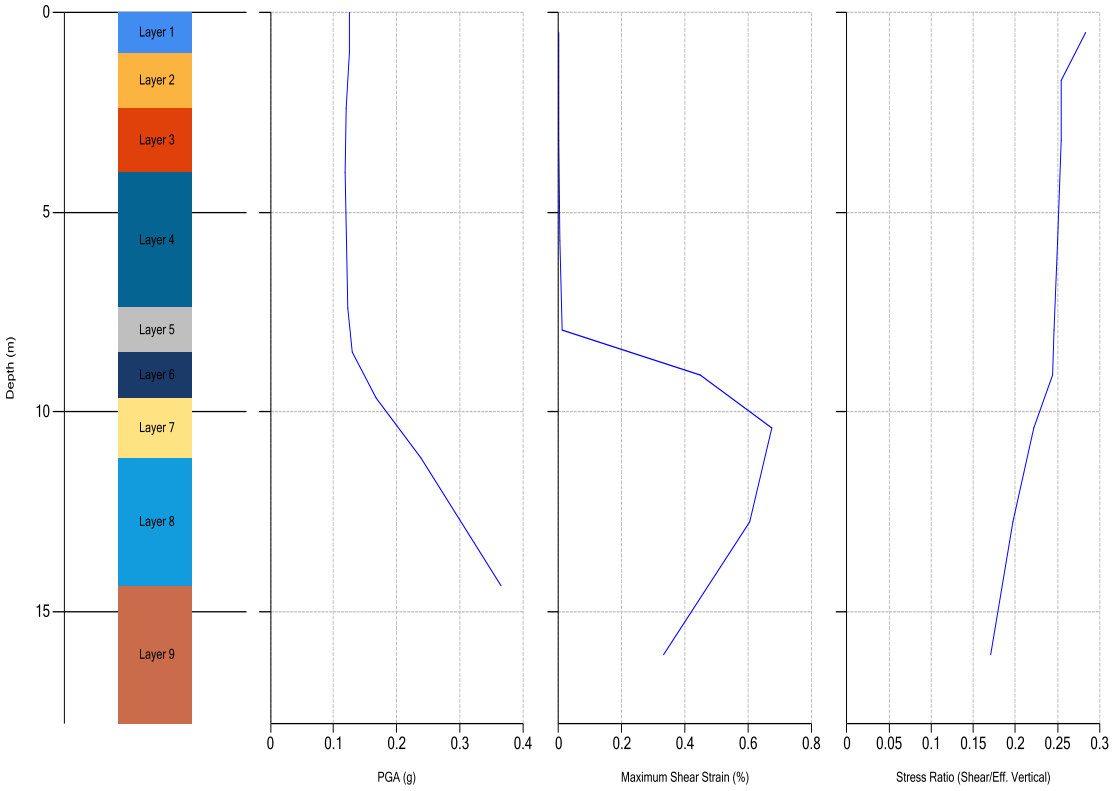

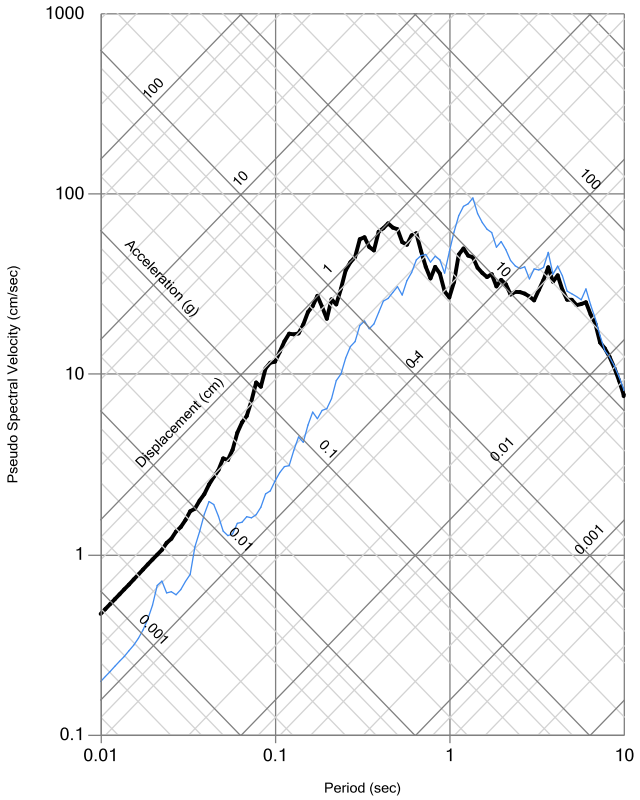

Layer #	Layer Name	Thickness (m)
1	sand	1
2	sand to silty sand	1.4
3	sand to silty sand	1.6
4	sillty sand to sandy silt	3.4
5	sandy silt to clayey silt	1.1
6	silty sand to sandy silt	1.15
7	silty clay to clay	1.5
8	clay	3.2
9	clayey silt to silty clay	3.45

C.2 Results of CPT 2

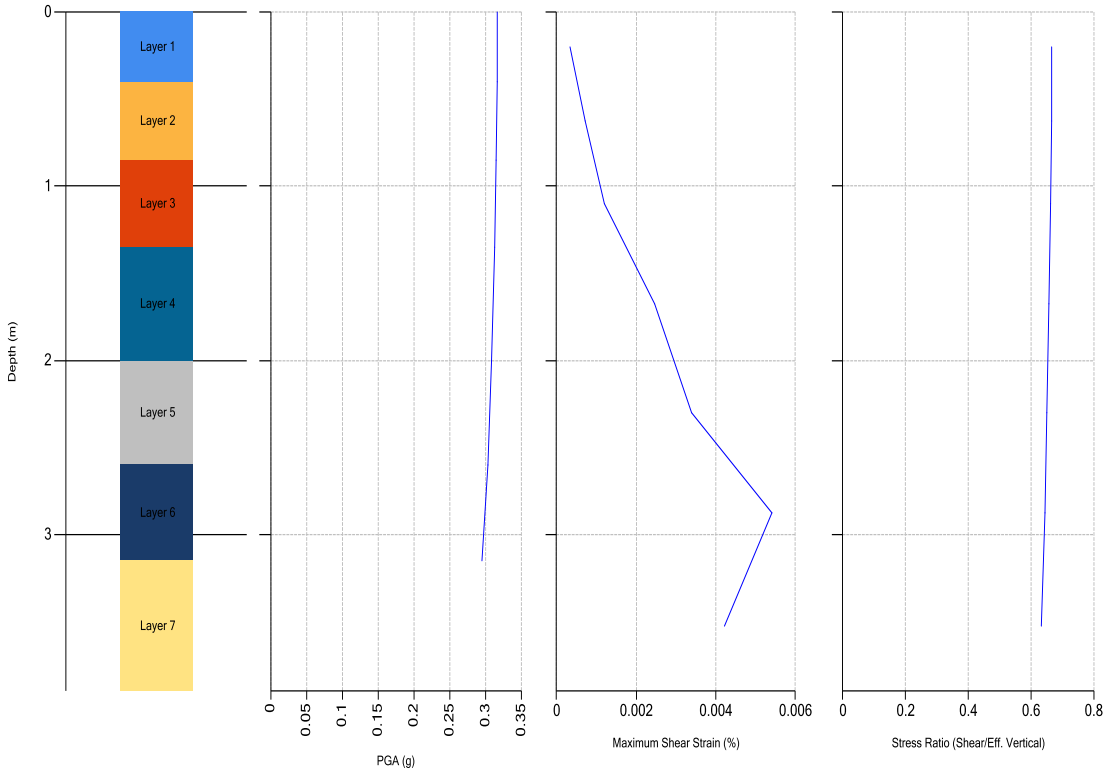

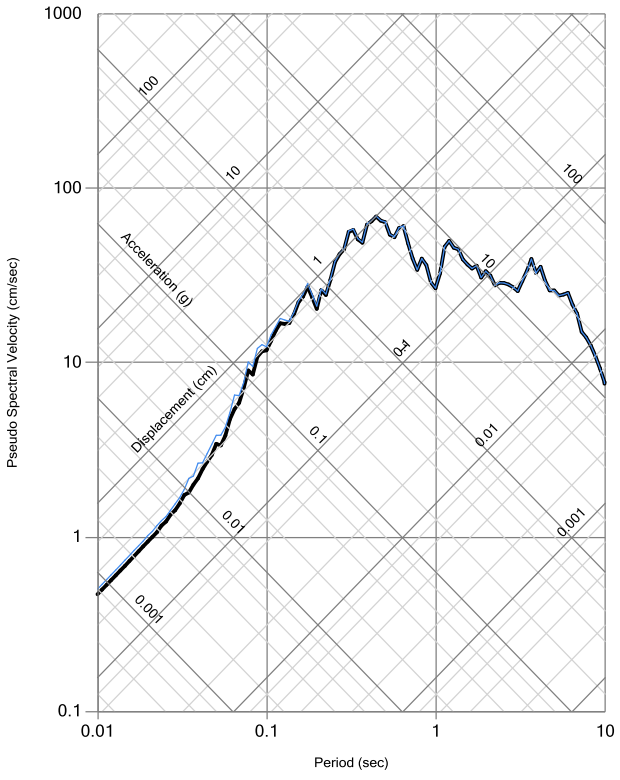

Layer #	Layer Name	Thickness (m)
1	sand to silty sand	0.4
2	sand	0.45
3	silty sand to sandy silt	0.5
4	sand to silty sand	0.65
5	sand	0.6
6	sand to silty sand	0.55
7	sand	0.75

C.3 Results of CPT 3

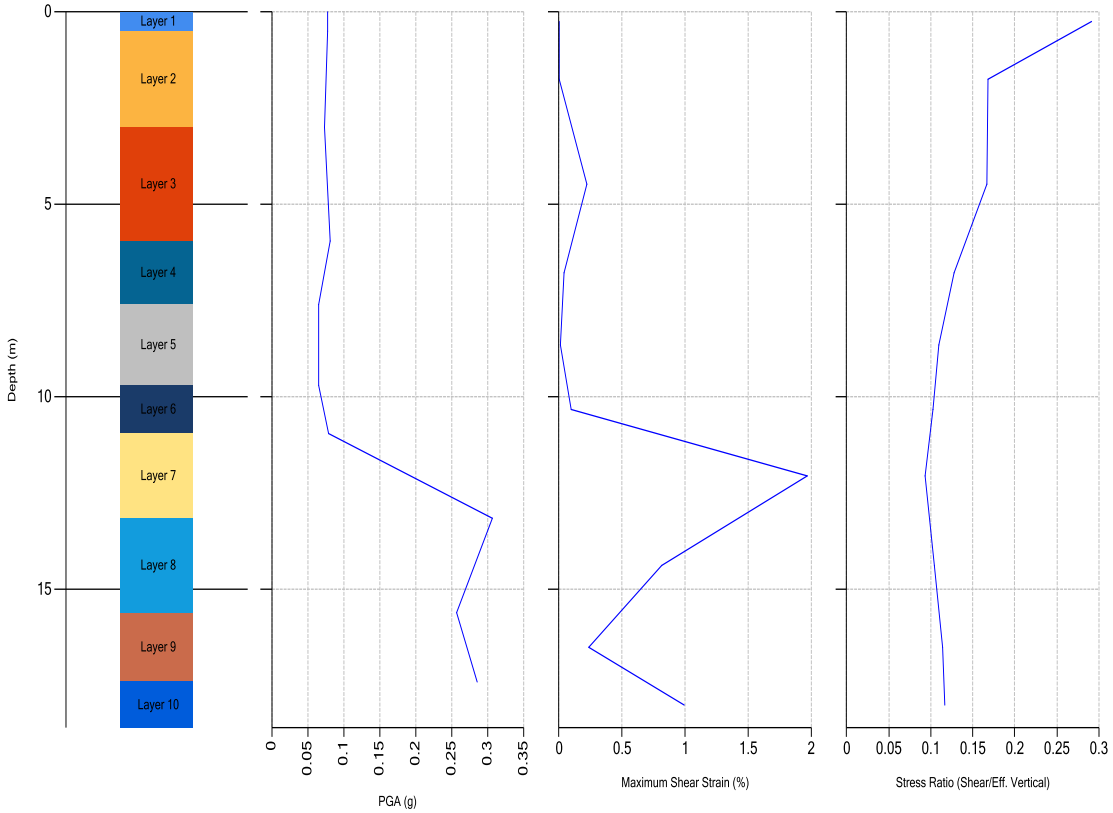

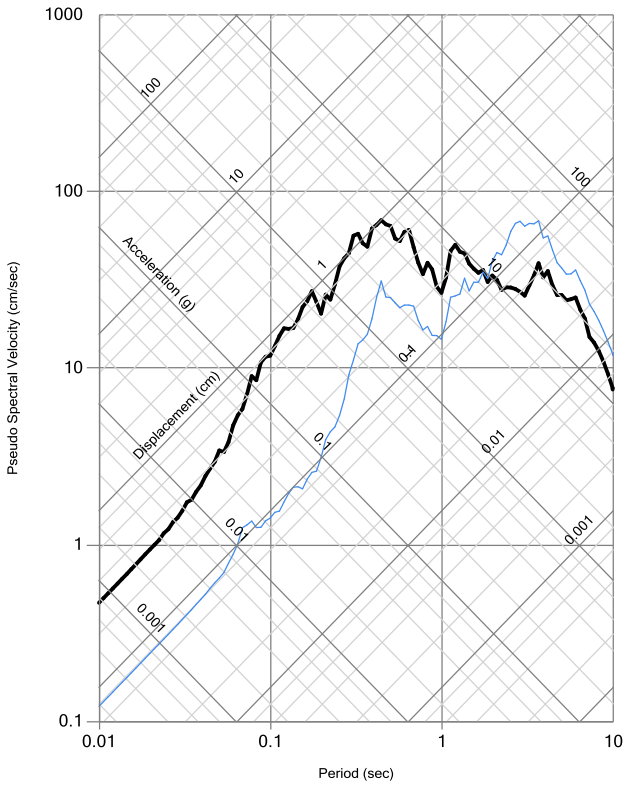

Layer #	Layer Name	Thickness (m)
1	silty sand to sandy silt	0.5
2	clay	2.5
3	clay	2.95
4	silty clay to clay	1.65
5	silty sand to sandy silt	2.1
6	clay	1.25
7	silty clay to clay	2.2
8	clay	2.45
9	silty clay to clay	1.8
10	clay	1.2

C.4 Results of CPT 4

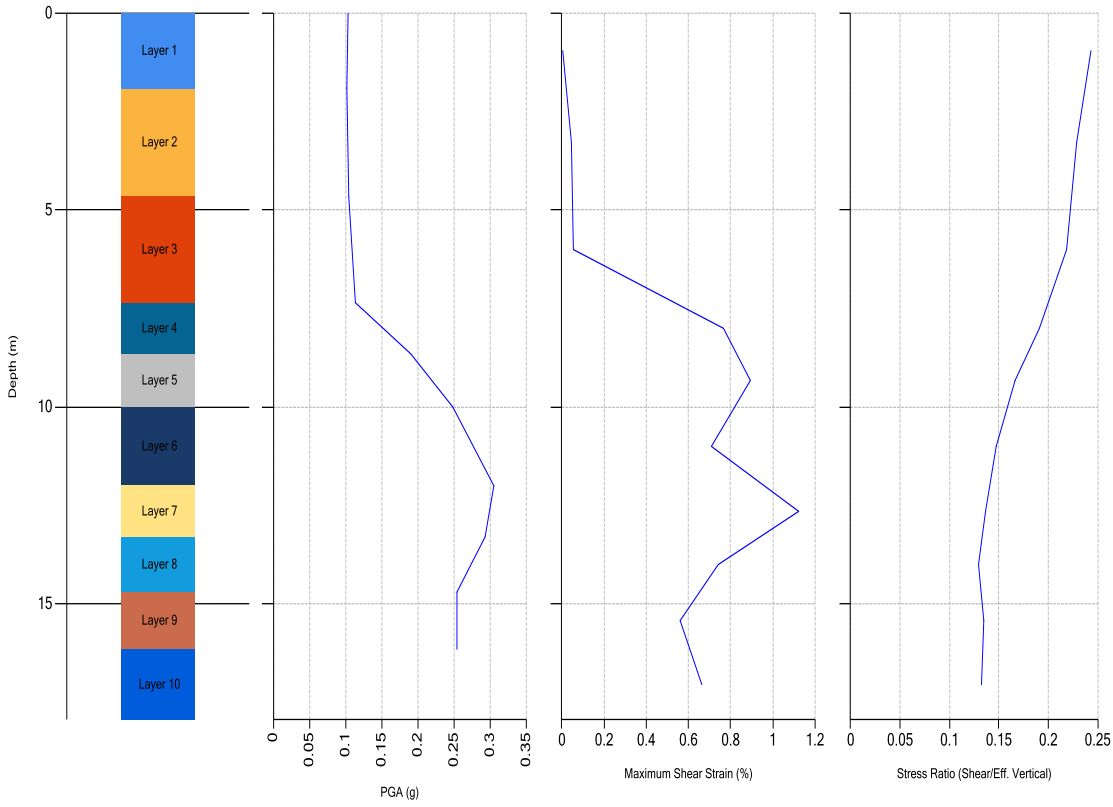

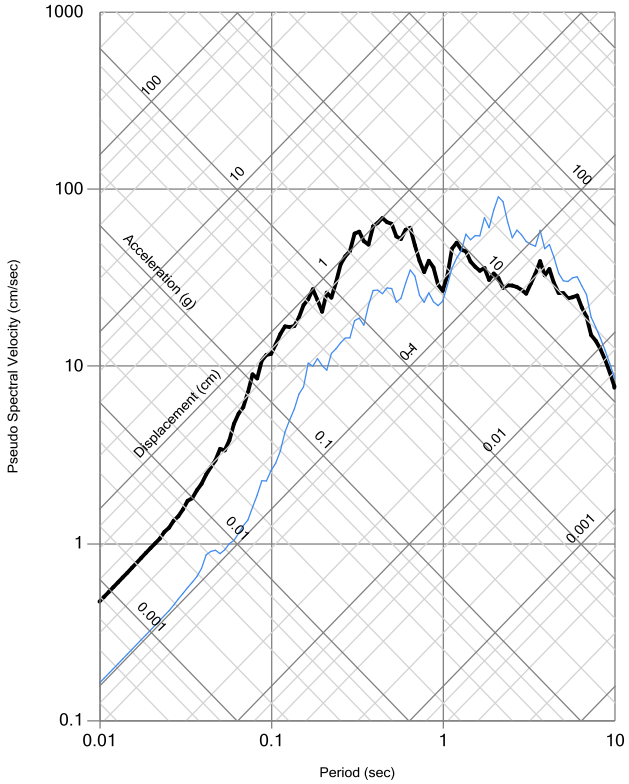

Layer #	Layer Name	Thickness (m)
1	clay	1.9
2	clayey silt to silty clay	2.75
3	clayey silt to silty clay	2.7
4	clay	1.3
5	clay	1.35
6	silty clay to clay	2
7	clay	1.3
8	clay	1.4
9	clay	1.45
10	silty clay to clay	1.8

C.5 Results of CPT 5

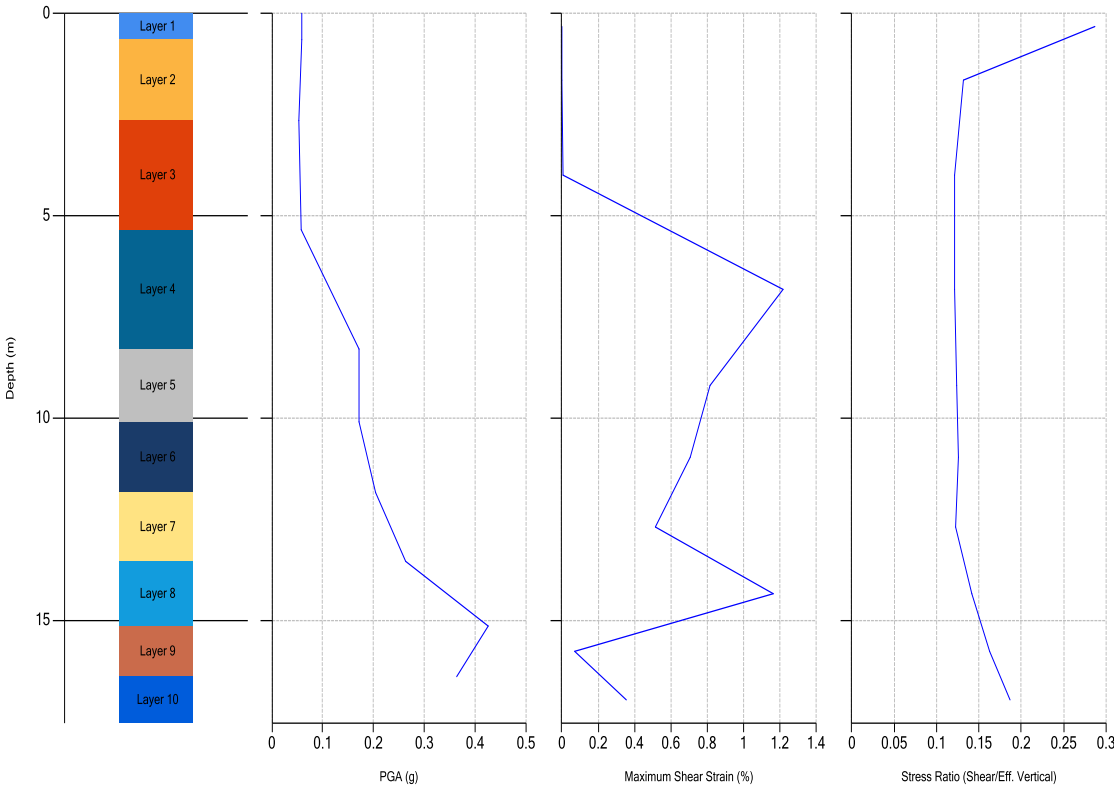

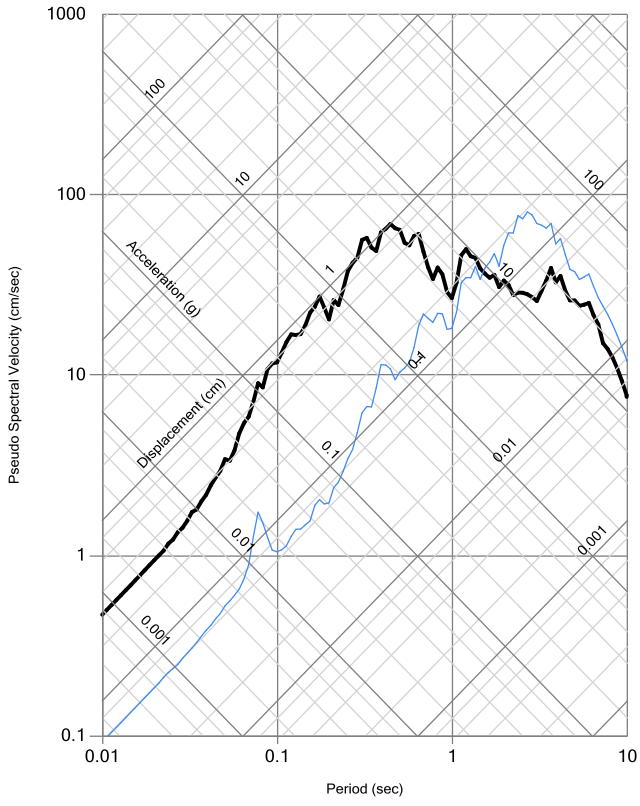

Layer #	Layer Name	Thickness (m)
1	silty sand to sandy silt	0.65
2	clay	2
3	clayey silt to silty clay	2.7
4	clay	2.95
5	clay	1.8
6	clay	1.75
7	clay	1.7
8	clay	1.6
9	clayey silt to silty clay	1.25
10	clay	1.15

C.6 Results of CPT 6

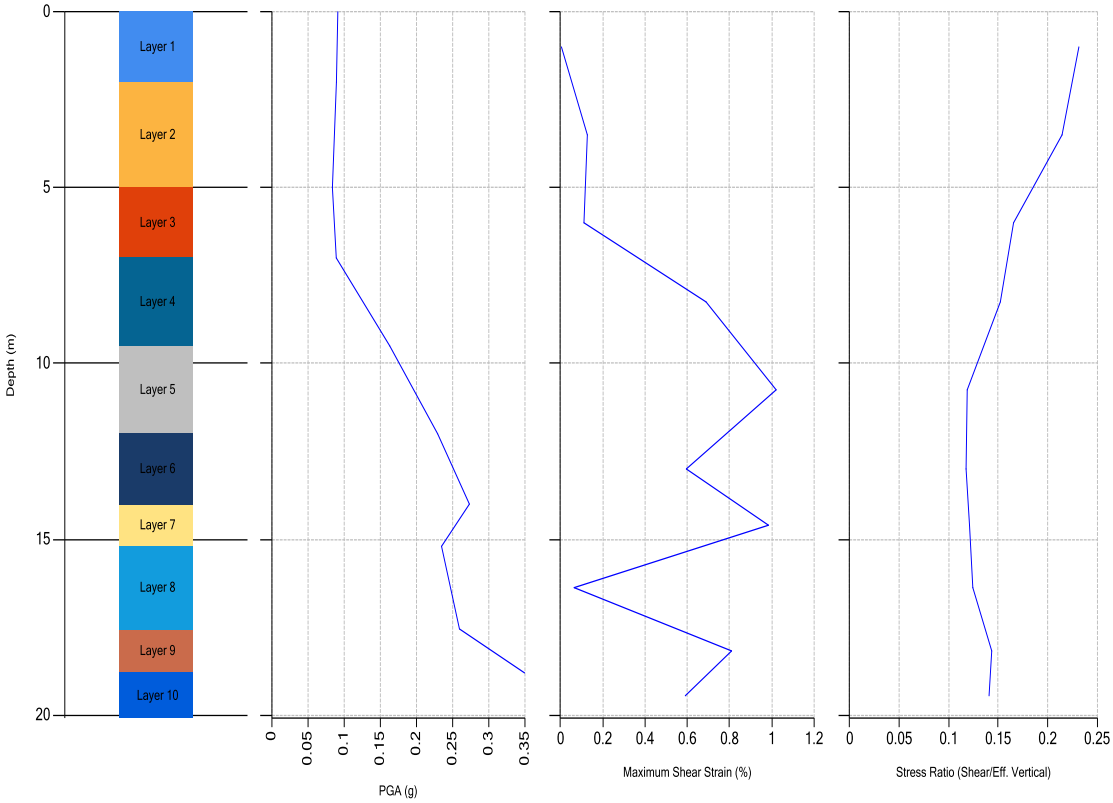

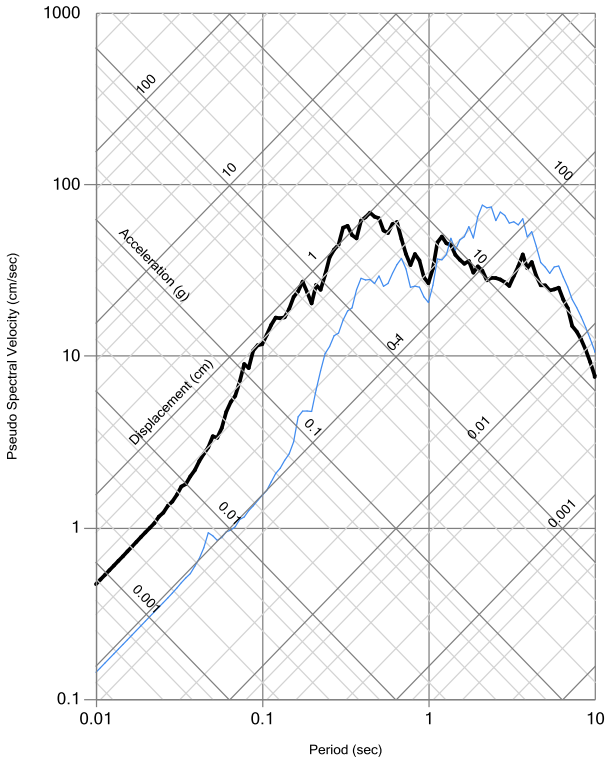

Layer #	Layer Name	Thickness (m)
1	clay	2
2	clay	3
3	silty clay to clay	2
4	clay	2.5
5	clay	2.5
6	clay	2
7	clay	1.2
8	clayey silt to silty clay	2.35
9	clay	1.25
10	clay	1.3

C.7 Results of CPT 7

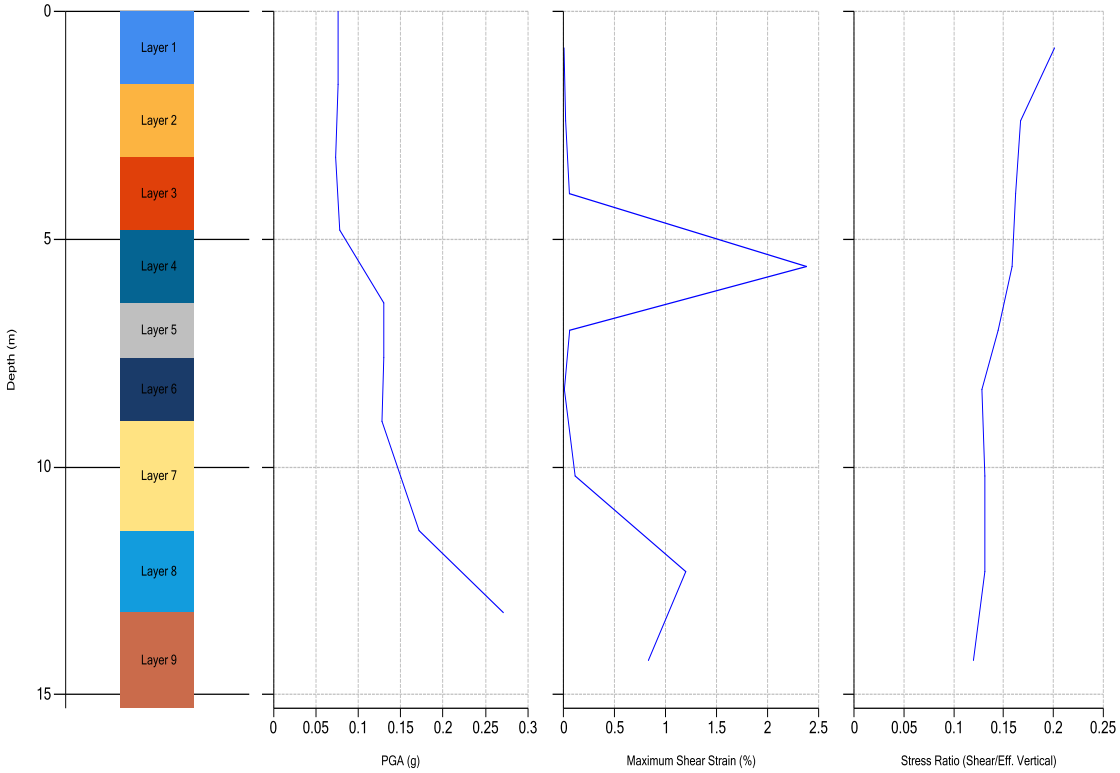

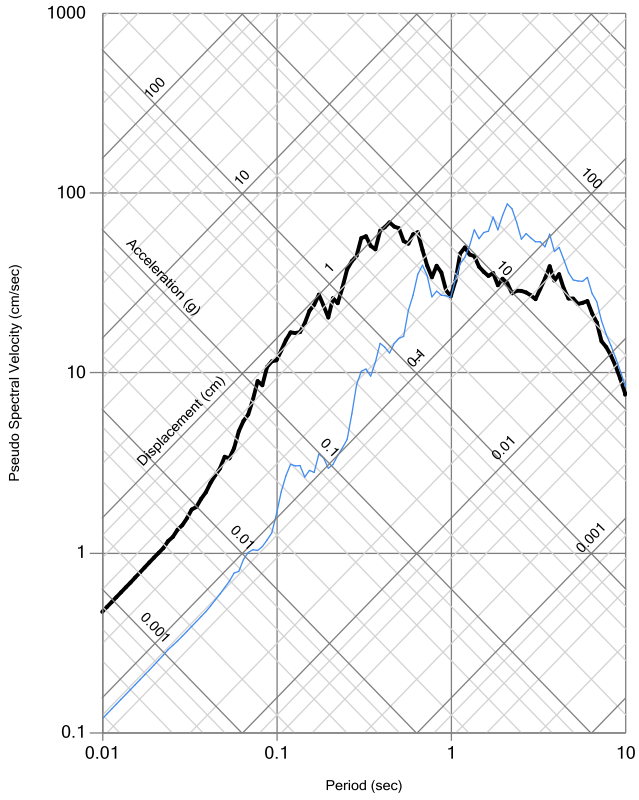

Layer #	Layer Name	Thickness (m)
1	clay	1.6
2	clay	1.6
3	clay	1.6
4	clay	1.6
5	clay	1.2
6	sand to silty sand	1.4
7	clayey silt to silty clay	2.4
8	silty clay to clay	1.8
9	clay	2.1

C.8 Results of CPT 8

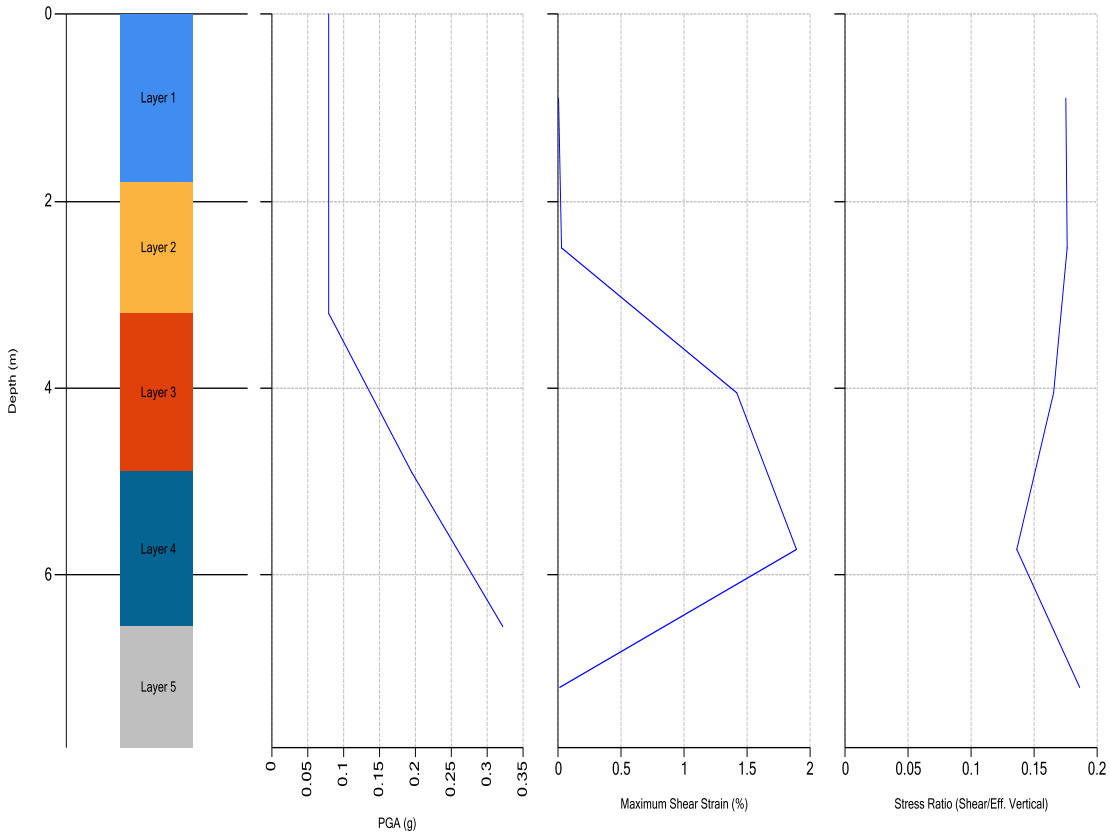

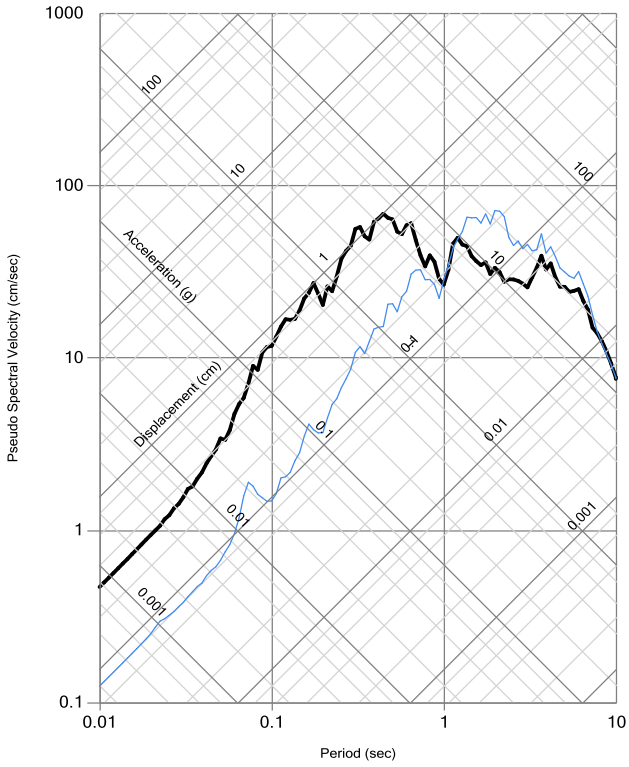

Layer #	Layer Name	Thickness (m)
1	clay	1.8
2	clay	1.4
3	clay	1.7
4	clay	1.65
5	clay	1.3

C.9 Results of CPT 9

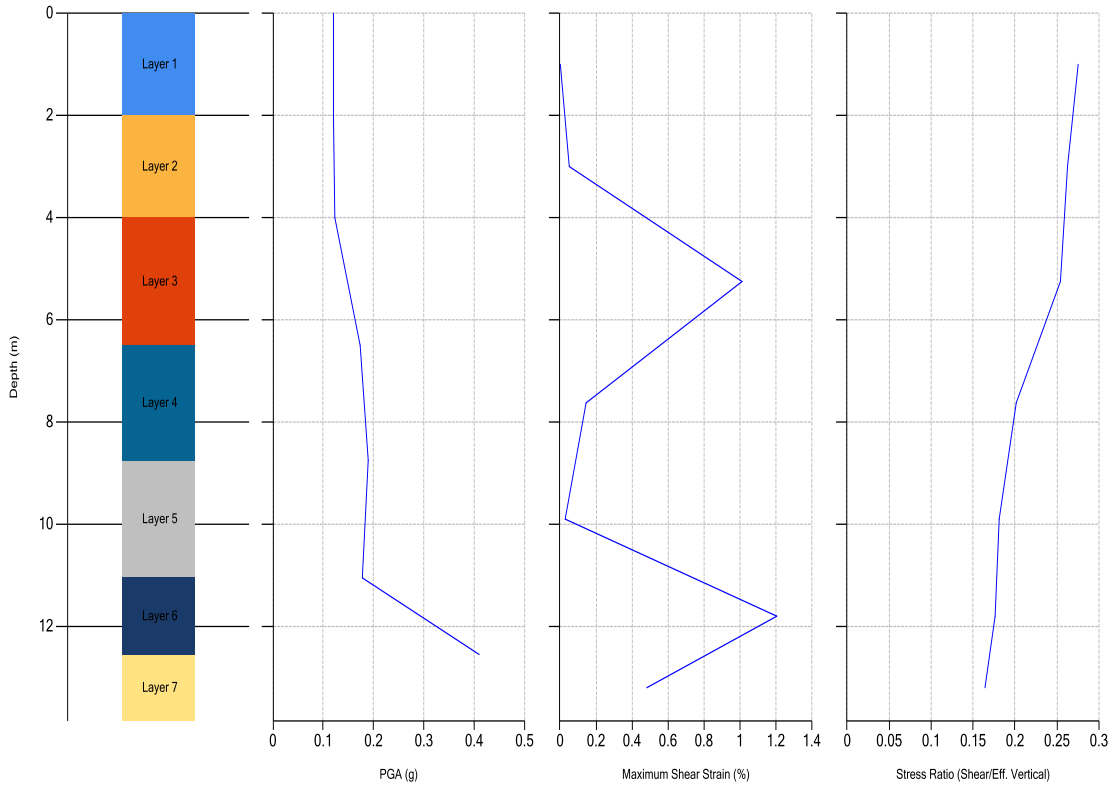

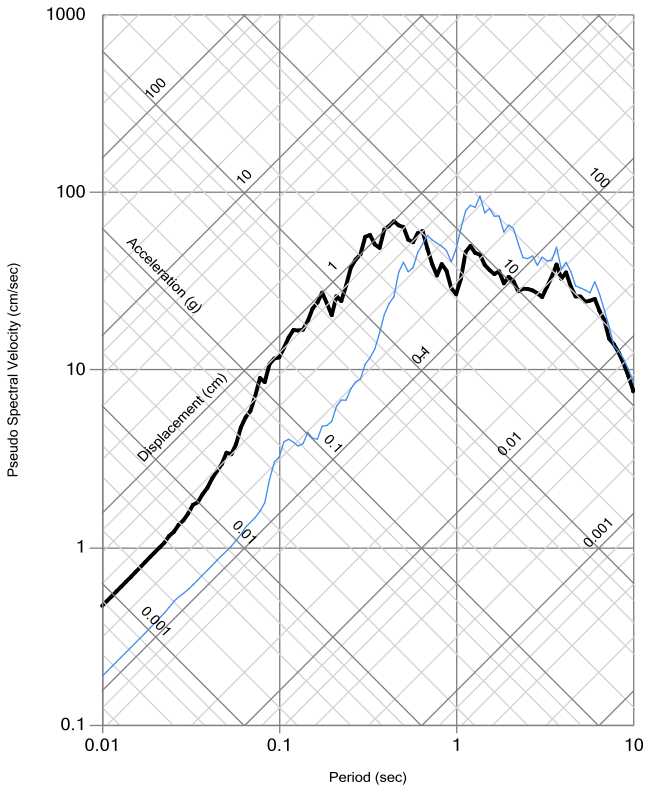

Layer #	Layer Name	Thickness (m)
1	clayey silt to silty clay	2
2	clay	2
3	clay	2.5
4	silty clay to clay	2.25
5	clayey silt to silty clay	2.3
6	clay	1.5
7	clay	1.3

C.10 Results of CPT 10

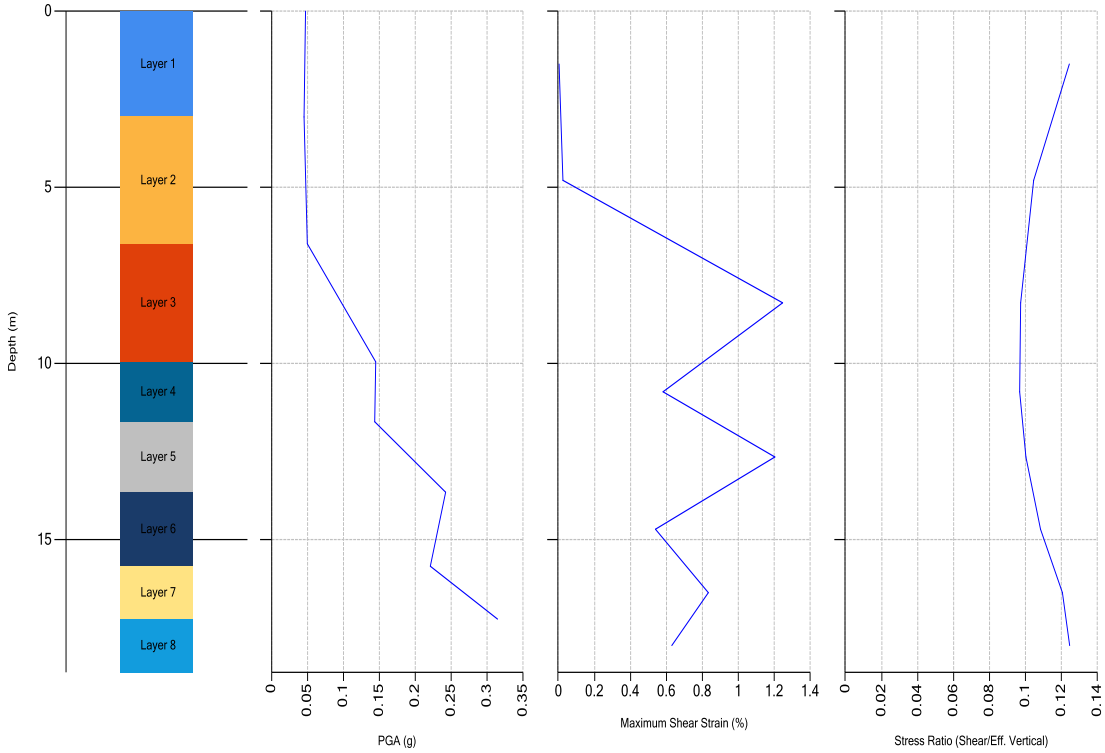

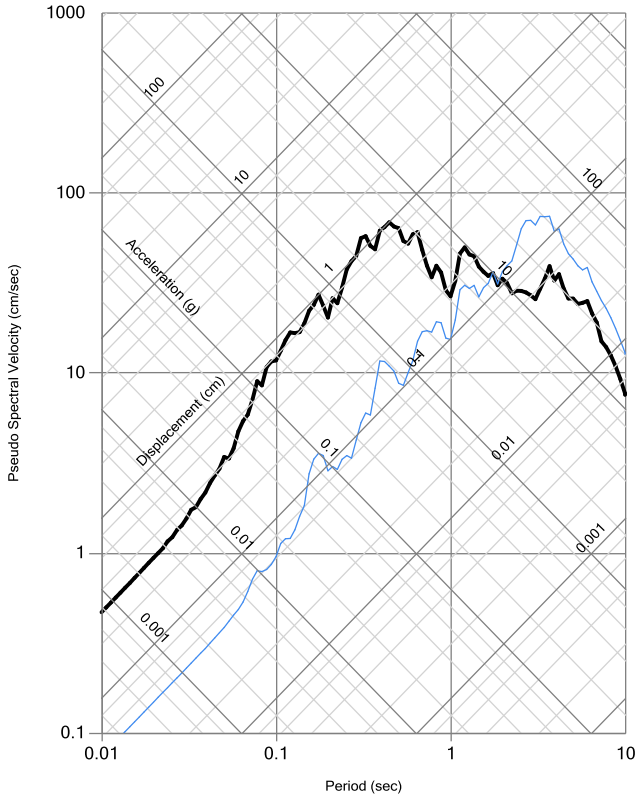

Layer #	Layer Name	Thickness (m)
1	clay	3
2	clay	3.6
3	silty clay to clay	3.35
4	clay	1.7
5	silty clay to clay	2
6	clay	2.1
7	silty clay to clay	1.5
8	silty clay to clay	1.5